

ASSOCIATION AND DIFFERENTIATION OF SMOKELESS POWDERS UTILIZING NON-TARGETED MASS SPECTROMETRY AND MULTIVARIATE STATISTICAL ANALYSIS

By

Kristen Leigh Reese

A THESIS

Submitted to
Michigan State University
in partial fulfillment of the requirements
for the degree of

Forensic Science - Master of Science

2016

ABSTRACT

ASSOCIATION AND DIFFERENTIATION OF SMOKELESS POWDERS UTILIZING NON-TARGETED MASS SPECTROMETRY AND MULTIVARIATE STATISTICAL ANALYSIS

By

Kristen Leigh Reese

Smokeless powders, low explosives that serve as propellant in ammunition, are typically analyzed in the unburned or burned forms. Forensic laboratories utilize chemical profiles for confirmation of powder type or association of evidence at a crime scene to a potential suspect. Recent research utilized targeted liquid chromatography (LC)-mass spectrometry (MS) to distinguish powders according to ammunition brand. This work demonstrated use of a non-targeted approach for compound identification combined with multivariate statistical analysis for association and discrimination of powders. Smokeless powders, both unburned and burned, were analyzed from commercial ammunition of different caliber, manufacturer, primer composition, and age. Preliminary morphological analysis was limited. Chemical analysis was performed using LC-atmospheric pressure chemical ionization-time-of-flight MS with multiplexed collision-induced dissociation for non-targeted compound identification (LC-APCI-multiplexed CID-TOF-MS). Increasing collision energies fragmented ions to different extents, providing structural information and facilitating compound identification, even without suitable reference standards. Principal components analysis of the chemical profiles generated distinct groupings of powders based on the presence of ethyl centralite, 1-methyl-3,3-diphenylurea, diphenylamine (DPA), N-nitroso-DPA, and dibutyl phthalate. Hierarchical cluster analysis produced a complementary analysis with the same groupings. Association of burned powders to unburned counterparts was possible, although the extent of association was dependent on the unburned powder composition and the extent of compound depletion during firing.

ACKNOWLEDGEMENTS

First, I would like to thank my advisor and committee member, Dr. Ruth Smith. Her guidance and encouragement throughout my graduate career have taught me how to better express my ideas and draw meaningful conclusions. She has been extremely patient in reading each draft of my thesis, for which I am extremely appreciative. I would like to thank Dr. Brian Hunter for serving on my committee, providing expertise, generously supplying ammunition, and securing firing range access. I would like to thank Dr. Steven Chermak for serving as the final member of my committee. The Bridgeport Lab of the State of Michigan's Police Department allowed use of their firing range. I would also like to acknowledge my Ph.D. advisor, Dr. A. Daniel Jones, for challenging my scientific curiosity and helping me become a better researcher.

I am extremely grateful for my fellow graduate students, both past and current, from the Forensic Chemistry Department and Chemistry Department. I cherish their friendship and support, especially during the unexpected times during my graduate career. A special thanks to those graduate students who have helped me shape research ideas and listened to countless presentations.

Finally, I would like to wholeheartedly thank my family, who have provided love and support throughout my project, especially during the most trying and stressful times. They have been my greatest encouragement throughout my graduate studies. This has been both a demanding and rewarding journey. I am grateful to everyone.

TABLE OF CONTENTS

LIST OF TABLES	vii
LIST OF FIGURES	viii
CHAPTER ONE: Introduction	1
1.1 Justification	1
1.2 Manufacture of Ammunition Components	2
1.3 Smokeless Powders Morphologies	4
1.3.1 General Morphologies	4
1.3.2 Comparison of Powder Morphologies	6
1.4 Chemical Analysis of Smokeless Powders	7
1.4.1 General Chemical Compounds Within Smokeless Powders	7
1.4.2 Current Methods for Chemical Analysis of Unburned Smokeless Powders and GSR..	9
1.4.2.1 Extraction of Smokeless Powder Additives.....	10
1.4.2.2 Chemical Analysis of Smokeless Powder Additives	11
1.4.3 Current Methods in Organic Compound Identification in GSR	13
1.4.4 Difficulties in Uniformity of Data Collection and Processing.....	15
1.5 Application of Multivariate Statistical Analysis for Chemical Components of Smokeless Powders.....	16
1.6 Thesis Objectives	19
REFERENCES	20
CHAPTER TWO: Instrumental and Statistical Theory	23
2.1 Separations- High Performance Liquid Chromatography (HPLC)	23
2.2 Mass Spectrometry.....	28
2.2.1 Ionization: Atmospheric Pressure Chemical Ionization	29
2.2.2 Mass Analyzer: Time of Flight	31
2.2.2.1 Multiplexed collision induced dissociation	35
2.2.3 Detectors- Microchannel Plate Detector	37
2.3 Data Output and Pre-Treatment	38
2.4 Multivariate Statistical Analysis	40
2.4.1 Principal Component Analysis	40
2.4.2 Hierarchical Cluster Analysis	42
REFERENCES	46
CHAPTER THREE: Materials and Methods	48
3.1 Materials	48
3.1.1 Acquisition of Commercial Ammunition	48
3.1.2 Chemical Solvents and Standards.....	50
3.2 Isolation of Unburned Smokeless Powder from Commercial Ammunition.....	50
3.3 Analysis of Physical and Chemical Attributes of Unburned Smokeless Powders	51
3.3.1 Morphology.....	51
3.3.2 HPLC-MS Analysis of Chemical Extracts	53

3.4 Analysis of Chemical Attributes of Fired Smokeless Powders	56
3.4.1 Collection of Burned Smokeless Powders	56
3.4.2 Extraction and HPLC-MS Analysis of Chemical Extracts from Spent Cartridges	56
3.5 Data Pretreatment.....	57
3.6 Data Analysis	59
3.6.1 Principal Component Analysis (PCA).....	60
3.6.2 Hierarchical Cluster Analysis (HCA)	60
REFERENCES	61

CHAPTER FOUR: Association and Discrimination of Unburned Commercial Smokeless

Powders Using Physical Properties, Chemical Properties, and Multivariate Statistical Analysis	63
4.1 Introduction.....	63
4.2 Morphological Analysis of Smokeless Powder Samples.....	63
4.3 Identification of Organic Compounds in Smokeless Powders	66
4.3.1 Multiplexed-CID Confirmation of Identity of Reference Standards	66
4.3.2 Multiplexed-CID to Identify Compounds in Unburned Smokeless Powders.....	72
4.3.3 Comparison of Chemical Profiles for Powders from Ammunition Containing Lead and Lead-Free Primers.....	83
4.3.4 Comparison of Chemical Profiles for Powders from Aged Ammunition and New Counterparts.....	89
4.4 Multivariate Statistical Analysis of Chemical Profiles from Unburned Powders	94
4.4.1 Principal Components Analysis.....	94
4.4.2 Hierarchical Cluster Analysis	98
4.5 Summary.....	101
APPENDICES	103
APPENDIX 4.1 Stereomicroscopic Images of Unburned Smokeless Powders	104
APPENDIX 4.2 Representative Chromatograms of the Chemical Profile from Unburned Smokeless Powders.....	112
APPENDIX 4.3 Morphological Characteristics for Unburned Smokeless Powders.....	120
REFERENCES	122

CHAPTER FIVE: Association and Discrimination of Burned Commercial Smokeless Powder

Residue Using Chemical Properties and Multivariate Statistical Analysis	124
5.1 Introduction.....	124
5.2 Analysis of Organic Compounds within Burned Smokeless Powders	124
5.2.1 Identification and Comparison of Chemical Profiles from Burned Smokeless Powders	124
5.2.2 Comparison of Chemical Profiles between Burned and Corresponding Unburned Smokeless Powders.....	132
5.3 Multivariate Statistical Analysis of Chemical Profiles from Burned Smokeless Powders Compared to their Corresponding Unburned Counterparts	133
5.3.1 Introduction.....	133
5.3.2 Example of Association by PCA and HCA	134
5.3.3 Example of Association by PCA and HCA	136
5.3.4 Example of No Association by PCA or HCA.....	138
5.3.5 Hypothetical Examples for Inclusion within a Forensic Lab.....	140

5.4 Summary	142
APPENDICES	144
APPENDIX 5.1 Extracted Ion Chromatograms Representing the Chemical Profile from Burned Smokeless Powders	145
APPENDIX 5.2 Multivariate Statistical Analysis Results for Burned Smokeless Powders ..	158
REFERENCES	176
CHAPTER SIX: Conclusions and Future Directions	178
6.1 Conclusions	178
6.2 Future Directions	180

LIST OF TABLES

Table 3.1 List of commercial cartridges from which smokeless powders were obtained	49
Table 3.2 HPLC Conditions.....	55
Table 3.3 APCI Probe Conditions	55
Table 3.4 MarkerLynx Software Chromatography and Mass Spectrometry Parameters	58
Table 4.1 Summary of Chromatographic and Mass Spectral Data for Explosive Reference Standards.....	67
Table 4.2 Summary of Chromatographic and Mass Spectral Data for Multiplexed-CID Identified Compounds	80
Table 4.3 Summary of organic compounds identified in unburned smokeless powders.....	82
Table A.4.3.1 Summary of Morphological Characteristics for Unburned Smokeless Powders.	120

LIST OF FIGURES

Figure 1.1 Components of Ammunition Cartridge.....	3
Figure 1.2 Common morphologies for smokeless powders, including (A) ball, (B) cylinder or tubular, (C) cylinder or tubular with perforation, (D) lamel, (E) disk, and (F) perforated disk.	5
Figure 1.3 Common chemical additives present in smokeless powders (A) diphenylamine, (B) 4-nitro diphenylamine, (C) 2,4-dinitrodiphenylamine, (D) ethyl centralite, (E) 2,4-dinitrotoluene, (F) dibutyl phthalate, and (G) 1-methyl-3,3-diphenylurea (Akardite II).	8
Figure 2.1 HPLC Workflow	24
Figure 2.2 Chromatogram of well-separated, Gaussian peaks	26
Figure 2.3 Typical chromatogram displaying chemical compounds as a function of the detector signal at a given retention time	27
Figure 2.4 Flowchart of the components comprising a mass spectrometer	28
Figure 2.5 Schematics for an atmospheric pressure chemical ionization (APCI) source.	30
Figure 2.6 Schematic for a Waters LCT Premier Time-of-Flight Mass Spectrometer operating in V-mode (www.waters.com).....	32
Figure 2.7 Chromatogram detailing the calculation of resolution for chromatography peaks	35
Figure 2.8 Workflow for increasing voltages during multiplex-CID fragmentation.....	36
Figure 2.9 A microchannel plate detector cross-section, with individual schematic representative of an individual channel.....	37
Figure 2.10 Representation of data plotted on a Y vs X axis with processing for PCA analysis.	41
Figure 2.11 An illustration of samples to be clustered (A, B, C, and D) with coordinates on an Y vs. X plot.....	43
Figure 2.12 An illustration of samples clustered using HCA. Samples A and B were initially clustered (black line) with Euclidean distance. The dashed lines indicate the possible linkage methods: single (green), average (red), and complete (blue).....	44
Figure 2.13 Example dendrogram output of HCA utilizing the example data.	45
Figure 3.1 Visual representation of Image J processed pictures. A) Raw picture of Magtech 7.62x39mm, Aged B) Binary representation, C) Altered binary representation D) Processed samples with outlines around defined kernels.	53

Figure 4.1 Representative morphology of smokeless powder kernels from (A) Win9NoPb and (B) PMC9Pb that were deemed distinguishable and from (C) Mag9NoPb and (D) Bzr9NoPb that were deemed indistinguishable.	65
Figure 4.2 Representative chromatogram of explosive reference standards analyzed by HPLC-APCI-multiplexed-CID-TOF-MS in positive mode. For each peak, the compound identification is given, along with the retention time (t_R) and the m/z of the molecular ion for the compound. 68	68
Figure 4.3 Multiplexed-CID spectra of DBP collected at collision energies of (A) 10 V, (B) 25 V, and (C) 40 V.....	69
Figure 4.4 Proposed fragmentation pathway for DBP based on multiplexed-CID spectra (shown in Figure 4.3).....	71
Figure 4.5 Representative chromatogram of Win9Pb, indicating the presence of DPA, EC, and DBP, as well as two unidentified compounds at t_R 4.18 min and t_R 6.67 min. For each peak, the compound identification is given, along with the retention time (t_R) and the m/z of the molecular ion for the compound.....	73
Figure 4.6 Multiplexed-CID spectra for peak at t_R 4.18 min in Win9Pb collected at different collision energies (A) 10 V, (B) 25 V, (C) 40 V, and (D) 55 V.	74
Figure 4.7 Proposed structure of peak at t_R 4.18 min based on multiplexed-CID spectra.....	76
Figure 4.8 Multiplexed-CID spectra for peak at t_R 6.61 min in Win9Pb collected at different collision energies (A) 10 V, (B) 25 V, and (C) 40 V.....	77
Figure 4.9 Proposed structure of peak at t_R 6.61 min based on multiplexed-CID spectra.....	79
Figure 4.10 Plot of normalized relative abundance of each identified compound in each powder originating from ammunition with lead-containing (Pb) and lead-free (NoPb) primer.....	84
Figure 4.11 Representative chromatogram of powder from (A) Fed9Pb and (B) Rem9Pb, indicating the presence of Akardite II, N-nitroso-DPA, DPA, EC, and DBP.	86
Figure 4.12 Representative chromatogram of powder from (A) Bzr9NoPb and (B) Mag9NoPb, indicating the presence of EC, (C) Extracted ion chromatograms (XIC) of m/z 170.1 corresponding to DPA in Bzr9NoPb, (D) m/z 170.1 in Mag9NoPb, (E) m/z 169.1 corresponding to N-nitroso-DPA in Bzr9NoPb, and (F) m/z 169.1 in Mag9NoPb.....	87
Figure 4.13 Representative chromatogram of powder from (A) Win9NoPb and (B) SB9NoPb, indicating the presence of organic compounds. The distinguishing compound in Win9NoPb was DBP while SB9NoPb contained EC.	88
Figure 4.14 Plot of normalized relative abundance of each identified compound in each powder originating from ‘aged’ ammunition (denoted with ‘A’) and corresponding new counterparts (denoted with ‘N’).....	90

Figure 4.15 Replicate chromatograms of powder from PMC9A, (A)-(E) represent replicates 1-5.	93
Figure 4.16 Principal components analysis based on chemical profiles of the unburned smokeless powders (A) scores plot and (B) loadings plot for the first two principal components.....	95
Figure 4.17 Hierarchical cluster analysis dendrogram based on chemical profiles of unburned smokeless powders. Groups indicate similar chemical profiles as determined during PCA analysis. Red numbers indicate similarity level at which each group was formed.....	99
Figure A.4.1.1 Representative pictures of (A) Win9Pb, (B) Rem9Pb, (C) Fed9Pb, (D) Horn9Pb, and (E) PMC9Pb taken with front lighting.	104
Figure A.4.1.2 Representative pictures of (A) Win9NoPb, (B) Rem9NoPb, (C) Bzr9NoPb, (D) Mag9NoPb, and (E) SB9NoPb taken with front lighting.	105
Figure A.4.1.3 Representative pictures of (A) Win12N, (B) PMC44N, and (C) SB7.62N taken with front lighting.	106
Figure A.4.1.4 All replicates of Win12A taken with front lighting.....	107
Figure A.4.1.5 All replicates of PMC44A taken with front lighting.	108
Figure A.4.1.6 All replicates of Mag7.62A taken with front lighting.	109
Figure A.4.1.7 All replicates of PMC9A taken with front lighting.	110
Figure A.4.1.8 All replicates of CCI22A taken with front lighting.....	111
Figure A.4.2.1 Representative chromatograms of (A) Win9Pb, (B) Rem9Pb, (C) Horn9Pb, (D) Fed9Pb, and (E) PMC9Pb.....	112
Figure A.4.2.2 Representative chromatograms of (A) Win9NoPb, (B) Rem9NoPb, (C) Bzr9NoPb, (D) Mag9NoPb, and (E) SB9NoPb.....	113
Figure A.4.2.3 Representative chromatograms of (A) Win12N, (B) PMC44N, and (C) SB7.62N.	114
Figure A.4.2.4 Chromatograms for Replicates 1-5 (A-E) of Win12A.	115
Figure A.4.2.5 Chromatograms for Replicates 1-5 (A-E) of PMC44A.....	116
Figure A.4.2.6 Chromatograms for Replicates 1-5 (A-E) of Mag7.62A.....	117
Figure A.4.2.7 Chromatograms for Replicates 1-5 (A-E) of PMC9A.....	118
Figure A.4.2.8 Chromatograms for Replicates 1-5 (A-E) of CCI2	119

Figure 5.1 Chromatograms of smokeless powder extracts from (A) unburned Win9Pb, and five replicates of burned Win9Pb (B-F)..... 125

Figure 5.2 Representative XIC chromatograms of extract obtained from a fired cartridge of Win9Pb (Replicate 4) displaying the abundances of (A) dibutyl phthalate at m/z 279.2, (B) ethyl centralite at m/z 269.2, (C) akardite II at m/z 227.1, (D) diphenylamine at m/z 170.1, and (E) N-nitroso-diphenylamine at m/z 169.1. 127

Figure 5.3 Graphical representation of the most abundant compounds across all chemical profiles of the extracts from fired cartridges of Pb vs NoPb: (A) DBP (m/z 279.2, t_R 12.12 minutes), (B) EC (m/z 269.2, t_R 8.45 minutes), (C) Akardite II (m/z 227.1, t_R 4.33 minutes), (D) DPA (m/z 170.1, t_R 7.75 minutes), and (E) N-nitroso-DPA (m/z 169.1, t_R 7.17 minutes). Alternating red and blue shading denote five replicates within an ammunition brand..... 128

Figure 5.4 Graphical representation of the most abundant compounds across all chemical profiles of the aged and newly manufactured ammunition: (A) DBP (m/z 279.2, t_R 12.12 minutes), (B) EC (m/z 269.2, t_R 8.45 minutes), (C) Akardite II (m/z 227.1, t_R 4.33 minutes), (D) DPA (m/z 170.1, t_R 7.75 minutes), and (E) N-nitroso-DPA (m/z 169.1, t_R 7.17 minutes). Alternating red and blue shading denote five replicates within an ammunition brand..... 131

Figure 5.5 Representation of the multivariate statistical analysis for a smokeless powder (SB9NoPb) able to have a good association via (A) PCA scores plot visual analysis and (B) HCA dendrogram providing a numerical analysis. 135

Figure 5.6 Representation of the multivariate statistical analysis for a smokeless powder (Rem9Pb) able to have a moderate association via (A) PCA scores plot visual analysis and (B) HCA dendrogram providing a numerical analysis..... 137

Figure 5.7 Representation of the multivariate statistical analysis for a smokeless powder (SB7.62N) with a poor association via (A) PCA scores plot visual analysis and (B) HCA dendrogram providing a numerical analysis. 139

Figure 5.8 Representation of a series of chemical profiles for hypothetical unknown samples for comparison against a known database of chemical profiles for unburned and burned smokeless powders analysis. 141

Figure A.5.1.1 Extracted ion chromatogram (XIC) of extract from fired cartridge of Win9Pb. Labels indicate m/z used for XIC analysis of listed compound..... 145

Figure A.5.1.2 Extracted ion chromatogram (XIC) of extract from fired cartridge of Rem9Pb. Labels indicate m/z used for XIC analysis of listed compound..... 146

Figure A.5.1.3 Extracted ion chromatogram (XIC) of extract from fired cartridge of Fed9Pb. Labels indicate m/z used for XIC analysis of listed compound..... 147

Figure A.5.1.4 Extracted ion chromatogram (XIC) of extract from fired cartridge of Hornday9Pb. Labels indicate m/z used for XIC analysis of listed compound..... 148

Figure A.5.1.5 Extracted ion chromatogram (XIC) of extract from fired cartridge of PMC9Pb. Labels indicate m/z used for XIC analysis of listed compound.....	149
Figure A.5.1.6 Extracted ion chromatogram (XIC) of extract from fired cartridge of Win9NoPb. Labels indicate m/z used for XIC analysis of listed compound.....	150
Figure A.5.1.7 Extracted ion chromatogram (XIC) of extract from fired cartridge of Rem9NoPb. Labels indicate m/z used for XIC analysis of listed compound.....	151
Figure A.5.1.8 Extracted ion chromatogram (XIC) of extract from fired cartridge of Bzr9NoPb. Labels indicate m/z used for XIC analysis of listed compound.....	152
Figure A.5.1.9 Extracted ion chromatogram (XIC) of extract from fired cartridge of SB9NoPb. Labels indicate m/z used for XIC analysis of listed compound.....	153
Figure A.5.1.10 Extracted ion chromatogram (XIC) of extract from fired cartridge of Mag9NoPb. Labels indicate m/z used for XIC analysis of listed compound.	154
Figure A.5.1.11 Extracted ion chromatogram (XIC) of extract from fired cartridge of Win12N. Labels indicate m/z used for XIC analysis of listed compound.....	155
Figure A.5.1.12 Extracted ion chromatogram (XIC) of extract from fired cartridge of PMC44N. Labels indicate m/z used for XIC analysis of listed compound.....	156
Figure A.5.1.13 Extracted ion chromatogram (XIC) of extract from fired cartridge of SB7.62N. Labels indicate m/z used for XIC analysis of listed compound.....	157
Figure A.5.2.1 Comparison of chemical profile for Fired Win9Pb versus profiles from unburned smokeless powder (A) PCA scores plot and (B) HCA dendrogram.....	158
Figure A.5.2.2 Comparison of chemical profile for Fired Rem9Pb versus profiles from unburned smokeless powder (A) PCA scores plot and (B) HCA dendrogram.....	159
Figure A.5.2.3 Comparison of chemical profile for Fired Horn9Pb versus profiles from unburned smokeless powder (A) PCA scores plot and (B) HCA dendrogram.....	160
Figure A.5.2.4 Comparison of chemical profile for Fired Fed9Pb versus profiles from unburned smokeless powder (A) PCA scores plot and (B) HCA dendrogram.....	161
Figure A.5.2.5 Comparison of chemical profile for Fired PMC9Pb versus profiles from unburned smokeless powder (A) PCA scores plot and (B) HCA dendrogram.....	162
Figure A.5.2.6 Comparison of chemical profile for Fired Win9NoPb versus profiles from unburned smokeless powder (A) PCA scores plot and (B) HCA dendrogram.....	163
Figure A.5.2.7 Comparison of chemical profile for Fired Rem9NoPb versus profiles from unburned smokeless powder (A) PCA scores plot and (B) HCA dendrogram.....	164

Figure A.5.2.8 Comparison of chemical profile for Fired Bzr9NoPb versus profiles from unburned smokeless powder (A) PCA scores plot and (B) HCA dendrogram.....	165
Figure A.5.2.9 Comparison of chemical profile for Fired Mag9NoPb versus profiles from unburned smokeless powder (A) PCA scores plot and (B) HCA dendrogram.....	166
Figure A.5.2.10 Comparison of chemical profile for Fired SB9NoPb versus profiles from unburned smokeless powder (A) PCA scores plot and (B) HCA dendrogram.....	167
Figure A.5.2.11 Comparison of chemical profile for Fired Win12N versus profiles from unburned smokeless powder (A) PCA scores plot and (B) HCA dendrogram.....	168
Figure A.5.2.12 Comparison of chemical profile for Fired PMC44N versus profiles from unburned smokeless powder (A) PCA scores plot and (B) HCA dendrogram.....	169
Figure A.5.2.13 Comparison of chemical profile for Fired SB7.62N versus profiles from unburned smokeless powder (A) PCA scores plot and (B) HCA dendrogram.....	170
Figure A.5.2.14 Comparison of chemical profile for Fired Win12A versus profiles from unburned smokeless powder (A) PCA scores plot and (B) HCA dendrogram.....	171
Figure A.5.2.15 Comparison of chemical profile for Fired PMC44A versus profiles from unburned smokeless powder (A) PCA scores plot and (B) HCA dendrogram.....	172
Figure A.5.2.16 Comparison of chemical profile for Fired Mag7.62A versus profiles from unburned smokeless powder (A) PCA scores plot and (B) HCA dendrogram.....	173
Figure A.5.2.17 Comparison of chemical profile for Fired CCI22A versus profiles from unburned smokeless powder (A) PCA scores plot and (B) HCA dendrogram.....	174
Figure A.5.2.18 Comparison of chemical profile for Fired PMC9A versus profiles from unburned smokeless powder (A) PCA scores plot and (B) HCA dendrogram.....	175

CHAPTER ONE: Introduction

1.1 Justification

Explosives serve a multitude of purposes, from non-military applications such as construction, demolition, and rock blasting, to a mixture of civilian and military purposes, specifically as the propellant, or energetic, component of ammunitions or improvised explosive devices. Explosives are broadly termed as materials that store a large amount of potential energy that can be rapidly released, usually with the generation of light, heat, sound, and pressure. Classification of explosives can be broadly termed high or low grade, depending on the rate of decomposition or pressure generation during release of the stored potential energy.

Smokeless powders are a low-grade explosive often used in ammunition cartridges. In this enclosed environment, the powder generates a large amount of pressure to launch the bullet. According to the Federal Bureau of Investigation (FBI), in 2011, 68% of murders, 41% of robbery offenses, and 21% of aggravated assaults in the United States were committed with some type of gun (1). Forensic scientists utilize smokeless powder evidence collected at a crime scene to identify the type of powder. In cases with a known suspect, the smokeless powder from the scene can be compared to powder obtained from the perpetrator.

After discharging a gun, both unburned and burned particles of smokeless powders are present. The most common forensic methods examine potential gunshot residue (GSR) for elemental composition and particle imaging. However, a greater awareness has more recently been given to the organic compounds present in the unburned, intact powder and GSR. This study examined the morphological characteristics of unburned smokeless powders. The organic compounds within unburned and corresponding burned GSR were extracted and analyzed with a non-targeted technique for comprehensive analysis, after which multivariate statistical analyses

were performed to determine which organic compounds can associate and discriminate the smokeless powder within different types of ammunition.

1.2 Manufacture of Ammunition Components

Ammunition is broadly identified based on either physical dimensions of cartridges or weight of ammunition. Handgun ammunition is classified on the basis of the diameter of the ammunition, commonly called caliber. Caliber can be measured in either metric (millimeters) or U.S. units (inches). Examples include the 9 mm Luger, denoting a bullet of 9 mm diameter, or the 7.62x39mm, where the bullet is 7.62 mm in diameter and 39 mm in length. For shotgun ammunition, the caliber is measured through the weight of the ammunition. Nomenclature is in terms of gauge (U.S.) or bore (U.K), most commonly the 12-gauge.

An ammunition cartridge (Figure 1.1) consists of the primer, propellant, bullet, and exterior casing. The primer consists of a sensitive mixture of a high explosive, oxidizing agent, and fuel, typically lead styphnate, barium nitrate, and antimony sulfide, respectively. The mixture is stable in the cartridge casing. During the firing process, pulling the trigger of the weapon initiates the firing pin to strike the primer. The primer material detonates, creating a spark to ignite the propellant. The burning propellant rapidly produces a large volume of gas which is trapped inside the casing. The amount of pressure generated depends upon the available surface area of the powder (see section 1.3.1 for further discussion). The expanding pressure is released through ejection of the bullet from the ammunition case. Expelled gases and GSR residue are simultaneously released with the bullet. GSR is composed of burned, partially burned, and

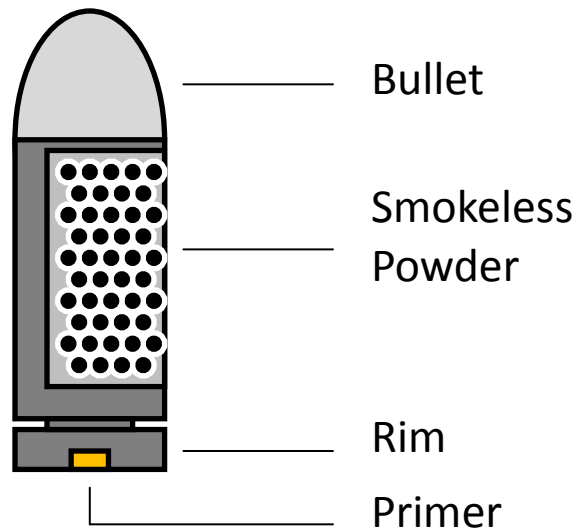


Figure 1.1 Components of Ammunition Cartridge

unburned particulates originating from the case, primer, propellant, lubricants, and any residue in the barrel from previously fired ammunition.

The assembly of ammunition consists of components acquired from a number of different companies. The companies may also produce different types of primers, propellants, or bullets. For example, the smokeless powder manufacturer Hodgdon produces products with names such as Titegroup, HP038, HS-6, Universal, etc (2). These designations indicate different burn rates and maximum pressure generated. Ammunition manufacturers such as Remington, Federal, Winchester, etc. purchase the smokeless powder for inclusion in their own ammunition. As a result, 9 mm ammunition from Remington and from Winchester could conceivably contain the same smokeless powder produced by Hodgdon.

Additionally, costs and product availability from a smokeless powder manufacturer (e.g., Hodgdon) may force an ammunition company (e.g., Remington or Winchester) to buy different powder manufacturer products over time, but this information is not conveyed to the consumer. Therefore, two boxes of ammunition cartridges of the same caliber produced by the same

manufacturer may actually contain different smokeless powders. Thus, forensic identification of smokeless powder focuses on 1) the similarities between chemical properties of a questioned sample recovered from a scene to known samples from suspects or 2) the identification of smokeless powder type from unburned particles present from recovered evidence.

1.3 Smokeless Powders Morphologies

1.3.1 General Morphologies

During the production of smokeless powders, manufacturers prepare a mixture of propellant and chemical additives into different shaped morphologies. Different morphologies will burn at different rates due to available surface area. For example, for two smokeless powders of the same overall shape but different individual kernel sizes, the powder with the smaller sized kernels will burn at a faster rate due to a larger exposed surface area. The burn rate determines where peak pressure is generated after powder ignition, which may need to be tailored in different ammunitions for optimal performance.

Common morphologies include lamel, ball, tubular, disk, and flake (Figure 1.3). The ball powders also contain sub-categories of “flattened” morphology, where the powder is pressed between rollers. Some powders contain perforations, or long holes, through the length of the powder. Perforations increase the amount of surface area to expedite the rate of burning. Due to the manufacturing process, many of the flattened ball powders contain imperfections, such as cracked edges or irregular forms due to small broken pieces. Other irregular shapes, such as teardrops, dumbbells, or striations, may be intentional or unintentional. The variation in kernel

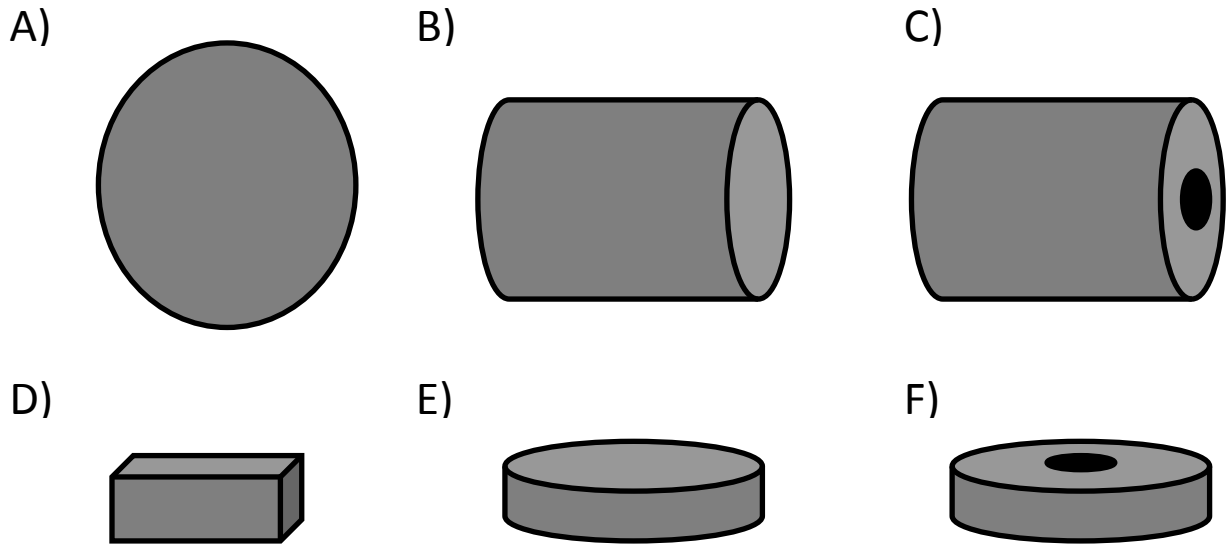


Figure 1.2 Common morphologies for smokeless powders, including (A) ball, (B) cylinder or tubular, (C) cylinder or tubular with perforation, (D) lamel, (E) disk, and (F) perforated disk.

shape can facilitate determination of a powder manufacturer, or, if the defect is extremely unique, association of the powder collected from a suspect to powder collected from a scene.

Additional characteristics of the powder appearance include luster, color, colored markers, and physical dimensions. Luster indicates the reflectance of light off the kernels when illuminated. The color of a powder is typically black or gray due to the addition of graphite as an outer coating. However, powder colors also include green, brown, gold, orange, and red. Colored kernels are an optional feature manufacturers include as markers to allow enthusiasts that prefer to disassemble ammunition to easily identify a commercial brand. Colored markers are commonly red, blue, green, orange, purple, and white. The measurement of smokeless powder dimensions, such as length, width, diameter, and so on, are characteristic of the manufacturing process and can discriminate among powders from different manufacturers. As the nomenclature for powders varies depending on the laboratory and/or country, all terminology, shapes, and physical measurements used in this thesis will conform to the national database of the Technical

Working Group for Fire and Explosions (TWGFEX) (3).

1.3.2 Comparison of Powder Morphologies

The TWGFEX national database is under the supervision of the National Center for Forensic Science (NCFS), incorporating more than 700 samples of smokeless powders of known origin (3). TWGFEX guidelines recommend at least 50 powder kernels should be characterized from each powder to obtain a representative sampling. The morphology is regarded as a better classifier of differentiating powders compared to other physical characteristics. Typically, picture documentation of the powder is recorded by photographing multiple kernels to examine one or more of the following characteristics, depending on morphology: length, width, thickness, diameter, area, and perforation. The measurements are typically reported on a millimeter scale and can be determined through either crude physical measurements, such as a ruler, or more intricate image-based processing software utilizing a reference scale, such as Image J (National Institutes of Health), or equivalent computer software. The type and manufacturer of an unknown powder can be determined through comparison of the morphological data to the database.

Based solely on morphological data, comparisons of powders have been performed. For example, Zack and House were able to distinguish 19 smokeless powders from three smokeless powder manufacturers based on shape and physical measurements of length and diameter (4). Database comparisons have been demonstrated by several sources (5). However, if a lab does not have an inclusive in-house reference collection, externally prepared databases are a useful tool. However, the use of morphological data alone, even in combination with a database, provides limited information. Therefore, the use of several techniques in combination with morphology

have been more recently utilized to better discriminate samples using the chemical profile of smokeless powders.

1.4 Chemical Analysis of Smokeless Powders

1.4.1 General Chemical Compounds Within Smokeless Powders

The broadest classification of smokeless powder relates to the composition of the energetic, or explosive, components. Single-based powders contain one energetic component, nitrocellulose. The addition of the energetic nitroglycerine creates a double-based powder, which increases the explosive content. The presence of nitroguanidine, nitroglycerine, and nitrocellulose signifies a triple-based powder. However, the triple-based powder is typically used in military-grade weapons, and is not encountered in common civilian ammunitions.

Manufacturers add chemical components to the energetic components in order to improve the powder longevity, burn rate, and pressure generation. The chemical structures of common additives are illustrated in Figure 1.2. Stabilizers, such as diphenylamine (DPA), ethyl centralite (EC), methyl centralite (MC), and 1-methyl-3,3-diphenylurea (commonly known as Akardite II) mitigate decomposition of nitrocellulose (NC). NC undergoes autocatalysis, where the breakage of weak nitrate ester bonds produces acids and nitric oxides that in turn accelerate further decomposition. Stabilizers, most of which contain aromatic groups, incorporate the free nitric oxides to form nitroaromatic compounds (Figure 1.2). With increasing age of the ammunition, the abundance of nitrated stabilizers increases, providing a potential

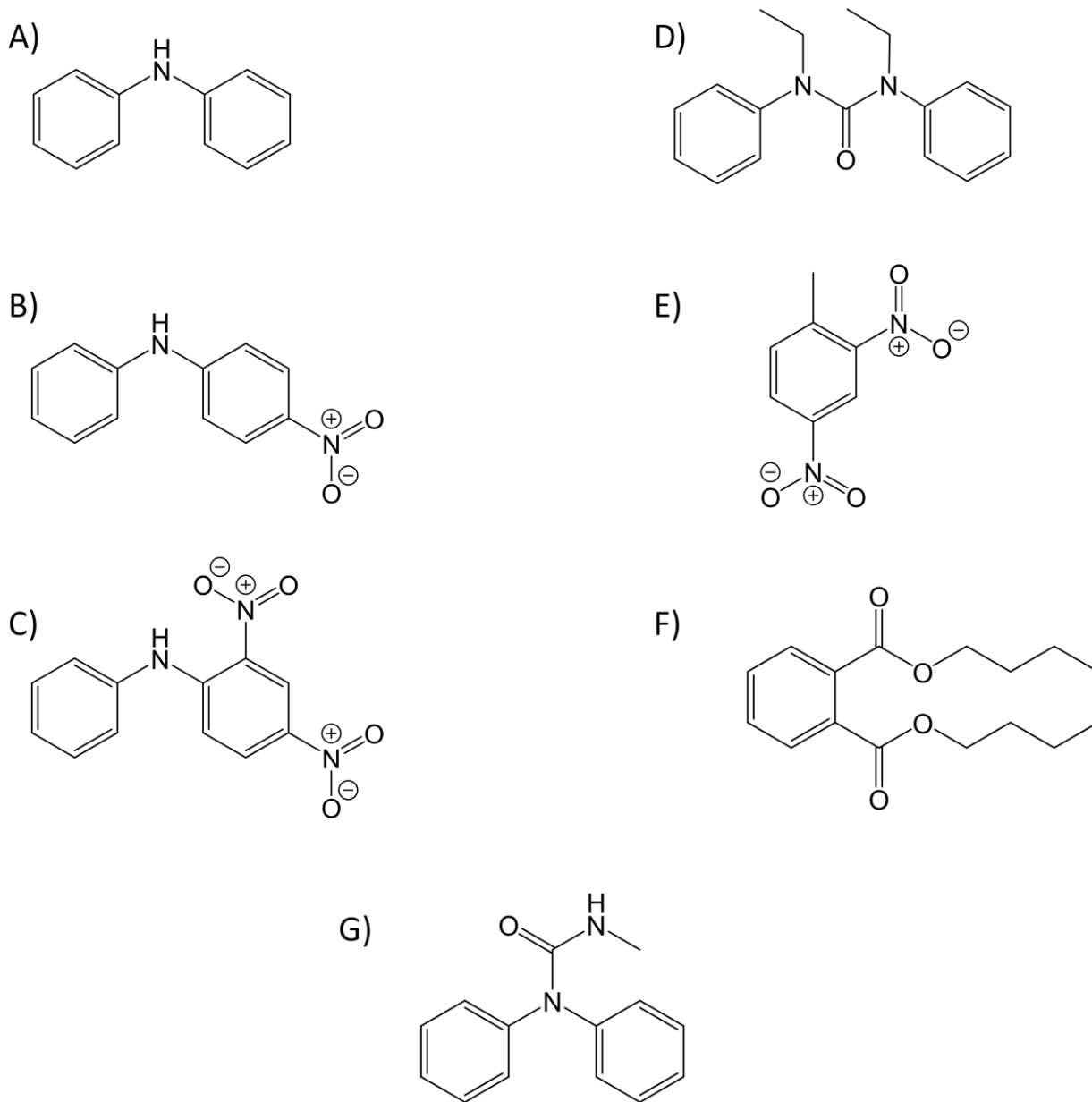


Figure 1.3 Common chemical additives present in smokeless powders (A) diphenylamine, (B) 4-nitro diphenylamine, (C) 2,4-dinitrodiphenylamine, (D) ethyl centralite, (E) 2,4-dinitrotoluene, (F) dibutyl phthalate, and (G) 1-methyl-3,3-diphenylurea (Akardite II).

indicator of age for an unknown powder. Nitration products reported in the literature include nitrated diphenylamine (2- or 4- nitroDPA), doubly nitrated diphenylamine (2,4-, 2,2- or 4,4-dinitro-DPA), N-nitroso-diphenylamine (N-nitroso-DPA), and singly nitrated ethyl centralite.

Plasticizers, such as alkylated phthalates, dinitrotoluene (DNT), and EC (Figure 1.2),

increase the flexibility of the powder to aid the manufacturing process. Plasticizers increase flexibility through incorporation into NC. The relatively small plasticizer molecules disrupt and reduce the intermolecular bonding between the larger nitrocellulose chains. Deterrents, including aromatic containing compounds such as dibutyl phthalate (DBP), DNT, EC, and MC, are applied as an external coating to control factors regarding the ignition of powders, such as flame temperature, initial burning rate, and overall ignitability. These help to increase the amount and efficiency of the burning process, leading to more control over the pressure generated during ignition.

1.4.2 Current Methods for Chemical Analysis of Unburned Smokeless Powders and GSR

Current analysis of the chemical compounds within smokeless powders or the resulting GSR have a range of objectives, including: 1) identification of an unknown material as an explosive material, 2) determination of a possible smokeless powder manufacturer, or 3) comparison of an unknown powder to a known powder. The first goal is generally determined through the presence or absence of an explosive material, particularly nitrocellulose. The other goals are determined through the detection and abundance of inorganic and/or organic compounds.

In forensic laboratories, scanning electron microscopy and energy dispersive x-ray analysis (SEM/EDS) is typically used for the definitive identification of GSR. This technique generates both morphology and elemental analysis of the GSR, focusing on the presence of the inorganic components (antimony, barium, and lead) that originate in the primer. There is an increasing body of research that demonstrates analysis of organic compounds in GSR and smokeless powders. The research documented in this thesis will focus on the organic

compounds, analyzing these compounds in unburned smokeless powders as well as the corresponding burned residues.

1.4.2.1 Extraction of Smokeless Powder Additives

The chemical analysis of smokeless powders is dependent upon the ability of separating the chemical additives from nitrocellulose within smokeless powders. Typically, the unburned powder is extracted through a liquid extraction process (6). Solvents have different chemical properties which affect the quality and quantity of compounds that can be extracted.

Solvents used in many liquid extraction processes for smokeless powders are dichloromethane (DCM), chloroform, or methanol (6-8). The polarities of these solvents affect the time necessary to extract the organic compound additives. The lower polarity of DCM will not dissolve nitrocellulose, while most nitrated aromatics, centralites, phthalates, etc. are extracted after an extended period of time, typically hours. The higher polarity of methanol allows easier penetration between the polymer linkages of nitrocellulose, providing a shorter extraction time.

Thomas *et al.* performed a study extracting smokeless powders in either methanol or DCM (8). Methanol extractions were tested at 15 minutes and 6 hours, while DCM was extracted only for 6 hours. Through abundance of chromatographic peaks, they concluded that DCM extracted a higher abundance of nitroglycerin, diphenylamine, and ethyl centralite than any of the methanol extractions at both time points. However, they acknowledged the study was performed on only two powders, therefore needing a larger sample size to make definitive conclusions. Scherperel *et al.* reported on the recovery of total organic material from seven powders extracted in methanol (7). The extraction procedure included a 10 second vortexing

step. The percentage of organic compounds extracted from the smokeless powders ranged from 12%– 53%, depending on the commercial ammunition.

These studies demonstrate the choice in extraction solvent and technique used can determine the reliability of experimental data as the quantitative recovery of additives from smokeless powders assists in identification and discrimination purposes.

1.4.2.2 Chemical Analysis of Smokeless Powder Additives

Once the chemical additives are isolated from smokeless powders, the resulting extracts must be properly analyzed. Moreover, the additives cover a wide range of compound classes, such as nitrated aromatics, amines, phthalates, and centralites. Therefore, an analytical technique should have the largest range of selectivity for differentiating different compounds, instrumental sensitivity to changes in concentration, large dynamic range, cost efficiency, and still provide quantitative results.

Several techniques have been used for initial analysis of smokeless powder extracts, such as capillary electrophoresis (CE), gas chromatography (GC), and liquid chromatography (LC). CE is typically used for the analysis of cations and anions resulting from salt additives, such as sulfates, nitrates, nitrites, and thiocyanates. GC and LC are used for the analysis of organic compounds at limits of detection in the nanogram range. However, GC employs high temperatures in the sample injection port for volatilization of compounds and high temperature programmed runs to achieve efficient separations, reaching temperatures of up to 300 °C. The high temperatures are not suitable for analysis of all thermally labile compounds. In particular, the thermal instability of nitrated, diphenylamine-based compounds (N-nitroso-DPA) has been reported in previous literature, resulting in an artificial increase in diphenylamine in the

chromatographic data. LC is preferred for the analysis of the thermally labile and low volatility compounds in smokeless powders. One or more solvents may be used as the mobile phase, but due to the large range of polarities within smokeless powders, a gradient is typically employed to achieve better resolved separations.

Various detectors for gas and liquid chromatography are used for the analysis of smokeless powders. These include ultraviolet (UV) detectors (7), thermal energy analyzer (TEA) detectors (9), electron capture detectors (ECD) (10), and mass spectrometry (MS) methods (8, 11). Of these, MS methods are superior to most detection systems due to increased sensitivity, selectivity, and a wide dynamic range. Most importantly, MS methods obtain structural information capable of providing definitive identification of compounds.

The usefulness of MS in the detection of smokeless powders has been documented in the literature. (7, 8) For example, Scherperel *et al.* (2009) optimized the detection of MC, EC, and DPA through direct flow injection with a nanoelectrospray ionization and quadrupole ion trap mass analyzers (7). Further fragmentation of individual mass spectral peaks for structural analysis was achieved through tandem mass spectrometry (MS/MS). MS/MS analysis was achieved using collision induced dissociation (CID) energies optimized for each compound. Combined with each powder's morphology and extraction efficiency in methanol, the chemical composition was able to successfully discriminate five of the seven powders as belonging to separate manufacturers. The remaining two powders were consistent with originating from the same source.

Reports in the literature also utilize mass spectrometry with the use of LC methods. For example, Thomas *et al.* (2011) detected diphenylamines, centralites, nitrotoluenes, nitroglycerin, and phthalates in smokeless powder samples in both positive and negative ion mode using ultra-

high performance LC (UPLC) combined with electrospray ionization (ESI) and atmospheric pressure chemical ionization (APCI) with tandem mass spectrometry (MS/MS) (8). Multiple reaction monitoring (MRM) was utilized to identify compounds based on pre-defined precursor and product ion pairs. The optimized method was applied to investigate lot-to-lot differences in a single brand of unburned smokeless powders. Individual lots could be differentiated, indicating that smokeless powder chemical compositions change over time.

These research studies show that abundances of organic compounds can be of use in distinguishing commercial ammunition brands. However, during the data processing, masses of fragment ions aid in constituent identification, but targeted MS/MS methods are usually limited by user-defined precursor ions which may preclude detection of novel or unanticipated compounds. A technique that does not rely on previously known compounds in smokeless powders would be ideal for novel or unanticipated compounds. A potential technique for identifying unknown compounds involves the application of multiple collision energies during the mass spectral analysis for the simultaneous generation of molecular and fragment ions for all compounds that elute during an analysis. Termed multiplex-collision induced dissociation (multiplexed-CID), this technique has been utilized previously in the analysis of plant metabolites (12, 13). This non-targeted, comprehensive approach has potential for structural determination of unknown compounds in cases where no reference standards are available to aid in the identification.

1.4.3 Current Methods in Organic Compound Identification in GSR

Most of the pre-firing smokeless powder mass is converted to gaseous products post-firing. Therefore, many compounds generated during the firing process are extremely volatile.

Detection of any of the more volatile compounds has been used in determination of the amount of time since firing (14). However, unburned material or less volatile burned material can be present in either the general vicinity of a fired weapon, such as residue remaining within the spent cartridge casing or on the skin of the shooter.

Recently, Gallidabino et al. (2015) analyzed quantities of volatile organic compounds (VOCs) from nine different types of fired cartridges using headspace-sorptive extraction (HSSE) (14). Samples were collected at various post-firing time intervals, and VOCs were identified or quantified using GC-MS. Compound classes identified included substituted aromatics, polycyclic aromatic hydrocarbons, and hetero-aromatics formed as a result of the explosion. The leftover unburned residue also provided compounds resulting from stabilizers, plasticizers, and deterrents. No correlation was observed between the quantities of unburned organic additives and VOCs. Principal component analysis (PCA) was performed on all the compounds recoverable from the fired cartridges and successful discrimination of the nine ammunition types was demonstrated. However, the limitation in this study was that the evidence must be analyzed very soon after firing as the volatile compounds were most important.

Other methods to collect organic compounds from GSR include solvent swabs or collection stubs typically used for SEM/EDS analysis. These collection methods have the advantage that they are not limited to collecting only the volatile compounds. A study by Szomborg et al. (2013) reported a systematic characterization of the background contamination present from different collection mediums for GSR collection prior to ion chromatography analysis (15). The collection technique with the minimal amount of interference involved a direct solvent extraction from the interior of the spent cartridge. However, the method was not subsequently tested on any powder samples.

Laza et al. (2009) analyzed GSR collected by a hand-swabbing method from the hands of shooters(11). Fifteen different ammunitions, spanning three calibers, were used. A HPLC-MS multiple reaction monitoring (MRM) method for the simultaneous detection of akardite II, EC, DPA, MC, N-nitroso-DPA, 2- and 4-nitroDPA was developed. EC and DPA in positive ion mode were detected as the most common stabilizers remaining in the GSR. However, a disadvantage of the technique is the necessary selection of precursor to fragment ion transitions during MRM. Compounds without these chosen transitions are not monitored, thus creating the potential to overlook novel or unexpected compounds. This disadvantage could be overcome with a technique such as multiplexed-CID, which non-selectively fragments all compounds.

1.4.4 Difficulties in Uniformity of Data Collection and Processing

Regardless of the successful literature detailing morphological measurements, extraction techniques, and chemical instrumentation used, the analysis of smokeless powders is not a uniform practice. For example, MacCrehan and Reardon (2002) conducted an inter-laboratory qualitative comparison of the analysis of smokeless powders (5). Two powders were prepared and distributed to participants. Qualitative compound identification was submitted by each lab using a variety of techniques for separation (GC, HPLC, CE) and detection (MS and cathodoluminescence). All labs identified nitroglycerin (NG) and the most abundant stabilizers, EC and DPA. However, the minor or trace compounds within each powder were inconsistently identified across labs. The differences were attributed to sample heterogeneity between kernels at trace levels and differences in chosen method sensitivities. The authors cautioned against relying only on qualitative chemical data for powder association and discrimination. Several labs reported on morphology characteristics in powder differentiation, with inter-lab measurements

being consistent.

Simultaneously studied by MacCrehan and Reardon was a quantitative analysis of chemical data provided from the previous study (16). Five laboratories provided quantitative data for NG, EC, DPA, N-nitroso-DPA, and trace compounds in mg of compound per gram of smokeless powder. Separation was achieved with either LC and CE, while detection was achieved with diode array absorbance or UV absorbance. For the major compounds, within laboratory precision was 1-5%, which was less than the between-laboratory variation of 5-10%. The quantitation of stabilizers was more reproducible than that of NG due to the inability to prepare an accurate and stable chemical standard for NG. However, trace compounds, such as 2- or 4- nitrodiphenylamine and 4-nitroEC, were not reproducibly detected in each powder between laboratories. These anomalies were attributed to sample preparation and variations in the manufacturing process. No analogous study has been found in literature since the early 2000's. Therefore, the analysis of chemical compounds within smokeless powders still requires further analysis for an objective, reproducible method.

1.5 Application of Multivariate Statistical Analysis for Chemical Components of Smokeless Powders

In 2009, the National Academy of Sciences (NAS) under the National Research Council issued a report entitled *Strengthening Forensic Science in the United States: A Path Forward* (17). The report, in part, highlighted the need to establish more objective analysis of data as well as the need for uniformity in generally accepted practices across forensic science disciplines. Therefore, analysts in separate labs would be able to come to the same conclusions regarding data from a submitted piece of evidence. For example, utilizing image-based software for

morphological measurements is preferred to hand-based measurements to reduce subjectivity. Likewise, for the analysis of chemical components, the chosen separation and detection schemes should provide the same results regardless of lab location and scientist. However, a single analytical technique is not all-encompassing to obtain the desired data, nor is it feasible to have identical equipment in every laboratory. Therefore, the report indicated that incorporating a statistical evaluation of data generated from evidence would reduce the likelihood of false positives and negatives, therefore being more suitable for testifying in court.

Multivariate statistical analyses can be used to provide an objective interpretation of data sets containing many variables and/or samples. Principal component analysis (PCA) is one such method that reduces the dimensionality of complex data to those variables that best differentiate samples in the data set. PCA has been applied to the association and discrimination of samples for ignitable liquids (18), paints (19), and glass (20). Hierarchical cluster analysis (HCA) is another multivariate statistical method complementary to PCA that assesses similarities among samples in a data set. All dimensions of the data are simultaneously assessed and plotted. The visual interpretation of the output can be utilized in comparison of samples. Both PCA and HCA have been applied to the analysis of smokeless powders (21).

Mahoney et al. utilized PCA with data from a time-of-flight secondary ion mass spectrometry (TOF-SIMS) to analyze three unburned smokeless powders and six unburned black powder samples (21). Two double-based powders, a ball and disk shape, and one single-based powder, rod shaped, were analyzed. The mass spectral data were indicative of organic compounds, such as NG, EC, and DBP, and inorganic additives, such as polydimethylsiloxane, potassium nitrates and perchlorates, and a sodium salt of dioctyl sulphosuccinate. Utilizing PCA, the smokeless powders and black powder samples were separately analyzed, where smokeless

powders showed a much higher variation between samples compared to black powders. The authors additionally used imaging techniques in SIMS to determine coating compositions. Limitations of this study included the use of only three smokeless powders compared to the multitude of commercially available samples.

Perez et al. utilized laser electrospray mass spectrometry (LEMS) for a direct and rapid detection of five smokeless powders (22). No prior sample preparation was required, and centralites, phthalates, DPA, and salt adducts of these compounds were detected. Association and discrimination of replicate mass spectra from five different powders was accomplished with PCA coupled with K-nearest neighbors and linear discriminant analysis. The advantage of this method was 100% classification across all smokeless powders in training sets to the correct manufacturers in test sets. However, a significant limitation of this study included the inability to identify a large amount of mass spectral peaks because tandem mass spectrometry was not utilized. The classification techniques utilized these compounds for differentiation, but the authors could not identify the origin of the compound.

HCA is typically utilized with PCA as a complimentary technique. A review of literature did not provide any work where mass spectral data from smokeless powders or gunshot residue were analyzed with PCA and HCA. However, Salles et al. (2012) analyzed gunshot residues with a gold microelectrode in an attempt to determine the type of handgun and ammunition used by a suspect (23). Their PCA scores plot and the HCA dendrogram indicated that ammunition discrimination was successful while discrimination based upon the gun used was less successful.

1.6 Thesis Objectives

The objectives of this thesis are:

1. To develop a multiplexed-CID method for non-mass selective, comprehensive analysis and identification of organic compounds extracted from smokeless powders, including unexpected or novel compounds. The technique will utilize high performance liquid chromatography, atmospheric pressure chemical ionization, and a time-of-flight mass analyzer. The full method is labeled HPLC-Atmospheric Pressure Chemical Ionization (APCI)-multiplexed CID-Time-of-flight (TOF)-MS.
2. To characterize unburned smokeless powders based upon morphology and organic composition determined via HPLC-APCI-multiplexed CID-TOF-MS.
3. To characterize burned smokeless powders based on organic compounds extracted directly from spent cartridges and analyzed via HPLC-APCI-multiplexed CID-TOF-MS. An investigation of the chemical changes that occur during the firing process will also be conducted.
4. To investigate differentiation of unburned and burned smokeless powders based on chemical composition using PCA and HCA.

REFERENCES

REFERENCES

1. Crime In The United States. In: Investigation FBo, editor.; 2011.
2. Hodgdon. Hodgdon Shotgun and Pistol Powders. 2015 [updated 2015; cited 2015 10/6/15]; Available from: <https://www.hodgdon.com/shotpist.html>.
3. Smokeless Powders Database [database on the Internet]. 2006 [cited 10/6/15].
4. House J, Zack P. Propellant Identification by Particle Size Measurement. *Journal of forensic sciences*. 1978;23(1):74-7.
5. MacCrehan WA, Reardon MR. A qualitative comparison of smokeless powder measurements. *Journal of forensic sciences*. 2002 Sep;47(5):996-1001.
6. Department of Forensic Science Trace Evidence Procedures Manual. In: Science VDoF, editor. Virginia; 2015.
7. Scherperel G, Reid G, Waddell Smith R. Characterization of smokeless powders using nanoelectrospray ionization mass spectrometry (nESI-MS). *Anal Bioanal Chem*. 2009 2009/08/01;394(8):2019-28.
8. Thomas JL, Lincoln D, McCord BR. Separation and detection of smokeless powder additives by ultra performance liquid chromatography with tandem mass spectrometry (UPLC/MS/MS). *Journal of forensic sciences*. 2013 May;58(3):609-15.
9. Muller D, Levy A, Vinokurov A, Ravreby M, Shelef R, Wolf E, et al. A novel method for the analysis of discharged smokeless powder residues. *Journal of forensic sciences*. 2007 Jan;52(1):75-8.
10. Harper RJ, Almirall JR, Furton KG, editors. Discrimination of smokeless powders by headspace SPME-GC-MS and SPME-GC-ECD, and the potential implications upon training canine detection of explosives; 2005.
11. Laza D, Nys B, Kinder J, Kirsch D, Mesmaeker A, Moucheron C. Development of a quantitative LC-MS/MS method for the analysis of common propellant powder stabilizers in gunshot residue *Journal of forensic sciences*. 2007;52:842-50.
12. Ekanayaka EAP, Celiz MD, Jones AD. Relative Mass Defect Filtering of Mass Spectra: A Path to Discovery of Plant Specialized Metabolites. *Plant Physiology*. 2015 02/06 10/09/received 02/05/accepted;167(4):1221-32.
13. Stagliano MC, DeKeyser JG, Omiecinski CJ, Jones AD. Bioassay-directed fractionation for discovery of bioactive neutral lipids guided by relative mass defect filtering and multiplexed collision-induced dissociation. *Rapid communications in mass spectrometry : RCM*. 2010 Dec 30;24(24):3578-84.

14. Gallidabino M, Romolo FS, Bylenga K, Weyermann C. Development of a novel headspace sorptive extraction method to study the aging of volatile compounds in spent handgun cartridges. *Analytical chemistry*. 2014 May 6;86(9):4471-8.
15. Szomborg K, Jongekrijg F, Gilchrist E, Webb T, Wood D, Barron L. Residues from low-order energetic materials. the comparative performance of a range of sampling approaches prior to analysis by ion chromatography. [Article]. 2013 12/10;233(1-3):55-62.
16. MacCrehan WA, Reardon MR, Duewer DL. A quantitative comparison of smokeless measurements. *Journal of forensic sciences*. 2002 Nov;47(6):1283-7.
17. Academies NRCotN. Strengthening Forensic Science in the United States: A Path Forward. In: Academies NRCotN, editor.; 2009.
18. Baerncopf JM, McGuffin VL, Smith RW. Association of ignitable liquid residues to neat ignitable liquids in the presence of matrix interferences using chemometric procedures. *Journal of forensic sciences*. 2011 Jan;56(1):70-81.
19. Schnegg M, Massonnet G, Gueissaz L. Motorcycle helmets: What about their coating? *Forensic Sci Int*. 2015 Jul;252:114-26.
20. Tripathi MK, Chattopadhyay PP, Ganguly S. Multivariate analysis and classification of bulk metallic glasses using principal component analysis. *Computational Materials Science*. 2015 9//;107:79-87.
21. Mahoney CM, Gillen G, Fahey AJ. Characterization of gunpowder samples using time-of-flight secondary ion mass spectrometry (TOF-SIMS). *Forensic Science International*. 2006 4/20//;158(1):39-51.
22. Perez JJ, Flanigan PM, Karki S, Levis RJ. Laser Electrospray Mass Spectrometry Minimizes Ion Suppression Facilitating Quantitative Mass Spectral Response for Multicomponent Mixtures of Proteins. *Analytical chemistry*. 2013 2013/07/16;85(14):6667-73.
23. Salles MO, Naozuka J, Bertotti M. A forensic study: Lead determination in gunshot residues. *Microchemical Journal*. 2012 3//;101:49-53.

CHAPTER TWO: Instrumental and Statistical Theory

2.1 Separations- High Performance Liquid Chromatography (HPLC)

Chromatography is a technique through which a mixture of compounds are separated through interaction with a stationary and mobile phase. The two most commonly used mobile phases are gas and liquid. The stationary phase is either a packed solid material or a liquid phase coated onto the inner walls of the column. Compounds of interest are carried with the mobile phase across the immobile stationary phase. Liquid chromatography (LC) and gas chromatography (GC) are coupled to a variety of detectors, especially mass spectrometry, to provide a higher degree of certainty in compound identification and quantitation (1). LC is commonly employed in the analysis of compounds found within smokeless powders.

A common workflow for LC is shown in Figure 2.1. A pump draws solvent from a reservoir through a sample injector loop. A sample prepared for LC analysis is injected as a small aliquot of sample prior to the start of a column. A constant flow of the mobile phase, such as a gradient of acetonitrile (ACN):water, through the injector moves the aliquot of sample onto the column. The attraction of each analyte to the mobile or stationary phase determines the amount of time spent on the column (1). Elution occurs when the separated analytes leave the column and travel to the detector. Compounds with a lower attraction for the stationary phase elute faster while those with a higher attraction for the stationary phase elute later. The time for an analyte to progress through the entire column and reach the detector is referred to as the retention time. The data output from an LC is a chromatogram, which is a plot of analyte abundance versus retention time.

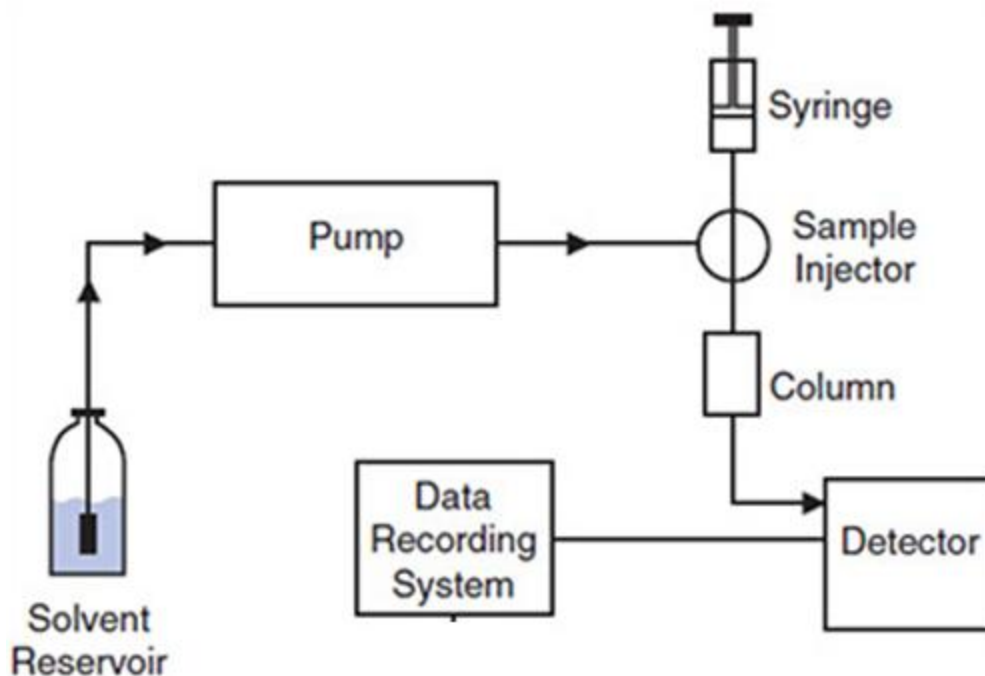


Figure 2.1 HPLC Workflow

The relative polarities of the stationary and mobile phases can be tailored to affect elution order of the analytes. Liquid chromatography can be normal phase or reverse phase. Normal-phase chromatography employs a polar stationary phase and a non-polar mobile phase. Reverse-phase chromatography employs a non-polar stationary phase and polar mobile phase. For smokeless powders, reverse-phase chromatography is more common.

A multitude of liquid mobile phases can be chosen for reverse-phase chromatography. The mobile phase employed can be a single solvent or multiple solvents. Typically, a binary mixture of organic and aqueous solutions is used. Methanol or acetonitrile are commonly used as the organic component of the mobile phase, while the aqueous phase consists of a dilute acid,

such as formic acid, or a buffer system, such as ammonium formate. The mobile phase composition can either be constant throughout the run or employ a gradient ramp at a constant rate. The constant composition requires an ample amount of time to elute all compounds. The gradient ramp gradually increases the polarity of the mobile phase, creating a solvent with a higher eluting strength. Both methods will separate the compounds, but the gradient ramp is utilized to decrease the possibility of two peaks co-eluting at the same time and decrease the overall time for elution (1).

As mentioned before, the mobile phase carries the analytes of interest through a stationary phase to achieve separation. Reverse-phase chromatography columns employ a non-polar phase where alkane chains, typically 8 or 18 carbons in length, are chemically bonded to the walls of packed silica particles with a siloxane bond. Upon introduction to the column, the analyte can transition into the stationary phase. The length of time spent within each phase depends on the relative affinity of the compound for the phases. If a compound has a greater affinity for the stationary phase, it will interact strongly with the alkane chains and spend little time in the mobile phase, causing a slow migration through the column. Conversely, if a compound has a greater affinity for the mobile phase, it will travel more quickly through the column. Two compounds of different polarities will therefore be separated through unique interactions with the stationary and the mobile phases. Utilization of a mobile phase gradient with a proper selection of stationary phase will produce an efficient separation.

The criteria for an efficient separation obtained with chromatography can be defined as the resolution between two sequentially eluting compounds in the chromatogram and the overall peak shape. Gaussian-like peak distributions for each peak and a clear separation between

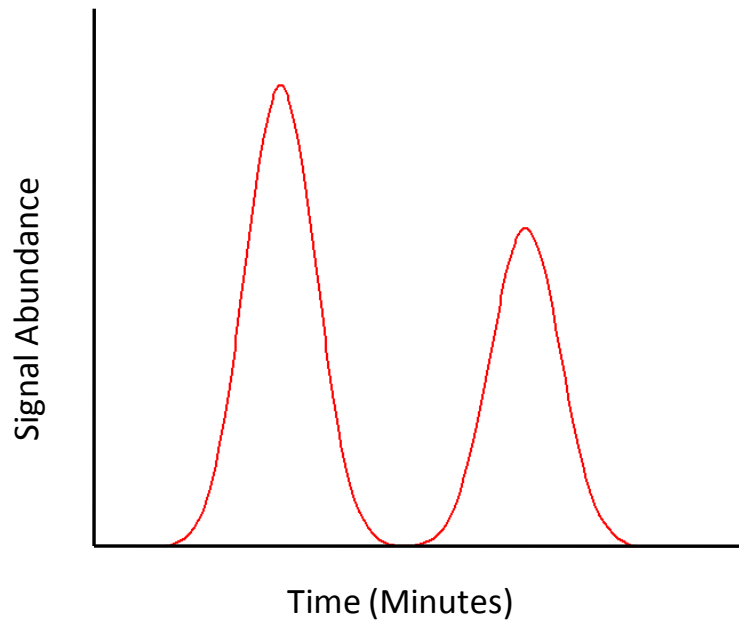


Figure 2.2 Chromatogram of well-separated, Gaussian peaks

compounds indicates efficient separation. An example of well separated peaks, with baseline resolution, is seen in Figure 2.2.

Diffusion through the packed column, peak broadening, and mass transfer rates can affect the peak shape and separation of closely eluting compounds. Diffusion through the packed column is affected by particle size. Typical HPLC columns contain silica particle sizes of 3-5 microns. Smaller particles are able to pack together more efficiently, creating fewer paths for the analyte to travel through the stationary phase. As a result, there are narrower peak widths with smaller diameter particles. Peak broadening occurs naturally as molecules migrate from regions of high concentration to low concentration. Therefore, although the sample starts off as a narrow band at the injection port of the chromatography system, it will gradually broaden due to molecular diffusion. However, peak broadening in LC is relatively little as diffusion rates in liquids are small. Additionally, higher flow rates decrease the effects of peak broadening as samples have less time to migrate. Finally, mass transfer concerns the rate at which analytes

transfer between the two phases and amount of time before equilibrium is established. A high flow rate may not allow sufficient time for equilibrium to establish between mobile and stationary phase. An analyte retained in the stationary phase will lag behind the flow of analyte in the mobile phase, leading to peak broadening. If factors affecting peak broadening are not considered, two closely eluting peaks may overlap to form one peak, thus precluding accurate identification and/or quantitation.

The final output for a chromatogram is seen in Figure 2.3, hypothetically for six compounds. The total time, typically in minutes, is displayed on the x-axis while detector signal is displayed on the y-axis. The retention time can be identified for each compound at the apex of the corresponding chromatographic peak. Peaks with earlier retention times are less attracted to the stationary phase, while those at a later retention times are more attracted to the stationary phase. Utilizing the same stationary phase composition, mobile phase composition, gradient, and detector should provide reproducible chromatographic data for a given sample.

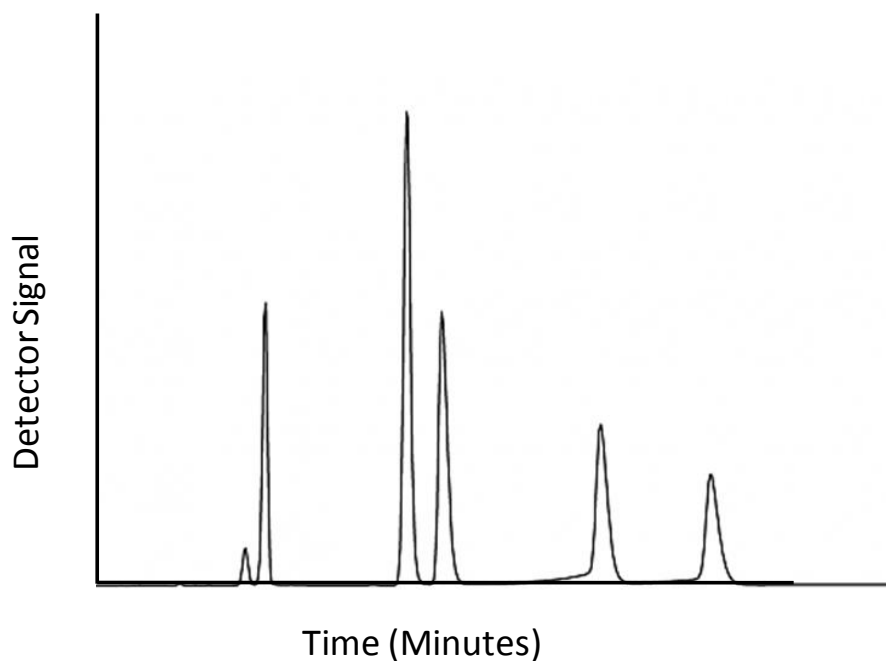


Figure 2.3 Typical chromatogram displaying chemical compounds as a function of the detector signal at a given retention time

2.2 Mass Spectrometry

Mass spectrometry (MS) is a useful technique for forensic applications due to the ability to provide definitive identification of compounds from chromatographic separations or direct infusions. The detection of analytes present within a complex mixture can be accomplished with speed, sensitivity, and specificity (2). Mass spectrometry serves as a detector for the analytes separated via liquid chromatography. Eluted compounds travel via a capillary tube connected from the end of the chromatography column to the ionization source. Molecules are converted into ions in the ionization source, separated according to the ion's mass-to-charge (m/z) ratio within a mass analyzer, detected, and converted into a mass spectrum via a data processing system (2) (Figure 2.4).

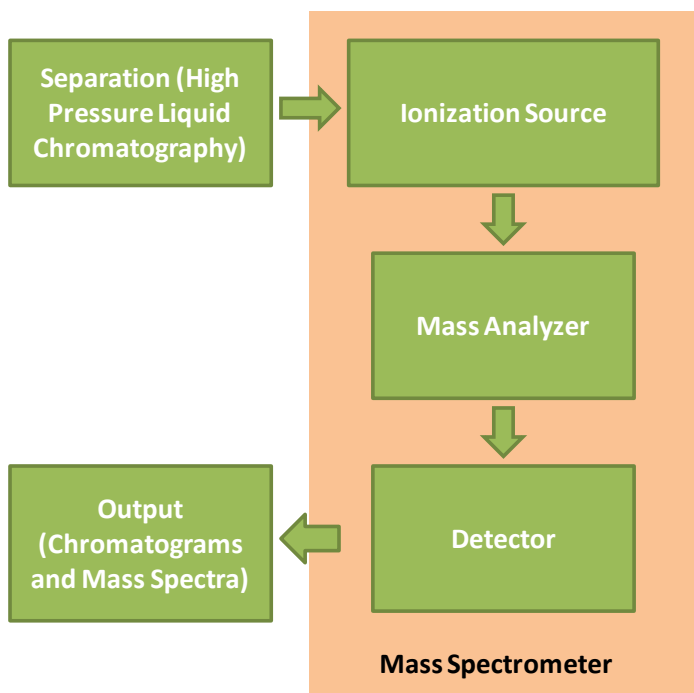


Figure 2.4 Flowchart of the components comprising a mass spectrometer

2.2.1 Ionization: Atmospheric Pressure Chemical Ionization

The ionization source is the component of the mass spectrometer where molecules are converted into ions. Ionization can be performed via a “hard” or “soft” technique. The “hard” ionization source leaves the molecules as highly energized molecular ions, which easily fragment into smaller ions that are characteristic of functional groups within the molecule (2). However, the molecular ion is of low abundance or not observed in the mass spectrum depending on the lability of the compound. While this technique is useful for identification, the fragment ions of similar compounds may produce the same fragments, thus impeding absolute identification. Conversely, the “soft” ionization techniques impart less energy to the molecule, leaving mostly unfragmented molecular ions which are extremely useful for compound identification. A commonly used “soft” ionization technique is atmospheric pressure chemical ionization (APCI), which can be used with LC.

Eluted compounds from the LC column enter the ionization source via a small diameter capillary tube connected to the outlet of the chromatography column (Figure 2.5). A nebulizing gas (e.g., nitrogen) pushes the incoming eluent through the source. Analyte and solvent molecules are nebulized in a heated region, where the solvent is evaporated and all molecules enter the gas phase.

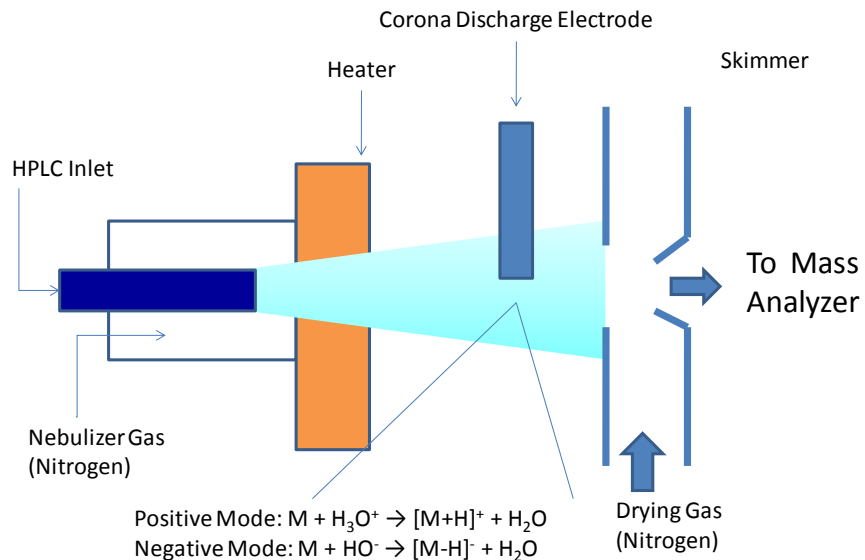
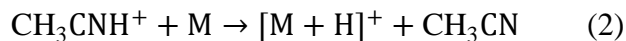
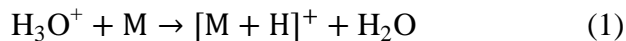


Figure 2.5 Schematics for an atmospheric pressure chemical ionization (APCI) source.

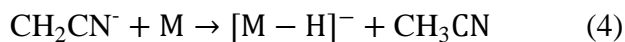
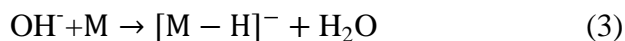
The gas flow passes through a corona discharge field, created and maintained by a strong electrical potential applied to the end of a needle. The gasses N_2 , O_2 , NO , H_2O (g), and reagent gas, all present in the ionization source, are ionized. A series of reactions between the ions and analyte molecules simultaneously produce both positive and negative ions of each analyte. However, the positive and negative ions are separately analyzed.

To analyze the positive ions of the analyte, the gas molecules of the analyte require a higher proton affinity than those of the reagent gas ions. Analyte molecules with relatively higher affinities for protons will remove free hydrogens from adjacent gas molecules. For example, the following equations show the protonation of the analyte molecule (M) with protonated water or acetonitrile, a commonly used organic solvent for HPLC:



In positive ion mode, the inlet to the mass spectrometer is negatively charged, attracting the positively charged ions that are produced.

Conversely, for negative ion mode, the gas molecules of the analyte should have a lower proton affinity than those of the reagent gas ions. Therefore, hydrogen will be removed from the analyte molecule. A positively charged mass spectrometer inlet draws in generated ions with a proton removed. Analogous to the examples for positive ion mode, the following equations show the removal of a proton from the analyte molecule using water or acetonitrile:



As discussed previously, APCI provides an extremely useful purpose in providing molecular ions, either protonated in positive mode or deprotonated in negative mode. However, simultaneous detection of the molecular and fragment ions improves the accuracy of analyte identification. The use of multiplexed collision induced dissociation (multiplexed-CID) (see section 2.2.2 for further discussion) allows the ability to fragment the molecular ions created through APCI to obtain both types of ions for enhanced identification purposes.

2.2.2 Mass Analyzer: Time of Flight

The goal of a mass analyzer is to separate individual ions generated in the ion source based upon their intrinsic mass-to-charge (m/z) ratio. A time of flight (TOF) mass analyzer measures the amount of time an ion requires to travel a known distance after the ion is imparted with kinetic energy via acceleration in an electrostatic field. A diagram of a commercial TOF

analyzer is shown in Figure 2.6. Ions leaving the ionization source are focused into a small beam of ions with sub-mm length in ion guides. A packet of ions are imparted with a uniform kinetic energy by the pusher and directed into a magnetic field-free region, seen in the diagram in blue. The speed at which they travel the pre-determined path (V shape) to the detector can be directly related to their m/z ratio.

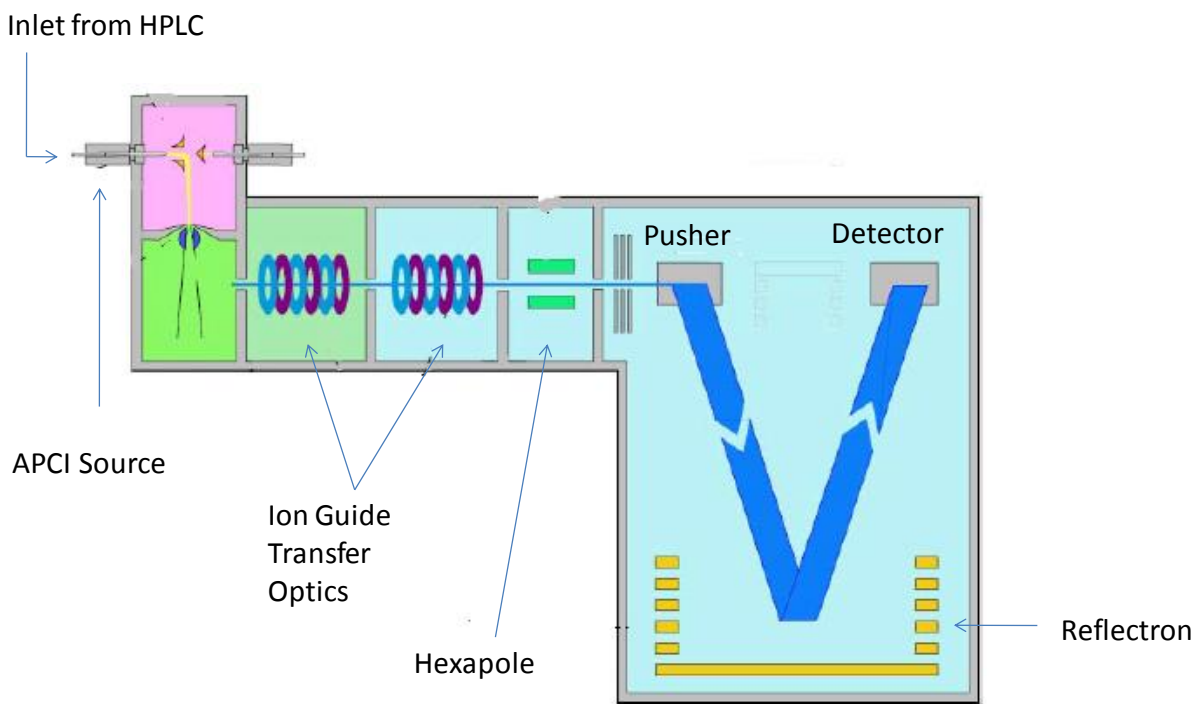


Figure 2.6 Schematic for a Waters LCT Premier Time-of-Flight Mass Spectrometer operating in V-mode (www.waters.com)

The distance travelled through the field-free region in a known amount of time can be related to m/z via the following equations (Lemière, 2001):

$$\frac{mv^2}{2} = qV \quad (1)$$

$$q = ze \quad (2)$$

$$t = \frac{d}{v} \quad (3)$$

$$\frac{m\left(\frac{d}{t}\right)^2}{2} = (ze)V \quad (4)$$

$$\frac{m}{z} = t^2 \left(\frac{2Ve}{d^2}\right) \quad (5)$$

where m is the mass, v is the velocity of the ion, q is the charge on the ion, V is the applied acceleration voltage, z is the charge on the ion, e is the charge on an electron, d is the distance travelled by the ion, and t is the flight time the ion takes to travel distance d . Fixed parameters include an electron charge (e) and the distance travelled (d), as the precise dimensions of the mass analyzer are carefully crafted by the manufacturer. Therefore, at a given setting of the applied acceleration voltage (V), measurement of the flight time, t , yields an experimentally measured m/z value.

The accuracy of the determined m/z value can be influenced by differences in the distribution of kinetic energy to each ion. Ions are decelerated and subsequently accelerated to impart a uniform kinetic energy. Minute differences in the spatial distribution of ions can affect the kinetic energy imparted. Acceleration energy is applied at the pusher. Ideally, the ions of a single molecule travel as a packet from pusher to detector, all having the same rate and flight time and thus m/z value. However, slight differences in the kinetic energy are imparted at the

pusher. Ions located closer to the pusher can have slightly more kinetic energy versus ions further from the pusher. If the pulsed ion packet has a wide variation of ion position, the measured time for migration across the flight tube will vary considerably. This will inflate the variation in measured m/z value. Modern TOF instrumentation attempts to lessen this spread via the use of a reflectron in the flight tube, as demonstrated in Figure C. This is a small area within the TOF where an electric field is induced to curve the flight path of the ions. Ions with more kinetic energy can travel slightly further into the curve of the reflectron and have a longer flight path, while ions with the same m/z but slightly less energy have a shorter path. The ion detector (see section 2.2.3 for further discussion) is positioned at a spot where the ions with slightly different energies will intersect on their flight paths.

Another commonly used technique to reduce flight time differences at the accelerator is to place the flight tube at a ninety-degree angle to the ion path from the source, known as an orthogonal TOF setup. A series of carefully timed changes in electric fields at the pusher direct ions perpendicularly into the field-free region of the TOF analyzer. The orthogonal orientation minimizes differences in the path length of ions, thereby reducing the differences in position of ions before introduction into the pusher.

One of the benchmarks by which mass analyzers are compared is the measure of resolution, or the ability to distinguish between ions of similar m/z ratios. The resolution is measure between two adjacent peaks in a spectrum, as seen in Figure 2.7

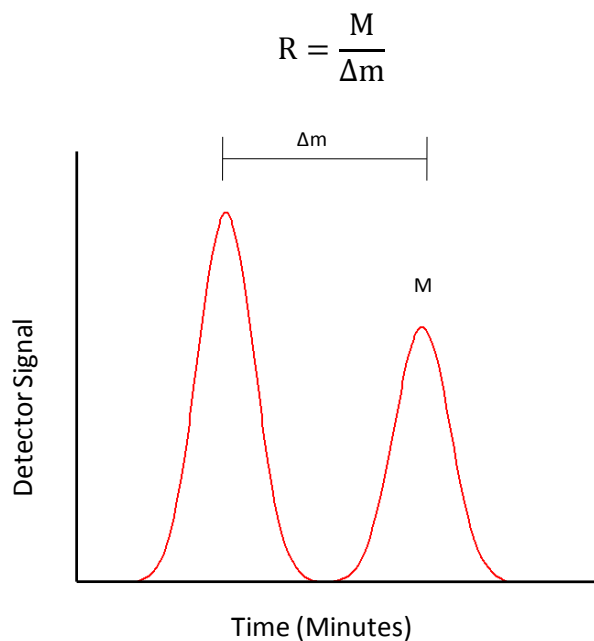


Figure 2.7 Chromatogram detailing the calculation of resolution for chromatography peaks

Higher resolution indicates better separation between two peaks. Low resolution mass analyzers, such as quadrupole mass analyzers, can only distinguish ions differing by 1 mass unit and have resolution values on the order of 1×10^2 . High resolution mass analyzers, such as TOFs, can distinguish ions with less than one mass unit difference, where resolution values are on the order of $1 \times 10^3 - 1 \times 10^5$ depending on instrumentation.

2.2.2.1 Multiplexed collision induced dissociation

The information obtained from both molecular and fragment ions is invaluable to compound identification. Traditionally, mass analyzers can be combined in order to isolate and separately fragment a molecular ion of interest in a process known as tandem mass spectrometry, commonly denoted MS/MS. Examples of these mass analyzers include a combination quadrupole-TOF, a triple quadrupole, or quadrupole ion trap-Orbitrap mass analyzers. However,

these analyzers typically rely on user-defined selection of the isolated molecular ion. Utilizing the time-of-flight mass analyzer, multiplexed collision induced dissociation (multiplexed-CID) is a non-targeted, non-selective technique utilized for simultaneously collecting mass spectral information on molecular and fragment ions generated using a soft ionization technique (3, 4).

Increasing collision voltages, applied in stepwise increments of user-selected parameters, are selected as “acquisition functions”. The voltages are applied to accelerate the ions at the point indicated in Figure 2.8. The intact, molecular ions are collided with nitrogen gas to achieve fragmentation. Successively higher functions impart ions with increasing amounts of excess energy, thus leading to a greater extent of fragmentation within the mass spectrometer (Figure 2.8).

A series of multiplexed-CID conditions allow rapid analysis of all acquisition functions and a parallel, but separate, mass spectrum for each function. Each acquisition is collected

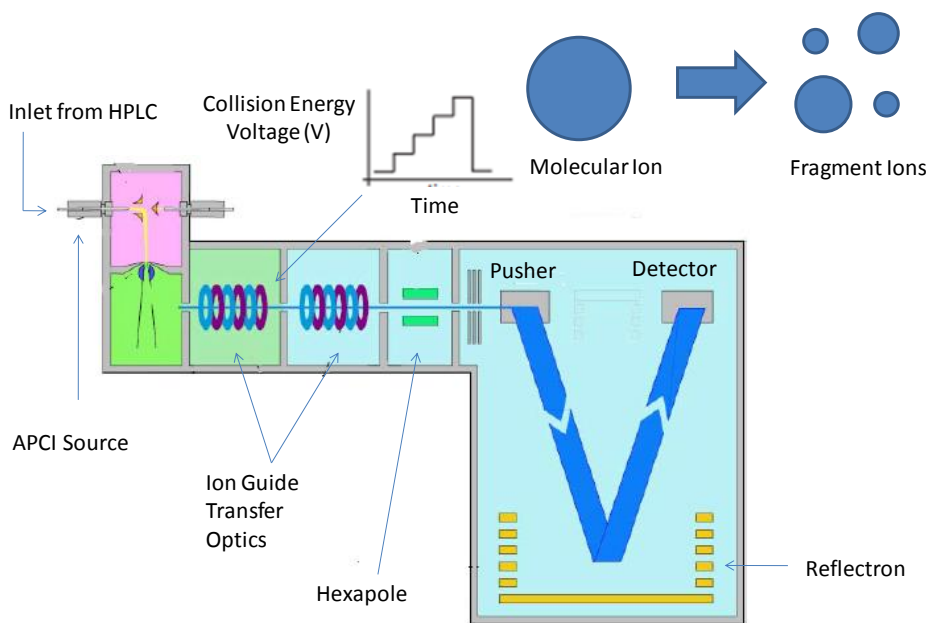


Figure 2.8 Workflow for increasing voltages during multiplex-CID fragmentation

rapidly, around 0.1 seconds per function. Therefore, data on both the molecular and fragment ions of a particular chromatographic peak can be acquired almost simultaneously, thus leading to more definitive compound identification. The technique was developed and used previously for the quantitative and qualitative assessment of specialized plant metabolites, bioactive compounds, etc (3), and has a wide potential for utilization as a pseudo-MS/MS method.

2.2.3 Detectors- Microchannel Plate Detector

Once separated in the mass analyzer, the ions travel towards a detector. The detector converts the flow of ions into a more easily read signal, such as an electrical current. A common detector is the microchannel plate detector (MCP) (Figure 2.9).

The MCP plate contains several hundred to several million separate channels, each of which acts as an individual electron multiplier. A single ion that travels through the mass analyzer encounters a converter which emits electrons when struck with an ion. An electrical field is applied across both faces of the MCP, which draws the electrons into a channel within the MCP. When the electron strikes the surface of the channel, secondary electrons are emitted.

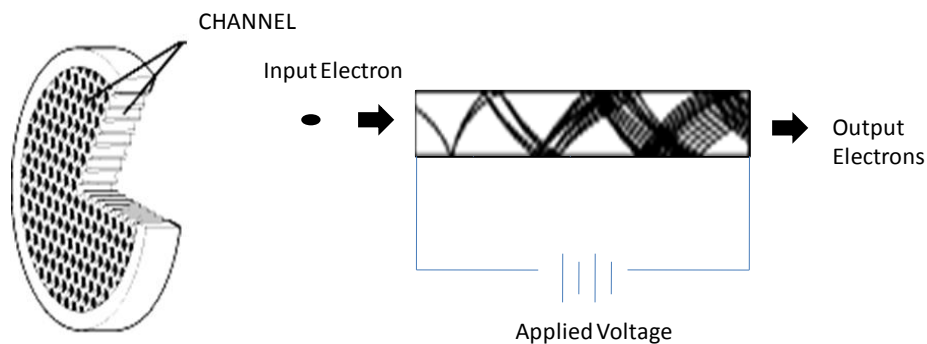


Figure 2.9 A microchannel plate detector cross-section, with individual schematic representative of an individual channel.

Electrons are drawn further through the MCP via the applied electrical field. Multiple collisions of electrons with the surface of the channel cause a large emission of electrons to result from the collision of one original ion, called a cascade effect. The original signal can be amplified 1×10^6 or more. The electrons are recorded as an electrical signal that corresponds to the abundance of a singular m/z value under a known set of instrumental conditions.

2.3 Data Output and Pre-Treatment

Data generated from LC-MS consists of a total ion chromatogram (TIC) with a mass spectrum for each time point. The TIC is generated from the summation of mass spectral peak abundances within each mass spectrum. Therefore, every chromatographic peak in the TIC corresponds to a separated compound. With multiplex-CID, each chromatogram also contains mass spectra obtained at higher collision energies.

The retention time and mass spectral peaks from molecular and/or fragment ions can be used in combination for definitive identification of compounds. This can be done through comparison of the retention time and mass spectrum with suitable reference standards analyzed on the same instrument under the same conditions. In the absence of such a reference standard, identification can be achieved through comparison of the compound's mass spectrum with mass spectra available in literature sources. However, in these instances, retention time cannot be compared as retention times vary depending on the stationary phase, mobile phase composition and gradient, and other instrument conditions.

The complexity of chromatographic and associated mass spectral data leads to the generation of multiple mass spectral peaks at each retention time, generating hundreds of variables. Even after compound identification through molecular and fragment ion comparisons,

comparison of multiple samples is difficult and time-consuming. Therefore, multivariate statistical procedures can be utilized for identification of similarities and differences among samples in a data set. Pretreatment procedures on the chromatographic data can be applied before data analysis in order to minimize variation due to the instrumentation that is not due to chemical differences in sample.

Compounds introduced during the analysis process that are not due to the samples are eliminated through background subtraction. This background noise can come from a number of sources, such as contaminants in the mobile phase, buffers (ammonium formate), or instrumentation noise. Therefore, a common practice is to run a solvent blank analyzed in the same manner as a sample. The chromatogram of the solvent blank is subtracted from the chromatogram of a sample. Therefore, peaks originating from the mobile phase, buffer, or instrumentation are reduced.

Retention-time alignment can be applied to the TIC to minimize shifts in instrumental conditions over time that affect elution of analytes within a sample. For example, the internal components of an HPLC system, such as pumps and solvent reservoirs, that are constantly in use may not consistently provide the same output for every sample run. Therefore, even with the same HPLC parameters, the same compounds may leave the chromatography system at different retention times between sample runs. If the same retention times are utilized across all chromatograms, accurate identification may not be possible. Many different alignment algorithms are available for correcting drifts in retention time. The specific alignment used for this study is detailed in the methods (Section 3.5).

Normalization is applied after retention-time alignment. Normalization of each peak area to total area of the chromatogram accounts for differences in volume of sample injected, source

conditions, or mass analyzer conditions. As long as the relative ratios of compounds are similar, normalization corrects for minute differences, leading to greater consistency in sample replicates.

2.4 Multivariate Statistical Analysis

2.4.1 Principal Component Analysis

Principal component analysis (PCA) is an exploratory statistical procedure that determines patterns in the variables within a data set. Visualization of the pattern facilitates association and discrimination of samples. Patterns are determined through the presence and abundance of individual compounds. The complexity of the data set can be simplified through transformation of the variables that explain the highest amount of diversity. For LC-MS, the variables are the mass spectral peaks at a given retention time in the chromatograms, which represent chemical compounds within the sample of interest, i.e. nitroaromatics, phthalates, toluenes, and other additives within smokeless powders.

Each compound in a complex mixture represents a distinct dimension, or variable, of the data set. PCA compares different dimensions to determine which compounds have the greatest contribution to the overall variance of the data set. PCA determines orthogonal, linear combinations of variables from a covariance matrix. New variables are determined which incorporate the greatest variance. The original multivariate data are projected into the resulting lower dimensional plots for visual association and discrimination.

An illustration to simplify the explanation of PCA processing is shown in Figure 2.10. Figure 2.10, Panel A shows an hypothetical data set plotted according to the abundance of hypothetical variable Y versus hypothetical variable X. A point labeled as Sample A would have an abundance of variable Y and variable X, giving the coordinates X_A and Y_A . Figure 2.10, Panel

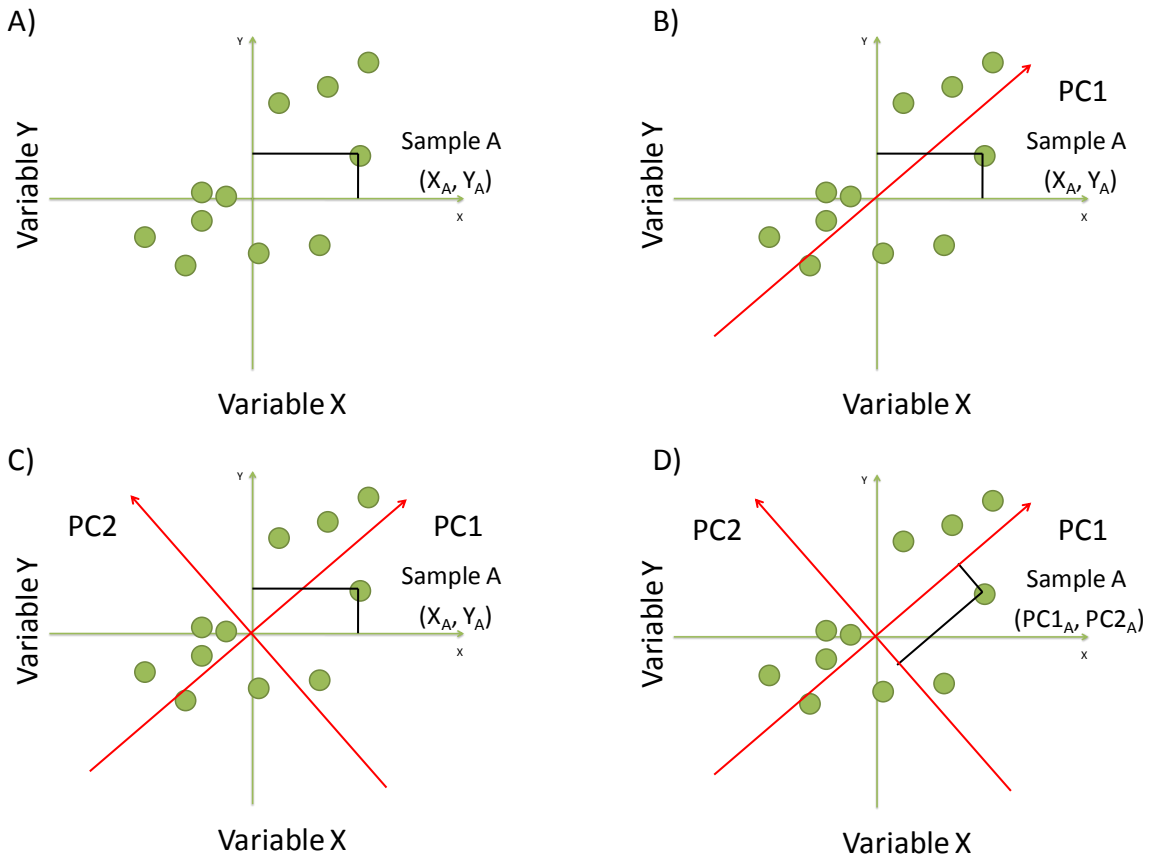


Figure 2.10 Representation of data plotted on a Y vs X axis with processing for PCA analysis

B shows the plot of Principal Component 1 (PC1). PC1 explains more of the variance in the data set compared to variable Y or variable X. Figure 2.10, Panel C shows the plot of PC2, the placement of which is constrained by being orthogonal to PC1 while explaining the second highest spread of data. Figure 2.10, Panel D shows Sample A with new coordinates relative to the axes of PC1 and PC 2. While only two variables were compared for simplicity of illustration, this process is repeated pair-wise between all principal components that can be defined for the system.

The number of PCs possible is the same as the number of total samples or variables, whichever number is smaller. Typically, the first few PCs (i.e. PC 1, PC 2, PC 3, etc) describe the majority of variance within the dataset. Visualization of PC 1 vs PC 2 on a two-dimensional XY scatterplot or PCs 1, 2, and 3 on a three-dimensional plot will adequately explain general trends among samples. This is extremely useful for data analysis and comprehension, as the data set does not have to be abstractly interpreted with thousands of dimensions, depending on the number of variables.

PCA generates two general plots: scores plots and loadings plots. Scores plots are scatterplots of different PCs (such as PC1 vs. PC2), where typically the highest amount of variance within the data set can be visualized. Samples that are chemically similar are positioned close to each other in the scores plot and separately from compounds with dissimilar chemical compositions. Loadings plots indicate the contributions of each chemical to the scores plot and can be used to explain the placement of samples within the scores plot. Samples further from the origin of the scores plot are composed mainly of variables that have greater contribution to the overall variance.

2.4.2 Hierarchical Cluster Analysis

Hierarchical cluster analysis (HCA) is a second exploratory multivariate statistical procedure that measure similarity among samples in a data set. Agglomerative clustering is utilized in this research, where samples are iteratively merged with the next closest group. The final product is a single cluster containing all samples.

The process for HCA is illustrated in Figure 2.11. The axis X and Y indicate two variables, in this case chemical compounds. The complete data set for HCA analysis can have

hundreds of variables, so there are many more axes than X and Y. However, multidimensional space cannot be represented. On the comparison of axis X and Y, four samples have been identified (A-D). Each sample begins as an individual cluster. In order to join samples into one cluster, a distance must be calculated in multidimensional space. The most common distance metric in HCA is Euclidean distance, shown in the following equation using the variables in Figure 2.11.

$$d = \sqrt{(X_A - X_B)^2 + (Y_A - Y_B)^2}$$

The two samples with the shortest distance are initially joined together in a cluster, indicating the greatest similarity, in this case samples A and B. Next, Euclidean distances are again calculated for the samples, but there must be a method to measure the distance the combined group AB versus C or D.

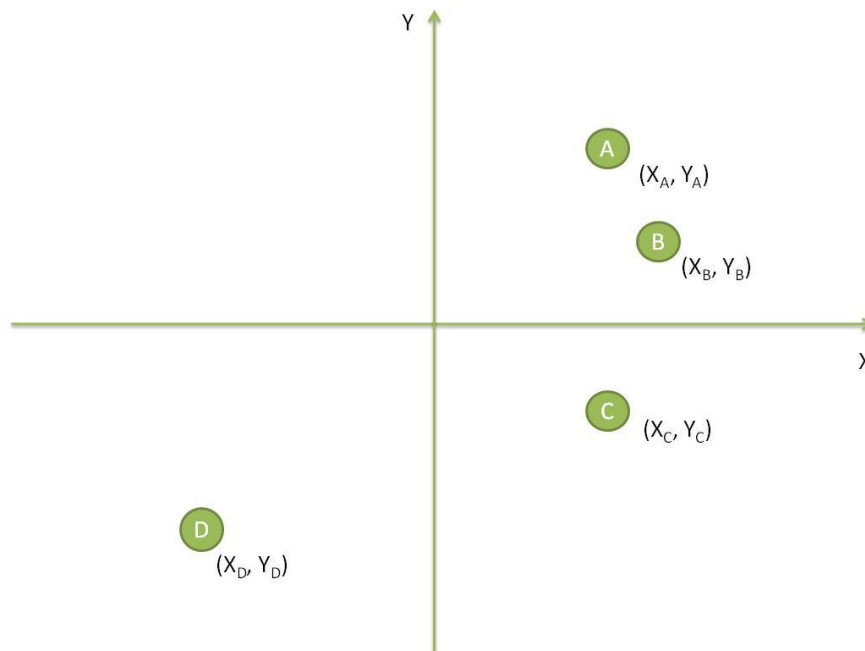


Figure 2.11 An illustration of samples to be clustered (A, B, C, and D) with coordinates on an Y vs. X plot.

The linkage method calculates the distance when already clustered samples are compared to a single sample or other clustered samples. Single linkage joins clusters that contain the smallest Euclidean distance between the closest pair of samples, one from each cluster. For example in Figure 2.12, B and C have the shortest calculated distance (green dashed line). Sample C would be linked to AB. Complete linkage measures the distance between the furthest pairs, and joins clusters separated by the shortest total distance between pairs. In Figure 2.12, A and C have the shortest overall distance (blue dashed line) compared to sample D. Average-linkage attempts to join clusters separated by the shortest total distance between the average of each cluster (Figure 2.12, red dashed line). AB would still be linked to sample C. This example was a simplified version of HCA, but generalizes the concept when applied to hundreds of variables.

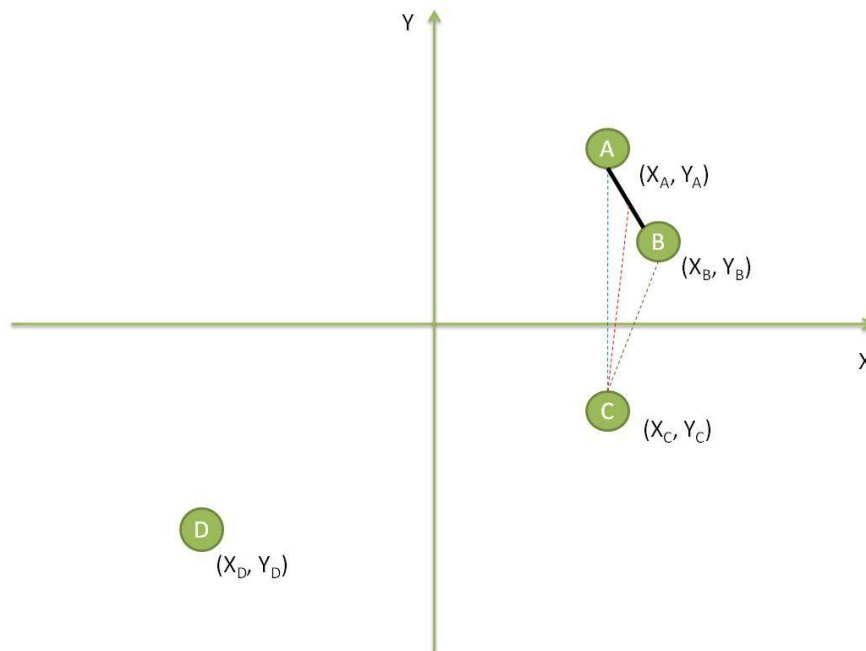


Figure 2.12 An illustration of samples clustered using HCA. Samples A and B were initially clustered (black line) with Euclidean distance. The dashed lines indicate the possible linkage methods: single (green), average (red), and complete (blue).

The clusters generated by HCA analysis can be represented through a dendrogram. Similarity levels provide a numerical indicator of the similarity between clusters. Similarity levels are calculated with the following equation:

$$\text{Similarity Level} = 1 - \frac{\text{Individual Euclidean Distance}}{\text{Maximum Euclidean Distance}}$$

Similarity levels are reported on the range of 0.0 to 1.0. The greater the similarity between samples, the higher the similarity level. An example of the dendrogram provided by the above example is illustrated in Figure 2.13. HCA observes patterns of similarity within the data, while PCA observes differences within the data set. Therefore, the techniques are complimentary, with both having advantages and disadvantages that can be overcome through analysis of both results.

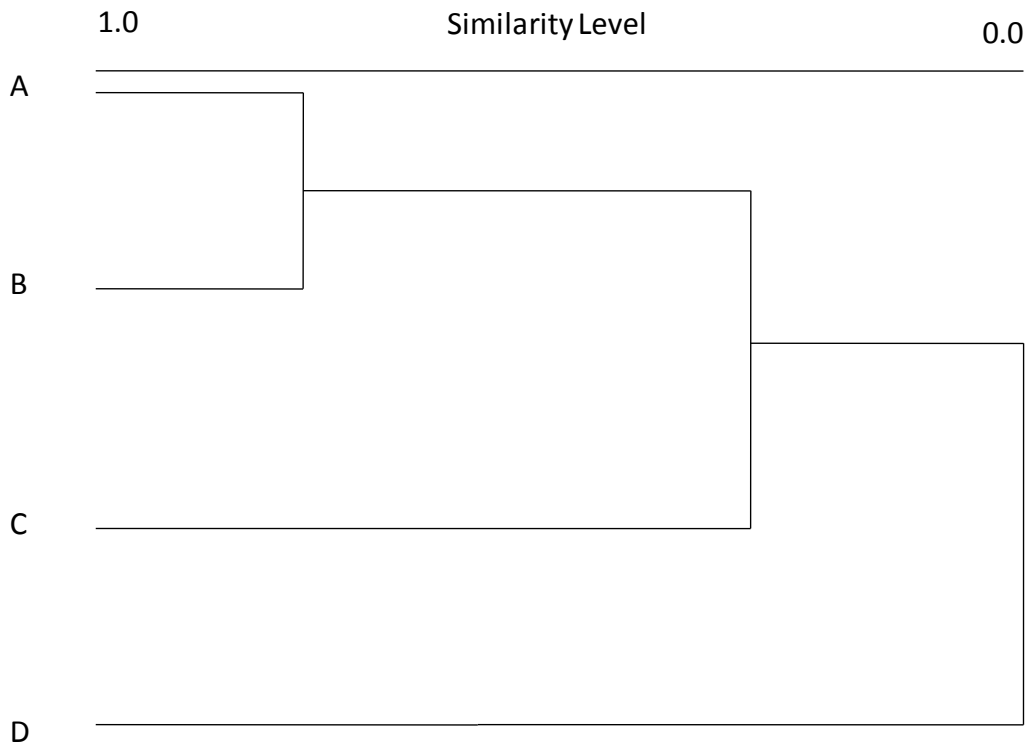


Figure 2.13 Example dendrogram output of HCA utilizing the example data.

REFERENCES

REFERENCES

1. Skoog D, Holler F, Crouch S. Principles of Instrumental Analysis. 6th ed, 2007.
2. Watson JT, Sparkman OD. Liquid Chromatography/Mass Spectrometry. Introduction to Mass Spectrometry: John Wiley & Sons, Ltd; 2008;639-88.
3. Stagliano MC, DeKeyser JG, Omiecinski CJ, Jones AD. Bioassay-directed fractionation for discovery of bioactive neutral lipids guided by relative mass defect filtering and multiplexed collision-induced dissociation. Rapid communications in mass spectrometry : RCM. 2010 Dec 30;24(24):3578-84.
4. Ekanayaka EAP, Celiz MD, Jones AD. Relative Mass Defect Filtering of Mass Spectra: A Path to Discovery of Plant Specialized Metabolites. Plant Physiology. 2015 02/0610/09/received 02/05/accepted;167(4):1221-32.

CHAPTER THREE: Materials and Methods

3.1 Materials

3.1.1 Acquisition of Commercial Ammunition

Ammunitions of different calibers were obtained from a variety of commercial manufacturers. The cartridge manufacturer, caliber, primer type, source of acquisition, approximate age, and additional information are detailed in Table 3.1. For simplification of nomenclature during this study, each commercial ammunition was designated by an abbreviated acronym. The assignments for each ammunition brand are referenced in Table 3.1.

Some of the ammunitions were purchased specifically for this project (denoted ‘new’) from Cabela's (5/31/14, Dundee, MI), while others were obtained from a collaborator (denoted ‘aged’). Of the aged ammunitions, samples were either obtained from the original packaging or a collection of "loose" ammunition that were not contained in a storage box. Five cartridges were chosen from each ammunition box to assess any apparent changes in the morphological and/or chemical profiles among different cartridges. For the aged samples, the five cartridges of a particular brand within the original packaging were assumed to have been produced at the same time. However, for the “loose” ammunition, the five cartridges were not assumed to have been produced at the same time.

Table 3.1 List of commercial cartridges from which smokeless powders were obtained

Cartridge Manufacturer	Caliber	Primer	Grains	Jacket	Approx. Age	Obtained From	Abbrev.
Winchester	9mm	Lead	115	FMJ	New	Cabela's	Win9Pb
Remington	9mm	Lead	115	MC	New	Cabela's	Rem9Pb
Federal	9mm	Lead	115	FMJ	New	Cabela's	Fed9Pb
Hornady	9mm	Lead	115	FTX	New	Cabela's	Horn9Pb
PMC	9mm	Lead	115	JHP	New	Cabela's	PMC9Pb
Winchester	9mm	No Lead	147	BEB	New	Hogg**	Win9NoPb
Remington	9mm	No Lead	147	NEB	New	Hogg**	Rem9NoPb
Blazer	9mm	No Lead	124	TMJ	New	Hogg**	Bzr9NoPb
Magtech	9mm	No Lead	115	FEB	New	Hogg**	Mag9NoPb
Sellier and Bellot (SB)	9mm	No Lead	115	FMJ	New	Hogg**	SB9NoPb
Winchester	12-Gauge	Lead	n/a	n/a	New	Cabela's	Win12N
PMC	0.44	Lead	180	JHP	New	Cabela's	PMC44N
Sellier and Bellot (SB)	7.62x39 mm	Lead	123	FMJ	New	Cabela's	SB762N
Winchester	12-Gauge	Lead	n/a	n/a	At least 15 y.o.	U.S.* Loose	Win12A
PMC	0.44	Lead	n/a	n/a	At least 15 y.o.	U.S.* Box	PMC44A
PMC	9mm	Lead	n/a	n/a	At least 15 y.o.	U.S.* Loose	PMC9A
Magtech	7.62x39 mm	Lead	n/a	n/a	At least 15 y.o.	U.S.* Box	Mag762A
CCI	0.22 LR	Lead	n/a	n/a	At least 15 y.o.	U.S.* Loose	CCI22A

*U.S. indicates "Unknown Source", provided by Dr. Brian Hunter. "Box" specifies all replicates originate from the same source, "Loose" specifies replicates possibly from different sources

** Ammunition was obtained from the work of a previous graduate student (Seth Hogg, 2013)

3.1.2 Chemical Solvents and Standards

Methanol (CHROMASOLV grade), acetone (CHROMASOLV grade), ethyl centralite ((1,3-diethyl-1,3-diphenyl-urea, 99%), methyl centralite (1,3-dimethyl-1,3-diphenyl-urea, 99%), dibutyl phthalate, 4-nitrotoluene, 2,4-dinitrotoluene, 2,4-dinitrodiphenylamine, and N-(3,5-dinitro-2-pyridinyl)-phenylalanine were purchased from Sigma Aldrich (St. Louis, MO, USA). Acetonitrile (HPLC grade) and the Milli-Q Ultra Pure Water Filtration System were purchased from Millipore (Billerica, MA, USA). Dichloromethane (HPLC grade) was purchased from J.T. Baker (Avantor Performance Materials, Center Valley, PA, USA). Ethanol (190 Proof) was purchased from Koptec (King of Prussia, PA, USA). Diphenylamine (sulfate salt) was purchased from Eastman Organic Chemicals (Rochester, NY, USA). Diethyl phthalate and dibutyl phthalate were purchased from Alfa Aesar (Heysham, LA, USA). 4-aminodiphenylamine was purchased from Acros Organics (Geel, Belgium).

3.2 Isolation of Unburned Smokeless Powder from Commercial Ammunition

For each ammunition type, except all 12-gauge samples, the smokeless powder was removed from five individual cartridges using an inertia-based bullet puller (Lyman Magnum Inertia Bullet Puller, Lyman Products Corp. Middletown, CT). Powder from each cartridge was separately collected within 20 mL glass scintillation vials and appropriately labeled. Between different brands and/or calibers, excess powder within the bullet puller was removed with three washes of an ethanol/water mixture (1:1 v/v). Preliminary testing indicated three washes were sufficient to remove all residue. The smokeless powder was removed from all 12-gauge samples by disassembling the plastic casing, transferring powder into 20 mL glass scintillation vials, and appropriately labeling.

3.3 Analysis of Physical and Chemical Attributes of Unburned Smokeless Powders

3.3.1 Morphology

Consistent with the methodology provided by Technical Working Group for Fire and Explosions (TWGFEX), 50 kernels from each unburned powder were analyzed for a representative sampling (1). All powders were compared on the basis of physical characteristics, such as shape, color, texture, and approximate size. Initial processing was performed with hand-drawn measurements in the free software Image J (version 1.49v, National Institutes of Health, Bethesda, MD, USA, <http://imagej.nih.gov/ij>). These measurements were subjective to visual determination of where the kernel edges were located, which introduced measurement error. For a more objective measurement, the individual powder kernels were separated and digitally processed. To facilitate measurements of the width of each kernel, samples were affixed to glass microscope slides (VMR Micro Slides, inch x 3 inch x 1.2 mm, Radnor, PA, USA) with double-sided tape.

Pictures of the unburned powders were taken at 10x magnification with a stereomicroscope (Nikon SMZ800, Nikon Corporation, Melville, NY, USA) connected to a digital camera (Nikon DCM1200F). Illumination was accomplished with an overhead light source (Schott Fostec light ACE I, Schott North America, Inc., Southbridge, MA) to enhance color, texture, shape, etc. Background lighting (Type 7200 Stir Light, Thermolyne Co., Dubuque, IA) provides objective physical measurements of total length and diameter. Images were recorded with the processing software (Automatic Camera Tamer 1 (ACT-1), version 2.62, Nikon Corporation). All image processing was performed using Image J. A universal measurement scale was utilized through repeated measurements of a 2 mm scale under the same

stereomicroscope conditions as smokeless powder samples, calculating total pixel count to a known distance scale (462 pixels/1 mm).

An initial study was conducted to assess the similarity between powder kernels acquired from all five cartridges within a single commercial brand. Subsequently, for all newly purchased samples, the kernels from one cartridge were assumed to be representative of the entire brand. For aged samples, kernels from each cartridge replicate were analyzed because powders could not be assumed as originating from the same source, as previously described.

An example of processing is shown in Figure 3.1 using the Mag7.62A, Replicate 1. Figure 3.1A shows the raw data file when the light source is directed behind the sample. The picture was converted into an 8-bit image and made binary, creating a black and white picture shown in Figure 3.1B. The kernels length and approximate diameter were measured using a feature called Bounding Rectangle, which measured the maximum pixel length of each kernel relative to the x- and y- axis of the picture. Therefore, the length and diameter of each kernel were oriented to the x- and y- axis, respectively. Individual kernels were selected and rotated. Alterations for each picture were recorded and compared to the raw file. Figure 3.1C shows the altered picture for the Mag7.62A, Replicate 1. Finally, Figure 3.1D shows the number of kernels recorded when the particles were analyzed.

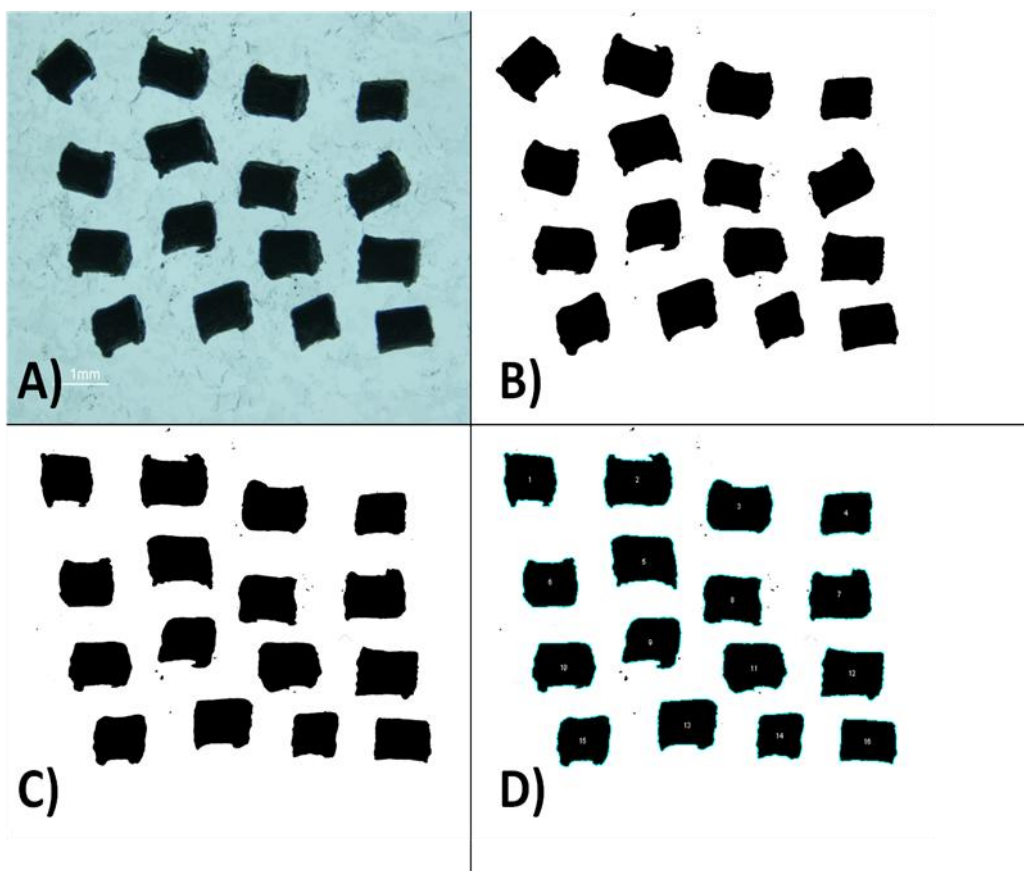


Figure 3.1 Visual representation of Image J processed pictures. A) Raw picture of Magtech 7.62x39mm, Aged B) Binary representation, C) Altered binary representation D) Processed samples with outlines around defined kernels.

3.3.2 HPLC-MS Analysis of Chemical Extracts

Reference standards were utilized for initial method development and determination of appropriate retention times and mass spectral analysis. A Shimadzu LC-20AD (Kyoto, Japan) HPLC was coupled with a Shimadzu SIL-5000 Auto Injector. An Ascentis Express C18 column (10cm x 2.1 mm, 2.7 μm beads) was utilized for separation of compounds. A Waters Micromass LCT Premier Mass Spectrometer (Waters Corporation, Milford, MA, USA) containing a time-of-flight (TOF) mass analyzer was equipped with an atmospheric pressure chemical ionization (APCI) source. The analytical technique is abbreviated as HPLC-APCI-multiplexed CID-TOF-MS.

Common organic compounds encountered in smokeless powders were selected as reference standards. These included methyl centralite (MC), ethyl centralite (EC), dibutyl phthalate (DBP), diphenylamine (DPA), 2,4-dinitrodiphenylamine (2,4-dinitro-DPA), and 2,4-dinitrotoluene (2,4-DNT). The internal standard in positive mode was 4-amino-diphenylamine and in negative mode was N-(3,5-dinitro-2-pyridinyl)-phenylalanine. Standards were prepared at concentrations ranging from 0.01 to 50 μ M in either acetonitrile or methanol.

For HPLC-MS analysis, preliminary studies were performed to optimize the instrumental conditions. The organic solvent used for HPLC separation, the rate of solvent flow, and the ramp of the solvent gradient were all varied. The gradient achieved a separation that washed the column of any residual material to prevent material carry-over into subsequent samples. The final HPLC conditions used are reported in Table 3.2.

The ionization source conditions were likewise adjusted to provide the highest signal intensity for the mass spectra of chemical standards. The most important conditions for signal strength were corona voltage, probe temperature, and desolvation gas flow. The final APCI probe conditions used are reported in Table 3.3.

TOF-MS conditions were varied for use with multiplex-CID analysis. Proper tuning of the instrument set most of the ion transfer conditions, including the hexapole RF multipole set at 100 Hz to allow a greater transmission of the lower m/z ions. Within multiplex-CID, collision energies ranging from 0 V to 80 V were analyzed. Five collision energies, 10 V, 25V, 40V, 55V, and 80V, were set in incremental steps to cover a wide range of fragmentation for each compound.

Table 3.2 HPLC Conditions

Time (minutes)	% 10 mM Ammonium Formate	% ACN	Flow ($\mu\text{L}/\text{min}$)
0	90	10	0.3
1	90	10	0.3
2	60	40	0.3
17	25	75	0.3
17.2	5	95	0.3
19.5	5	95	0.3
19.7	90	10	0.3
21	90	10	0.3

Table 3.3 APCI Probe Conditions

	APCI Positive	APCI Negative
Corona Voltage (μA)	4	20
Sample Cone Voltage	10	10
APCI Probe Temp	500	500
Cone Gas Flow (L/hr)	40	40
Desolvation Gas Flow (L/hr)	450	450
Mass Range (m/z)	50-1000	40-1000

After the five aliquots for each smokeless powder sample were measured for total organic material, the samples were stored as stock solutions. The percentage values for total material extracted for each powder were used to prepare each sample at a final concentration of 0.1 mg of extracted material/mL 1:1 ACN:water spiked with the appropriate internal standards for positive and negative ionization. Samples were analyzed by HPLC-APCI-multiplexed CID-TOF-MS.

3.4 Analysis of Chemical Attributes of Fired Smokeless Powders

3.4.1 Collection of Burned Smokeless Powders

Five cartridges of each ammunition were fired with the assistance of the Michigan State Police Laboratory (Bridgeport, MI). All 9 mm, 0.44 mm, 0.22 mm, 7.62x39mm, and 12-gauge ammunition were fired with a Ruger P95 DC, Ruger Super Redhawk, Browning Buckmark 22, Thompson Center Encore (Single Shot), and a pump action Bernelli 12-gauge, respectively. A plastic bag was carefully placed over the ejection port of each fired gun to collect the spent cartridge casings in an attempt to avoid inadvertent contamination with either the ground or undue handling. A universal gun cleaner was utilized to clean the barrel of each gun between different brands of ammunition. Spent cartridge casings were placed upright to avoid loss of loose residue. Samples were stored in a dry environment at room temperature prior to analysis.

3.4.2 Extraction and HPLC-MS Analysis of Chemical Extracts from Spent Cartridges

Spent cartridge casings were individually extracted with acetone and immediately transferred to a separate vial. The 12-gauge, 0.44, and 7.62x39 cartridges were each extracted with two, 750 mL aliquots of acetone. The 9 mm cartridges were each extracted with two 700 mL aliquots of acetone. The 0.22 LR cartridges were extracted with two 200 μ L aliquots of acetone. The two aliquots for each sample were collected in the same vial and labeled.

Acetone extracts were dried down with nitrogen gas. Three, 500 μ L aliquots of CH_2Cl_2 were used to extract the organic compounds for 10 minutes. All three aliquots were transferred to one vial and dried under nitrogen gas. Samples were re-suspended in CH_2Cl_2 at a ratio of 0.8 mL solvent / 1 mL of container volume for stock solutions. Aliquots of the stock solutions were dried

and re-suspended in ACN:water (1:1 v/v) containing 25 μM 4-aminodiphenylamine and 10 μM N-(3,5-dinitro-2-pyridinyl)-phenylalanine at a ratio of 0.4 mL solvent / 1 mL of container volume. All samples were analyzed with the same HPLC conditions and multiplexed-CID conditions used for the unburned smokeless powders.

3.5 Data Pretreatment

Initial data output was in the form of a total ion count (TIC) chromatogram. The TIC chromatogram was generated from the summation of the abundances of all mass spectral peaks at a given retention time. All chromatograms were generated in MassLynx Software (version 4.1, Waters, Milford, MA, USA). Pretreatment was necessary to minimize contributions of non-sample signals on subsequent data analysis. Utilizing a background subtraction function, the TIC chromatogram for each sample was background subtracted from the TIC chromatogram of 1:1 ACN:10mM ammonium formate spiked with internal standards.

A secondary software within MassLynx, called MarkerLynx (Version 4.1, Waters, Milford, MA, USA.) was utilized for simultaneously performing retention time alignment and area normalization on the background subtracted chromatograms. Peaks between only the specified initial and final retention times were analyzed. Each chromatographic peak was identified with user-specified parameters, as seen under the heading "Peak Parameters" (Table 3.4). The peak width at 5% height was an approximation of the amount of time, measured in seconds, comprising the width near the base of the peak. The peak to peak baseline noise specified the average noise in the chromatogram between adjacent peaks that was not due to eluting samples.

Each TIC peak had an associated mass spectrum, as previously stated. Parameters were once again defined for all mass spectra (Table 3.4). The high and low mass range specified a range for all m/z peaks analyzed within each mass spectra. The extracted ion chromatogram (XIC) window specified the mass accuracy tolerance of the acquired data. The intensity threshold specified a minimum abundance an individual mass spectral peak had to obtain in order to be considered above noise. The mass window specified a range in which mass spectral peaks are considered the same compound. Finally, the retention time window specified the range in which two eluting peaks with very similar mass spectral peaks were considered to be the same compound. Retention time alignment across all samples was performed with this technique, using the base peak values.

Table 3.4 MarkerLynx Software Chromatography and Mass Spectrometry Parameters

<u>Parameters</u>	<u>Value</u>
Initial Retention Time (min)	2
Final Retention Time (min)	13
Low Mass (m/z)	45
High Mass (m/z)	1000
XIC Window (Da)	0.5
<u>Peak Parameters</u>	
Peak Width at 5% Height (seconds)	15
Peak-to-Peak Baseline Noise	0.5
<u>Mass Spectral Collection Parameters</u>	
Marker Intensity threshold (counts)	10
Mass Window (m/z)	0.5
Retention Time Window (min)	2

All of the mentioned parameters were necessary to generate a list of data that encompassed the complexity of each information-rich sample. One sample can generate hundreds of entries, where each entry was a combination of a mass spectral peak at a specific retention time. Each entry, denoted 'marker', was a potential chemical compound of interest. The same m/z value at different retention times indicated similar core structures. For example, many markers contained m/z 170.11 at various retention times. Each of these compounds were found to contain diphenylamine (DPA) as a core structure, consistent with its protonated molecule.

Within a single sample, MarkerLynx software summed the intensities of all marker ions and normalized the total intensity to a count of 10,000. The individual intensity of each marker ion was normalized relative to the 10,000 count. For example, a marker with a count of 1500 would represent a single compound comprising 15% of the ionized organic profile. Across all samples, the normalized abundance of each marker was determined. Mean-centering of the normalized markers was performed as a pre-treatment to multivariate statistical analysis in EZ Info (Version 2.0, Umetrics, San Jose, CA, USA).

3.6 Data Analysis

Finally, the markers generated created a simplified profile of the compounds present in all samples (n=90). Association of replicates and discrimination of powders from separate ammunitions was accomplished through multivariate statistical analysis, specifically principal component analysis (PCA) and hierarchical cluster analysis (HCA).

3.6.1 Principal Component Analysis (PCA)

Principal components analysis was performed on the chemical profiles of all unburned smokeless powders using the statistical software EZ Info. Scores for each sample were generated and plotted on a scatter plot. Loadings plots were also generated, indicating which compound was most influential on each PC. Subsequently, the processed data representing the burned residues from each ammunition were overlaid as a prediction set on the scores plot generated from the unburned samples, which served as a training set. Positioning of the burned samples on the scores plot was dependent on the loadings plot of the unburned samples. The use of burned samples from different ammunitions did not influence the positioning of the unburned samples on the scores plot.

3.6.2 Hierarchical Cluster Analysis (HCA)

Agglomerative hierarchical cluster analysis (HCA) was performed on the processed marker data from MarkerLynx generated from all replicates of unburned smokeless powders or spent cartridge extracts using Pirouette (version 4.0, Infometrix Software, Inc., Bothell, WA, USA). Euclidean distance and complete linkage methods were used to create dendrograms that were analyzed for extent of similarity between replicates of either data set.

REFERENCES

REFERENCES

1. Technical Working Group for Fire and Explosions. Smokeless Powders Database. 2006 [cited 10/6/15]. <http://www.ilrc.ucf.edu/powders/>.

CHAPTER FOUR: Association and Discrimination of Unburned Commercial Smokeless Powders Using Physical Properties, Chemical Properties, and Multivariate Statistical Analysis

4.1 Introduction

In this study, the ammunition cartridge brands from which smokeless powder were obtained were coded as indicated in Table 3.1. Initial differentiation of powders was performed through analysis of their physical morphologies. A non-targeted, mass spectrometry analysis, termed multiplexed-collision induced dissociation (CID), subsequently generated chemical fingerprints of each unburned smokeless powder. Using multiplexed-CID, it was possible to identify compounds even in the absence of suitable reference standards. Finally, principal component analysis (PCA) and hierarchical cluster analysis (HCA) were conducted based on the chemical profiles to objectively associate and differentiate powders collected from a variety of ammunition manufacturers, primer compositions, calibers, and ages.

4.2 Morphological Analysis of Smokeless Powder Samples

Five cartridges from three different boxes of ammunition (Bzr9NoPb, SB9NoPb, Win9Pb) were disassembled and 50 kernels from each were viewed under a stereomicroscope. Morphologies of kernels from replicate cartridges of newly manufactured ammunition were visually similar. Hence, subsequent morphological analyses were performed on powder from one cartridge which was assumed to be representative of the ammunition. In contrast, the morphologies of kernels from replicate cartridges of aged ammunitions were not always visually similar. This was attributed to the manner in which the replicates were collected, i.e. loose ammunition stored in a large secondary container. As the exact source of the aged ammunition was unknown, powder from all five cartridge replicates was examined for the morphological

analyses. Pictures of all smokeless powders are in Appendix 4.1 and a summary of the morphological features is given in Table A.4.3.1.

Based only on morphology, visual discrimination of selected powders was possible. For example, Win9NoPb (Figure 4.1A) and PMC9Pb (Figure 4.1B) were distinguished based on surface features and physical dimensions. The powder from Win9NoPb was generally small irregularly flattened balls with a textured, rough surface and a relatively small average diameter of 0.58 mm +/- 0.08 mm. The powder from PMC9Pb contained rounder flattened balls with a smoother surface texture and a larger average diameter of 0.90 +/- 0.12 mm. Morphological analysis was sufficient to provide a reasonable measure of distinction among smokeless powders obtained from several different ammunition sources. However, consistent with practices in current forensic laboratories, verification of smokeless powder origin must be performed with further chemical analysis (1).

Several powders could not be distinguished only on morphology. For example, powders from the ammunition Mag9NoPb (Figure 4.1C) and Bzr9NoPb (Figure 4.1D) both contained rough-textured, black disks. The average diameters for Mag9NoPb and Bzr9NoPb were 0.90 +/- 0.05 mm and 0.91 +/- 0.06 mm, respectively. The average thicknesses for both Mag9NoPb and Bzr9NoPb were 0.21 +/- 0.02 mm. Both diameter and thickness measurements were not significantly different between the powders from each ammunition. The smokeless powders obtained from the following pairs of ammunitions could not be distinguished based upon morphology: Rem9Pb and Fed9Pb, Horn9Pb and Rem9NoPb, PMC44N and PMC44A, and Mag9NoPb and Bzr9NoPb. Most powders required careful analysis for differentiation, additionally limiting high-throughput analysis. A more definitive and easily interpretable means of differentiation for multiple samples was accomplished through analysis of the organic

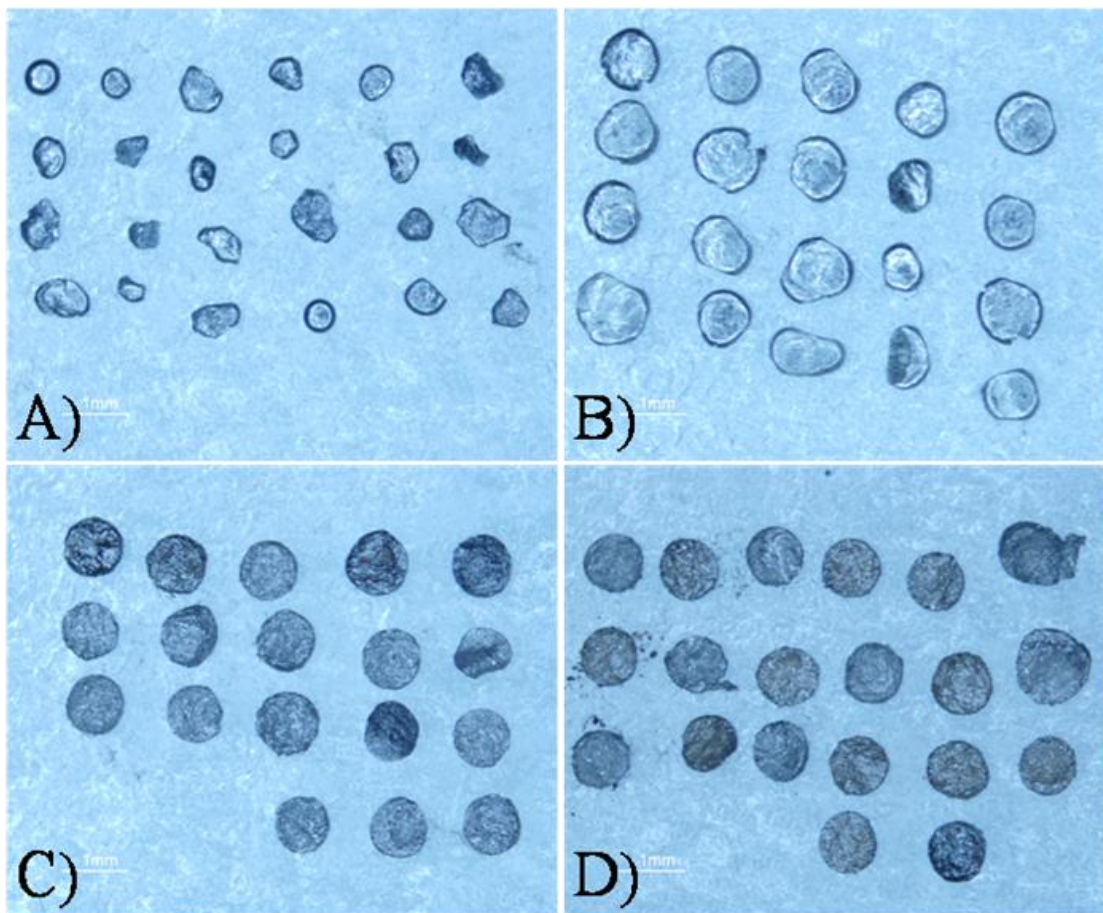


Figure 4.1 Representative morphology of smokeless powder kernels from (A) Win9NoPb and (B) PMC9Pb that were deemed distinguishable and from (C) Mag9NoPb and (D) Bzr9NoPb that were deemed indistinguishable.

compound fingerprint for each powder.

4.3 Identification of Organic Compounds in Smokeless Powders

4.3.1 Multiplexed-CID Confirmation of Identity of Reference Standards

Reference standards were analyzed in both positive and negative mode using high-performance liquid chromatography (HPLC) coupled to an atmospheric pressure chemical ionization source (APCI) for analysis with a time of flight (TOF) mass spectrometer (MS) utilizing multiplexed-CID (termed HPLC-APCI-multiplex CID-TOF-MS). Multiplexed-CID was used to identify and confirm the structures of each of the reference standards. The relevant mass spectral data are summarized in Table 4.1 and a representative chromatogram of a standard mixture containing 4-amino-diphenylamine (internal standard for positive mode), methyl centralite (MC), ethyl centralite (EC), and dibutyl phthalate (DBP) is shown in Figure 4.2.

To illustrate the use of multiplexed-CID for compound identification and confirmation, DBP is shown as an example. The multiplexed-CID spectra for this compound (retention time (t_R) 11.63 min) are shown in Figure 4.3. At a collision energy of 10 V (Figure 4.3A), the intact molecular ion at m/z 279.1414 was observed, which corresponds to protonated DBP. At a collision energy of 25 V (Figure 4.3B), fragment ions were observed at m/z 205.0860, 190.0458, and 149.0234 while at a higher collision energy (40 V), only the ions at m/z 190 and m/z 149 were still observed (Figure 4.3C).

Table 4.1 Summary of Chromatographic and Mass Spectral Data for Explosive Reference Standards

Reference Standard	Retention Time (Min)	Analysis Mode	Exact Mass of Molecular Ion (Da)	Exact Mass of Fragment Ions (Da) at Each Collision Energy
4-amino-diphenylamine	3.21	Positive	185.1303	10V: 185.1226 25 V: 185.1226 40 V: 185.1226, 167.0907, 139.0669, 93.0694 55 V: 185.1226, 167.0907, 139.0669, 93.0694
Methyl centralite	5.88	Positive	241.1595	10 V: 241.1595 25 V: 241.1595, 134.0635 40 V: 134.0635 55 V: 134.0635 106.0692
Diphenylamine	7.79	Positive	170.1243	10 V: 170.1110 25 V: 170.1110 40 V: 170.1110, 133.0406, 93.0688 55 V: 133.0954, 93.0688
Ethyl centralite	8.54	Positive	269.1853	10 V: 269.1674 25 V: 269.1674, 148.0784 40 V: 269.1674, 148.0784 55 V: n/a
Dibutyl phthalate	12.20	Positive	279.1819	10 V: 279.1819 25 V: 205.1104, 190.0683, 149.0411 40 V: 190.0683, 149.0411, 121.0437 55 V: 190.0683, 149.0411, 121.0437
N-3,5-DNPyr-DL-Phenylalanine	5.77	Negative	332.0677	10 V: 332.1184 25 V: 332.1184, 271.1193, 253.1044 40 V: 253.1044, 163.0388 55 V: 253.1044, 163.0388
2,4-dinitrodiphenylamine	4.89	Negative	259.0574	10 V: 259.0910, 242.0881, 211.0819 25 V: 242.0881, 211.0819 40 V: 242.0881, 211.0819 55 V: 211.0819, 165.0806
2,4-dinitrotoluene	7.63	Negative	182.0226	10 V: 182.0572, 165.0529, 152.0455 25 V: 182.0572, 165.0529, 152.0455, 135.0338 40 V: 152.0455, 135.0338, 105.0387 55 V: n/a

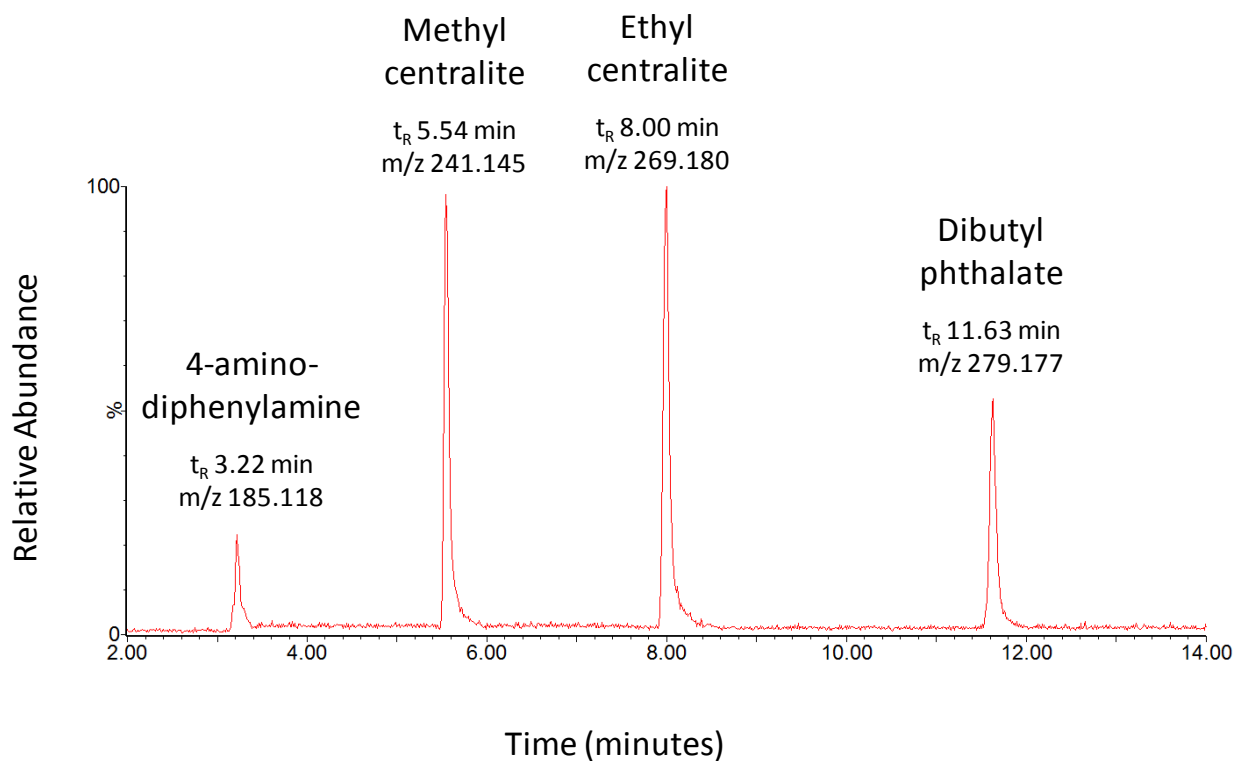


Figure 4.2 Representative chromatogram of explosive reference standards analyzed by HPLC-APCI-multiplexed-CID-TOF-MS in positive mode. For each peak, the compound identification is given, along with the retention time (t_R) and the m/z of the molecular ion for the compound

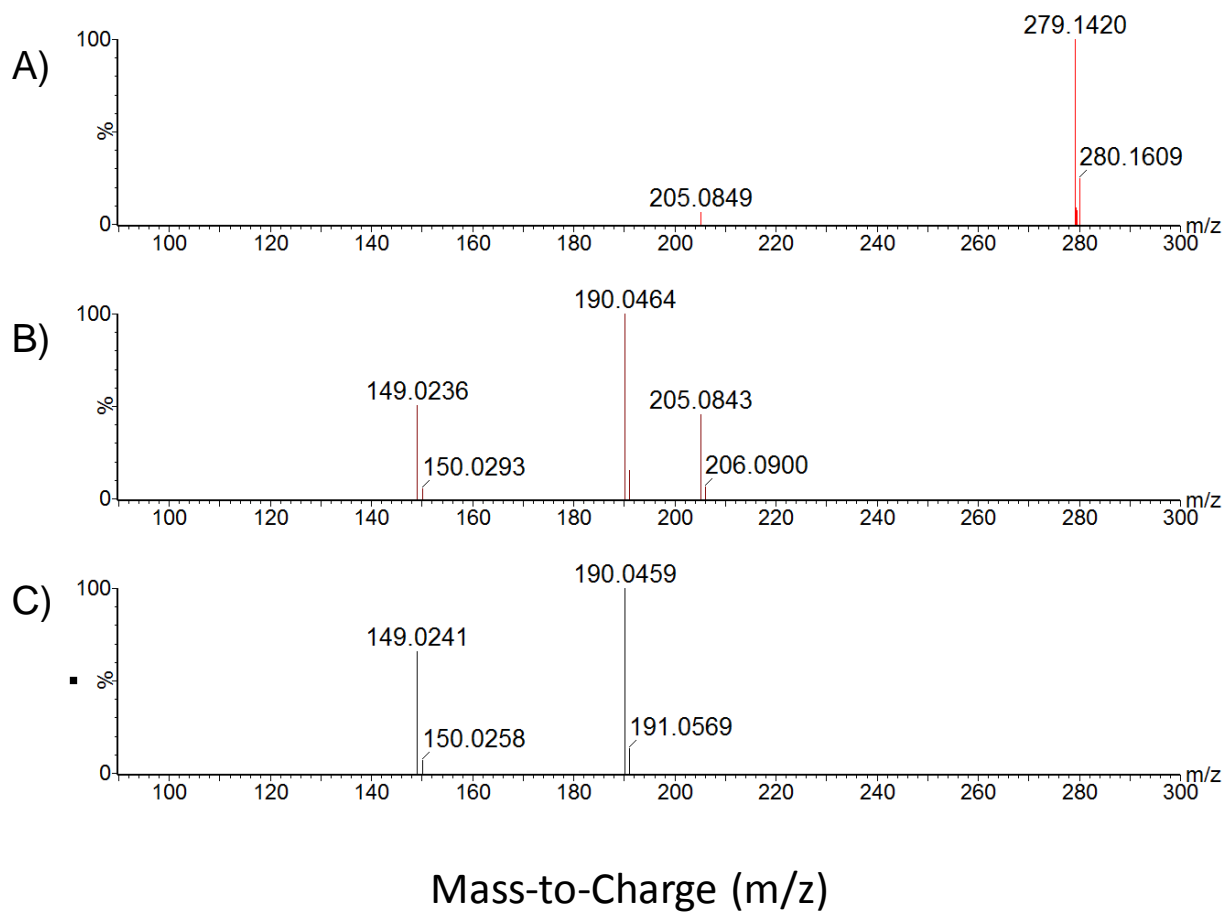


Figure 4.3 Multiplexed-CID spectra of DBP collected at collision energies of (A) 10 V, (B) 25 V, and (C) 40 V.

Structures corresponding to the fragment ions at m/z 279, 205, and 149 are shown in the fragmentation mechanism for DBP in Figure 4.4. Elucidation of the fragment structures was assisted with elemental composition analysis. The fragment ion at m/z 205 was consistent with a molecular formula of $C_{12}H_{13}O_3$, accurate to 2.4 ppm, resulting from the loss of one side chain $[-OC_4H_9]$ from either carbonyl. The fragment ion at m/z 190 likely contained an odd number of nitrogen atoms, thus generating an even molecular mass. This fragment was consistent with a molecular formula of $C_{10}H_8NO_3$, accurate to 24.2 ppm. The addition of a nitrogen suggested this compound was an adduct of a fragment with a solvent molecule. Analysis of the fragment at m/z 149 suggested a molecular formula of $C_8H_5O_3$, accurate to 3.4 ppm. The mass difference between the fragments at m/z 190 and m/z 145 were consistent with the addition of one molecule of the solvent acetonitrile, C_2H_3N , to the m/z 145 fragment. The acetonitrile adduct, m/z 190 ion, was reproducible in multiple analyses of the DBP standard, minimizing the possibility of error due to sample handling. The high mass accuracy of the time-of-flight mass analyzer used in this study allowed a higher confidence in elucidating the fragmentation mechanism for each chemical standard and the unknown compounds (Section 4.3.2).

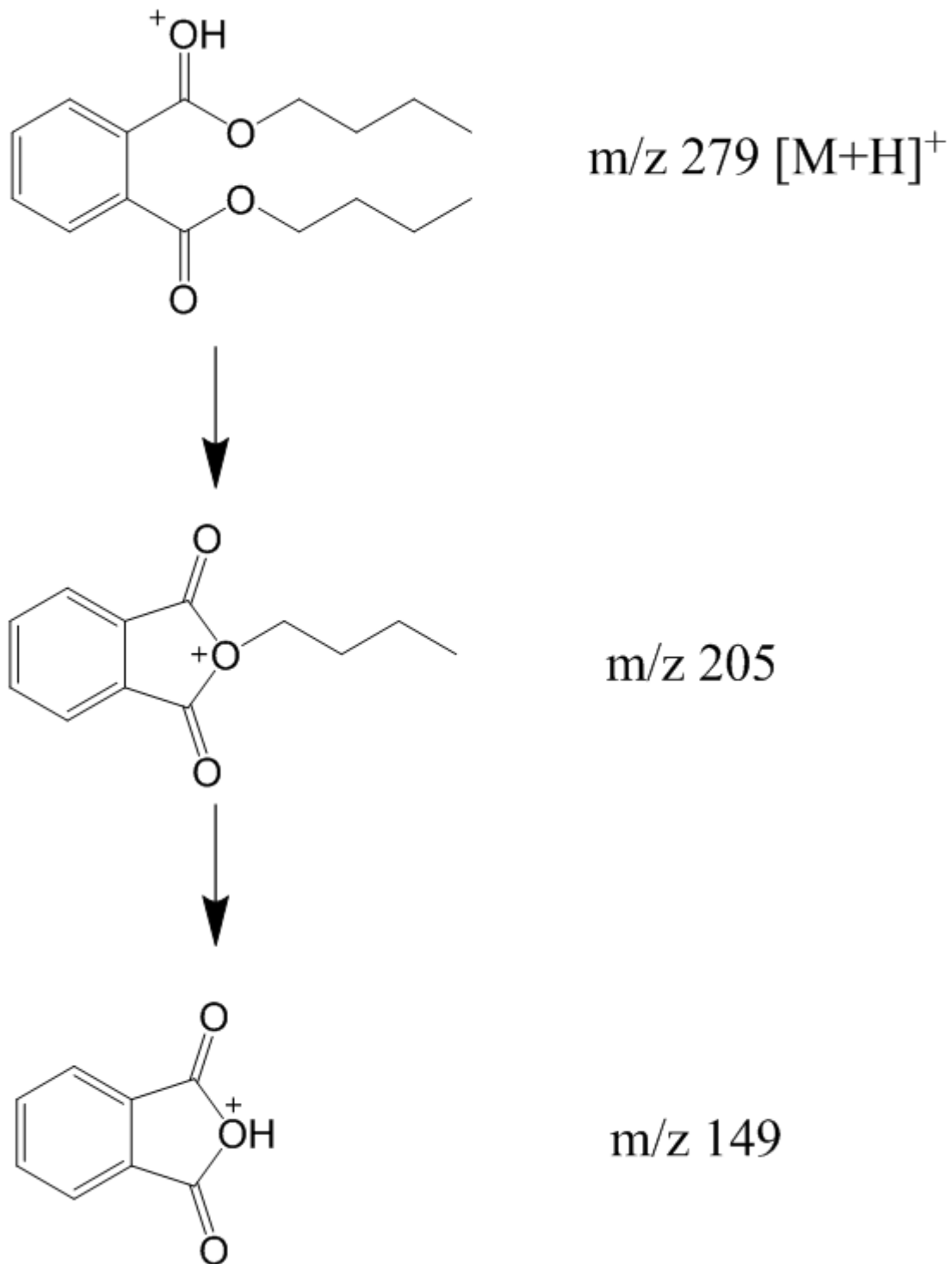


Figure 4.4 Proposed fragmentation pathway for DBP based on multiplexed-CID spectra (shown in Figure 4.3).

4.3.2 Multiplexed-CID to Identify Compounds in Unburned Smokeless Powders

The smokeless powder from a total of five cartridges in each ammunition was extracted and analyzed by HPLC-APCI- multiplexed-CID-TOF-MS. Compounds within each powder were identified through interrogation of the multiplexed-CID spectra with comparison to multiplexed-CID spectra from known reference standards. As an example, the chromatogram of an extract of Win9Pb in positive ion mode is shown in Figure 4.5. Based on comparison to the multiplexed-CID spectra of reference standards, DPA, EC, and DBP were identified in the powder. As none of the reference standards were consistent with the peaks eluting at t_R 4.18 min and t_R 6.67 min, multiplexed-CID assisted in the provisional identification of these compounds, even in the absence of a reference standard.

The multiplexed-CID spectra for the peak eluting at t_R 4.18 min are shown in Figure 4.6. As with the reference standards, elemental composition was performed on each fragment ion. At a collision energy of 10 V, the protonated molecule at m/z 227.1223 and an additional fragment at m/z 170.1111 were observed. At collision energies of 25 V and 40 V, an additional fragment ions at m/z 196.0941 was observed. The ion at m/z 196 represented a loss of 31 mass units from the protonated molecular ion, corresponding to a molecular formula of $C_{13}H_{10}NO$ and a fragment loss of $[-CH_5N]$. The ion at m/z 170 represented a loss of 57 mass units from the molecular ion, corresponding to a molecular formula of $C_{12}H_{12}N$ and a fragment loss of $[-C_2H_3NO]$. The ion at m/z 170 was consistent with the molecular ion for DPA and the fragment ions at m/z 133 and m/z 93 at higher collision energies (40 V and 55 V) were consistent with the fragmentation of DPA (Table 4.1). The proposed molecular formulas were most consistent with the mass spectral

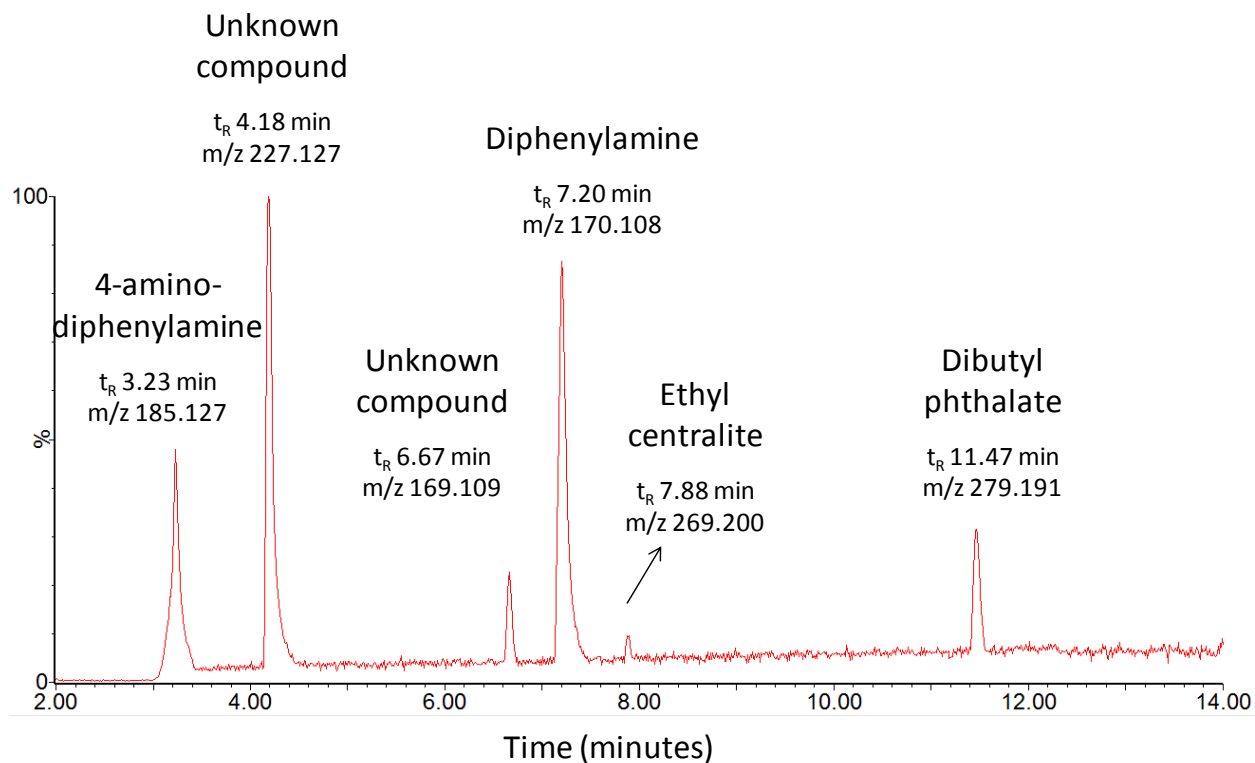


Figure 4.5 Representative chromatogram of Win9Pb, indicating the presence of DPA, EC, and DBP, as well as two unidentified compounds at t_R 4.18 min and t_R 6.67 min. For each peak, the compound identification is given, along with the retention time (t_R) and the m/z of the molecular ion for the compound

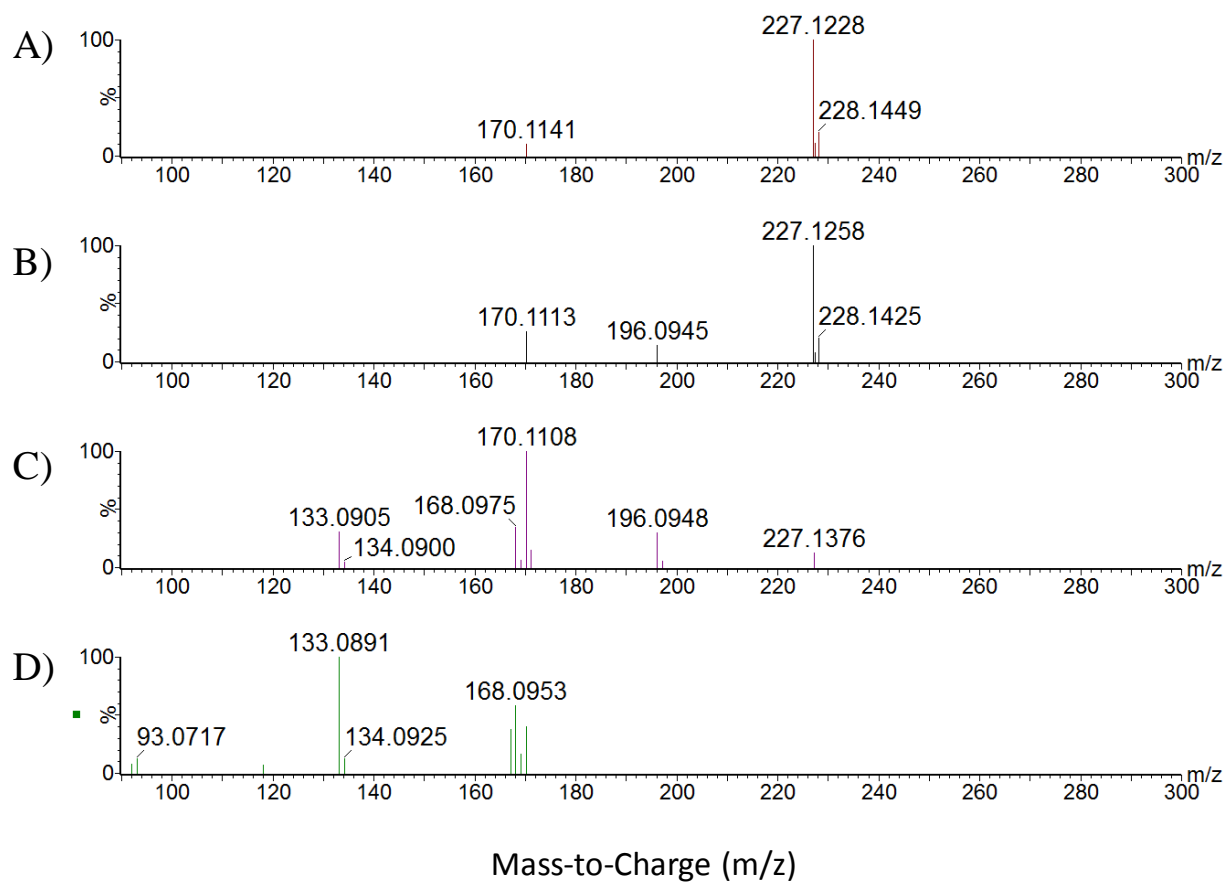


Figure 4.6 Multiplexed-CID spectra for peak at t_R 4.18 min in Win9Pb collected at different collision energies (A) 10 V, (B) 25 V, (C) 40 V, and (D) 55 V.

data. The compound with molecular ion m/z 227 was observed in a similar work by Scherperel *et al.* (2), who suggested the compound was a glycine attached to diphenylamine. However, based on the multiplex-CID spectra, the peak at t_R 4.18 min was provisionally identified as the stabilizer 1-methyl-3,3-diphenylurea, commonly known as akardite II (3) (Figure 4.7).

Li *et al.* previously analyzed unburned smokeless powders using DART-MS and compared the resulting chemical profiles to those generated for the same powders by GC-MS (4). Akardite II was identified in the powders but only when analyzed by DART-MS. The lack of detection using GC-MS was likely due to thermal degradation of Akardite II to form diphenylamine. This was analogous to degradation of N-nitroso-DPA to DPA that has been previously reported for GC-MS analysis of smokeless powders (5,6). Thus, the LC-APCI-multiplexed-CID-TOF-MS method used in this research has the advantage of detecting a more comprehensive organic chemical profile compared to instrumentation commonly used for smokeless powder analysis.

The peak eluting at t_R 6.61 min in the chromatogram of Win9Pb (Figure 4.5) was identified through interrogation of the multiplexed-CID spectra in a similar manner as described above. The multiplexed-CID spectra for the peak eluting at t_R 6.61 min are shown in Figure 4.8. At a collision energy of 10 V, the molecular ion at m/z 199.1070 was observed, while the base peak was observed at m/z 169.1040. The ion at m/z 169.1040 represented a loss of 30 mass units from the molecular ion, which corresponded to a loss of [-NO]. At collision energy of 25 V, only m/z 169 was observed. At collision energy 40 V and above, additional fragment ions at m/z 133.0903 and m/z 93.0702 were observed. The combination of ions at m/z 169, 133 and 93 at

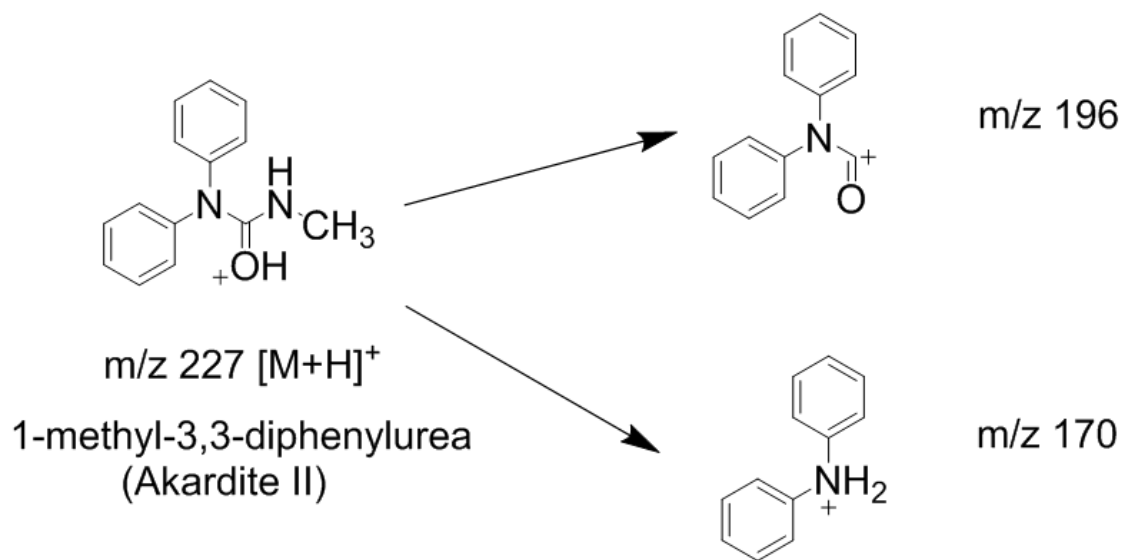


Figure 4.7 Proposed structure of peak at t_R 4.18 min based on multiplexed-CID spectra.

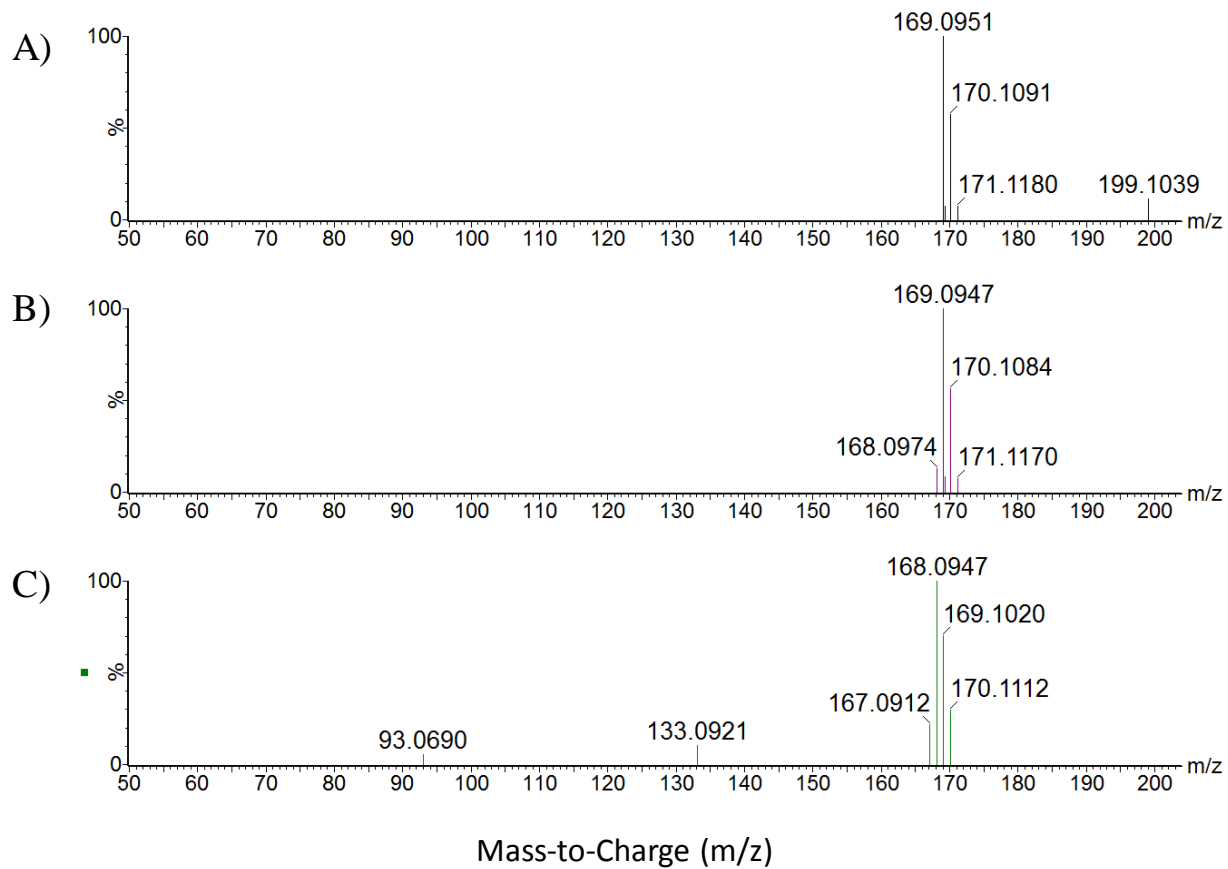


Figure 4.8 Multiplexed-CID spectra for peak at t_R 6.61 min in Win9Pb collected at different collision energies (A) 10 V, (B) 25 V, and (C) 40 V.

higher collision energies was consistent with the fragmentation of DPA (Table 4.1). Based on the multiplexed-CID spectra, the peak at t_R 6.61 min was identified as N-nitroso-diphenylamine (N-nitroso-DPA), which consists of a DPA molecule with a nitroso group replacing the hydrogen atom of the central amine (Figure 4.9).

Multiplexed-CID provisionally identified the compounds akardite II, N-nitroso-DPA, nitroglycerin, and diaminoaniline (7). The mass spectral fragments of each identified compound are summarized in Table 4.2. At least one of these compounds, all of which had no available reference standard, was present in the chemical profile of each smokeless powder along with compounds from the reference standards. Therefore, multiplexed-CID was essential for enabling the characterization of a comprehensive chemical profile for every smokeless powder.

A summary of the organic compound composition for each smokeless powder is summarized in Table 4.3. Representative chromatograms corresponding to each powder are shown in Appendix 4.2. The presence of nitroglycerin in all of the smokeless powders in this study, except Mag7.62A, indicated double-based explosives, while Mag7.62A was a single-based explosive. DBP was present as a plasticizer in most powders. N-nitroso-DPA and DPA were present in all but three powders. N-nitroso-DPA is the first nitration product formed with DPA after stabilizing the decomposition of nitrocellulose. As N-nitroso-DPA was present even in the newly manufactured ammunitions, decomposition occurred rapidly in the samples.

Certain compounds were present in a limited number of smokeless powders. EC, a plasticizer, was present in approximately one-third of the samples, both newly manufactured and

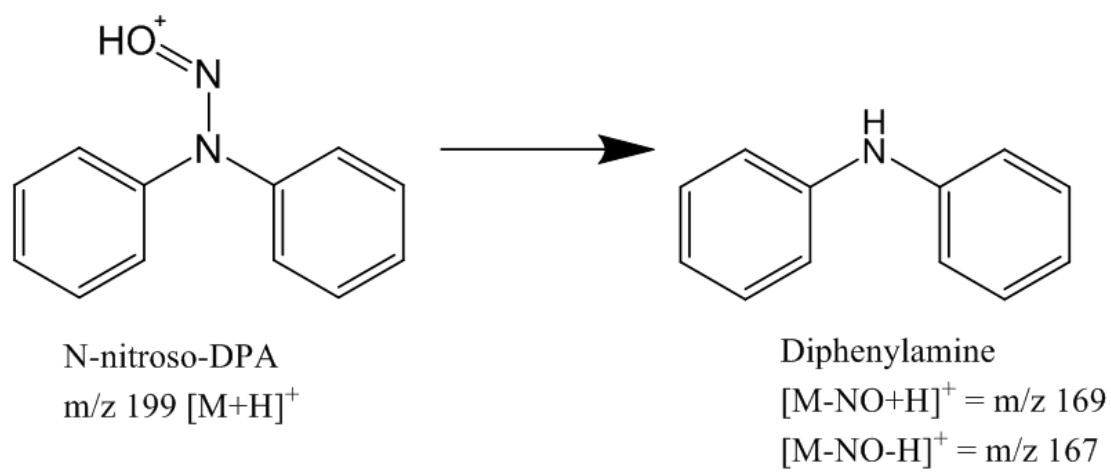


Figure 4.9 Proposed structure of peak at t_R 6.61 min based on multiplexed-CID spectra.

Table 4.2 Summary of Chromatographic and Mass Spectral Data for Multiplexed-CID Identified Compounds

Reference Standard	Chromatographic Retention Time (Min)	Analysis Mode	Exact Mass of Molecular Ion (Da)	Exact Mass of Fragment Ions (Da) at Each Collision Energy
Akardite II	4.18	Positive	227.1208	10V: 227.1208, 170.1115 25 V: 227.1208, 196.0944, 170.1115 40 V: 227.1208, 196.0944, 170.1115, 133.0895 55 V: 170.1115, 133.0895 80 V: 167.0905, 133.0895
N-nitroso-diphenylamine	6.14	Positive	199.1022	10 V: 199.1022, 169.0963 25 V: 169.0963 40 V: 168.0925, 133.0909 55 V: 167.0867, 139.0658, 118.0778 80 V: 167.0867, 139.0658, 118.0778
Diaminoaniline	4.73	Positive	123.1025	10 V: 123.1025 25 V: 123.1025 40 V: 123.1025, 108.0806, 106.0782 55 V: 118.0749 80 V: n/a
Nitroglycerin	4.87	Negative	289.0196	10 V: 289.0196 25 V: 61.9906 40 V: 61.9906 55 V: n/a 80 V: n/a

aged samples. Akardite II, a stabilizer, was present in approximately one-fourth of the samples, all of which were newly manufactured. 2,4-DNT was likewise present in approximately one-fourth of the samples, all of which were aged samples. 2,4-DNT resulted from increased NC decomposition, consistent with aging and corroborated the results seen for the more abundant compound N-nitroso-DPA. Finally, diaminoaniline was only present in Mag7.62A, thus providing discrimination of this powder from all other smokeless powders analyzed.

Twelve distinct chemical profiles were identified among all the smokeless powder samples in this study. These profiles were based only on the presence or absence of each organic compound. Several smokeless powders contained the same chemical profile. For example, the powders from Win9Pb, Rem9Pb, and Fed9Pb all contain Akardite II, N-nitroso-DPA, DPA, DBP, and NG. These were distinguished from the chemical profile for Horn9Pb, which contained EC but lacked the presence of Akardite II. However, differentiation of Win9Pb, Rem9Pb, and Fed9Pb had to come from a semi-quantitative analysis (Section 4.3.3).

Table 4.3 Summary of organic compounds identified in unburned smokeless powders

	Akardite II ¹	N-nitroso-DPA ¹	DPA	EC	DBP	Diamino-aniline ¹	Nitroglycerin ¹	2,4-DNT
Win9Pb	X	X	X		X		X	
Rem9Pb	X	X	X		X		X	
Fed9Pb	X	X	X		X		X	
Horn9Pb		X	X	X	X		X	
PMC9Pb		X	X				X	
Win9NoPb	X	X	X		X		X	
Rem9NoPb		X	X	X	X		X	
Bzr9NoPb			X	X	X		X	
SB9NoPb	X	X	X	X			X	
Mag9NoPb				X			X	
Win12N		X	X	X	X		X	
PMC44N		X	X		X		X	
SB7.62N	X			X			X	
Win12A(3,4) ²		X	X	X	X		X	X
Win12A(1) ²		X	X	X	X		X	
Win12A(2) ²		X	X	X	X		X	
Win12A(5) ²		X	X	X	X		X	
PMC44A		X	X		X		X	
Mag7.62A		X	X		X	X		X
PMC9A(1,2,4) ²		X	X		X		X	X
PMC9A(3,5) ²		X	X	X	X		X	X
CCI22A(1,3,4) ²		X	X	X	X		X	
CCI22A(2,5) ²		X	X				X	X

1. Compounds indicated were identified through multiplexed-CID

2. Parentheses indicate extraction replicates among five cartridges analyzed within each aged ammunition brand

4.3.3 Comparison of Chemical Profiles for Powders from Ammunition Containing Lead and Lead-Free Primers

The chemical composition of smokeless powders were compared to determine if chemical changes resulted among ammunitions containing lead (Pb) or lead-free (NoPb) primer. Although some discrimination was provided through the qualitative profiles, definitive conclusions had to be determined using a semi-quantitative analysis. The relative abundances of smokeless powders were compared to determine if differentiation of powders with the same qualitative profiles was possible.

The normalized relative abundances of each compound are shown in Figure 4.10 for the 9mm ammunition with Pb and NoPb primers. DPA and its nitration product N-nitroso-DPA were observed at similar levels in most samples, excluding Bzr9NoPb and Mag9NoPb. It's inclusion in most powder's organic compound formulations indicated its importance as a stabilizer for nitrocellulose degradation. DBP was likewise present in many samples. Meanwhile, Akardite II and EC were either present in low abundances or one of the most prominent compounds in the chemical profile. Thus, the compounds with more varied relative abundances served as more informative markers of discrimination among samples compared to the compounds with similar relative abundances.

Ethyl centralite had the largest difference in the relative abundance among samples, ranging from essentially no abundance in PMC9Pb to almost 80% of the organic profile of Bzr9NoPb and Mag9NoPb. Varied relative abundances were also seen within Akardite II, ranging from no abundance to 46% of the organic profile (Rem9Pb), and DBP, ranging from no abundance to 22% of the organic profile (Horn9Pb). DPA was more consistent among samples, being absent only in two samples while averaging around 20-30% of most organic profiles. The

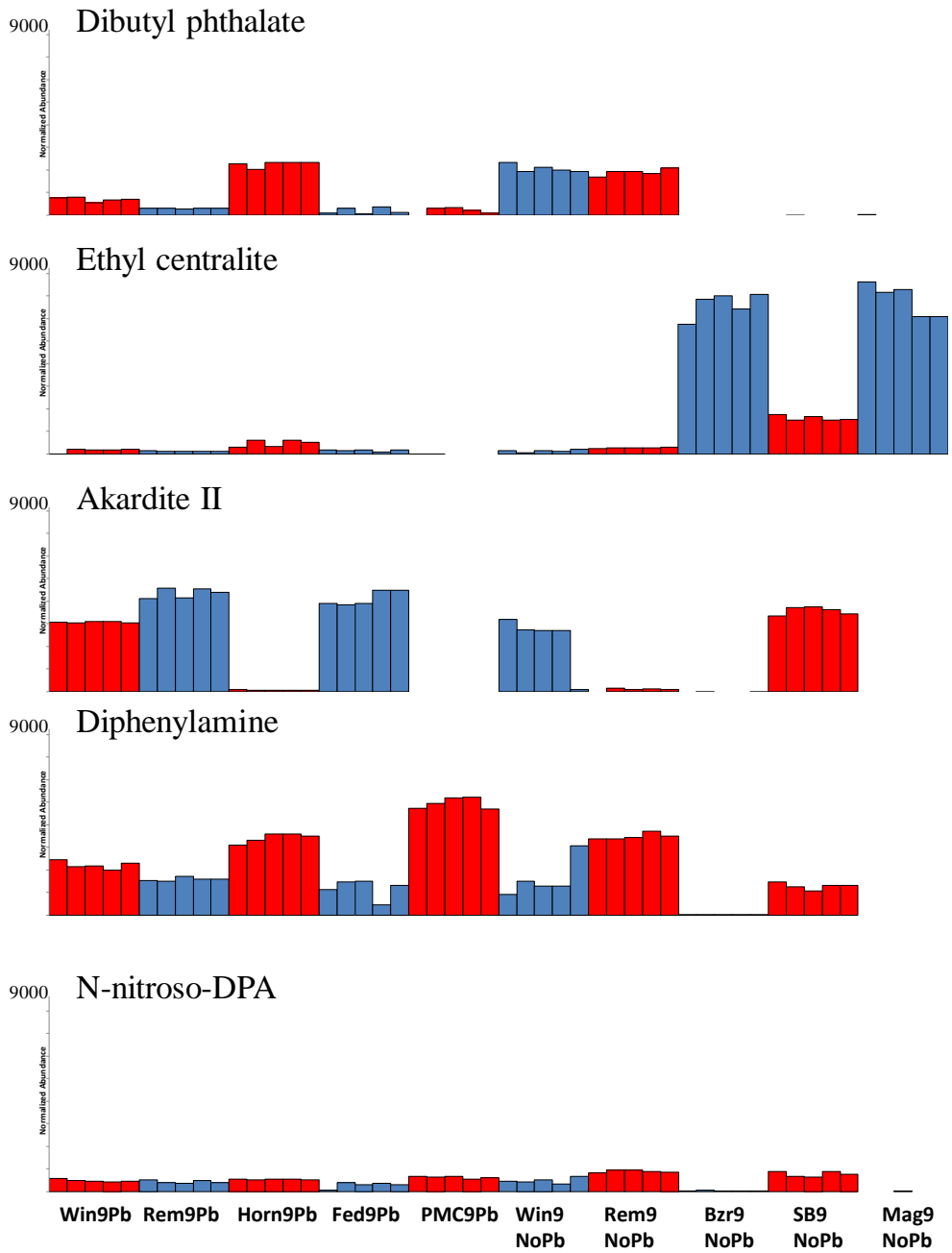


Figure 4.10 Plot of normalized relative abundance of each identified compound in each powder originating from ammunition with lead-containing (Pb) and lead-free (NoPb) primer.

compound with the most similar abundance among samples was N-nitroso-DPA. The contribution of N-nitroso-DPA to each chemical profile was less than 10%, due to these samples being newly manufactured. The compounds with the larger differences in relative abundances between samples have greater potential as diagnostic markers for the association and discrimination of powders when utilizing statistical methods.

For example, within the samples indistinguishable through qualitative analysis, Akardite II was more prominent in Win9Pb and Win9NoPb, distinguishing them from Rem9Pb and Fed9Pb. DBP was present in higher abundance in Win9NoPb, distinguishing this powder from Win9Pb. Figure 4.11 shows the chemical profiles of Rem9Pb and Fed9Pb, indistinguishable through both the qualitative and semi-quantitative analysis. As their morphologies were also indistinguishable (Section 4.2), this implied powders that originated from the same source. Further conclusions will be drawn after an objective analysis using statistical analysis (Section 4.4).

The powders from Bzr9NoPb and Mag9NoPb were also indistinguishable based on morphology (Section 4.2). A cursory assessment of the chemical profiles seemed to indicate both powders contained only EC (Figure 4.12A and B). However, further analysis with extracted ion chromatograms indicated DPA was present in Bzr9NoPb but was not present in Mag9NoPb while N-nitroso-DPA was present in higher relative abundance in Bzr9NoPb (Figure 4.12 C – F). The presence of these compounds, albeit at very low levels only observed using extracted ion chromatograms (XICs), allowed distinction of the two powders.

The chemical profiles of powders that were distinguished based on morphological differences were also compared. As an example, Figure 4.13 shows chemical profiles corresponding to Win9NoPb and SB9NoPb. While some compounds (Akardite II, DPA,

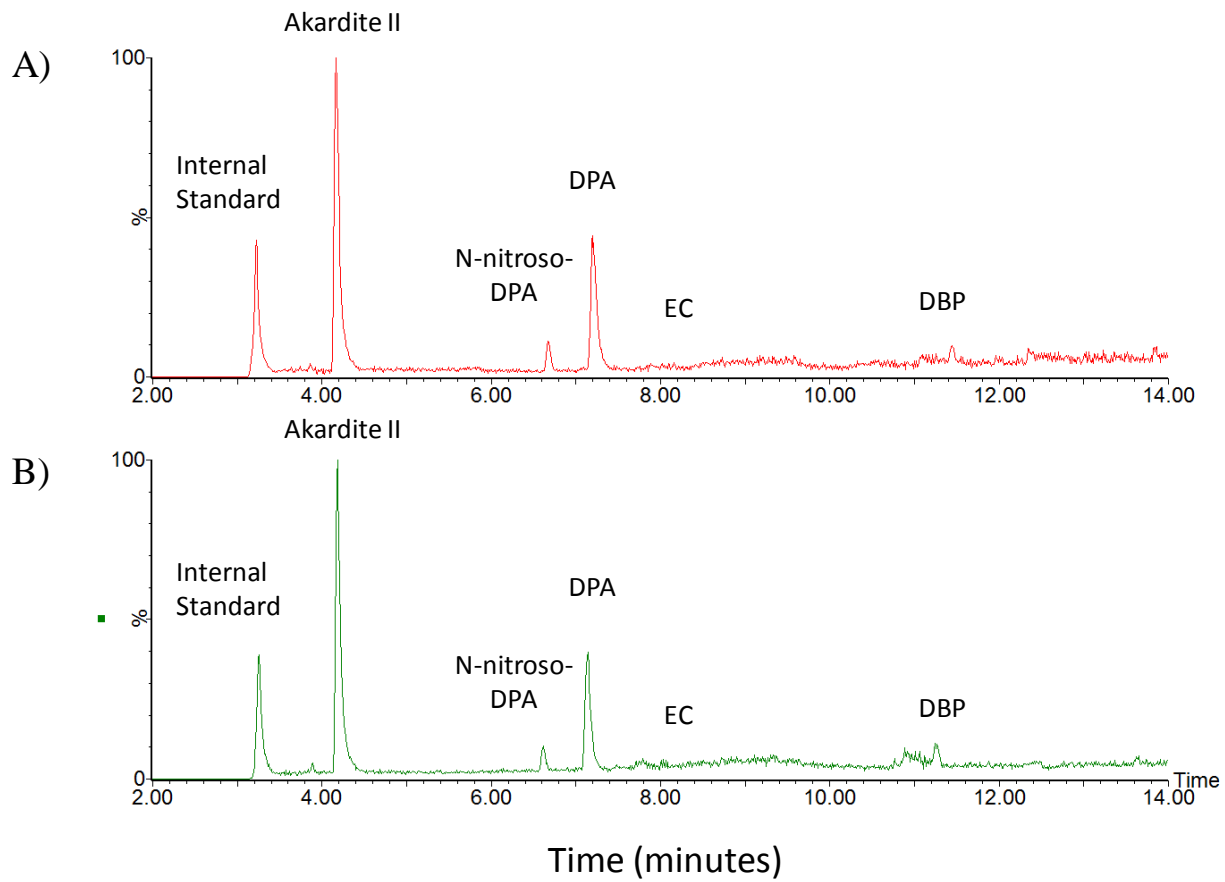


Figure 4.11 Representative chromatogram of powder from (A) Fed9Pb and (B) Rem9Pb, indicating the presence of Akardite II, N-nitroso-DPA, DPA, EC, and DBP.

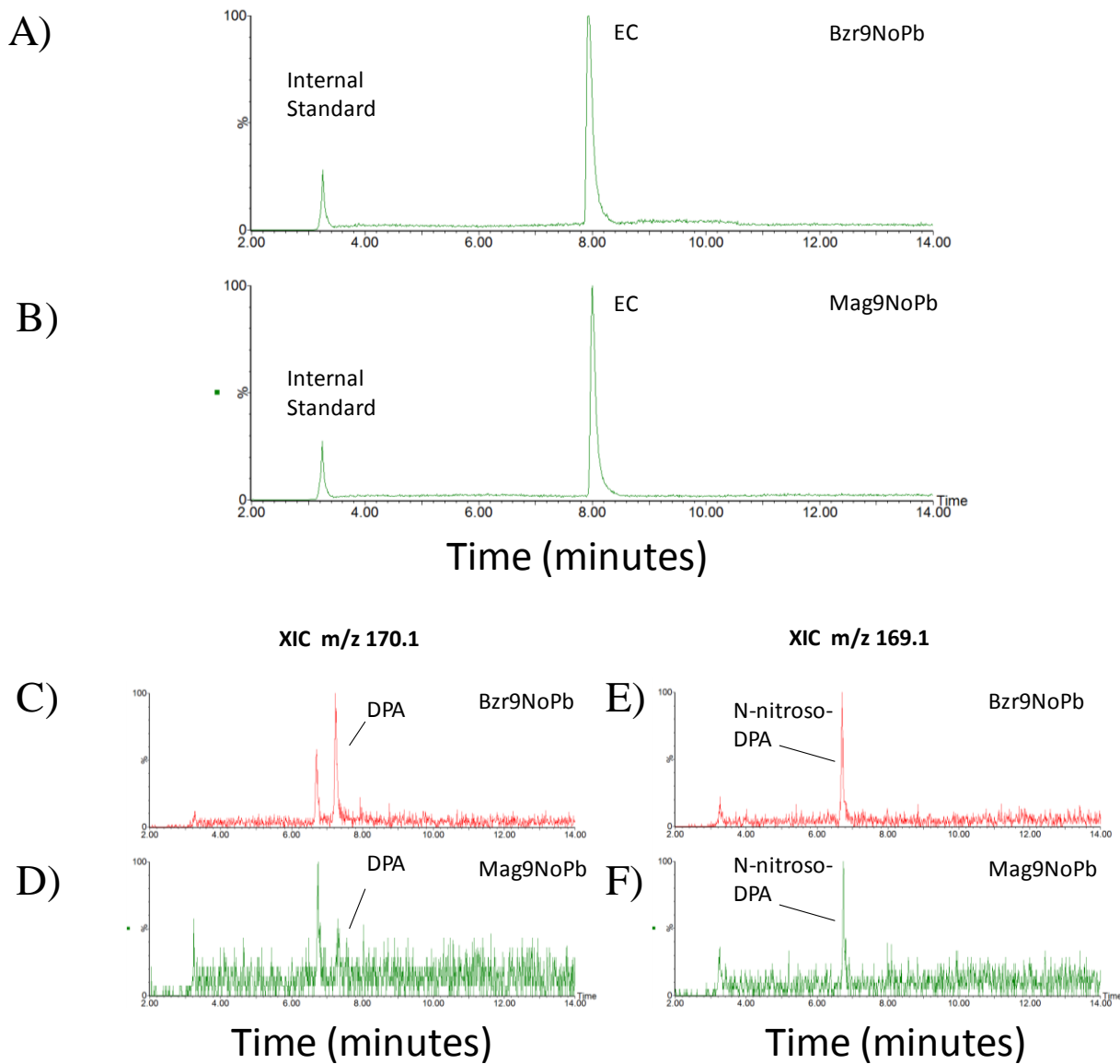


Figure 4.12 Representative chromatogram of powder from (A) Bzr9NoPb and (B) Mag9NoPb, indicating the presence of EC, (C) Extracted ion chromatograms (XIC) of m/z 170.1 corresponding to DPA in Bzr9NoPb, (D) m/z 170.1 in Mag9NoPb, (E) m/z 169.1 corresponding to N-nitroso-DPA in Bzr9NoPb, and (F) m/z 169.1 in Mag9NoPb.

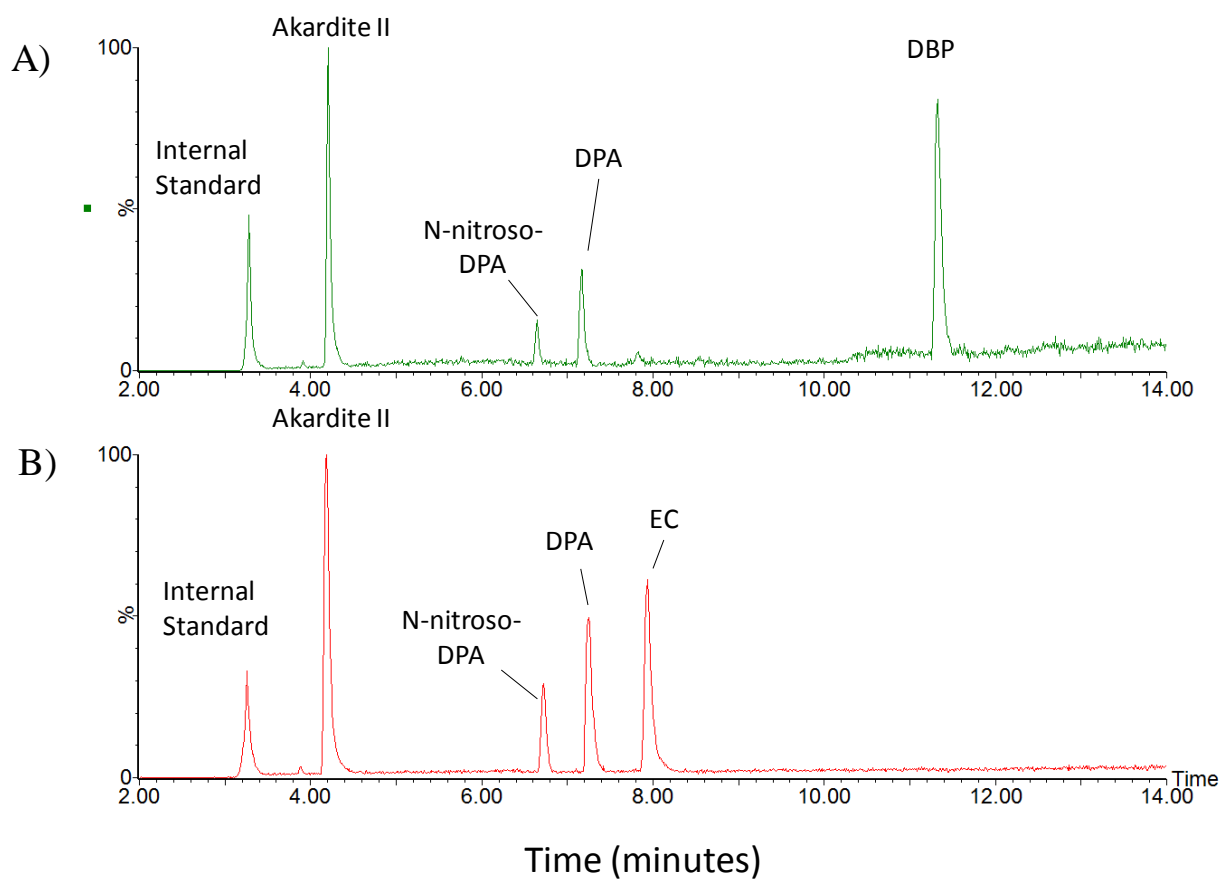


Figure 4.13 Representative chromatogram of powder from (A) Win9NoPb and (B) SB9NoPb, indicating the presence of organic compounds. The distinguishing compound in Win9NoPb was DBP while SB9NoPb contained EC.

N-nitroso-DPA, and nitroglycerin) were common to both powders, these compounds were present in different ratios. Further, DPA and EC were present only in Win9NoPb and SB9NoPb, respectively. Thus, the difference between these powders first indicated based on morphology was confirmed based on the chemical profiles of the two powders. A similar conclusion was reached for all Pb and NoPb powders that were morphologically different.

Overall, the presence of lead in the primer of the ammunition cartridge did not provide a characteristic compound or ratio of compounds that would have potential as a diagnostic marker for the association and discrimination of powders. This conclusion was not unexpected as the materials comprising the primer are physically distinct from the smokeless powder within the ammunition cartridge.

4.3.4 Comparison of Chemical Profiles for Powders from Aged Ammunition and New Counterparts

The chemical compositions of smokeless powders were compared to determine the effects, if any, of changing the caliber type or manufacturing age (new denoted by 'N', aged denoted by 'A'). The qualitative profiles (Table 4.3) were useful as an initial tool to provide some discrimination between powders. In particular, Mag7.62A lacked the presence of nitroglycerin, which was present in all other samples, and contained a unique compound provisionally identified as diaminoaniline (7), which may serve as either an explosive component or a stabilizer. However, many of the qualitative profiles were similar. Therefore, the relative abundances of each compound were utilized for differentiation of powders.

The normalized relative abundances of each compound were compared in Figure 4.14, with caliber type and ammunition manufacturer indicated. It was noted that the aged samples

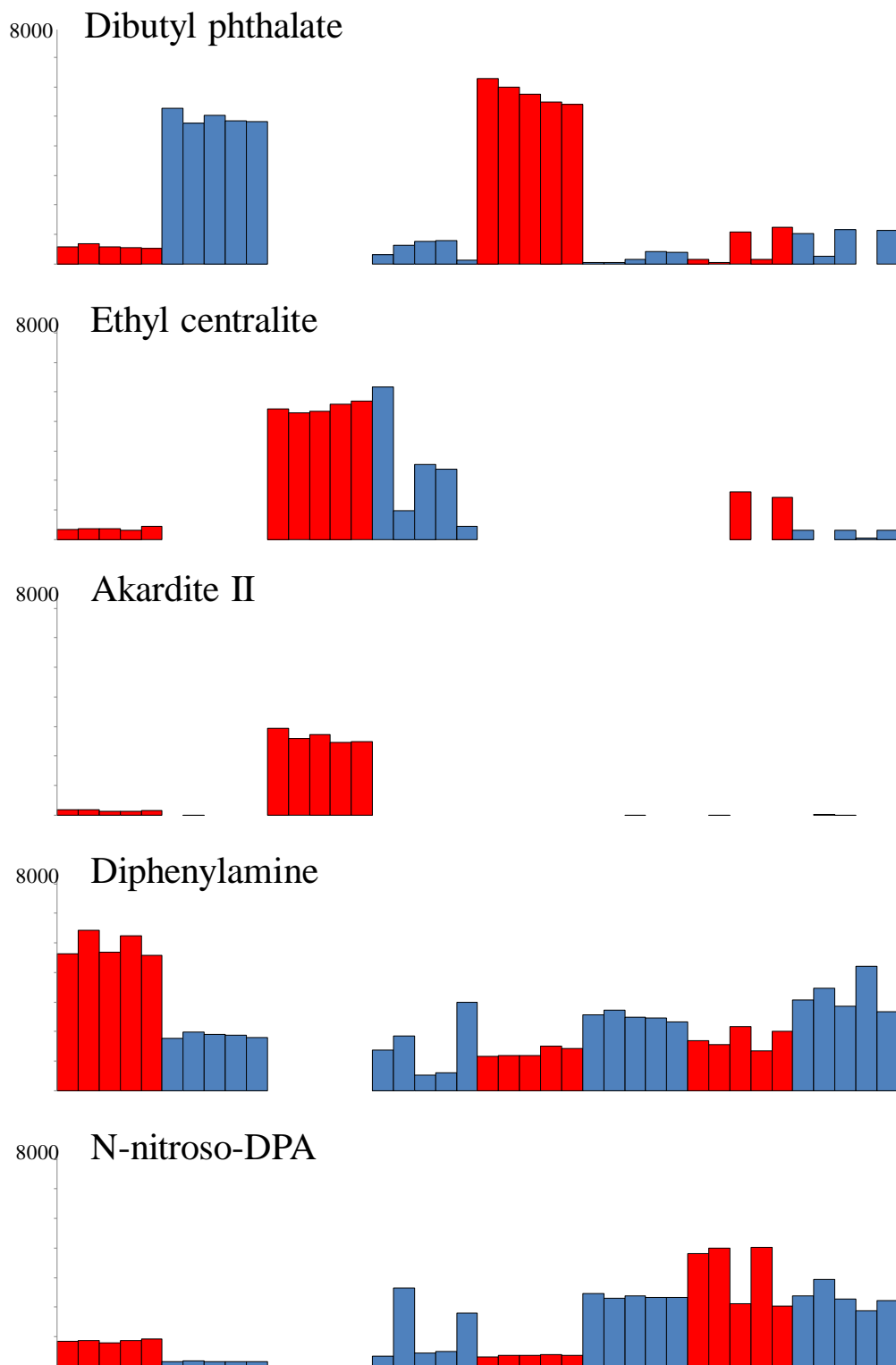


Figure 4.14 Plot of normalized relative abundance of each identified compound in each powder originating from 'aged' ammunition (denoted with 'A') and corresponding new counterparts (denoted with 'N').

contained differences in the abundances of compounds between the five replicates within a single ammunition manufacturer. For example, the qualitative profile of Win12A separated replicates 3 and 4 from 1, 2, and 5 (Table 4.3). The normalized relative abundances of each group showed replicates 3 and 4 have similar abundances while replicates 1, 2, and 5 have different profiles (Figure 4.14). Namely, replicates 1, 2, and 5 had higher abundances of EC, N-nitroso-DPA, and DPA than replicates 3 and 4. This is further supported by the morphological data, where replicate 1 consisted of large black disks with pink markers, replicates 2 and 5 were large, gray irregular flakes, and replicates 3 and 4 were small, gray flattened disks (Table A.4.3.1). Likewise, the replicates for PMC9A and CCI22A were separated into different profiles through the differences in the qualitative analysis, semi-quantitative normalized relative abundances, and morphological analysis (Table 4.3, Figure 4.14).

In comparison of the aged samples to their newly manufactured counterparts, DBP had the largest difference in relative abundance among samples, ranging from no abundance in SB7.62N to around 60% of the abundance in PMC44A and PMC44N. Varied relative abundances were also seen within EC, ranging from no abundance to 52% of the organic profile (SB7.62N). Akardite II was absent from most samples, only having significance in SB7.62N at around 30% of its organic profile. DPA was again consistent among samples, averaging around 10-20% of most organic profiles and averaging 50% in Win12N. Noticeably, the levels of N-nitroso-DPA were greatly increased, averaging about 5% in the new samples and 30-40% in select aged samples. The increase in N-nitroso-DPA was due to the degradation of nitrocellulose, as previously described. However, the increase in the relative abundance of N-nitroso-DPA was not consistent across all samples. The degradation of nitrocellulose was likely affected by ambient storage conditions of the ammunition, which were unknown for each aged sample.

The chemical profiles of different ammunitions, and even within an ammunition, were differentiated based upon the normalized abundances. For example, PMC 9A replicates 1, 2, and 4 contained a different normalized abundance profile from replicates 3 and 5, which was supported by the chromatograms of each replicate (Figure 4.15). Replicates 3 and 5 contained a higher normalized abundance of DBP, EC, and DPA, while containing lower normalized abundances of N-nitroso-DPA. Therefore, two profiles were developed for the normalized relative abundances of PMC9A (Table 4.3, Figure 4.15) for subsequent statistical analysis.

Overall, the chemical profiles for powders from different calibers did not provide a characteristic compound or ratio of compounds as a potential marker for powder association or discrimination. As smokeless powder serve as the propellant, the ammunition manufacturers likely adjust the amount of powder rather than adjusting the chemical composition. However, the several compounds, in particular DBP and N-nitroso-DPA, have value as diagnostic markers in statistical analysis for the association and discrimination of powder profiles. This will be further explored through PCA and HCA analysis (Section 4.4).

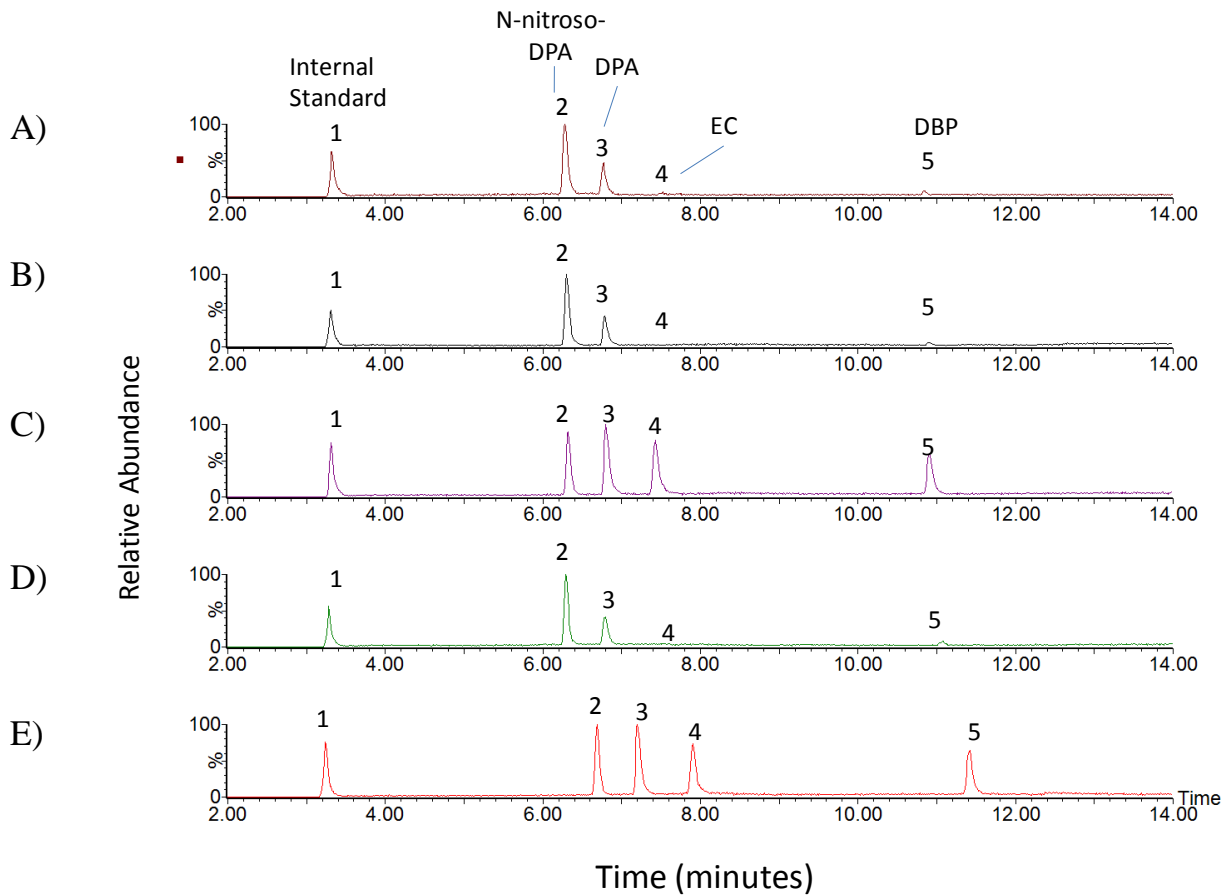


Figure 4.15 Replicate chromatograms of powder from PMC9A, (A)-(E) represent replicates 1-5.

4.4 Multivariate Statistical Analysis of Chemical Profiles from Unburned Powders

4.4.1 Principal Components Analysis

The organic chemical profiles from positive ion mode for all powders were subjected to principal component analysis (PCA) and hierarchical cluster analysis (HCA). The PCA scores plot for the first two principal components (PC1 and PC2) is shown in Figure 4.16A. In general, replicates of each powder were positioned closely in the scores plot. However, replicates were not closely positioned for some aged samples, for example PMC9A (blue crosses) and Win12A (black crosses). The wide range in positioning for the aged samples along the axes was consistent with the variation in total abundances seen in the semi-quantitative analysis (Figures 4.10 and 4.14).

From the scores plot, there was differentiation of powders into groups of similar chemical profiles. Groups 1 - 4 were indicated on the scores plot based upon positioning along PC1 and PC2. Group 1 was positioned high on the positive scale of PC2 while positioned around zero on PC1, distinguishing these samples from the remaining samples. Group 2 samples were positioned most positively on PC1. Groups 3 and 4 were positioned negatively on both PC1 and PC2. Group 4 was separated from Group 3 due to tight overlap in positioning along both axes while the samples in Group 3 covered a wider area.

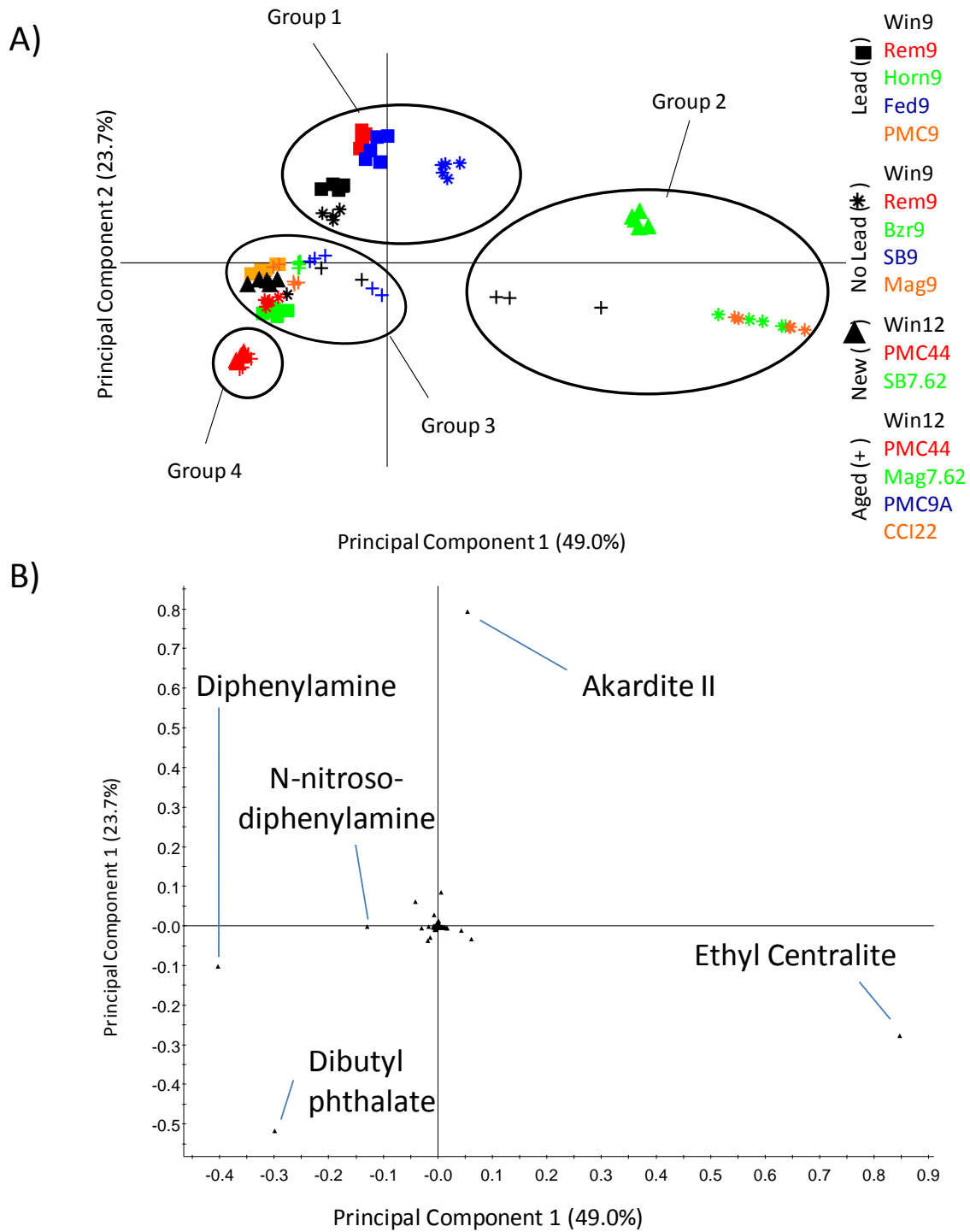


Figure 4.16 Principal components analysis based on chemical profiles of the unburned smokeless powders (A) scores plot and (B) loadings plot for the first two principal components.

The chemical contributions to the scores plot were explained through analysis of the loadings plot for PC1 and PC2 (Figure 4.16B). For PC 1, the compounds (variables) that were most influential in determining the position of a powder are EC, which is weighted positively, and DBP and DPA, which are both weighted negatively. For example, Group 2 was positioned most positively on PC1 and all the powders in this group contained EC at a very high relative abundance (Figure 4.10, 4.14), while the powders in Group 3 were positioned negatively on PC1 and all the powders in this group contained DPA and N-nitroso-DPA at a high relative abundance (Figure 4.10, 4.14).

The compounds that were most influential in determining position on PC2 are Akardite II, which is weighted positively, and EC and DBP, which were both positioned negatively. Group 1 was positioned positively on PC 2 and samples within this group contained a high abundance of Akardite II (Figure 4.10). Within Group 1, Win9Pb and Win9NoPb were positioned more negatively on PC 2 relative to Rem9Pb and Fed9Pb due to a higher relative abundance of DPA and DBP, which was weighted negatively on this PC. Group 4 was positioned most negatively on PC2 and samples within this group contained a high abundance of DBP (Figure 4.14), differentiating them from most smokeless powders.

The positioning of the samples on the scores plot (Figure 4.16) assisted in the differentiation of four similar chemical groups as well as some differentiation within the groups. However, the replicates of several powders overlapped each other. For example, Rem9Pb and Fed9Pb overlapped in Group 1, Bzr9NoPb and Mag9NoPb overlapped in Group 2, and PMC44N and PMC44A overlapped in Group 4. Each of these pairs of samples also had indistinguishable morphologies, leading to a greater probability that these powder samples originated from the same smokeless powder manufacturer. It is important to note that while some samples in Group

3 overlap in terms of their chemical composition, their physical morphologies were able to distinguish these powders. This highlighted the importance of a physical and chemical characterization of smokeless powders for increasing confidence in comparing samples.

The scores plot was further assessed to determine trends relating to the characteristics of the ammunition in terms of manufacturer, primer composition, caliber, and age. Four Winchester ammunitions were utilized in this study: 9mmPb, 9mmNoPb, 12-gauge (New) and 12-gauge (Aged). The symbols for these samples were all colored black on the scores plots. Both 9 mm samples were in Group 1, the 12-gauge (New) was in Group 3, and the 12-gauge (Aged) was in Group 2. Likewise, both Remington samples were not chemically similar, as the 9mmPb was in Group 1 and 9mmNoPb was in Group 3. Therefore, ammunition manufacturer had no effect on the chemical composition of the smokeless powder.

The positioning on the scores plots was also compared for primer compositions and calibers. Primer compositions, specifically the presence or absence of lead, were not found to have any effect on the chemical composition of the powder. The Pb-containing samples were contained within Groups 1 and 3, while the NoPb samples were located in Groups 1, 2, and 3. Likewise, the chemical composition was not affected by the calibers. More samples were classified as 9mm caliber relative to the other calibers. However, no caliber displayed organic compounds or relative abundances that could have been considered unique to that caliber type.

The age of the ammunition did influence the chemical composition, specifically the presence of N-nitroso-DPA. As previously stated, the decomposition of nitrocellulose was a gradual process which was mitigated by the amount of stabilizer, in this case DPA, present in the sample. The majority of aged samples were contained in Group 3 due to the presence of N-

nitroso-DPA. Meanwhile, the new counterparts were spread over the scores plot in groups 2, 3, and 4.

4.4.2 Hierarchical Cluster Analysis

The chemical profiles of all powders analyzed were subjected to hierarchical cluster analysis (HCA) and the resulting dendrogram is shown in Figure 4.17. The five extraction replicates of each new powder clustered at high similarity levels of 0.9 and above while extraction replicates from the aged powders tended to cluster at more moderate similarity levels ranging from 0.7 to 0.9.

After a similarity level of 0.38, five groups of the powders were apparent (as labeled in Figure 4.17). The first cluster formed at a similarity level of 0.840 and contained the new and aged PMC44 powders. As this was the first cluster formed, these two powders were the most similar in the data set. This similarity was also observed in the PCA scores plot as these samples were in Group 4, and they were differentiated as a result of their high abundance of DBP (Figure 4.16A).

The second cluster formed at a similarity level of 0.709 and this group contained SBNoPb, Fed9Pb, Rem9Pb, Win9NoPb, and Win9Pb. The relatively high similarity at which this group forms indicated that the chemical profiles of these powders are very similar. This was in agreement with the PCA scores plot as these samples were positioned in Group 1 and differentiated due to high abundance of Akardite II (Figure 4.16A).

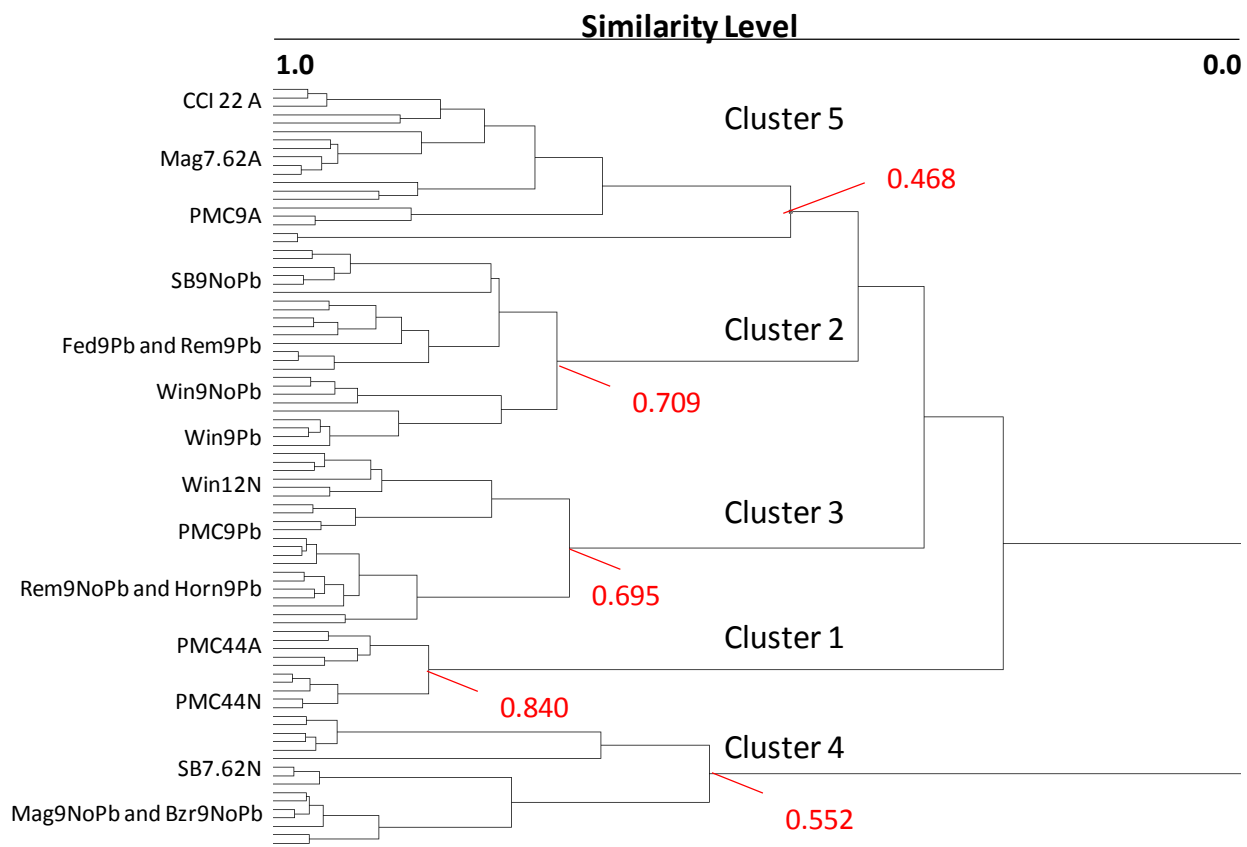


Figure 4.17 Hierarchical cluster analysis dendrogram based on chemical profiles of unburned smokeless powders. Groups indicate similar chemical profiles as determined during PCA analysis. Red numbers indicate similarity level at which each group was formed.

The third cluster formed at a similarity level of 0.695 and this group contained Win12N, PMC9Pb, Rem9NoPb, and Horn9Pb. The relatively high similarity at which this cluster formed indicated that the chemical profiles of these powders were very similar. This was in agreement with the PCA scores plot, where these samples were contained within Group 3 and differentiated based upon a more negative position on PC1 as a result of the higher relative abundances of DPA (Figure 4.16A).

The fourth cluster formed at a similarity level of 0.552 and this contained SB7.62N, Mag9NoPb, and Bzr9NoPb. The moderate similarity at which this cluster forms indicated that the chemical profiles of these powders were variable. This was in agreement with the PCA scores plot, where these samples were contained within Group 2 and differentiated based upon a more positive position on PC2 as a result of a higher relative abundance of akardite II. (Figure 4.16A).

The fifth cluster formed at a similarity level of 0.468 and contained Mag7.62A, CCI22A, and PMC9A. The moderate similarity at which this group forms indicated that the chemical profiles of these powders were variable. This was in agreement with the PCA scores plot as the remainder of Group 3 and differentiated based upon a slightly negative position on PC 2 as a result of a higher relative abundance of N-nitroso-DPA. (Figure 4.16A).

The data presented for HCA was in agreement with that of the PCA scores plot. However, PCA has the advantage of indicating the variables, or chemical compounds, that are responsible for the similarity and differentiation of the powders. HCA displays the similarity between samples of similar chemical composition without indication of how the clusters are formed. The advantage of HCA lies in the ability to provide a numerical measure of similarity. PCA interpretation is primarily a visual assessment. For example, the PCA analysis of samples in

the negative scale of PC 1 and PC 2 were primarily grouped into Groups 3 and 4 based upon visual similarity. However, HCA provided a numerical measure that the samples can be differentiated through the dominance of N-nitroso-DPA and DPA. Therefore, the use of both PCA and HCA in tandem is a powerful tool.

4.5 Summary

Previous research has shown differences in morphology and chemical composition can assist in the discrimination of smokeless powders from different smokeless powder manufacturers. While morphology provided an initial means of discrimination, the analysis was subjective and limited in drawing conclusions. Subsequently, definitive association and discrimination of powders was performed through an analysis of the extracts from a variety of commercial smokeless powders. Chemical standards were used to identify DBP, DPA, and EC, which were all prominent in the chemical profile. Multiplexed-CID was utilized to allow identification of the organic compounds for which no reference standards were available, such as the prominent Akardite II and N-nitroso-DPA. The analysis benefitted from the compounds identified using multiplexed-CID as these were present in multiple samples and significantly contributed to both statistical analyses. Additionally, powders with a unique organic compound profile were discriminated from powders indistinguishable by morphology alone.

Utilizing PCA and HCA, compounds common to all powders were analyzed to provide more objective measures of association and discrimination among the powders. The analysis of powders was independent of factors such as ammunition manufacturer, primer composition, and caliber, suggesting the possibility that ammunition manufacturers purchased smokeless powder from the same supplier. The age of the ammunition affected the chemical composition of the

powder. The decomposition of nitrocellulose was stabilized via the conversion of DPA to N-nitroso-DPA. Ultimately, most powders were able to be distinguished based upon morphological and chemical analysis, while pairs of powders that were unable to be distinguished were suspected to originate from the same smokeless powder manufacturer.

APPENDICES

APPENDIX 4.1 Stereomicroscopic Images of Unburned Smokeless Powders

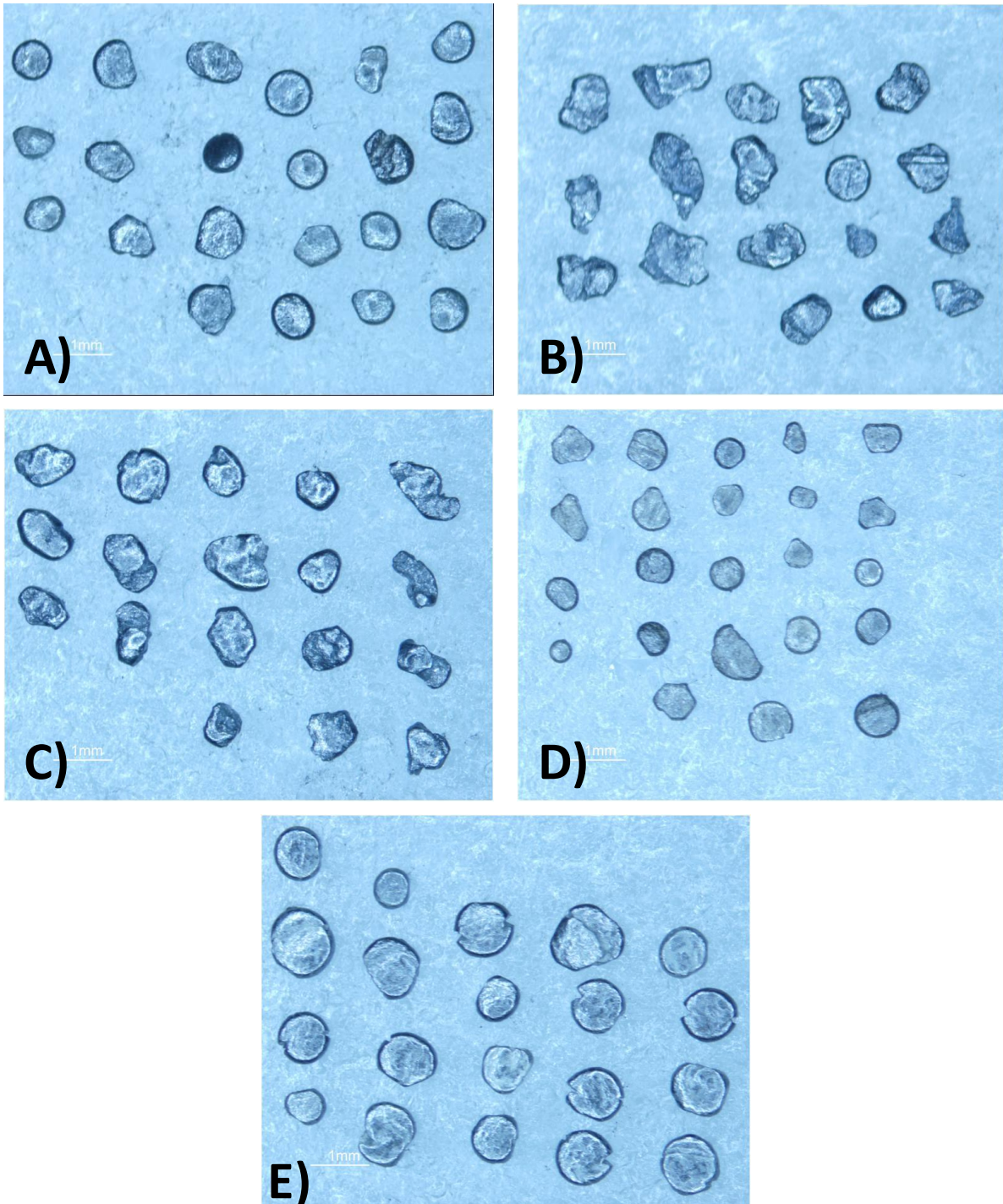


Figure A.4.1.1 Representative pictures of (A) Win9Pb, (B) Rem9Pb, (C) Fed9Pb, (D) Horn9Pb, and (E) PMC9Pb taken with front lighting.

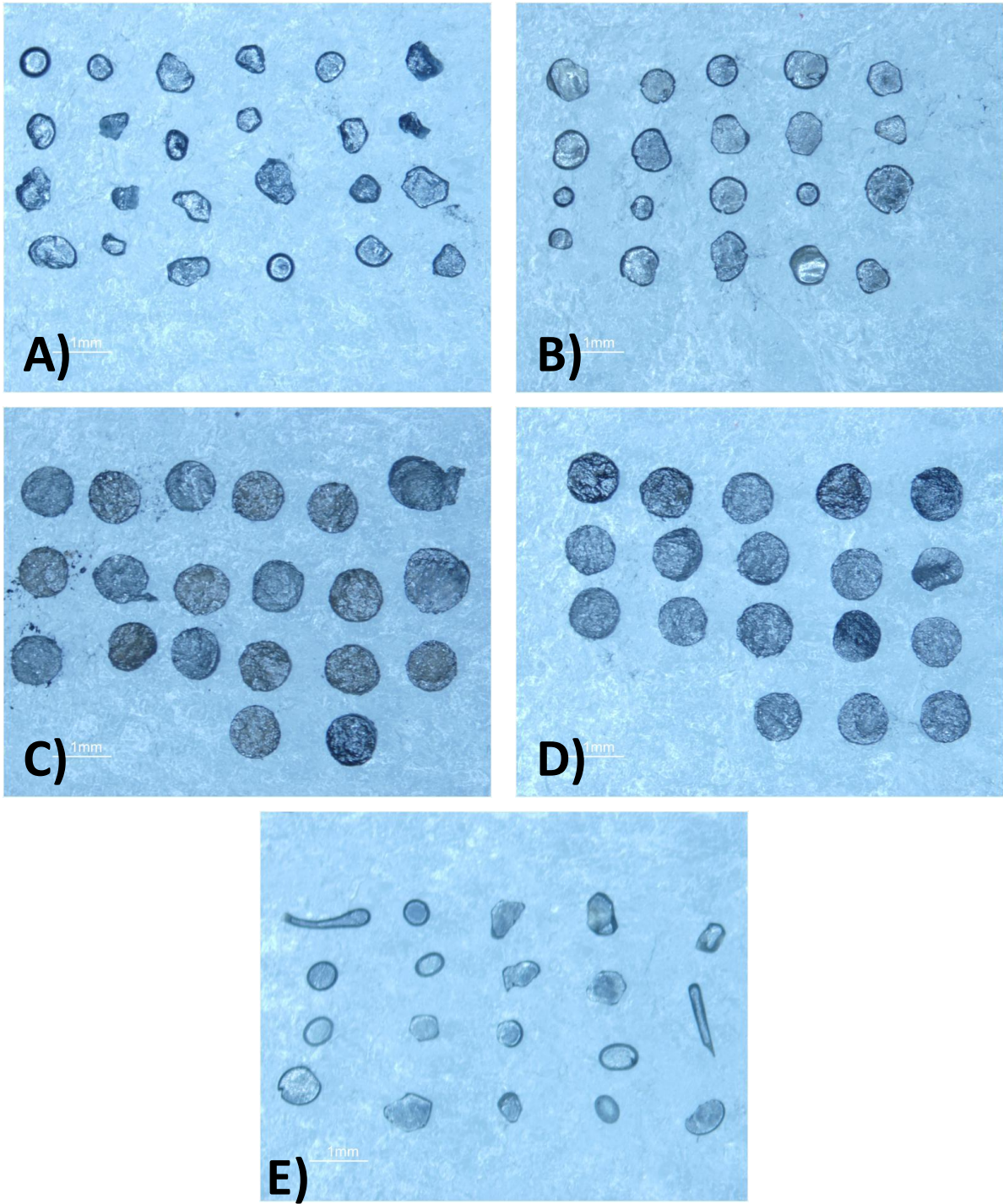


Figure A.4.1.2 Representative pictures of (A) Win9NoPb, (B) Rem9NoPb, (C) Bzr9NoPb, (D) Mag9NoPb, and (E) SB9NoPb taken with front lighting.

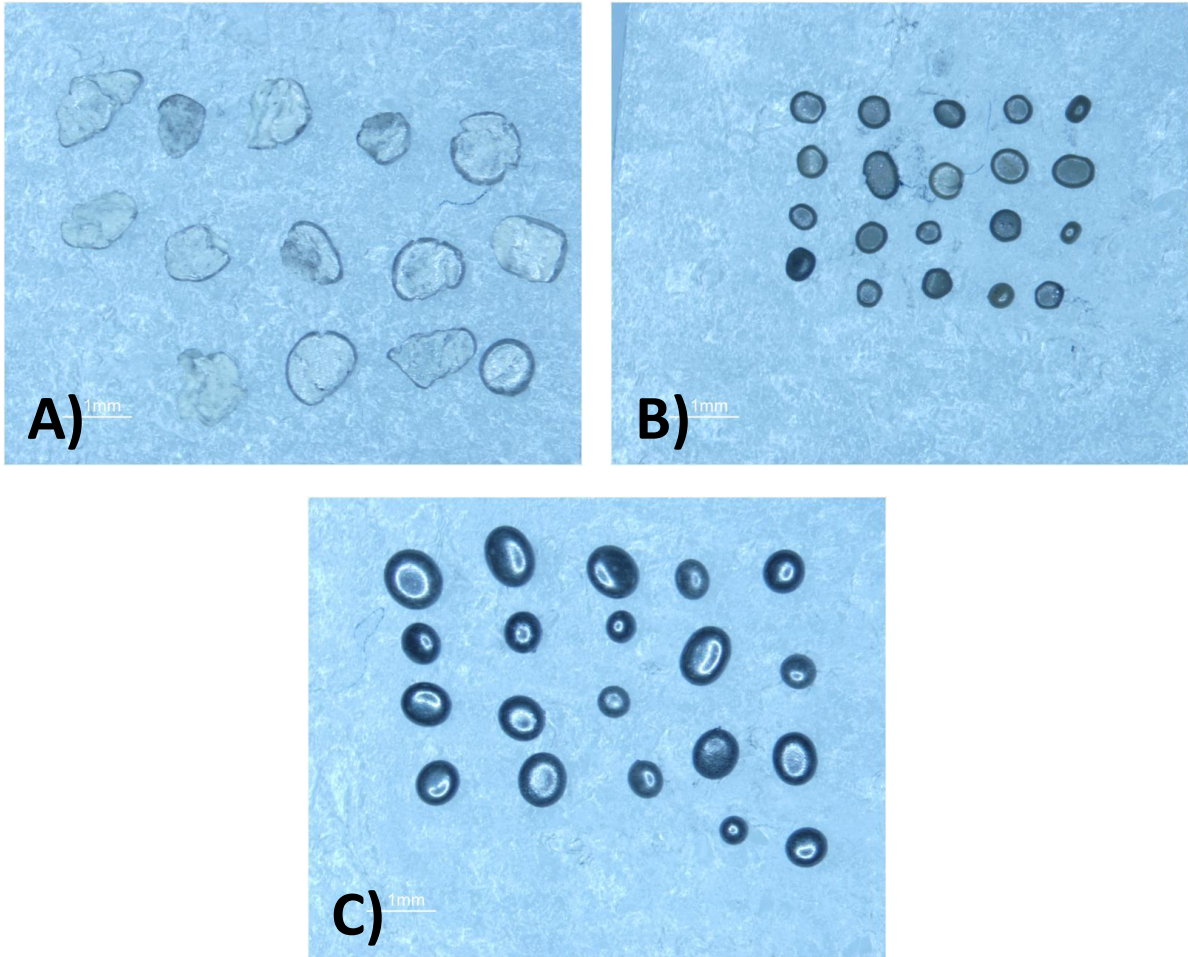


Figure A.4.1.3 Representative pictures of (A) Win12N, (B) PMC44N, and (C) SB7.62N taken with front lighting.

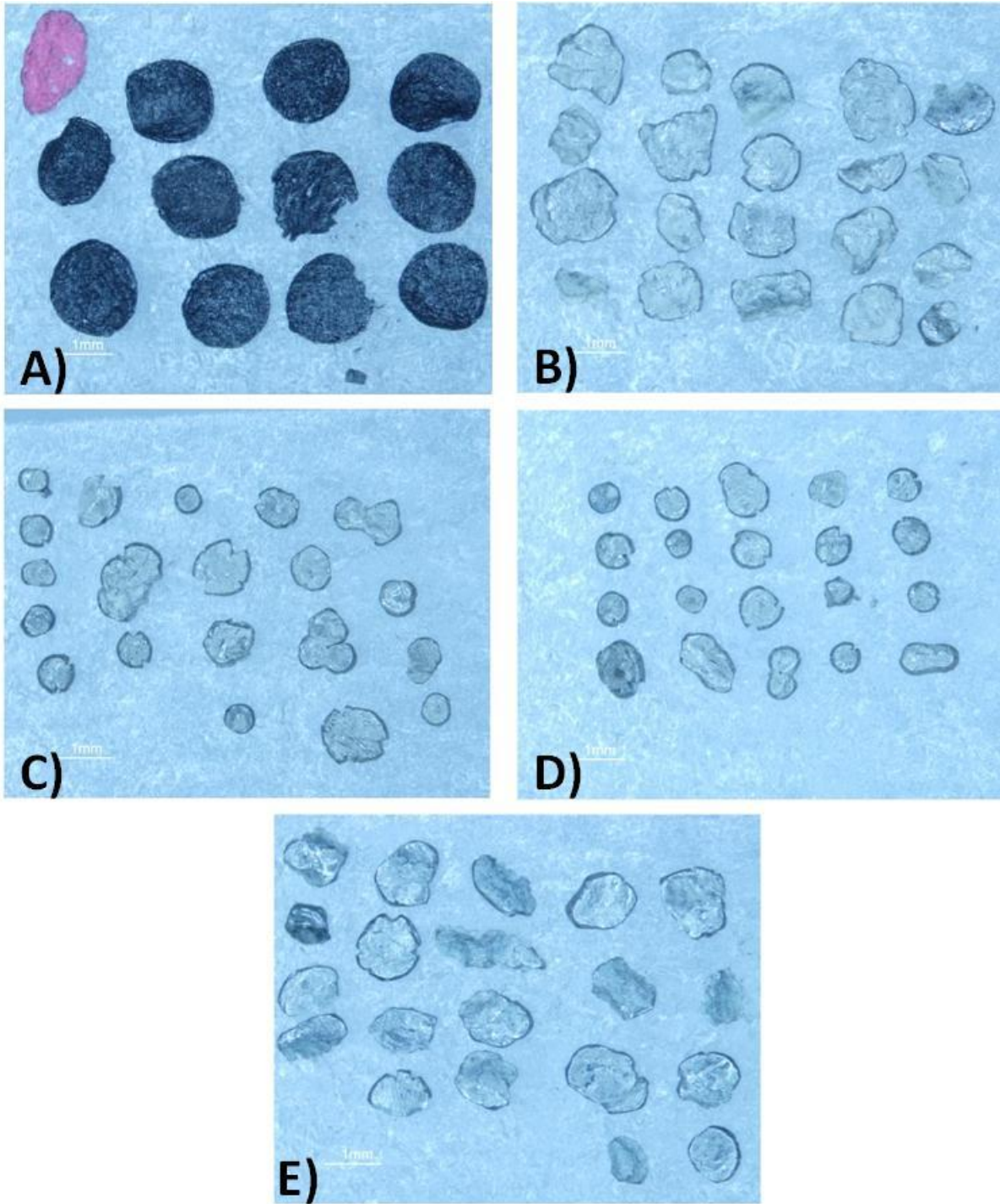


Figure A.4.1.4 All replicates of Win12A taken with front lighting.

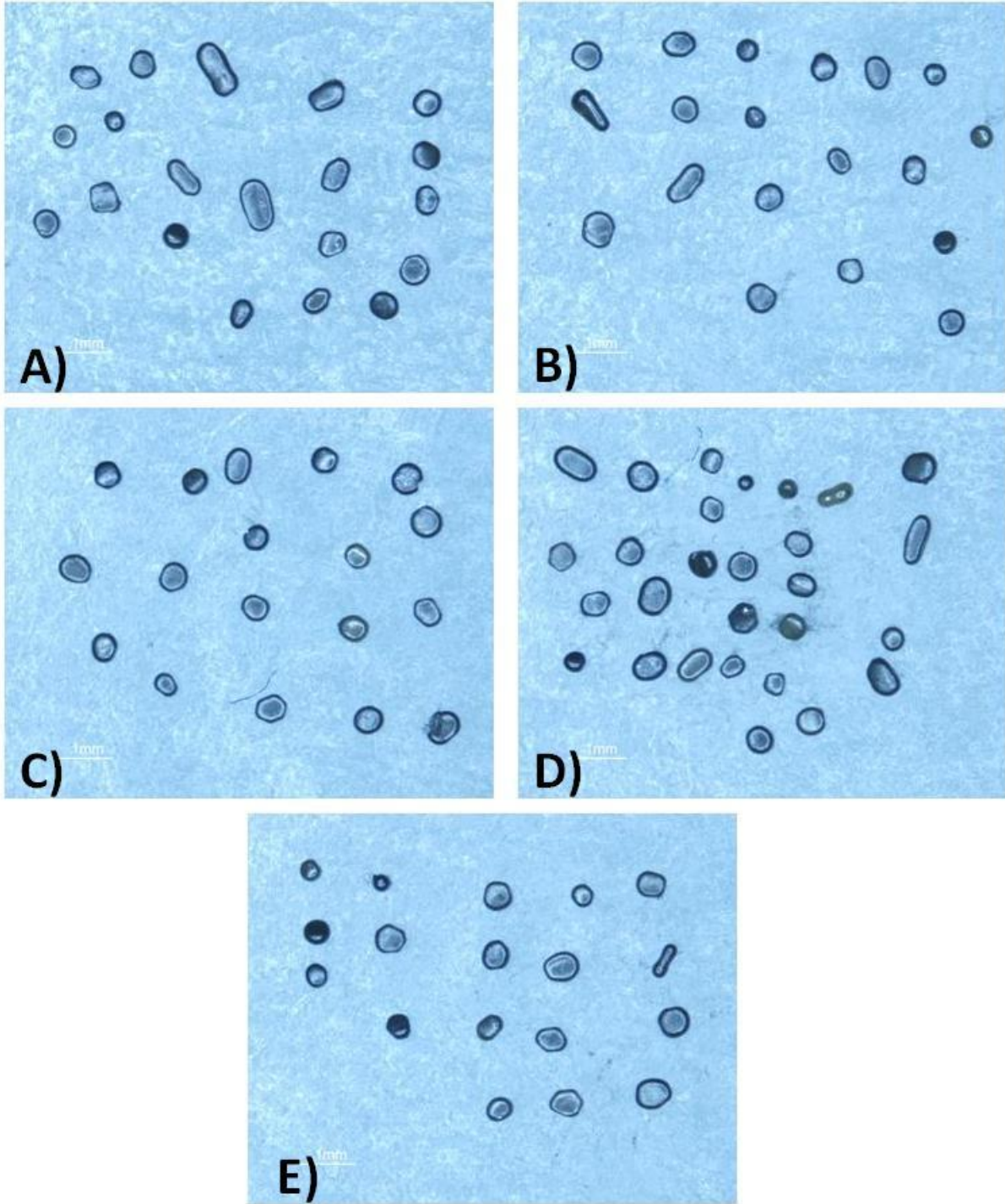


Figure A.4.1.5 All replicates of PMC44A taken with front lighting.

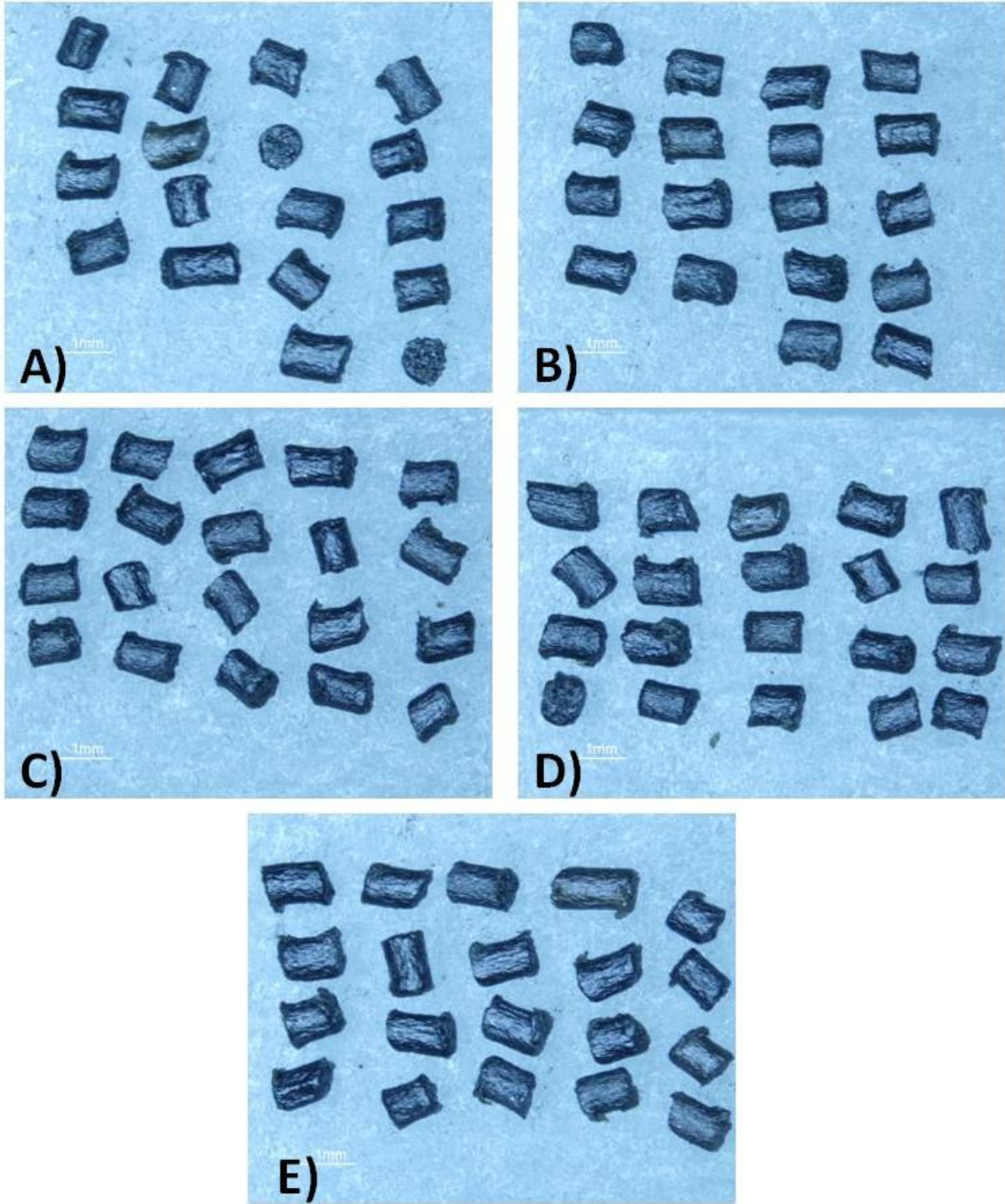


Figure A.4.1.6 All replicates of Mag7.62A taken with front lighting.

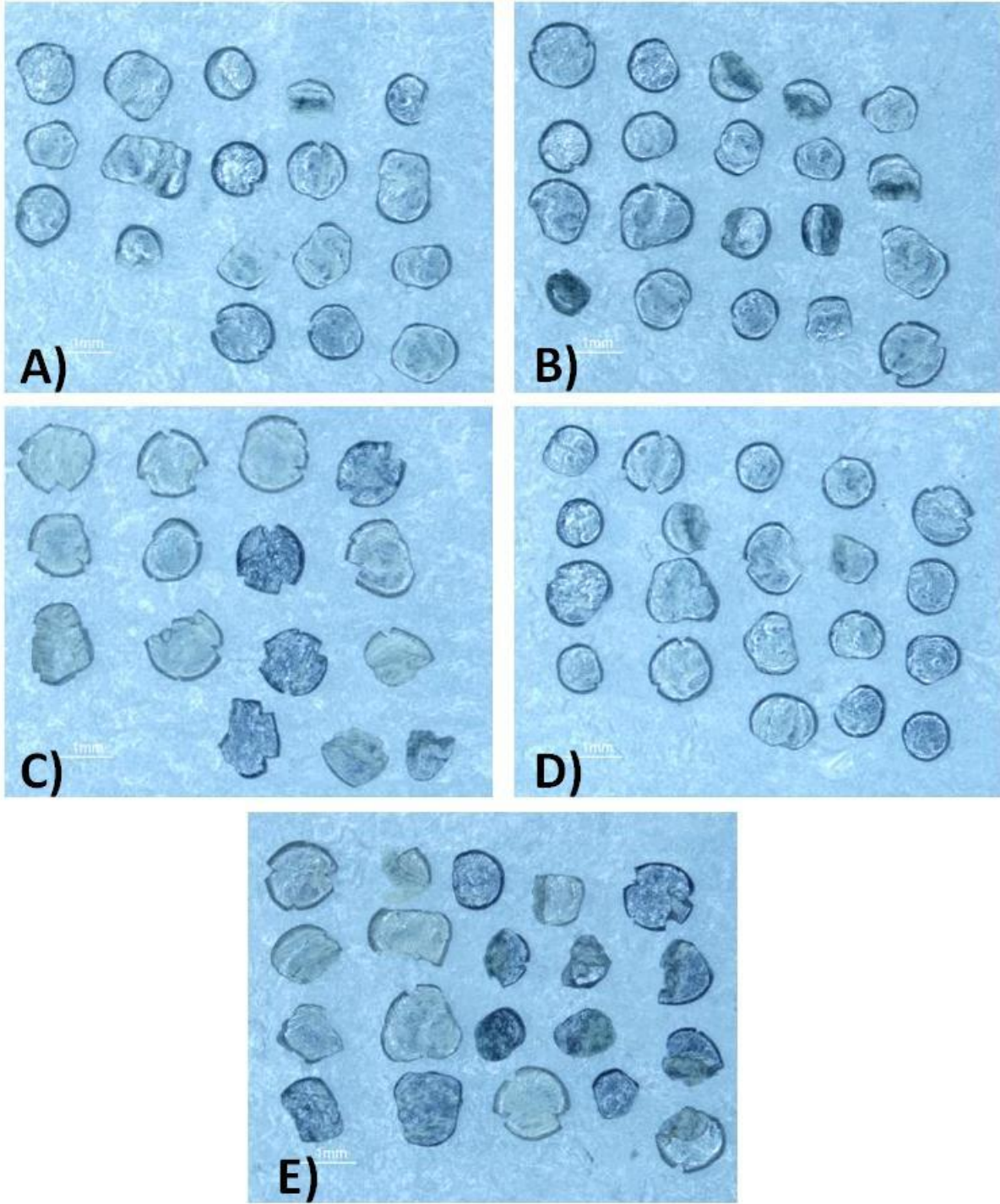


Figure A.4.1.7 All replicates of PMC9A taken with front lighting.

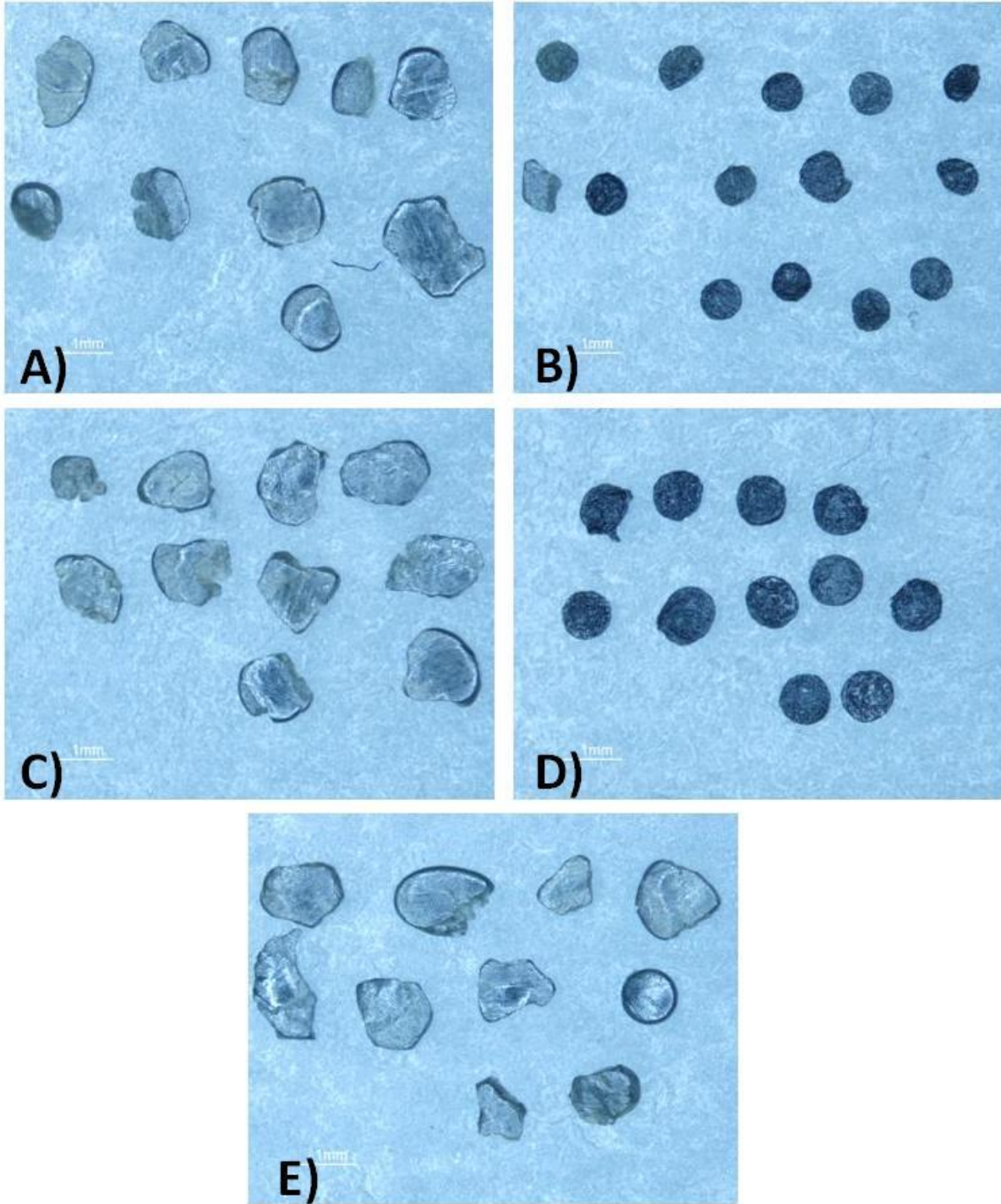


Figure A.4.1.8 All replicates of CCI22A taken with front lighting.

APPENDIX 4.2 Representative Chromatograms of the Chemical Profile from Unburned Smokeless Powders

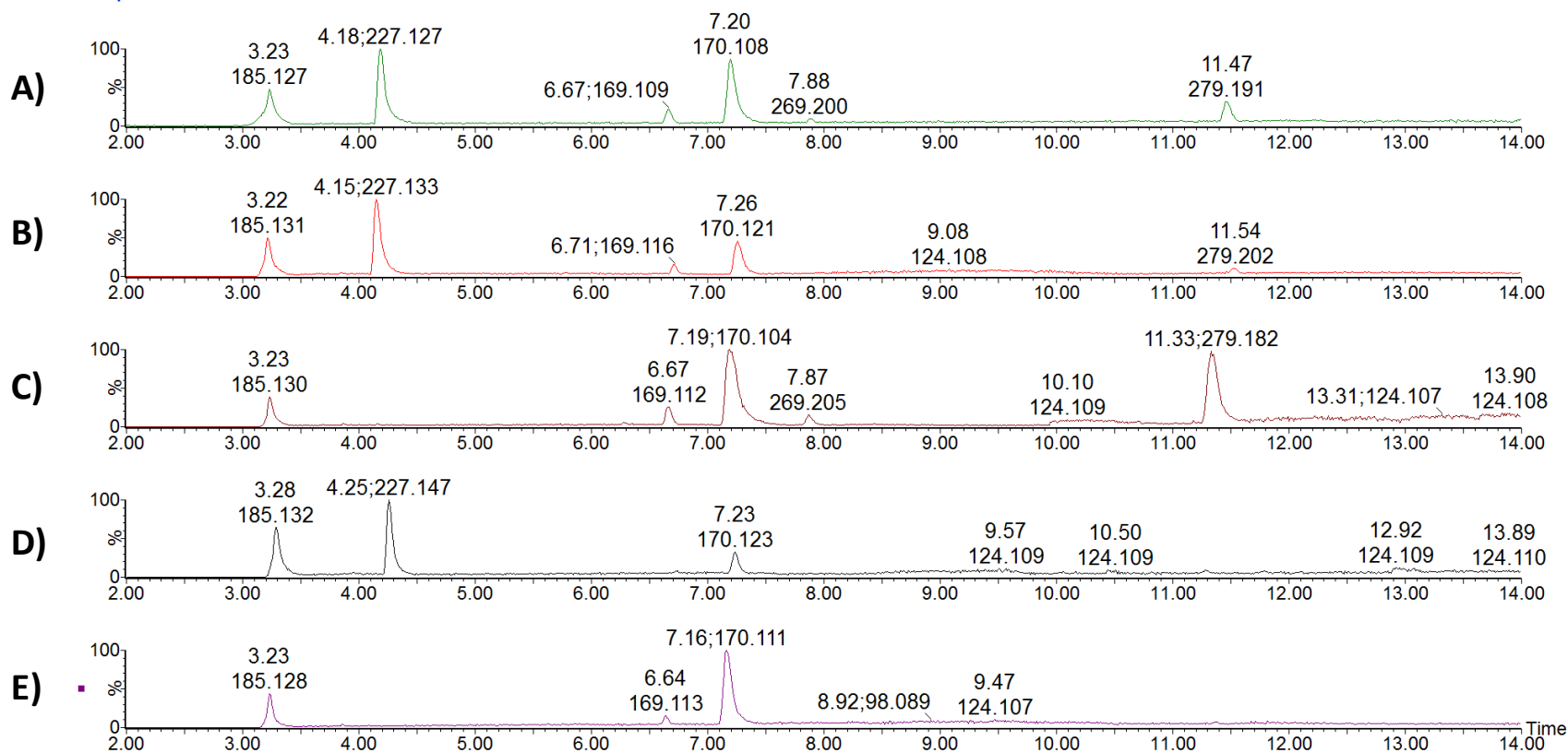


Figure A.4.2.1 Representative chromatograms of (A) Win9Pb, (B) Rem9Pb, (C) Horn9Pb, (D) Fed9Pb, and (E) PMC9Pb.

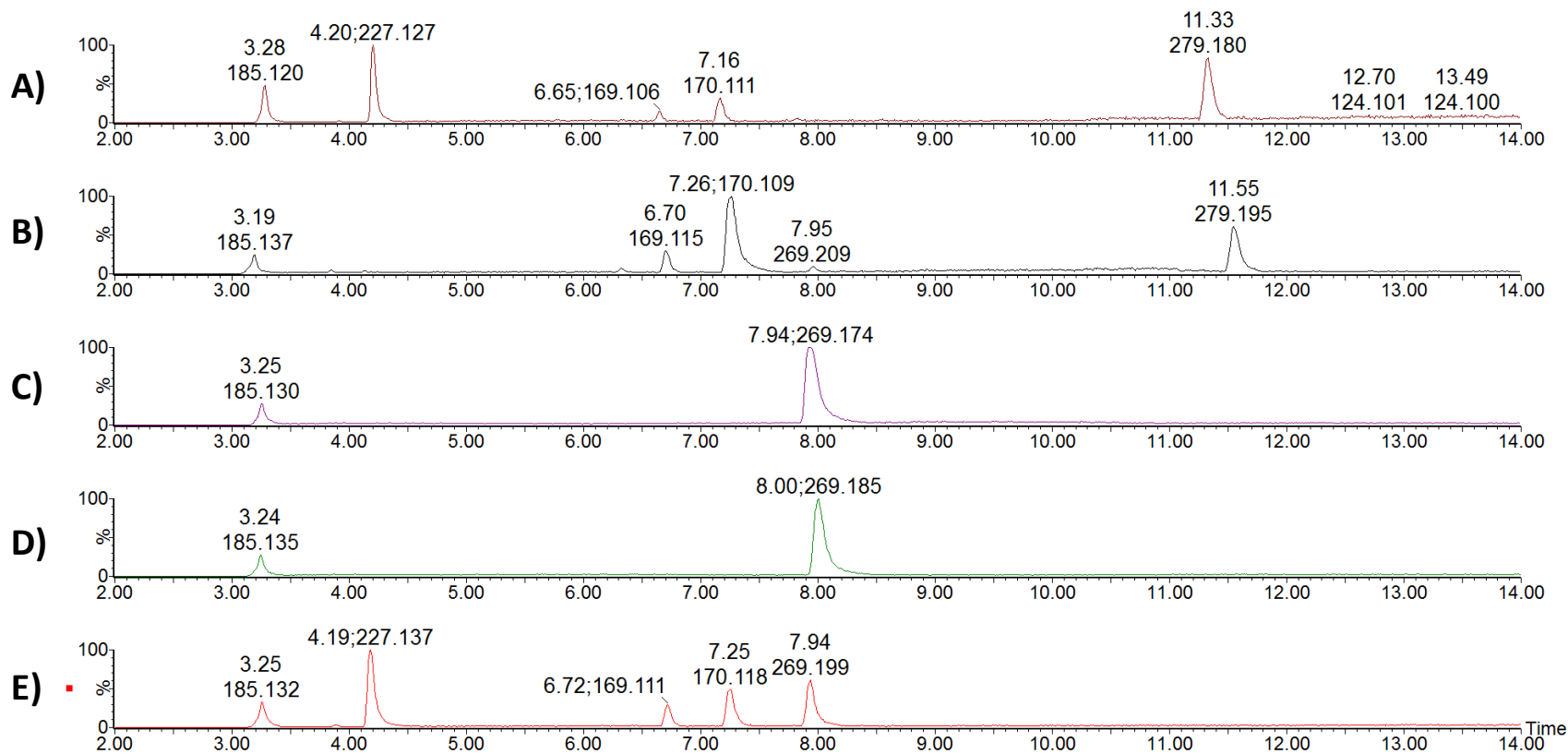


Figure A.4.2.2 Representative chromatograms of (A) Win9NoPb, (B) Rem9NoPb, (C) Bzr9NoPb, (D) Mag9NoPb, and (E) SB9NoPb.

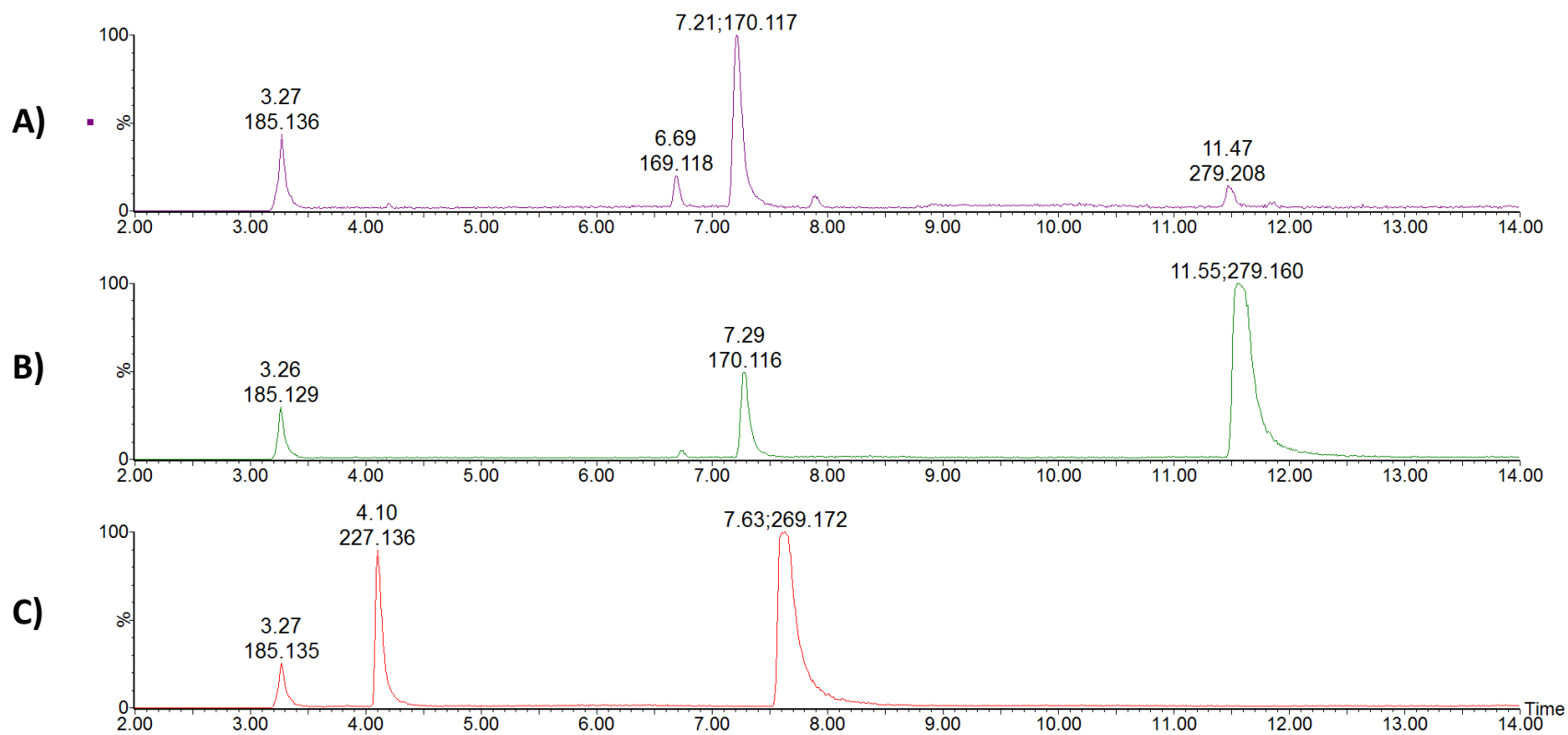


Figure A.4.2.3 Representative chromatograms of (A) Win12N, (B) PMC44N, and (C) SB7.62N.

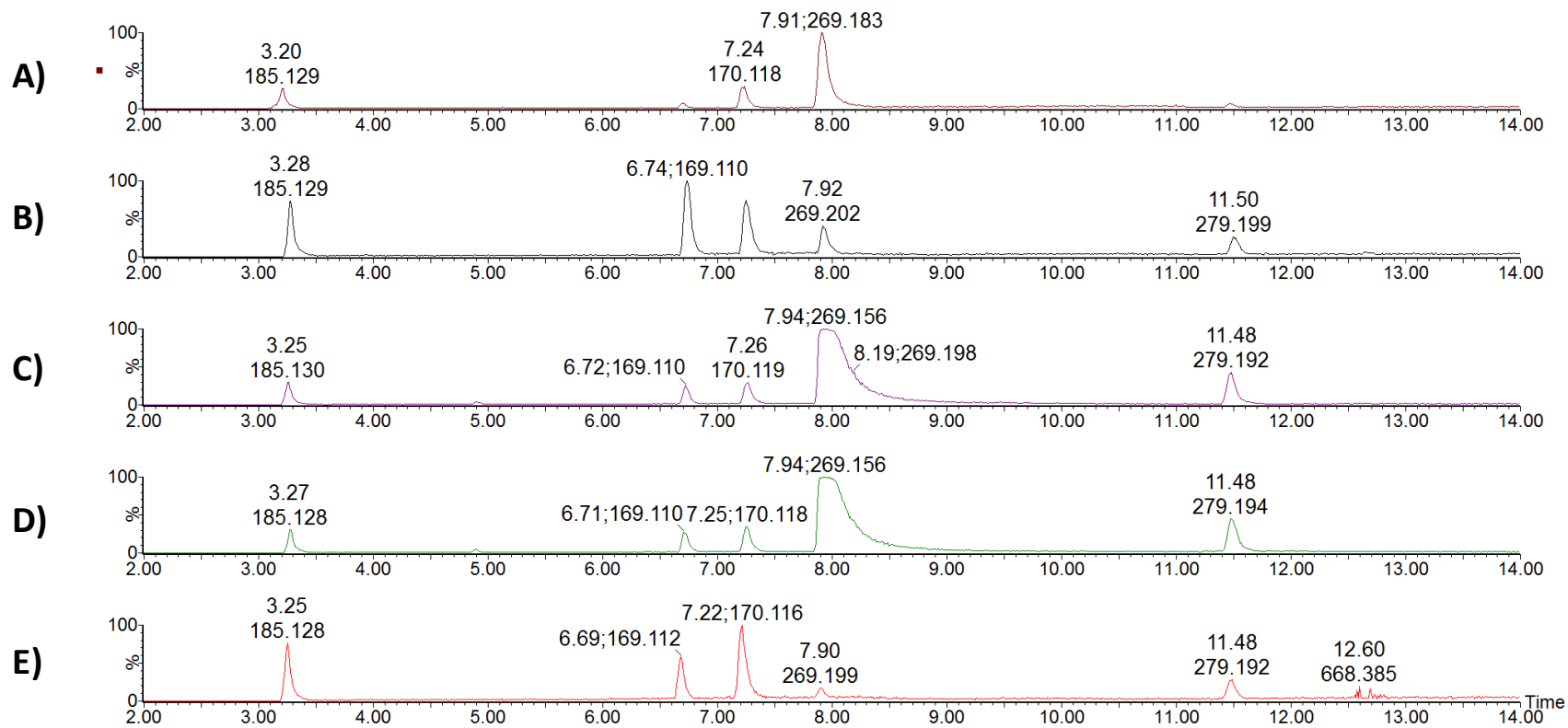


Figure A.4.2.4 Chromatograms for Replicates 1-5 (A-E) of Win12A.

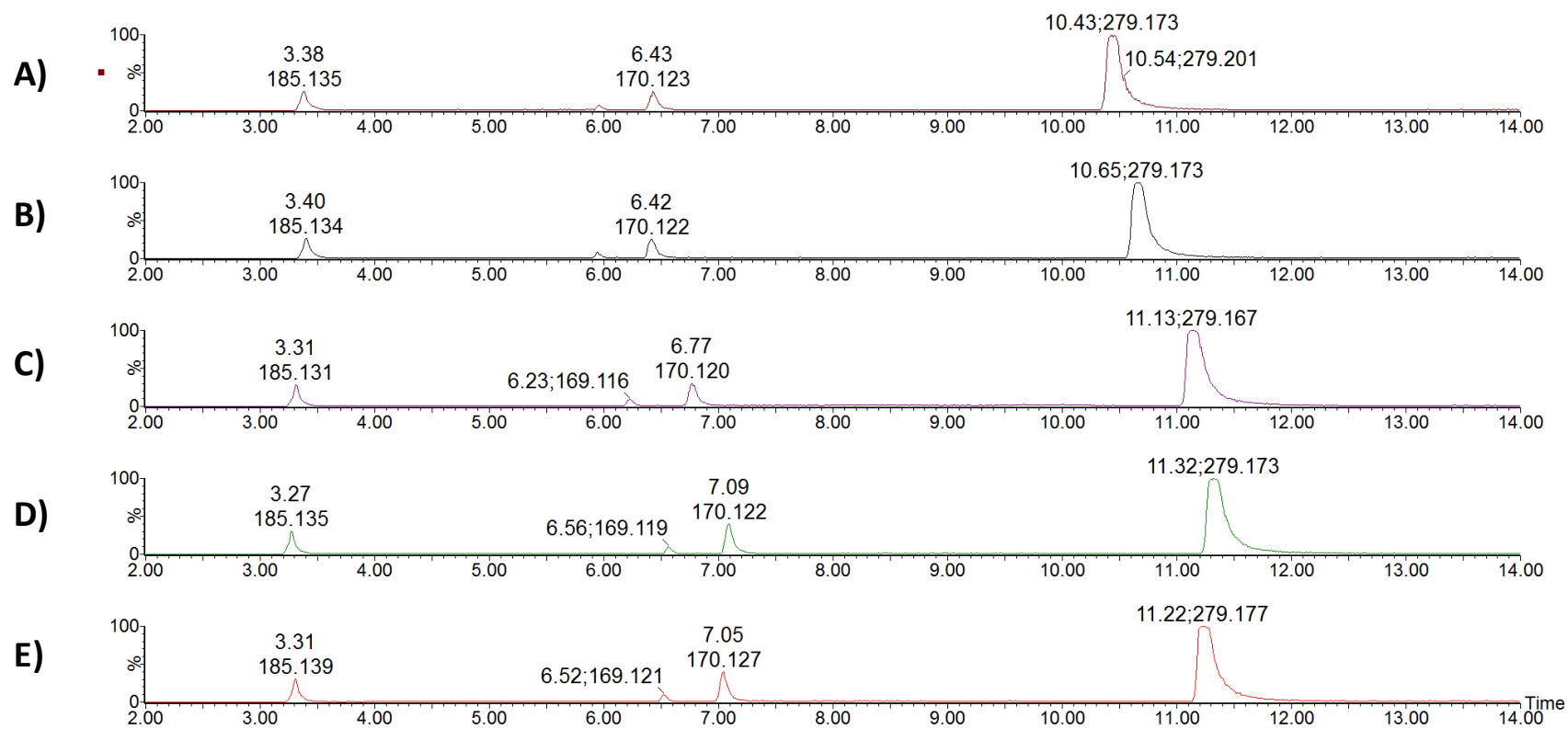


Figure A.4.2.5 Chromatograms for Replicates 1-5 (A-E) of PMC44A

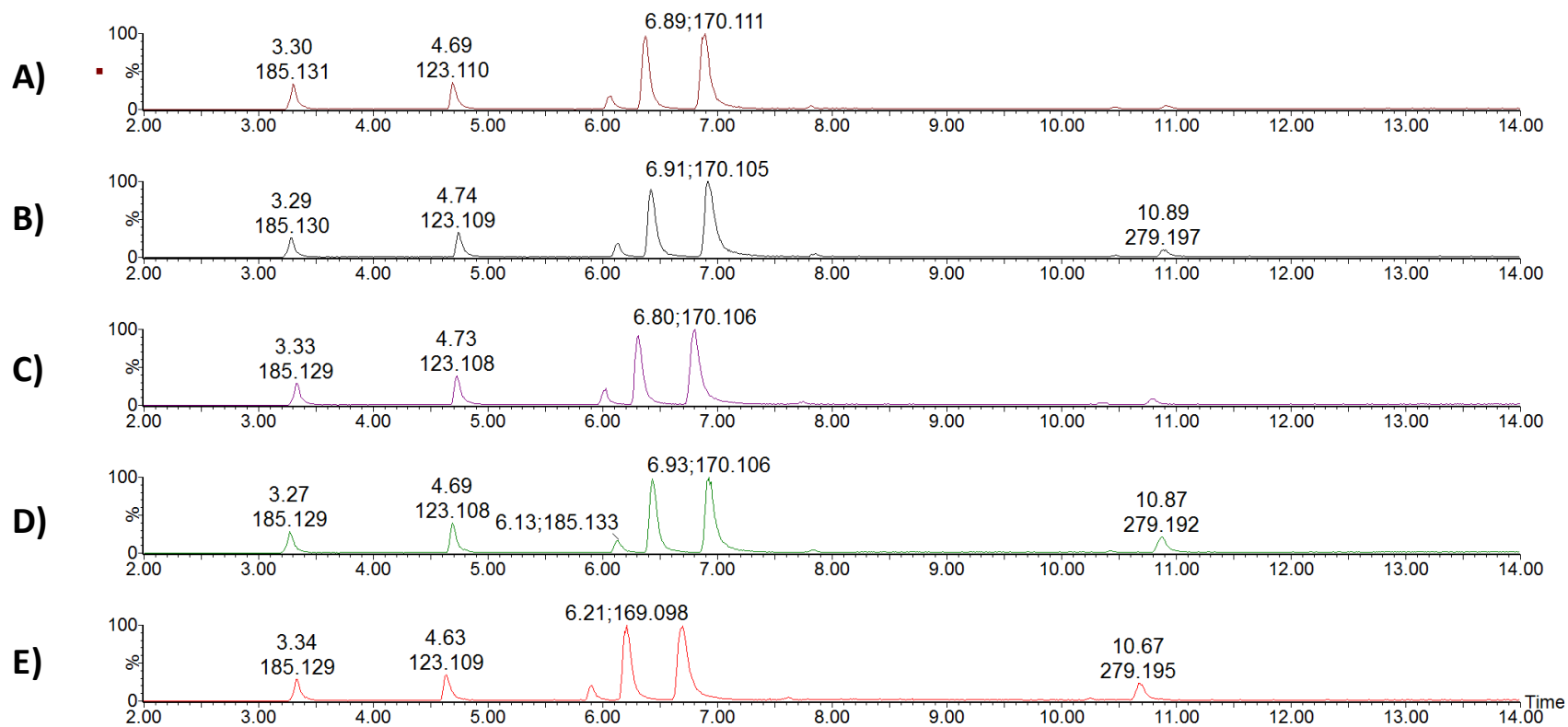


Figure A.4.2.6 Chromatograms for Replicates 1-5 (A-E) of Mag7.62A

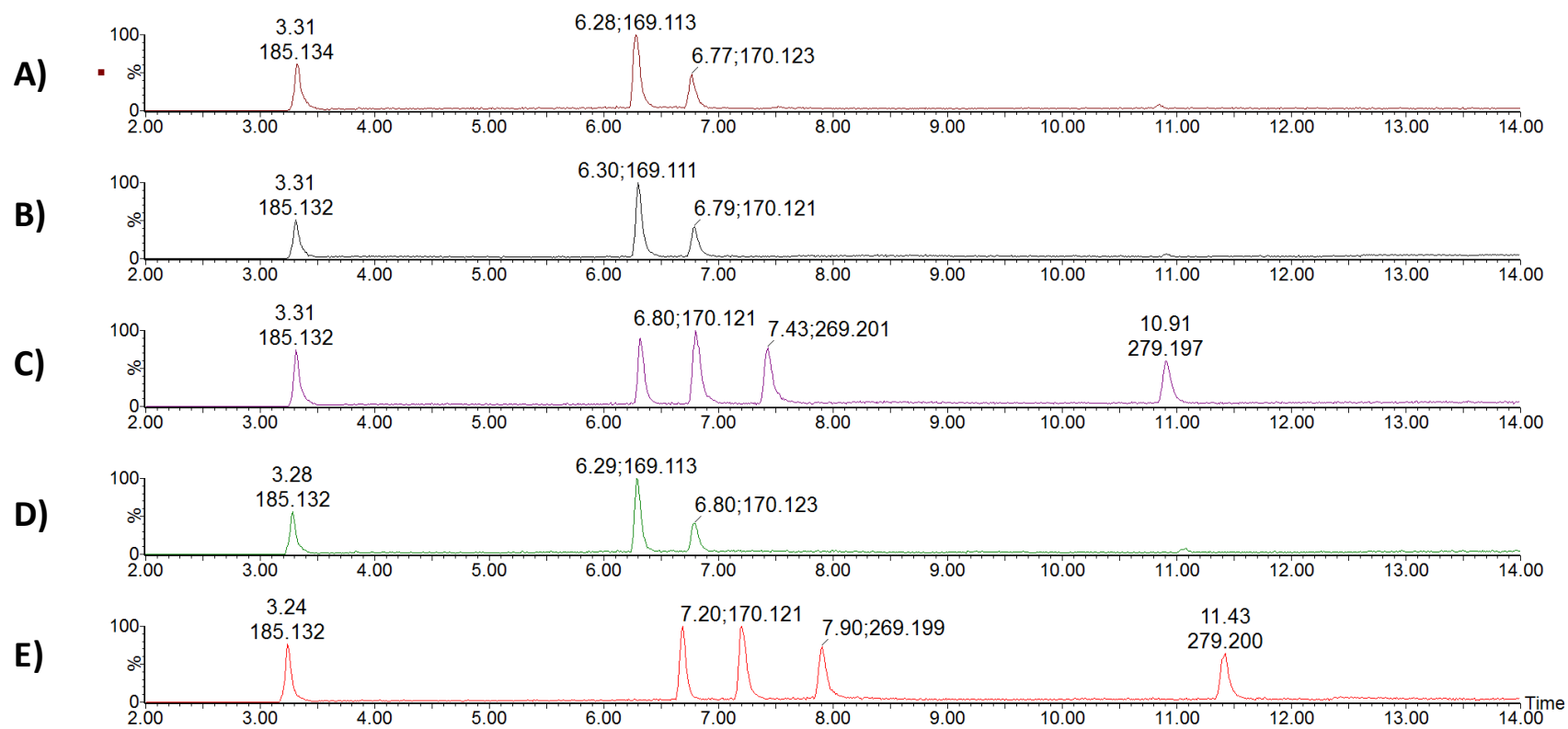


Figure A.4.2.7 Chromatograms for Replicates 1-5 (A-E) of PMC9A

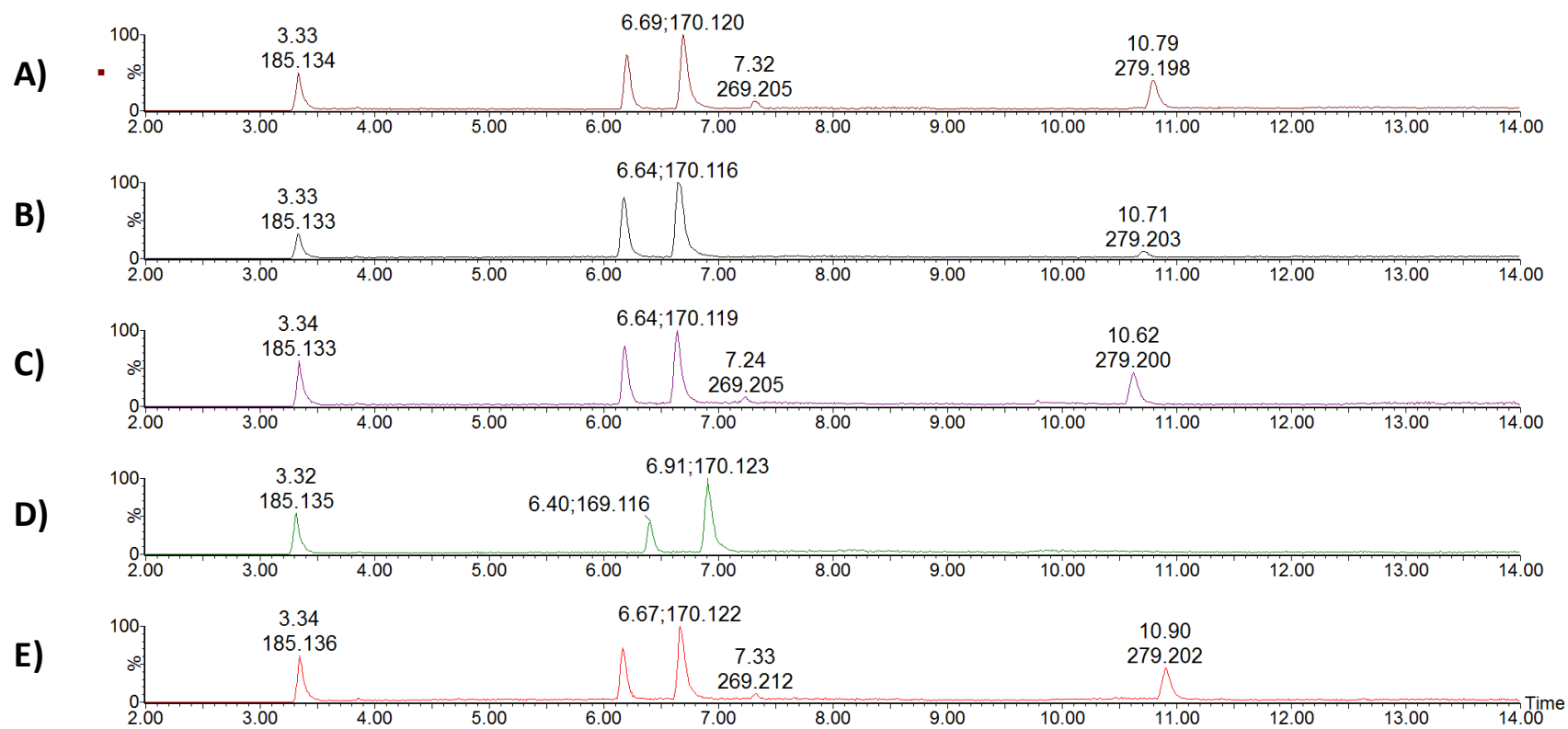


Figure A.4.2.8 Chromatograms for Replicates 1-5 (A-E) of CCI2

APPENDIX 4.3 Morphological Characteristics for Unburned Smokeless Powders

Table A.4.3.1 Summary of Morphological Characteristics for Unburned Smokeless Powders

<u>Cartridge Identifier</u>	<u>Color</u>	<u>Morphology (SWGFE Database)</u>	<u>Presence of Perforation</u>	<u>Distinguishing features (teardrop, dumb bells, texture)</u>	<u>Luster (Dull, Shiny)</u>	<u>Colored Marker</u>	<u>Length (mm)</u>	<u>Standard Deviation of Length (mm)</u>	<u>Thickness (mm)</u>	<u>Standard Deviation of Thickness (mm)</u>
<u>Win9Pb</u>	Gray	Flattened Ball and Irregular Flattened Ball	No	Smooth	Dull	No	0.776	0.098	0.239	0.037
<u>Rem9Pb</u>	Gray	Irregular with Flattened Ball	No	Rough Surface	Dull	No	0.892	0.171	0.187	0.017
<u>Fed9Pb</u>	Gray	Irregular with Flattened Ball	No	Rough Surface	Dull	No	0.865	0.113	0.197	0.022
<u>Horn9Pb</u>	Gray	Flattened Ball and Irregular Flattened Ball	No	Smooth	Dull	No	0.602	0.113	0.167	0.025
<u>PMC9Pb</u>	Gray	Flattened Ball	No	Smooth	Dull	No	0.903	0.116	0.253	0.018
<u>Win9NoPb</u>	Gray	Flattened ball and irregular	No	Rough Surface	Dull	No	0.580	0.084	0.173	0.029
<u>Rem9NoPb</u>	Gray	Flattened Ball and Irregular Flattened Ball	No	Smooth	Dull	No	0.613	0.11	0.162	0.015
<u>Bzr9NoPb</u>	Black	Disk	No	Rough surface	Dull	No	0.914	0.063	0.208	0.026
<u>Mag9NoPb</u>	Black	Disk	No	Rough surface	Dull	No	0.895	0.045	0.207	0.014
<u>SB9NoPb</u>	Gray	Flattened ball and irregular	No	Smooth surface; Rods, dumb bells	Dull	No	0.510	0.097	0.176	0.025
<u>Win12N</u>	Gray/White	Irregular flattened balls/flakes	No	Slightly rough surface, flakes	Dull	No	1.030	0.12	0.175	0.02

<u>PMC44N</u>	Black	Flattened Ball	No	Smooth surface; Rods	Dull	No	0.448	0.059	0.172	0.012
<u>SB7.62N</u>	Gray	Flattened ball and ball	No	Smooth surface; Tear-drops, rods	Shiny	No	0.646	0.124	0.35	0.041
<u>Win12A, Rep 1</u>	Black	Disk	No	Rough surface	Dull	Pink Flakes	1.496	0.068	0.131	0.033
<u>Win12A, Rep 2,5</u>	Gray	Irregular flattened disks	No	Rough surface; flakes	Dull	No	1.025	0.165	0.183	0.036
<u>Win12A, Rep 3,4</u>	Gray/green	Flattened Ball and Irregular Flattened Ball	No	Smooth	Dull	No	0.572	0.141	0.207	0.028
<u>PMC44A</u>	Black	Flattened balls	No	Smooth surface; Rods	Dull	No	0.389	0.069	0.185	0.027
<u>PMC9A, Rep 1,2,4</u>	Gray	Flattened Ball and Irregular Flattened Ball	No	Smooth	Dull	No	0.916	0.187	0.254	0.031
<u>PMC9A, Rep 3,5</u>	gray-green	Irregular with Flattened Ball	No	Smooth and Rough Surface	Dull	No	1.034	0.143	0.215	0.042
<u>CCI22A, Rep 1,3,5</u>	Black/green	Flattened Ball and Irregular Flattened Ball	No	Smooth and Rough Surface, striations	Dull	No	1.214	0.258	0.257	0.042
<u>CCI22A, Rep 2</u>	Black	Disk	No	Rough; some elongation	Dull	Green Flakes	0.704	0.059	0.17	0.028
<u>CCI22A, Rep 4</u>	Black	Disk	No	Rough; some flattened balls	Dull	No	0.833	0.048	0.263	0.034
<u>Mag7.62A</u>	Black	Cylinder (Tubular)	Yes	Rough surface	Dull	No	0.884	0.109	0.698	0.056

Note: In Aged samples, "Rep" refers to the replicate number, each a differentiable morphology. For example, "Rep 2" refers to replicate 2 of a powder

REFERENCES

REFERENCES

1. Department of Forensic Science Trace Evidence Procedures Manual. In: Science VDoF, editor. Virginia; 2015.
2. Scherperel G, Reid G, Waddell Smith R. Characterization of smokeless powders using nanoelectrospray ionization mass spectrometry (nESI-MS). *Anal Bioanal Chem.* 2009 2009/08/01;394(8):2019-28.
3. Meyer R, Kohler J, Homburg A. *Explosives.* Weinheim: Wiley, 2007.
4. Li, F. et al. Detection and Characterization of Chemical Attribute Signatures from Smokeless Powders by Dynamic Headspace Concentration and DART-MS. *ASMS 2013.*
5. Yinon J, editor. *Advances in Analysis and Detection of Explosives:* Springer, 1993.
6. Moorehead W. Characterization of Smokeless Powders. *Forensic Analysis on the Cutting Edge:* John Wiley & Sons, Inc.; 2007;241-68.
7. Platten WE, 3rd, Bailey D, Suidan MT, Maloney SW. Biological transformation pathways of 2,4-dinitro anisole and N-methyl paranitro aniline in anaerobic fluidized-bed bioreactors. *Chemosphere.* 2010 Nov;81(9):1131-6.

CHAPTER FIVE: Association and Discrimination of Burned Commercial Smokeless Powder Residue Using Chemical Properties and Multivariate Statistical Analysis

5.1 Introduction

In this study, ammunition cartridges from each commercial brand were fired to assess changes in the chemical profile after combustion. Each ammunition was denoted using the same abbreviations as given in Table 3.1. Changes in the chemical profiles as a result of firing were assessed. The chemical profiles from the residue of burned smokeless powders were individually compared to the chemical profiles of their corresponding unburned counterparts through principal component analysis (PCA) and hierarchical cluster analysis (HCA). The extent of association and discrimination of burned powders to their unburned counterparts was affected by the firing process.

5.2 Analysis of Organic Compounds within Burned Smokeless Powders

5.2.1 Identification and Comparison of Chemical Profiles from Burned Smokeless Powders

The extracted residue of five fired cartridges from each smokeless powder brand was separated through High Performance Liquid Chromatography (HPLC) and detected through mass spectrometry, specifically an atmospheric pressure chemical ionization (APCI) source coupled with a multiplexed-collision induced dissociation (multiplexed-CID) on a time-of-flight mass spectrometer (TOF-MS). Replicates from each burned powder residue were compared to assess the similarity of the chemical profiles across each ammunition box. Figure 5.1 displays representative total ion chromatograms (TIC) for Win9Pb at a collision energy of 10 V for the unburned powder and all five extracted residues after firing. This collision energy was selected to display primarily molecular ions. The unburned powder showed 1-methyl-3,3-diphenylurea,

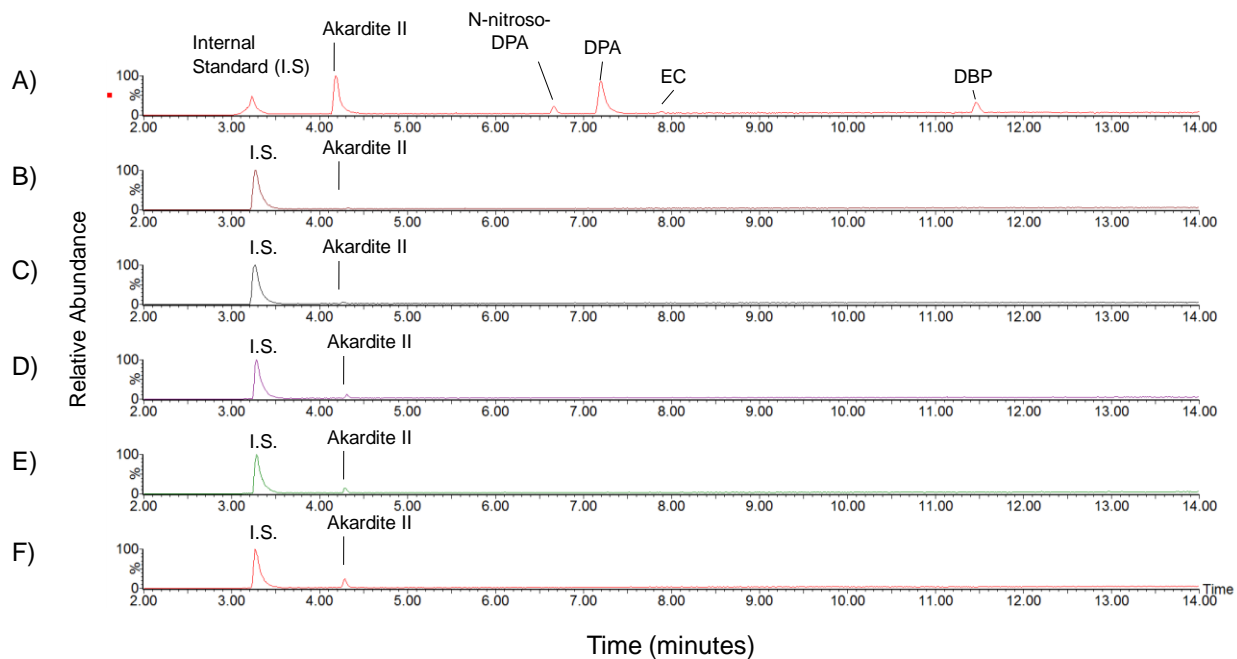


Figure 5.1 Chromatograms of smokeless powder extracts from (A) unburned Win9Pb, and five replicates of burned Win9Pb (B-F)

commonly known as akardite II, N-nitroso-diphenylamine (N-nitroso-DPA), diphenylamine (DPA), ethyl centralite (EC), and dibutyl phthalate (DBP), all present at large abundances within the chromatogram.

Subsequently, the burning process converted most of the solid smokeless powder to gaseous products. For example, when examining the chemical profiles of the burned residue of Win9Pb, only akardite II was observed at an appreciable amount relative to the internal standard, albeit at a substantially lower abundance than in the unburned powder.

Due to the low abundance of Akardite II in the TIC, extracted ion chromatograms (XIC) were generated, corresponding to the m/z of the molecular ion in each compound of interest. Representative XICs for Win9Pb replicate 4 are shown in Figure 5.2. From these, it was apparent that the residue contained DBP, EC, DPA, and N-nitroso-DPA, in addition to Akardite II. The remaining four residues all showed the same compounds although not necessarily at the same abundances due to the non-uniform distribution of residue within each spent ammunition cartridge. Representative XICs for extracts from all fired ammunitions collected at a collision energy of 10 V are shown in Appendix 5.1.

Figure 5.3 displays the relative abundance of DBP, EC, Akardite II, DPA, and N-nitroso-DPA in the extracts of the burned residues for all lead-containing and lead-free ammunition. While replicates of burned residues from different ammunitions contained the same qualitative profile, the abundances for each compound were not always comparable. This was attributed to the irreproducibility of burning during the firing process. Specifically, the efficiency of the combustion process within the cartridge was variable among replicates,

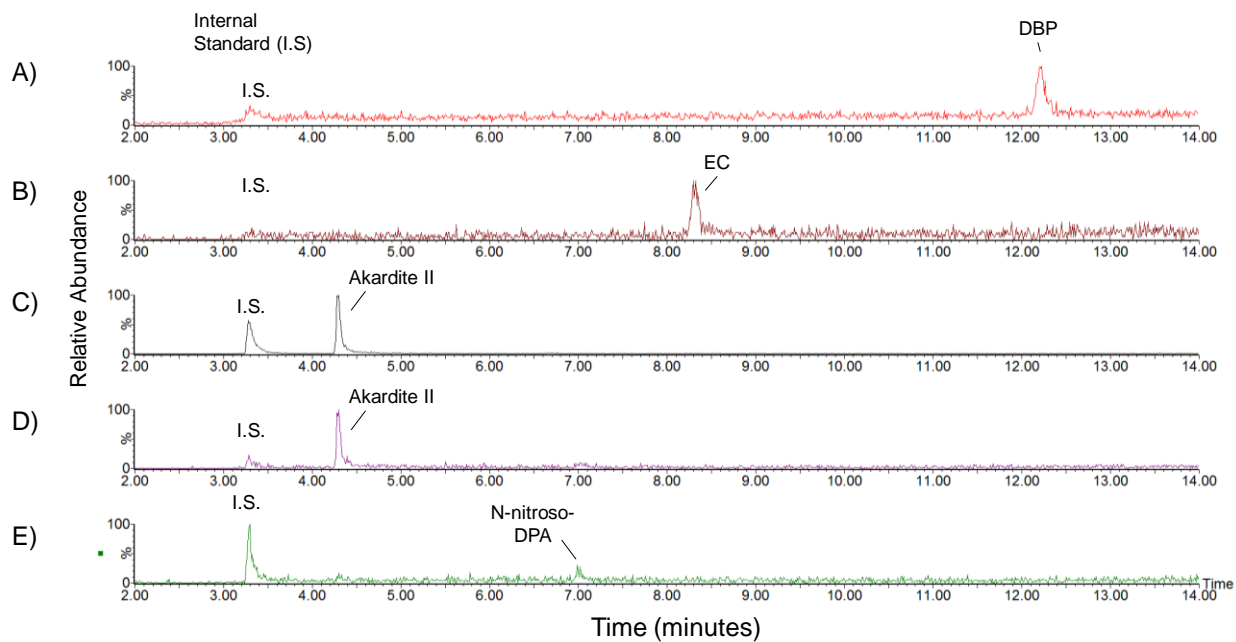


Figure 5.2 Representative XIC chromatograms of extract obtained from a fired cartridge of Win9Pb (Replicate 4) displaying the abundances of (A) dibutyl phthalate at m/z 279.2, (B) ethyl centralite at m/z 269.2, (C) akardite II at m/z 227.1, (D) diphenylamine at m/z 170.1, and (E) N-nitroso-diphenylamine at m/z 169.1.

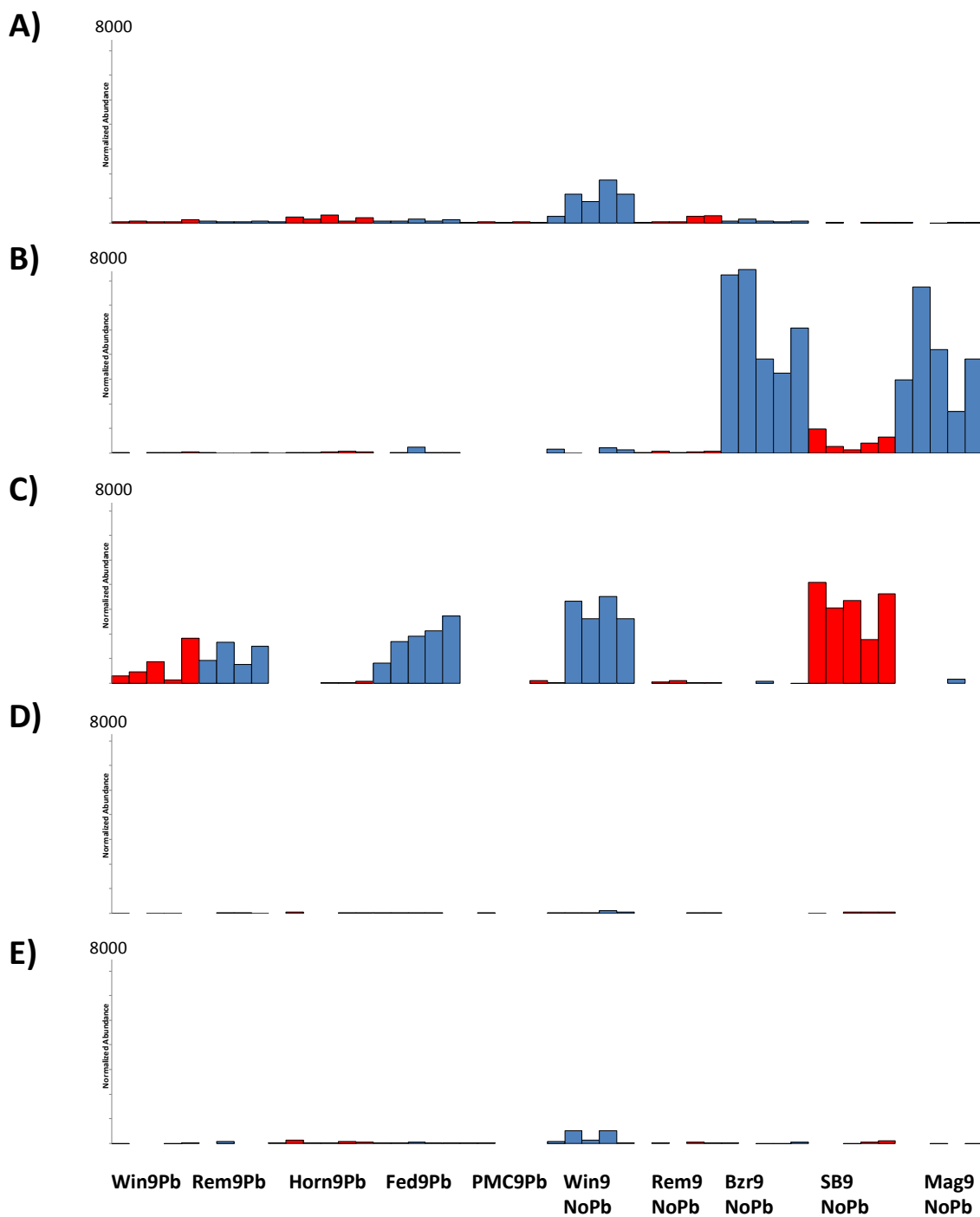


Figure 5.3 Graphical representation of the most abundant compounds across all chemical profiles of the extracts from fired cartridges of Pb vs NoPb: (A) DBP (m/z 279.2, t_R 12.12 minutes), (B) EC (m/z 269.2, t_R 8.45 minutes), (C) Akardite II (m/z 227.1, t_R 4.33 minutes), (D) DPA (m/z 170.1, t_R 7.75 minutes), and (E) N-nitroso-DPA (m/z 169.1, t_R 7.17 minutes). Alternating red and blue shading denote five replicates within an ammunition brand

leaving different abundances of residue for extraction from the cartridge. Differences in abundance among several ammunition brands were apparent across samples, such as the high abundance of EC or akardite II in select samples. DPA displayed the lowest abundance across all samples, likely as a result of its purpose as a stabilizer within the powder. This will be expanded upon when discussing the changes in chemical profiles between burned and corresponding unburned samples (Section 5.2.3).

Several comparisons among burned residues were made based upon previously determined morphologies. For example, Rem9Pb and Fed9Pb had indistinguishable morphologies (Section 4.2) and chemical composition in the unfired material (Section 4.3.3). Reference to Figure 5.3 showed the chemical profiles of the burned residues from these two powders also had similar qualitative profiles, with Akardite II being most prominent. However, the relative abundances of akardite II and the trace compounds were variable due to the irreproducibility of the burning during the firing process.

Unburned powders from Bzr9NoPb and Mag9NoPb had indistinguishable morphologies (Section 4.2); however, Bzr9NoPb was distinguished from Mag9NoPb based on the presence of DPA and abundance of N-nitroso-DPA (section 4.3.3). When comparing the burned residues, again XICs were used and indicated that DPA and N-nitroso-DPA were still present in Bzr9NoPb (Figure A.5.1.8) but not in Mag9NoPb (Figure A.5.1.10), allowing distinction of the two powders. Finally, samples that did not contain the same morphologies nor chemical composition in the unfired state likewise displayed distinguishing chemical features from extracts of the burned residues.

Extracts of burned residues from ammunition samples of at least 15 years of age were analyzed along with extracts from the corresponding burned residues of newly manufactured

samples. Figure 5.4 displays the normalized abundance of DBP, EC, Akardite II, DPA, and N-nitroso-DPA in extracts of residues from all aged ammunition and their newly manufactured counterparts. The burned residues extracted from the newly manufactured samples were consistent in the presence and ratio of compounds across all five replicates. For the aged ammunition, the samples designated 'U.S. Box' (Table 3.1) were obtained from the original packaging. Replicates residues extracted from these cartridges displayed a higher consistency in the presence and ratio of the compounds present. The aged ammunition samples designated 'U.S. Loose' were potentially obtained from different sources. These residues displayed varying chemical profiles across samples within the same brand.

The decrease in total abundance of organic compounds due to the burning process necessitated the use of XICs to investigate the individual compounds within the chemical profiles. The compound with the highest abundance was not consistent among replicates within each ammunition, which was attributed either to cartridges of different origin in the aged samples or different quantities of residue collected as a result of variation in the firing process. For most samples, DPA (Figure 5.4D) and N-nitroso-DPA (Figure 5.4E) were consistently present at low abundance, with the exception of PMC44N and PMC44A. Akardite II (Figure 5.4C), EC (Figure 5.4B), and DBP (Figure 5.4A) were present in high abundance in several samples.

The aged samples tended to show less reproducibility in the chemical profiles from burned residues as compared to the profiles from their newly manufactured counterparts. For example, Win12A contained great variability between replicates. Win12A replicates 1, 3, and 5 contained a notable amount of EC while the remaining replicates were depleted of EC. Multiple chemical profiles were recorded for different replicates within Win12A and other aged

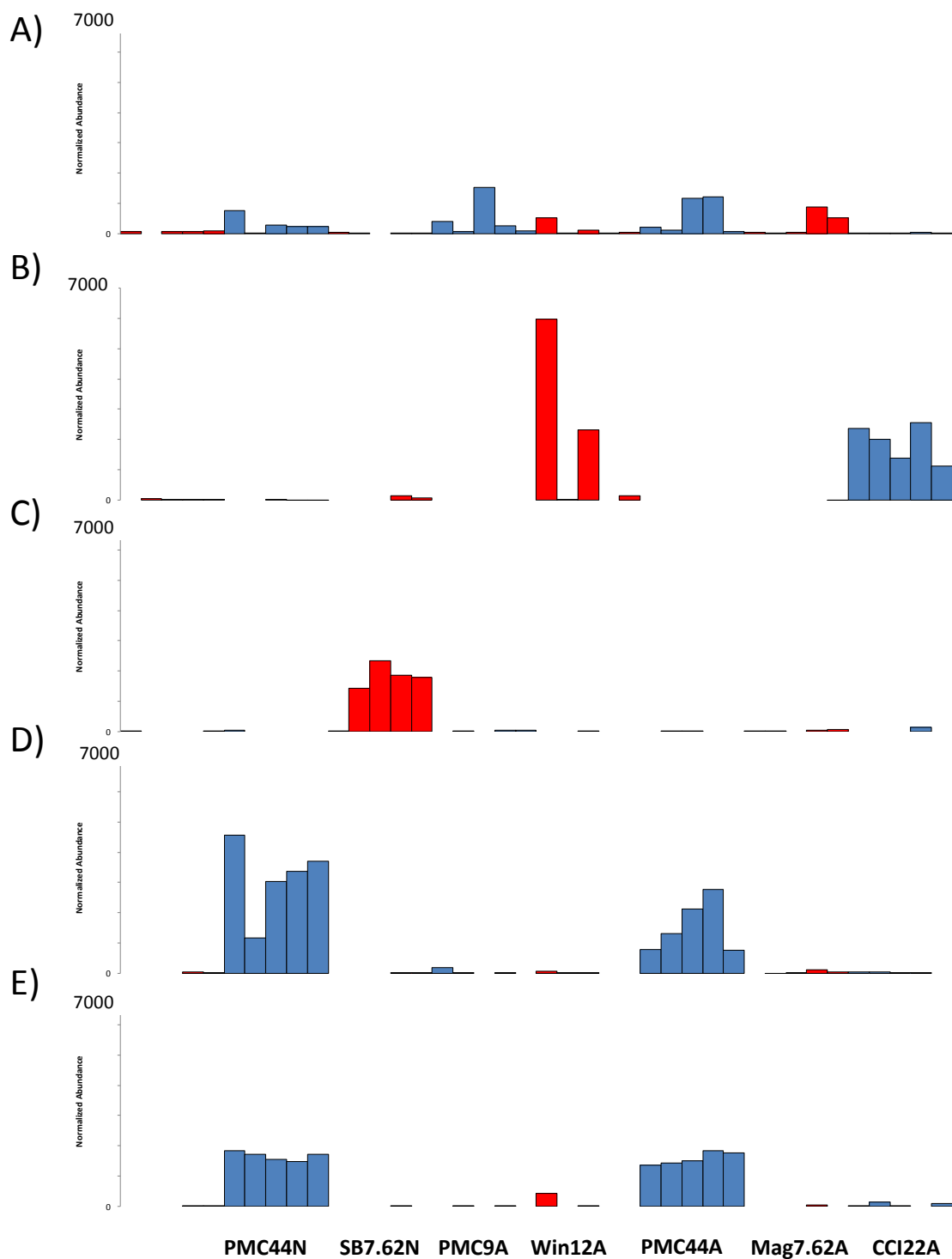


Figure 5.4 Graphical representation of the most abundant compounds across all chemical profiles of the aged and newly manufactured ammunition: (A) DBP (m/z 279.2, t_R 12.12 minutes), (B) EC (m/z 269.2, t_R 8.45 minutes), (C) Akardite II (m/z 227.1, t_R 4.33 minutes), (D) DPA (m/z 170.1, t_R 7.75 minutes), and (E) N-nitroso-DPA (m/z 169.1, t_R 7.17 minutes). Alternating red and blue shading denote five replicates within an ammunition brand.

ammunitions. With many of the aged samples, the designation of replicates 1-5 did not correspond to true replicates as it was not known whether the five cartridges actually originated from the same box. In contrast, Win12N and the newly manufactured samples consistently displayed similar qualitative profiles across a compound, but varied in their normalized abundances between replicates, which was attributed to variation in the firing process.

5.2.2 Comparison of Chemical Profiles between Burned and Corresponding Unburned

Smokeless Powders

When comparing the general chemical profiles of burned and corresponding unburned smokeless powders, differences were predominant in smokeless powders that contained DPA before firing. Many unburned smokeless powders, such as Horn9Pb, PMC9Pb, Rem9NoPb, Win12A, Mag7.62A, and CCI22A contained DPA as the most abundant compound. However, from the extracts of the burned smokeless powders, DPA (analyzed via XIC m/z 170.1) was either present in trace abundance or not detectable.

In addition to its role as a stabilizer, DPA has been shown to act as an antioxidant (1). The depletion of DPA was likely due to its interaction with nitrocellulose during the firing process. Nitrocellulose reacted with oxygen to produce gaseous products. There was generation and propagation of free radicals through the breakage of the nitrate ester bond (O-NO₂) within nitrocellulose, which lead to further free radical formation (1). Free radical production can be blocked with antioxidants. The abundance of DPA in smokeless powders, however, was insufficient to counteract the free radicals generated in the oxidation process. Therefore, this was a possible explanation to support the depletion of DPA after the firing process.

PMC44N and PMC44A, however, contained a high abundance of DPA and N-nitroso-DPA after firing. The chemical composition of each unburned smokeless powder sample contained a high abundance of DBP in addition to lower abundances of DPA and N-nitroso-DPA. A possible explanation for the ability of DPA to survive the combustion process may be the presence of DBP as an exterior coating around the propellant and DPA mixture. DBP is a known flame-deterrent, which is regularly applied to smokeless powders to control the burn rate and to produce constant pressure on the bullet during the firing process (2). A coating of EC has previously been reported for smokeless powders through MS imaging techniques (3). Residue of smokeless powders left post-firing could be from the inner core of the powder kernel, such as DPA. However, as MS imaging techniques were not utilized in this research, the coating hypothesis to explain the prevalence of DPA was not investigated further.

5.3 Multivariate Statistical Analysis of Chemical Profiles from Burned Smokeless Powders Compared to their Corresponding Unburned Counterparts

5.3.1 Introduction

The chemical profiles of the replicates from each ammunition were separately plotted against the chemical profiles of all unburned smokeless powders. Visual determination of the extent of association or discrimination was performed. Hierarchical cluster analysis was also performed on the data set to assess the extent of similarity of the burned residue to the unburned powder. The following sections illustrate different extents of association observed for the powders in the data set.

5.3.2 Example of Association by PCA and HCA

The scores plot and HCA dendrogram for a data set that included all unburned powders and the burned residue from SB9NoPb are shown in Figure 5.5. The burned residue replicates of SB9NoPb (red Xs) were positioned positively on PC 1 and positively on PC2. From the scores plot (Figure 5.5A), all five replicates were positioned closely to the unburned powder from SB9NoPb (blue *). The burned residue contained a high abundance of Akardite II (Figure 5.3), consistent with the high abundance of this compound in the corresponding unburned powder (Figure 4.10). There was some spread in the positioning of the replicates of the burned powder, although that was consistent with the variability in the firing process.

The HCA dendrogram (Figure 5.5 B) shows the clustering of a single replicate from SB9NoPb burned residue with the closest clustering unburned samples. The single replicate of SB9NoPb first formed a cluster with a single replicate of Fed9Pb. The cluster next incorporated all five replicates of unburned SB9NoPb at a similarity level of 0.78. Subsequently, SB9NoPb formed a cluster with the remaining samples in Group 1 at a similarity level of 0.71. Therefore, the burned residue of SB9NoPb were most similar to the corresponding unburned powder compared to all others in the data set. It was not as similar to Fed9Pb because all unburned replicates were not incorporated before the replicates of unburned SB9NoPb. Additional burned residues that closely corresponded to their unburned counterparts included the following samples: Win9Pb, Win9NoPb, Bzr9NoPb, and Mag9NoPb. The PCA scores plots and HCA dendrograms for these samples are included in Appendix 5.2.

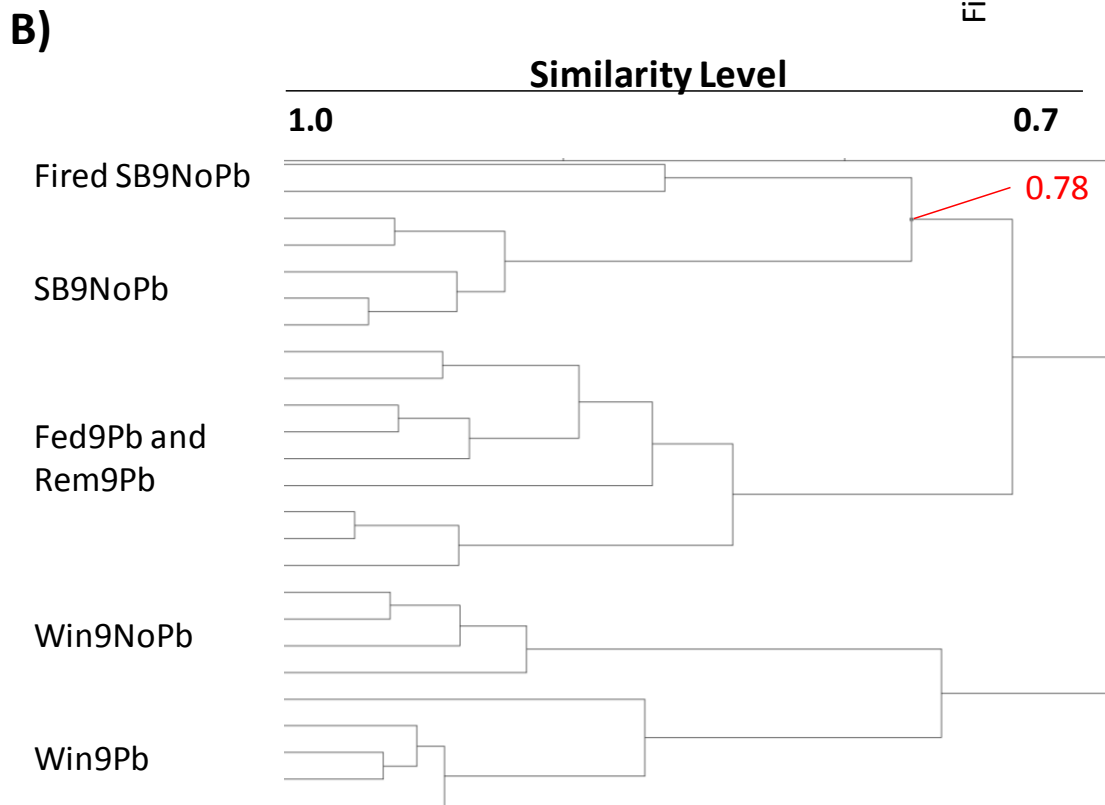
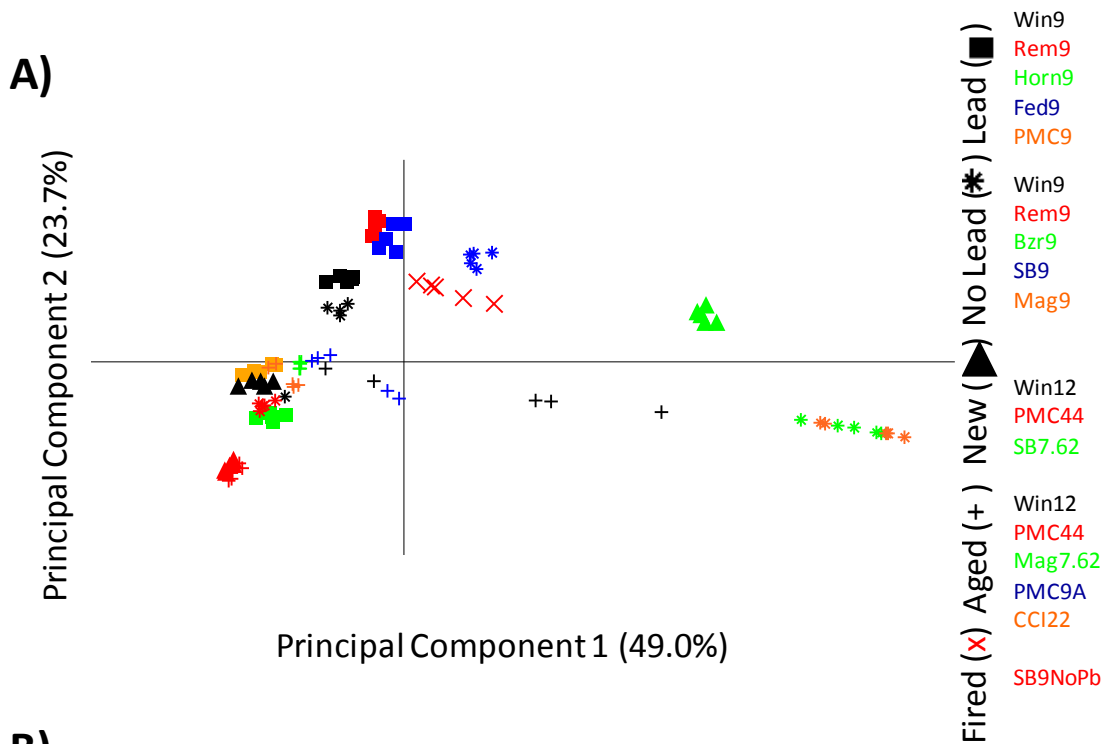


Figure 5.5 Representation of the multivariate statistical analysis for a smokeless powder (SB9NoPb) able to have a good association via (A) PCA scores plot visual analysis and (B) HCA dendrogram providing a numerical analysis.

5.3.3 Example of Association by PCA and HCA

The scores plot and HCA dendrogram for a data set that included all unburned powders and the burned residue from Rem9Pb are shown in Figure 5.6. The burned residue replicates of Rem9PB (red Xs) were positioned more positively on PC 1 but more negatively on PC2 compared to the unburned Rem9Pb powder (red squares), indicating only moderate association (Figure 5.6A). The shift in positioning on PC1 was due to the depletion of DPA while the more negative positioning on PC2 was due to a decrease in abundance of akardite II.

The HCA dendrogram (Figure 5.6B) shows the clustering of a single replicate from Rem9Pb burned residue with the closest clustering unburned samples. The single replicate of Rem9Pb clustered with a large group of unburned samples, including Rem9Pb, at a similarity level of 0.65. Thus, the burned residue did not cluster exclusively with the corresponding unburned powder but instead clustered with a larger group of unburned powders. Additional powders with burned residues that moderately corresponded to their unburned counterparts included the following samples: Fed9Pb, Win12A, Mag7.62A, and PMC9A. The PCA scores plots and HCA dendrograms for these samples are included in Appendix 5.2.

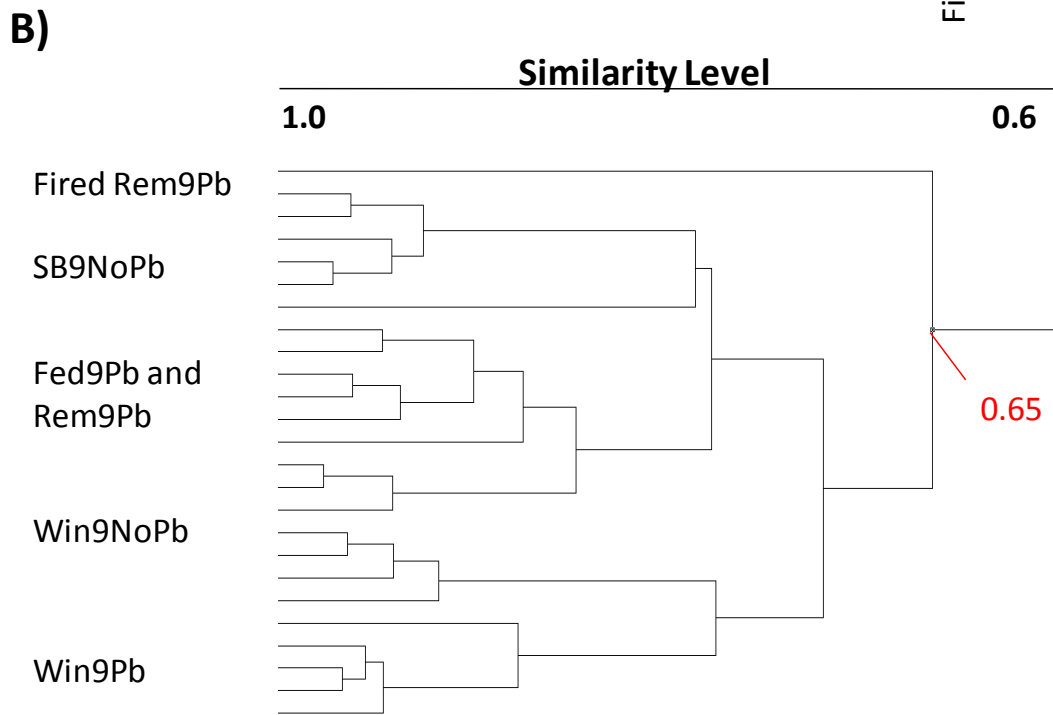
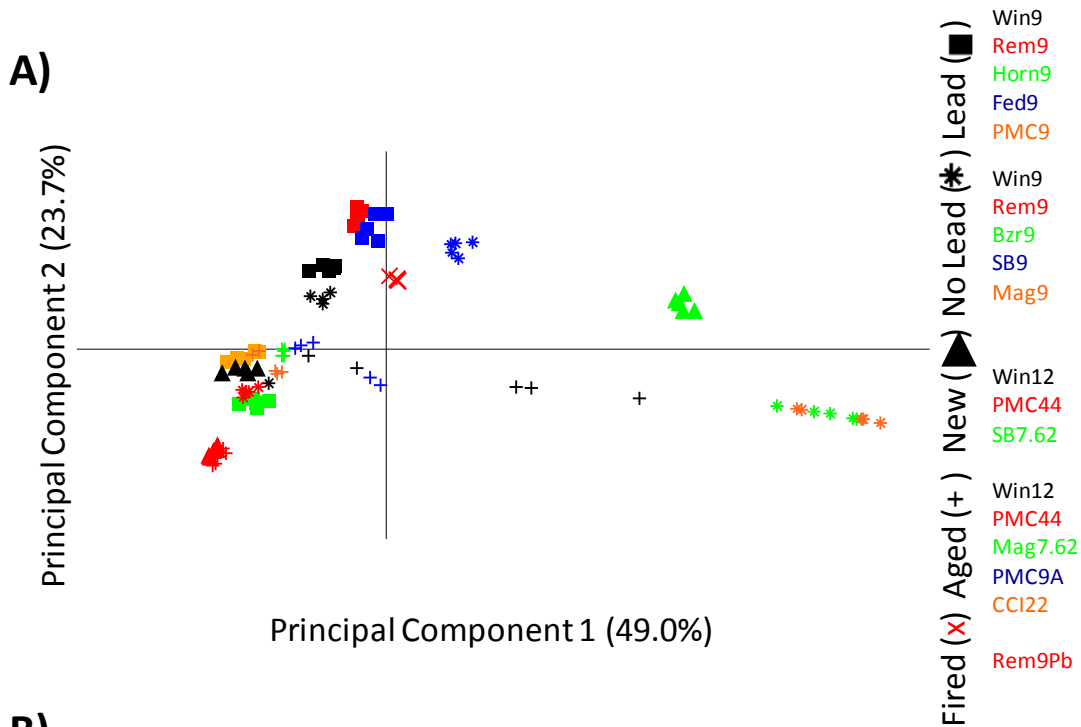


Figure 5.6 Representation of the multivariate statistical analysis for a smokeless powder (Rem9Pb) able to have a moderate association via (A) PCA scores plot visual analysis and (B) HCA dendrogram providing a numerical analysis.

5.3.4 Example of No Association by PCA or HCA

The scores plot and HCA dendrogram for a data set that included all unburned powders and the burned residue from SB7.62N are shown in Figure 5.7. In this example, there was poor association of the five burned replicates of SB7.62N (green X's) to the corresponding unburned SB7.62N (green *).

While the unburned samples were positioned positively in PC 1 in the area indicative of a prominence of EC in the chemical profile (Group 2), the chemical profiles for the burned residue were spread across PC2 in the area where Akardite II is a prominent compound (Group 1). The burned residues of SB7.62N contained a high abundance of Akardite II (Figure 5.4) whereas, for the unburned powder, EC was the dominant compound, with only a moderate abundance of Akardite II (Figure 4.14). Therefore, the apparent depletion of EC explained the large shift on PC1 between the chemical profiles of the unburned and burned residues. The wider spread of points along PC 2 in the scores plot was indicative of the irreproducibility of residue deposition within the spent cartridge during the burning process.

The HCA dendrogram (Figure 5.7B) shows the clustering of a single replicate of SB7.62N burned residue with all unburned chemical profiles. The single replicate of SB7.62N first clustered with a single replicate of Rem9NoPb. Next, a cluster was formed within all replicates of Rem9NoPb and Horn9Pb. Subsequently, the fired replicate of SB7.62N did not cluster with the unfired SB7.62N until all samples are included in a single cluster, a similarity score of 0.0. This type of analysis was poor, as the changes to chemical profile during the burning process precluded classification with its unfired counterpart. Additional powders with burned residues that poorly corresponded to their unburned counterparts included the following

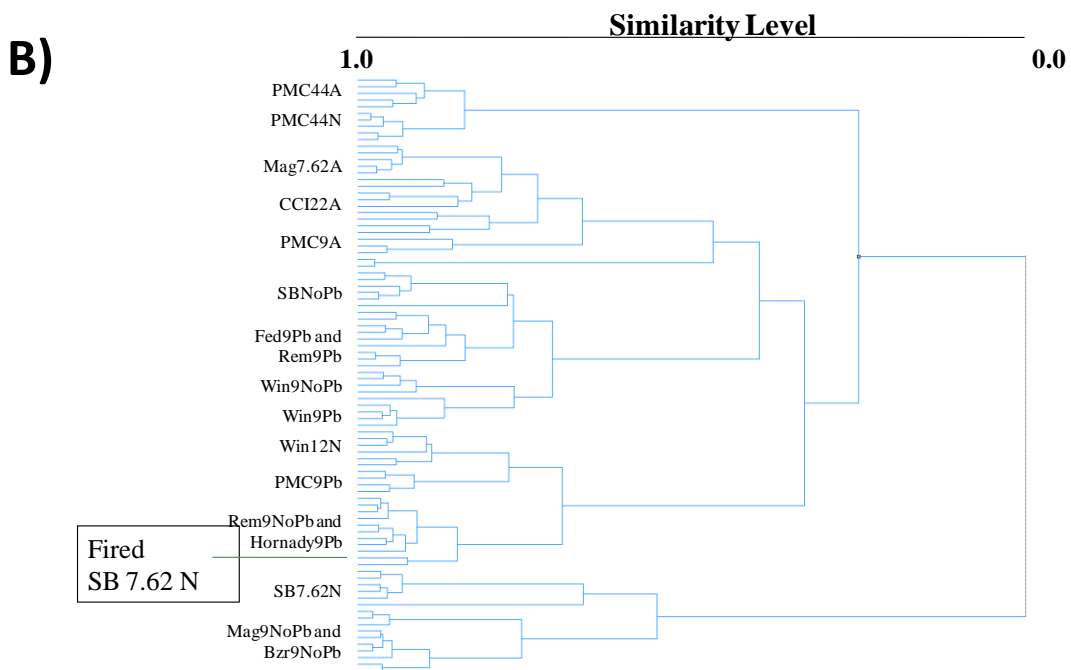
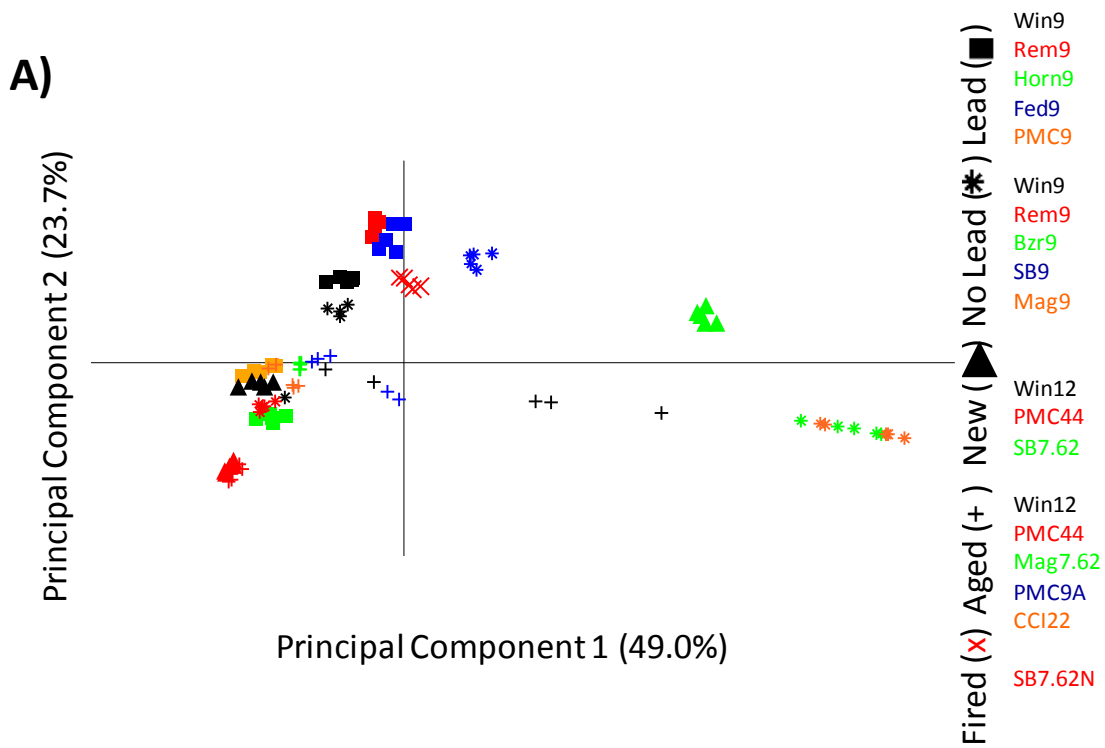


Figure 5.7 Representation of the multivariate statistical analysis for a smokeless powder (SB7.62N) with a poor association via (A) PCA scores plot visual analysis and (B) HCA dendrogram providing a numerical analysis.

samples: Horn9Pb, PMC9Pb, Rem9NoPb, Win12N, PMC44N, PMC44A, and CCI22A. The PCA scores plots and HCA dendrograms for these samples are included in Appendix 5.2.

5.3.5 Hypothetical Examples for Inclusion within a Forensic Lab

The association and discrimination of the chemical profiles for unburned smokeless powders and their corresponding burned residues were all performed on samples of known origin. However, for practical use in a forensic laboratory, comparisons could be made 1) between unknown ammunition found at a crime scene to ammunition from a potential suspect or 2) ammunition at a crime scene to a general reference collection. The chemical data collected from samples of known origin can serve as a reference collection against unknown samples for characterization and possible association.

A reference collection would be composed of known samples spanning a variety of manufacturers, calibers, primer compositions, and ages to obtain a comprehensive spread of the chemical profiles likely to be encountered at a crime scene. Ideally, all samples would have chemical profiles from extracts of unburned powders and corresponding burned residues. The chemical profiles would be subjected to PCA and HCA analysis.

An unknown sample would be analyzed in the same manner as the reference collection. The chemical profile would be plotted on a scores plot and a dendrogram. Figure 5.8 represents a series of three hypothetical chemical profiles from unknown burned residues plotted against the known samples from this project, simulating a reference collection.

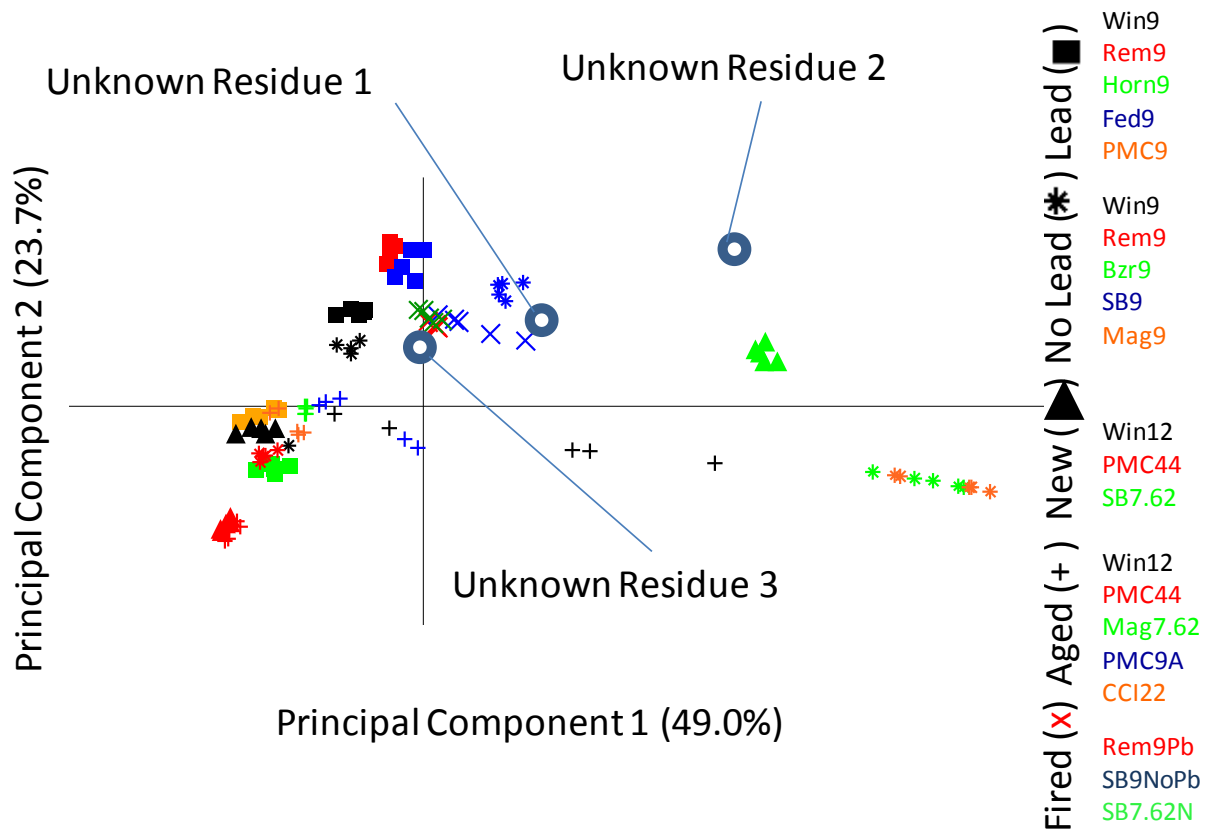


Figure 5.8 Representation of a series of chemical profiles for hypothetical unknown samples for comparison against a known database of chemical profiles for unburned and burned smokeless powders analysis.

The chemical profile of hypothetical burned residue 1 was positioned positively on PC1 and PC2, similar to the known unburned and burned SB9NoPb samples. The chemical profile of hypothetical burned residue 2 was positioned very positively on PC1 and positively on PC2, and was not similar to any of the known unburned or burned powders. However, the positioning of burned residue 2 indicates it was most consistent with the chemical profiles from samples defined the PCA scores plot as Group 2, containing an abundance of both akardite II and ethyl centralite. However, it can be excluded as having originated from a smokeless powder in the reference collection because it does not overlap a known data point. Finally, the chemical profile of hypothetical burned residue 3 was positioned positively on PC2 and around zero on PC1, close to the burned residues from Rem9Pb and SB7.62N.

5.4 Summary

The chemical composition of smokeless powders have been shown to change when comparing smokeless powders to the burned residue collected after firing. Comprehensive chemical profiles of burned residues were generated using HPLC-APCI-multiplexed CID-TOF-MS analysis. The abundance of organic compounds was greatly reduced after firing, prompting the use of XICs to provide a relative abundance of each compound. DPA was shown to be depleted in overall abundance for a majority of samples. EC and Akardite II were shown to be retained, while N-nitroso-DPA and DBP showed a reduced abundance.

Association of the compositions of the burned residue to the unburned smokeless powders were attempted using PCA and HCA. The chemical profiles from burned residues were individually compared to the entire collection of unburned powders. PCA was used to provide a means of visual association with scores plots, and HCA was used to compliment PCA with a

numerical measure of similarity. Burned powders were classified into categories depending on how well the chemical profiles were able to be associated with their unburned counterparts. Ultimately, more than half of the burned residues were able to be associated to their unburned counterparts through PCA and HCA (good association) or through one of the two methods (moderate association). The information obtained from known samples of unburned powders and burned residues can be applied to the analysis of hypothetical unknown chemical profiles of evidence types collected at crime scenes for characterization and association purposes.

APPENDICES

APPENDIX 5.1 Extracted Ion Chromatograms Representing the Chemical Profile from Burned Smokeless Powders

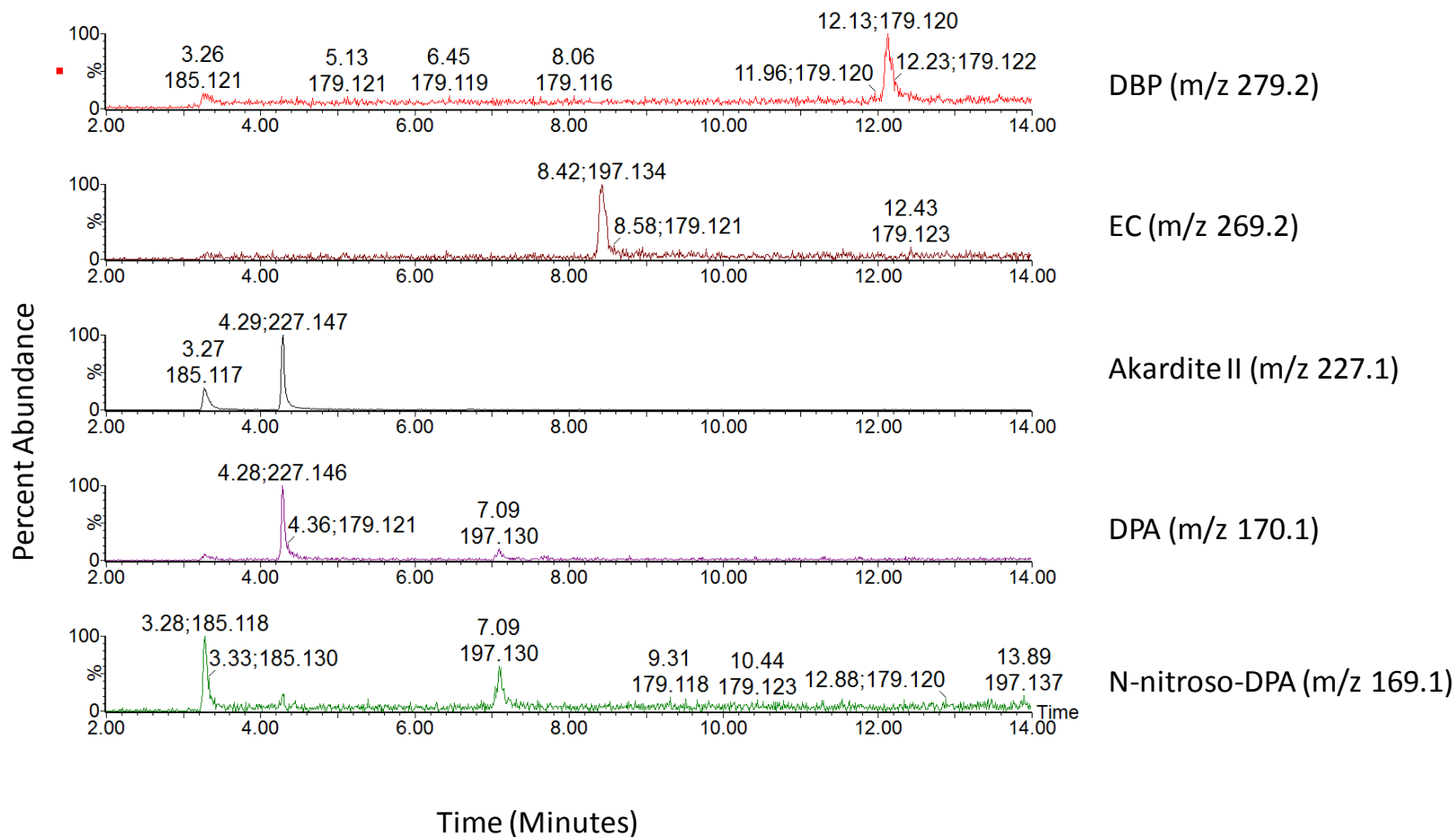


Figure A.5.1.1 Extracted ion chromatogram (XIC) of extract from fired cartridge of Win9Pb. Labels indicate m/z used for XIC analysis of listed compound.

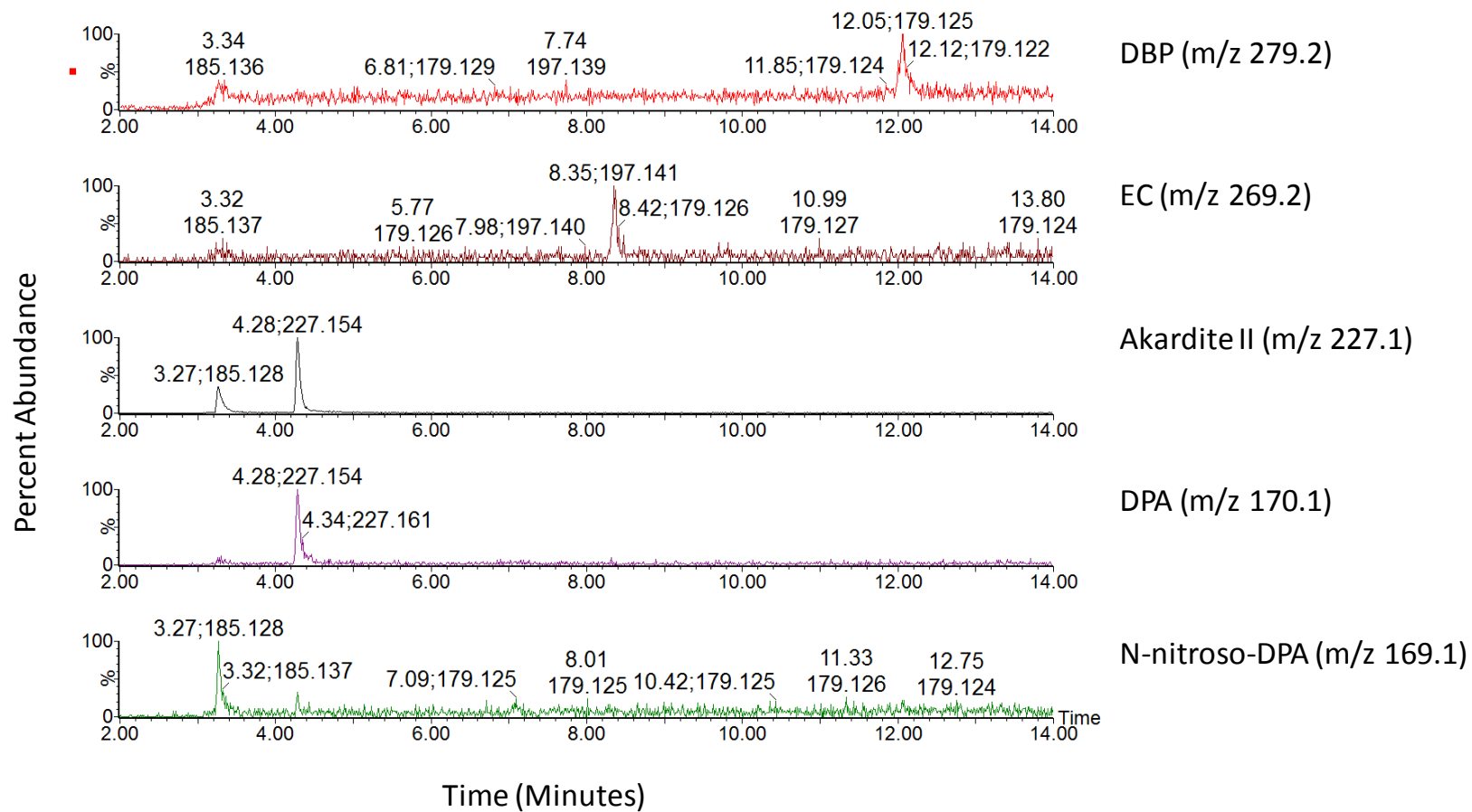


Figure A.5.1.2 Extracted ion chromatogram (XIC) of extract from fired cartridge of Rem9Pb. Labels indicate m/z used for XIC analysis of listed compound.

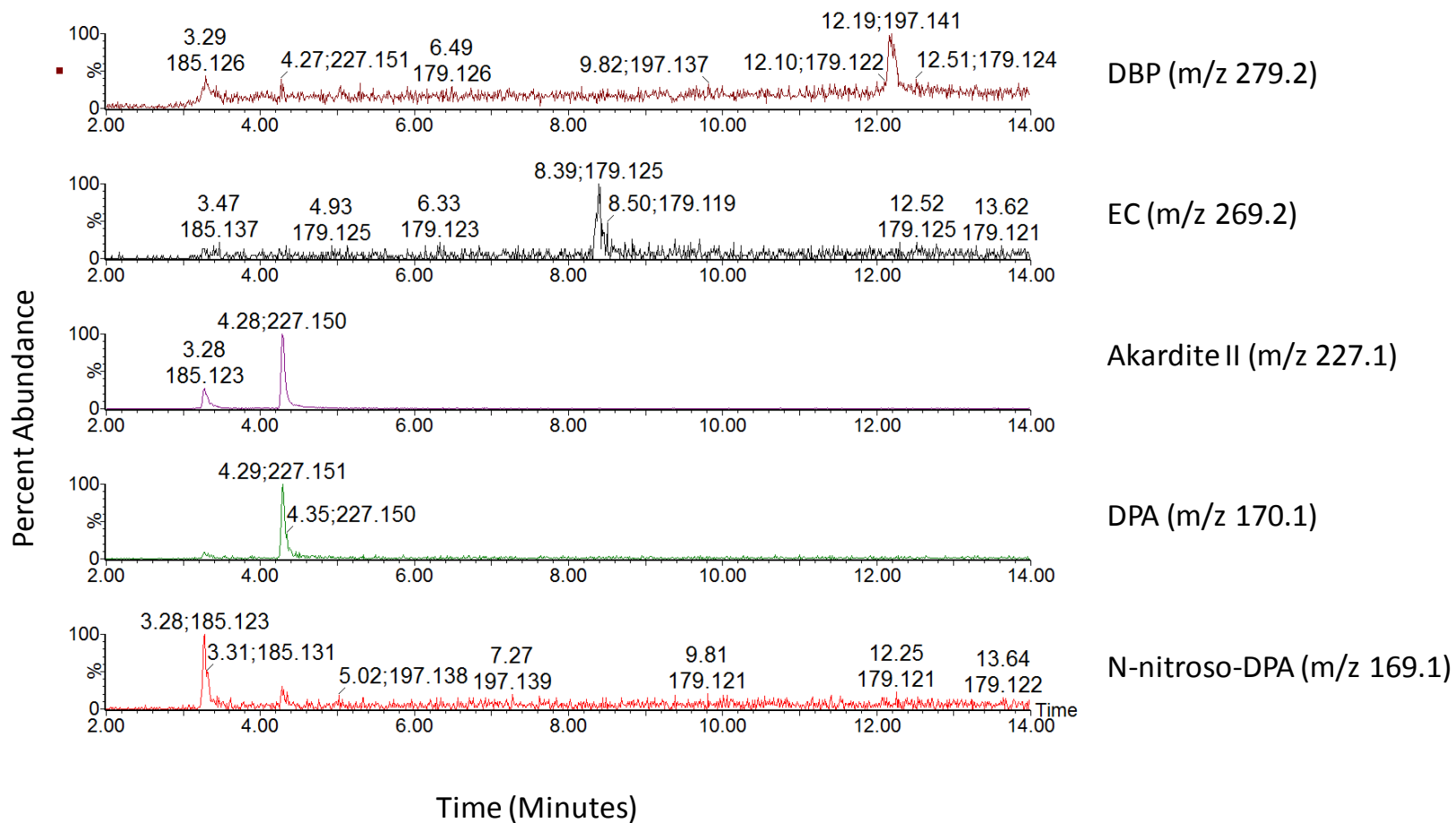


Figure A.5.1.3 Extracted ion chromatogram (XIC) of extract from fired cartridge of Fed9Pb. Labels indicate m/z used for XIC analysis of listed compound.

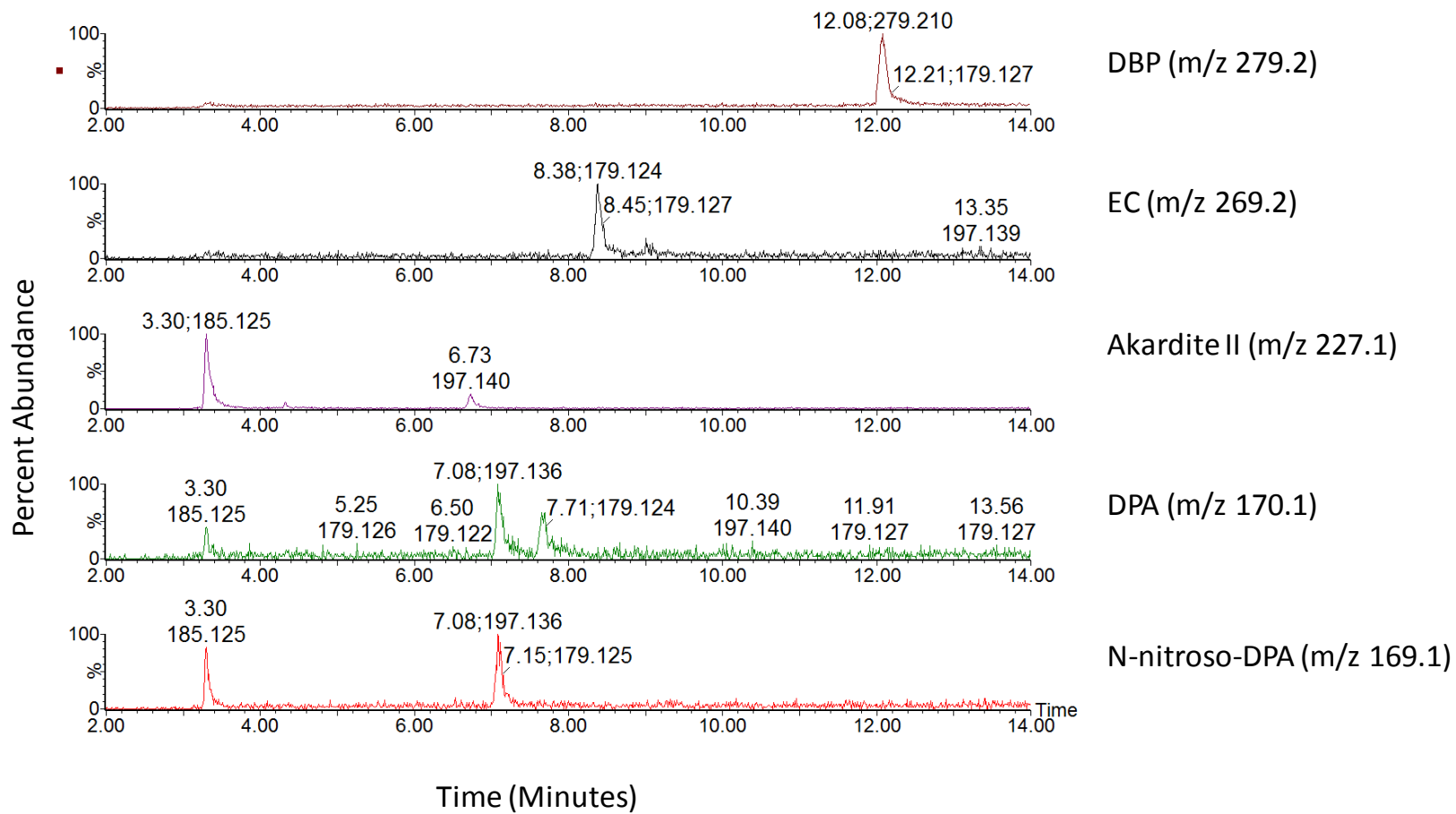


Figure A.5.1.4 Extracted ion chromatogram (XIC) of extract from fired cartridge of Hornday9Pb. Labels indicate m/z used for XIC analysis of listed compound.

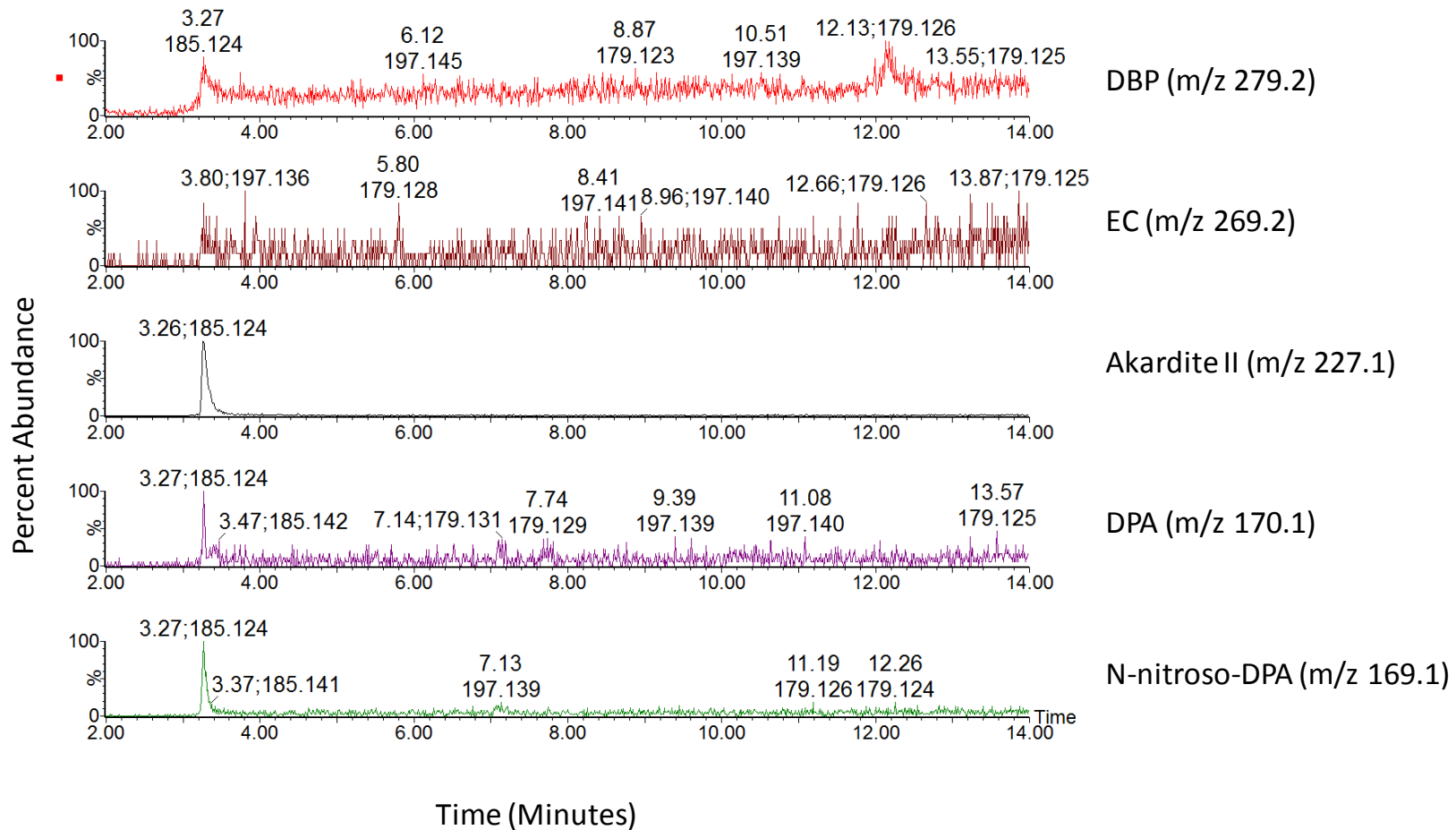


Figure A.5.1.5 Extracted ion chromatogram (XIC) of extract from fired cartridge of PMC9Pb. Labels indicate m/z used for XIC analysis of listed compound.

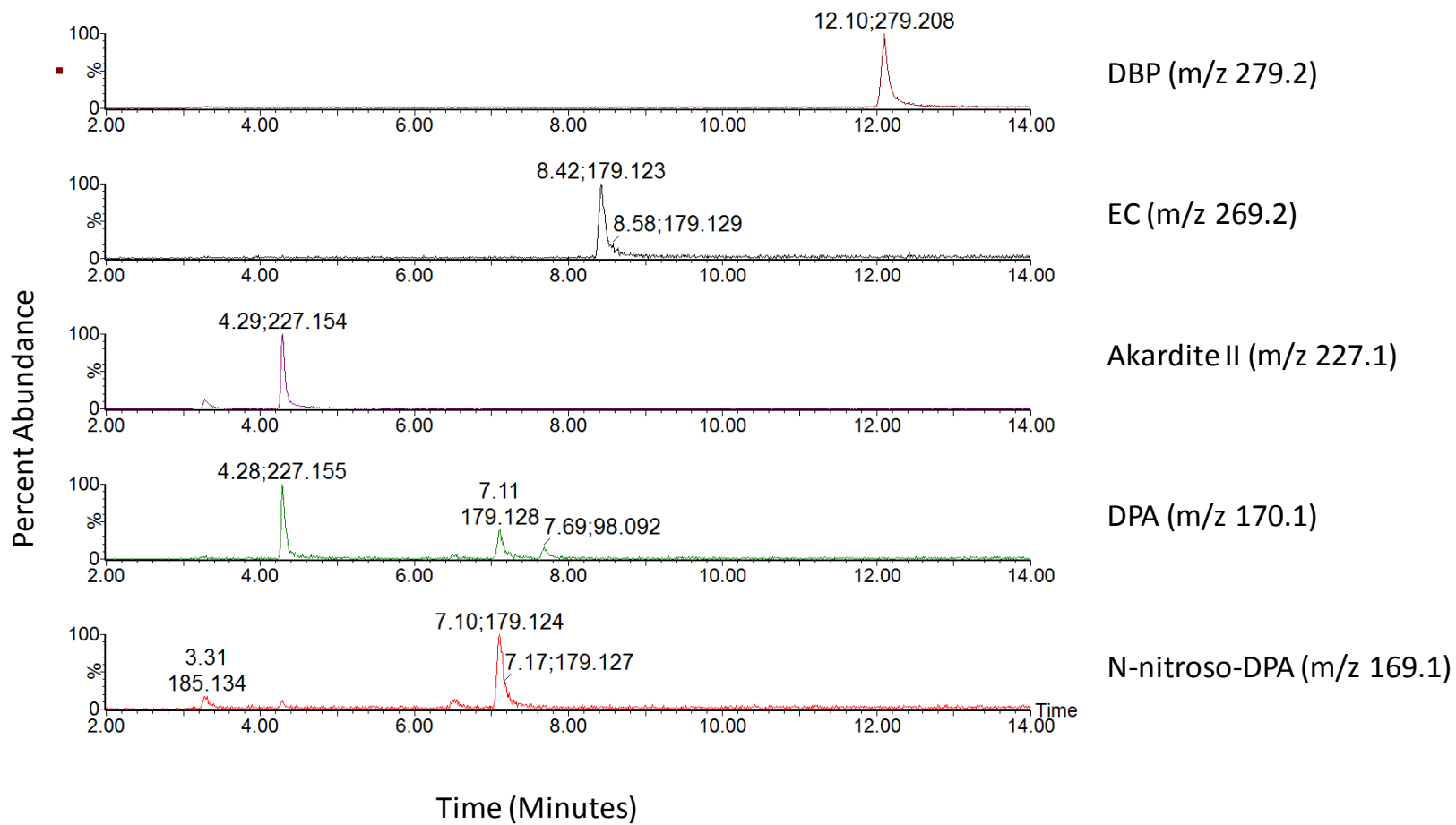


Figure A.5.1.6 Extracted ion chromatogram (XIC) of extract from fired cartridge of Win9NoPb. Labels indicate m/z used for XIC analysis of listed compound.

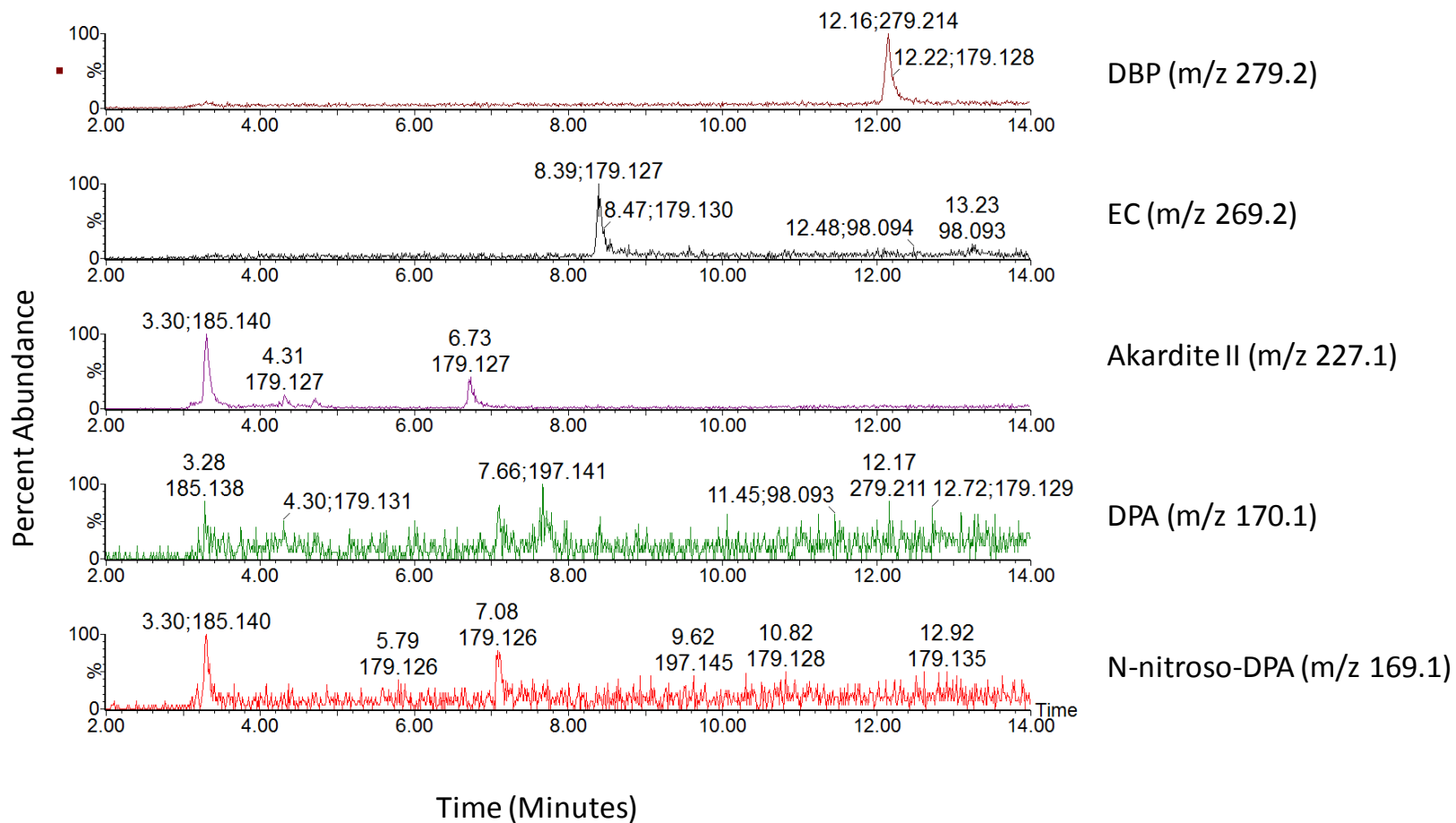


Figure A.5.1.7 Extracted ion chromatogram (XIC) of extract from fired cartridge of Rem9NoPb. Labels indicate m/z used for XIC analysis of listed compound.

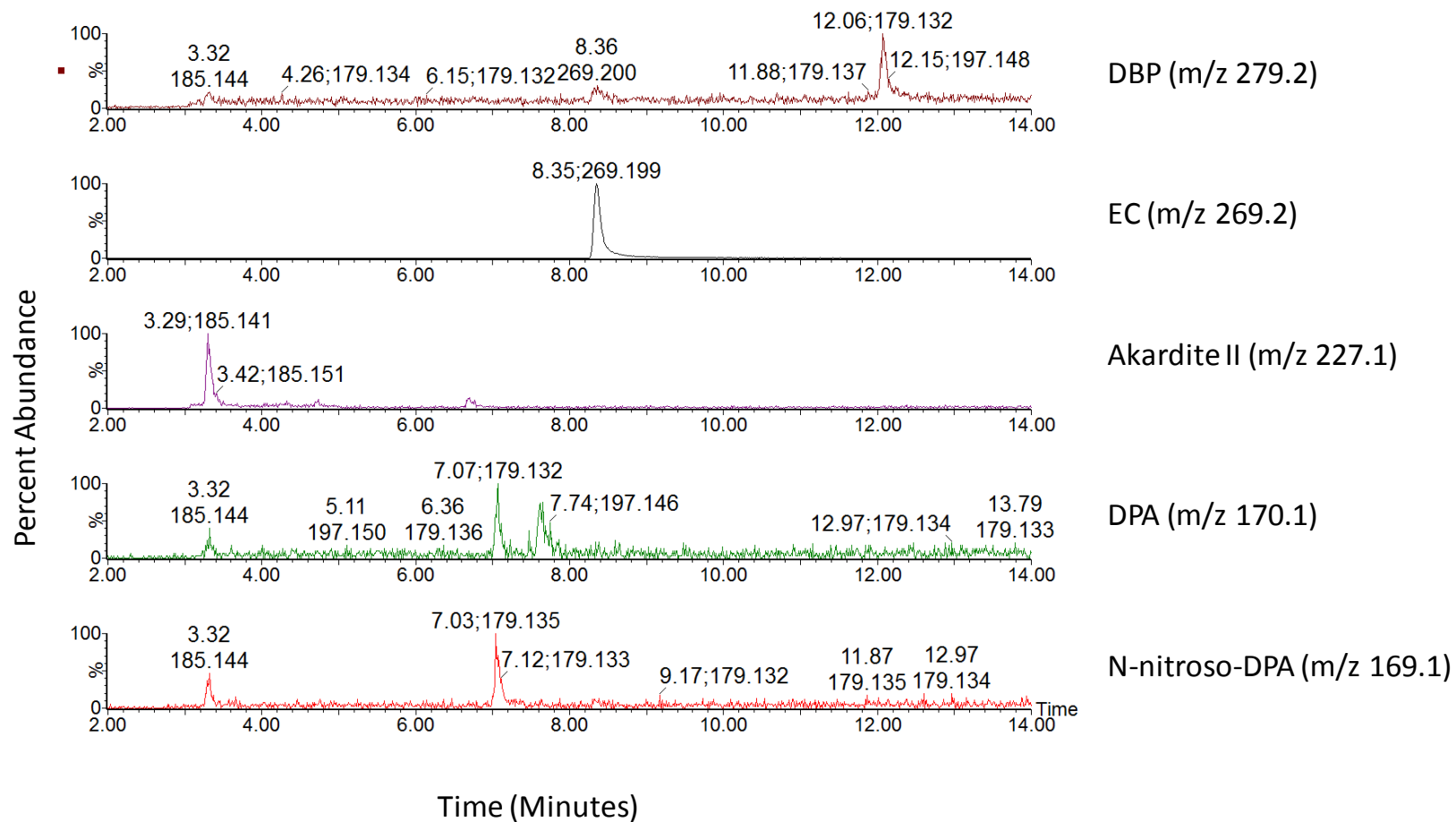


Figure A.5.1.8 Extracted ion chromatogram (XIC) of extract from fired cartridge of Bzr9NoPb. Labels indicate m/z used for XIC analysis of listed compound.

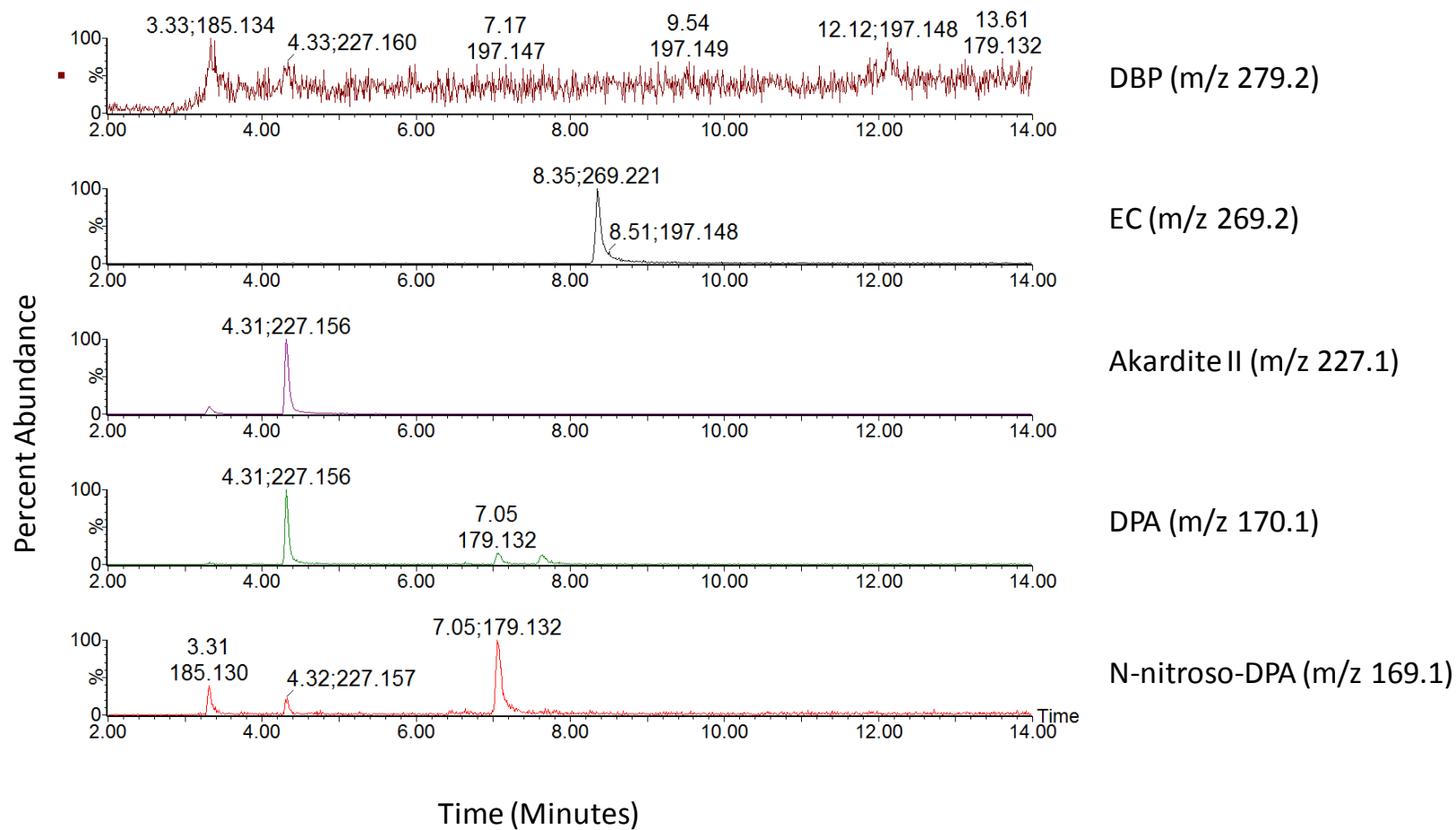


Figure A.5.1.9 Extracted ion chromatogram (XIC) of extract from fired cartridge of SB9NoPb. Labels indicate m/z used for XIC analysis of listed compound.

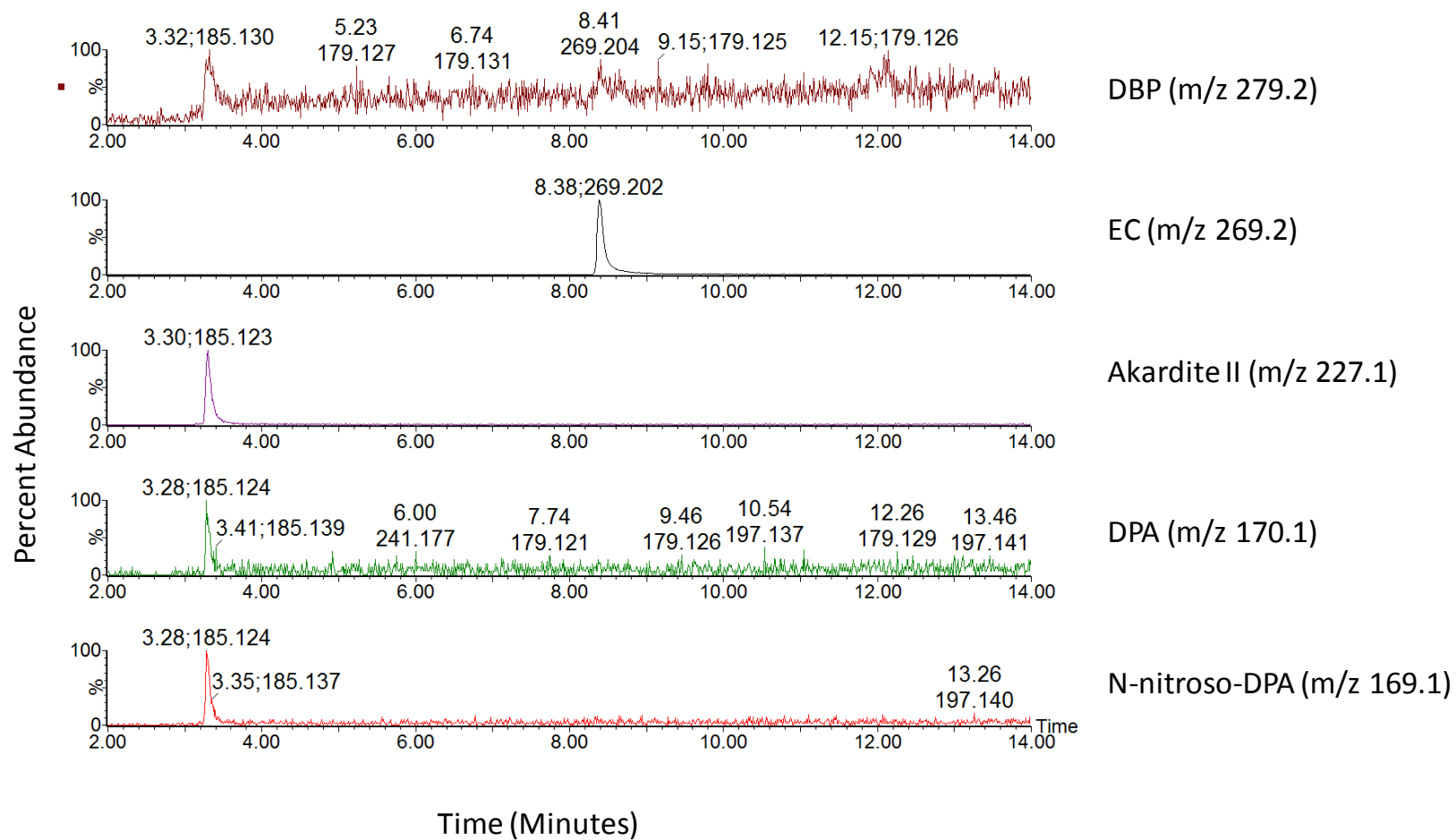


Figure A.5.1.10 Extracted ion chromatogram (XIC) of extract from fired cartridge of Mag9NoPb. Labels indicate m/z used for XIC analysis of listed compound.

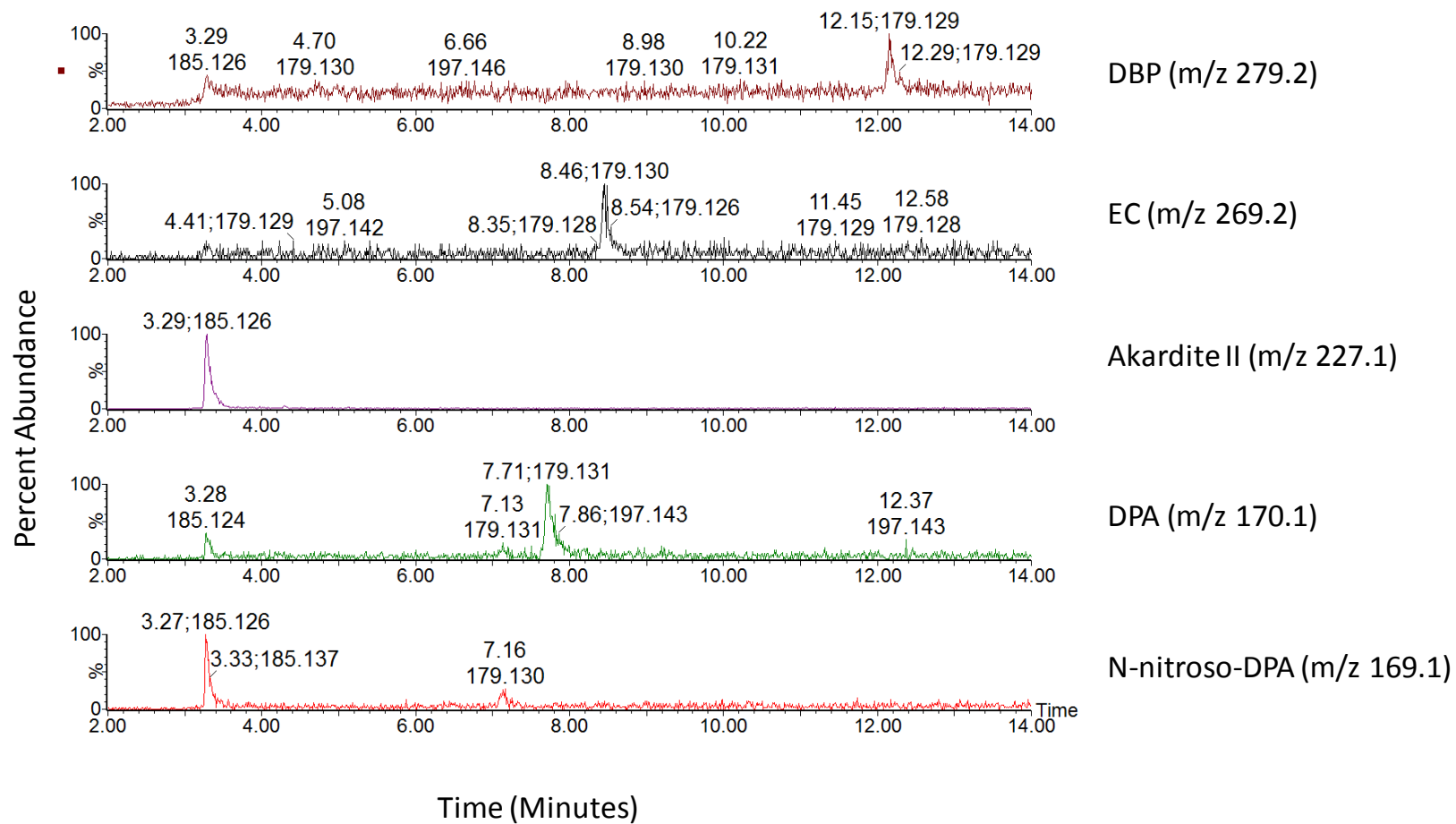


Figure A.5.1.11 Extracted ion chromatogram (XIC) of extract from fired cartridge of Win12N. Labels indicate m/z used for XIC analysis of listed compound.

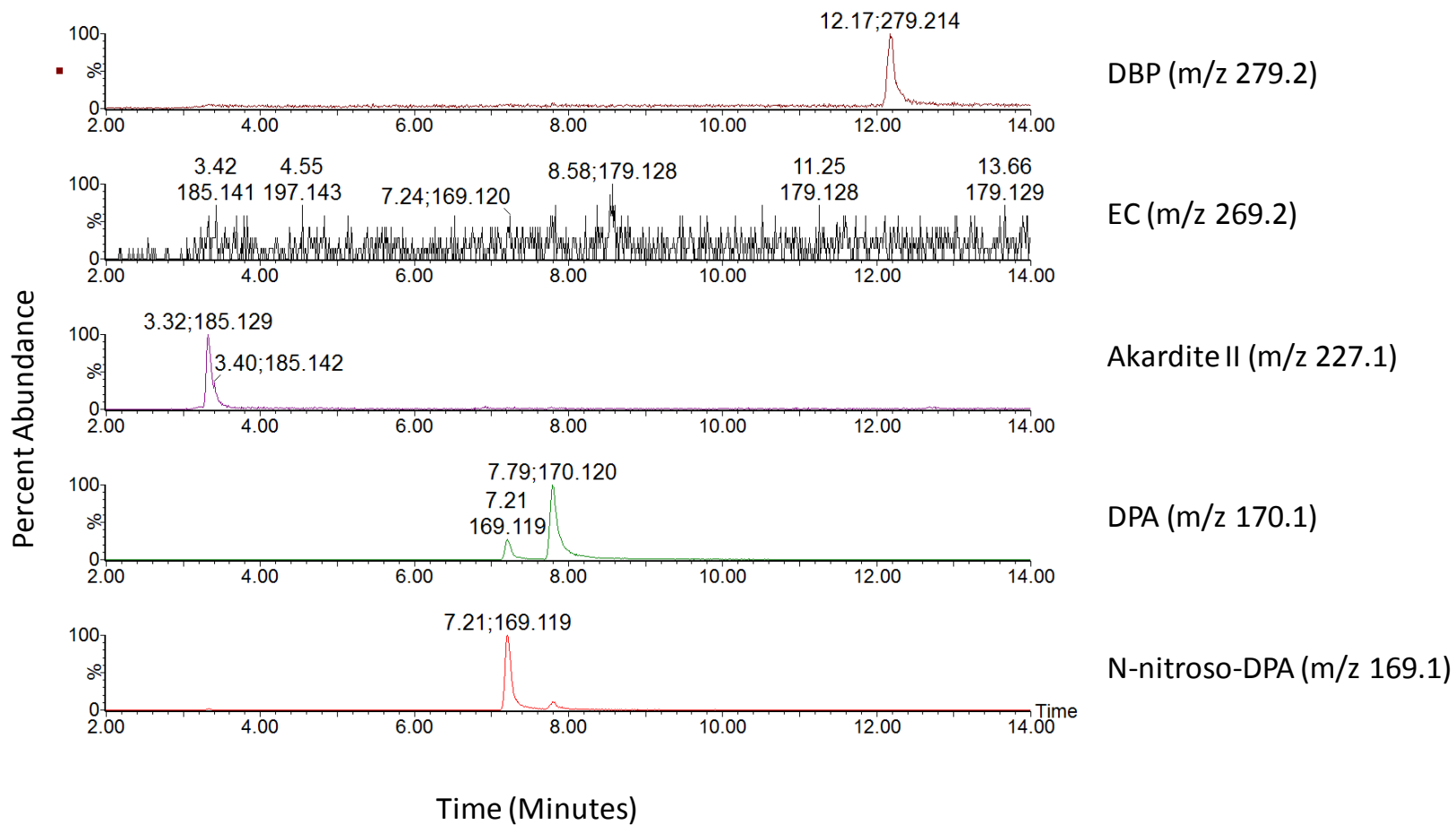


Figure A.5.1.12 Extracted ion chromatogram (XIC) of extract from fired cartridge of PMC44N. Labels indicate m/z used for XIC analysis of listed compound.

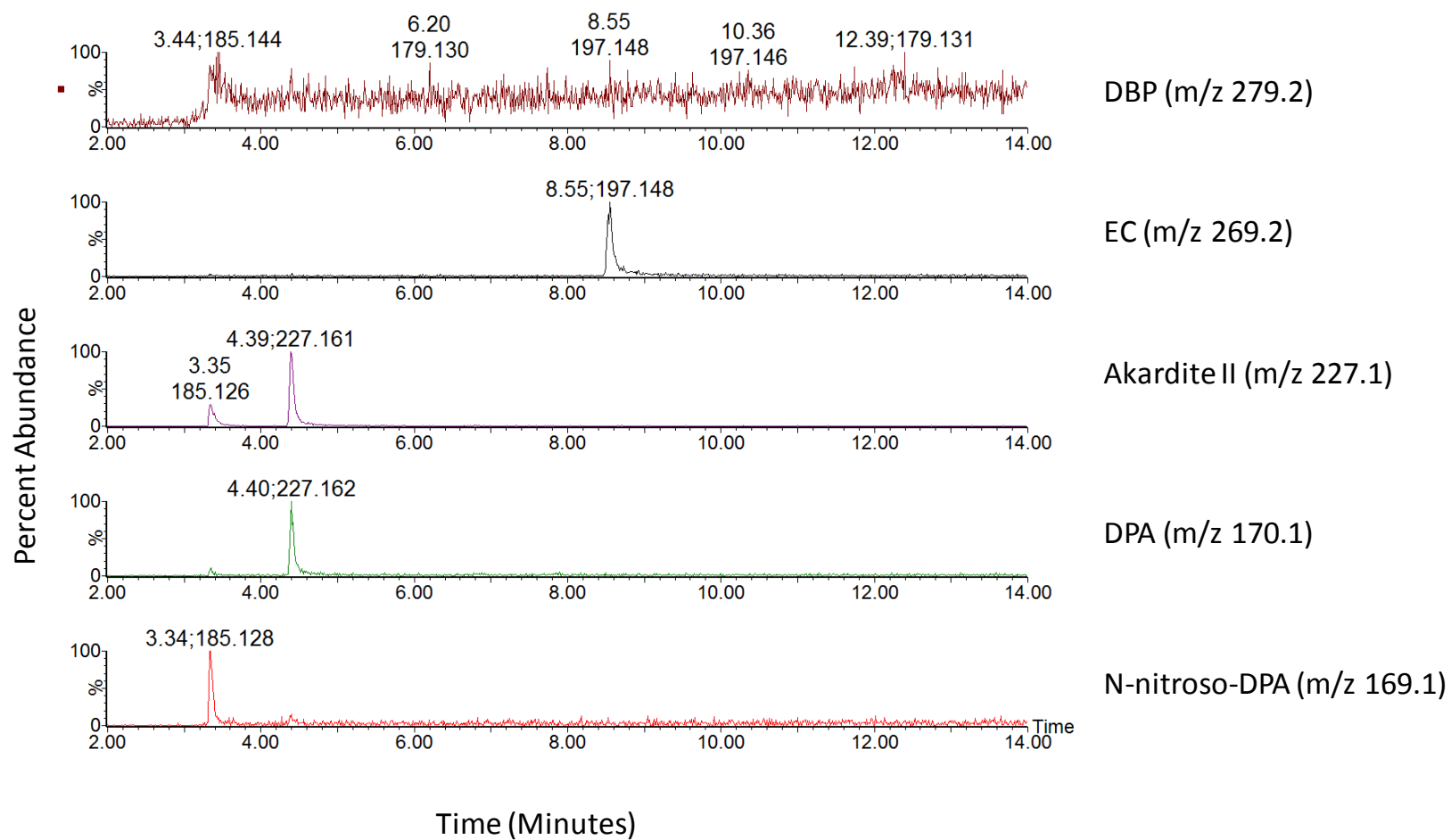


Figure A.5.1.13 Extracted ion chromatogram (XIC) of extract from fired cartridge of SB7.62N. Labels indicate m/z used for XIC analysis of listed compound.

APPENDIX 5.2 Multivariate Statistical Analysis Results for Burned Smokeless Powders

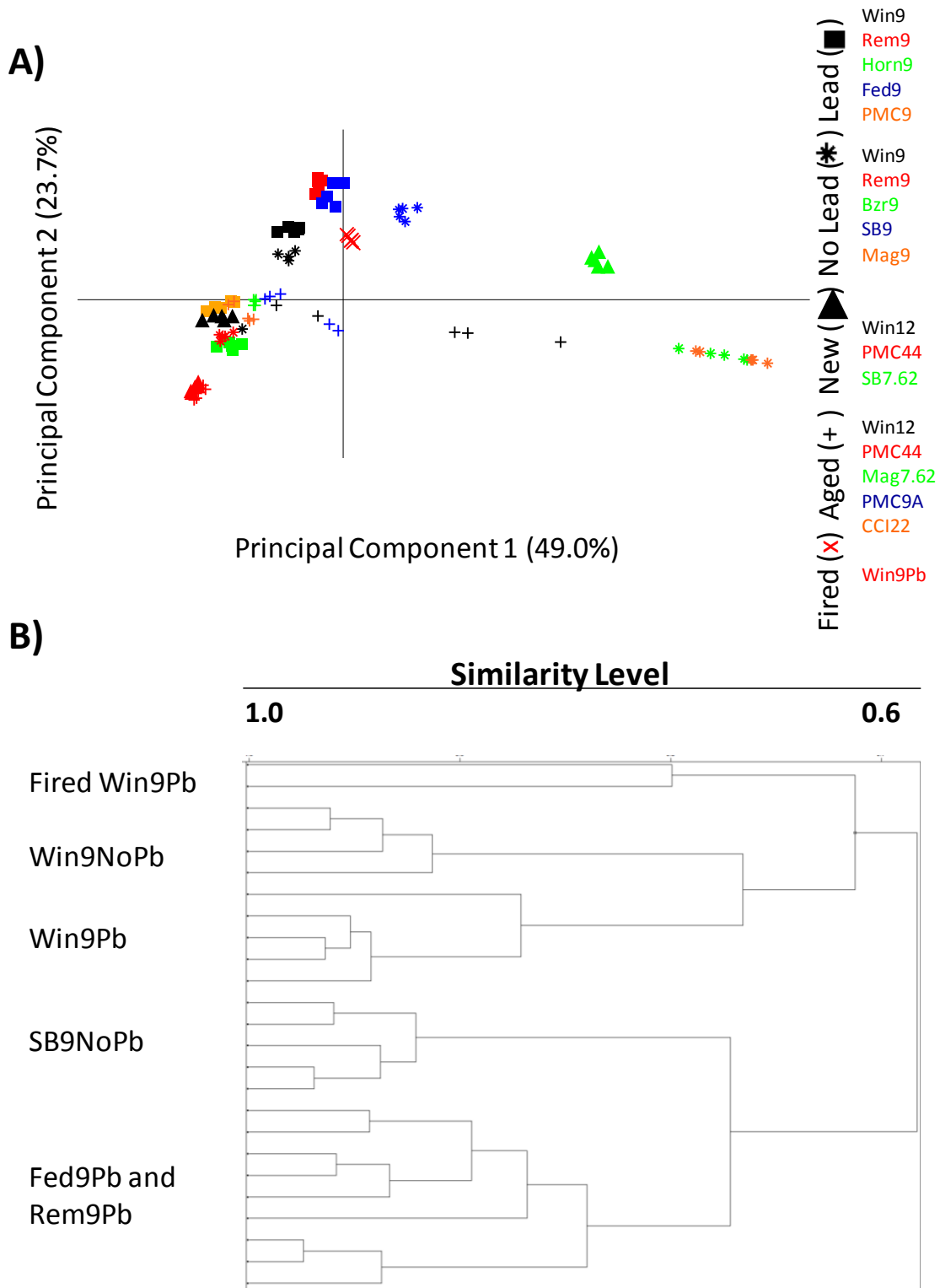


Figure A.5.2.1 Comparison of chemical profile for Fired Win9Pb versus profiles from unburned smokeless powder (A) PCA scores plot and (B) HCA dendrogram.

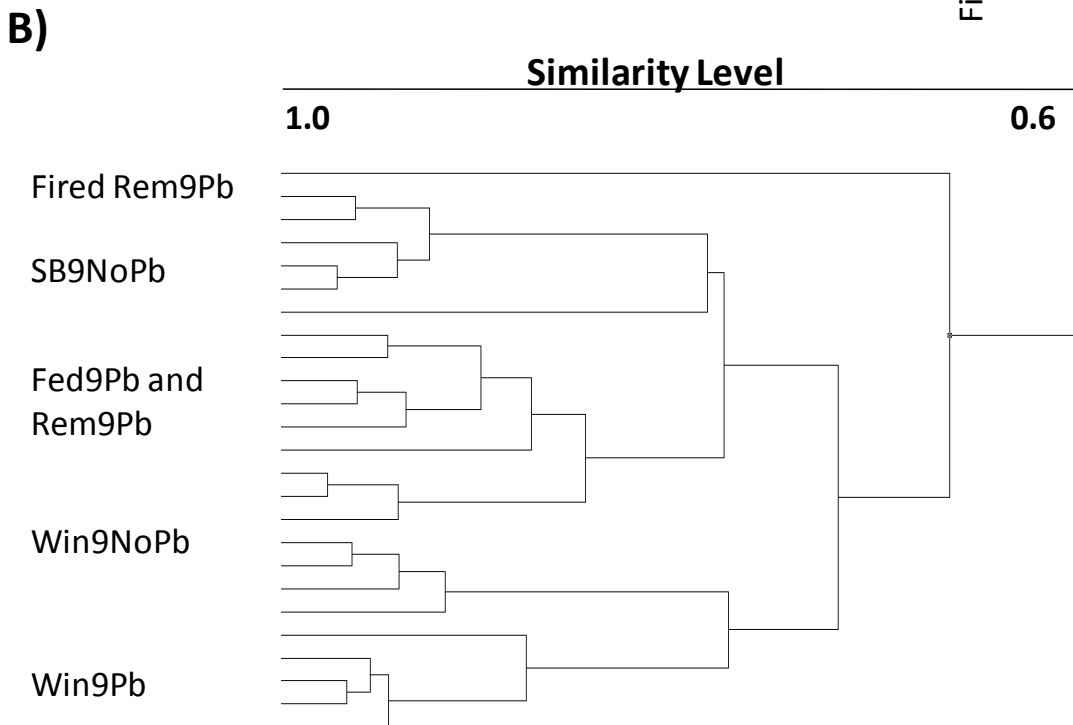
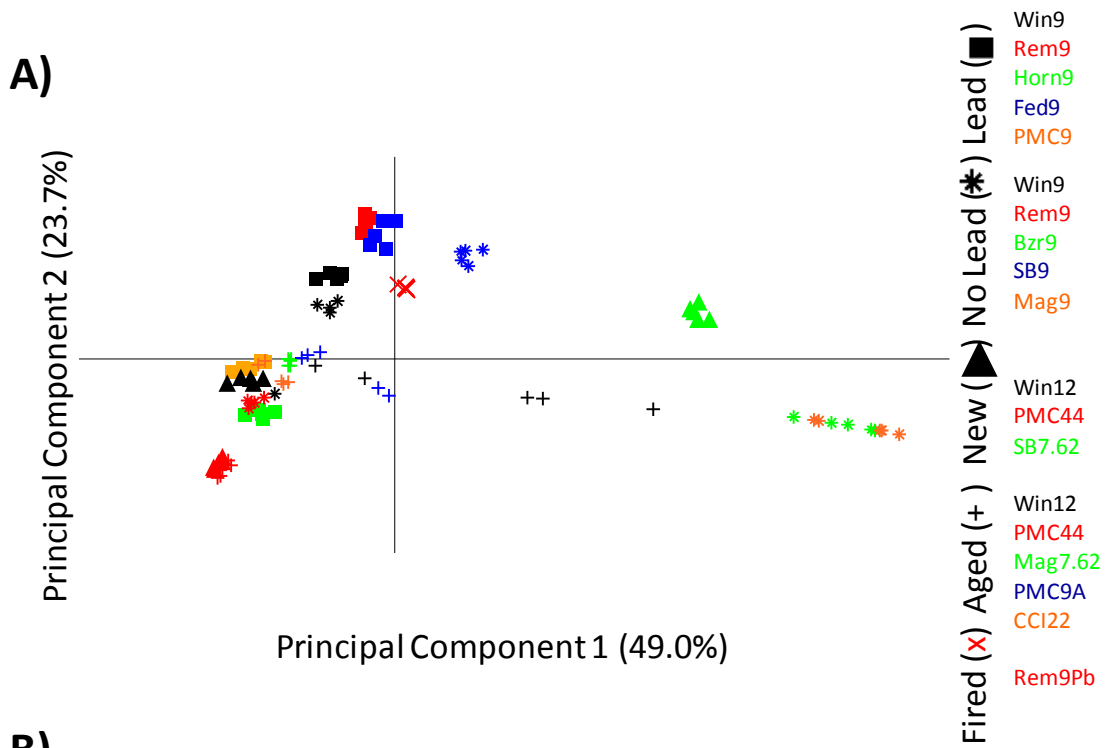


Figure A.5.2.2 Comparison of chemical profile for Fired Rem9Pb versus profiles from unburned smokeless powder (A) PCA scores plot and (B) HCA dendrogram

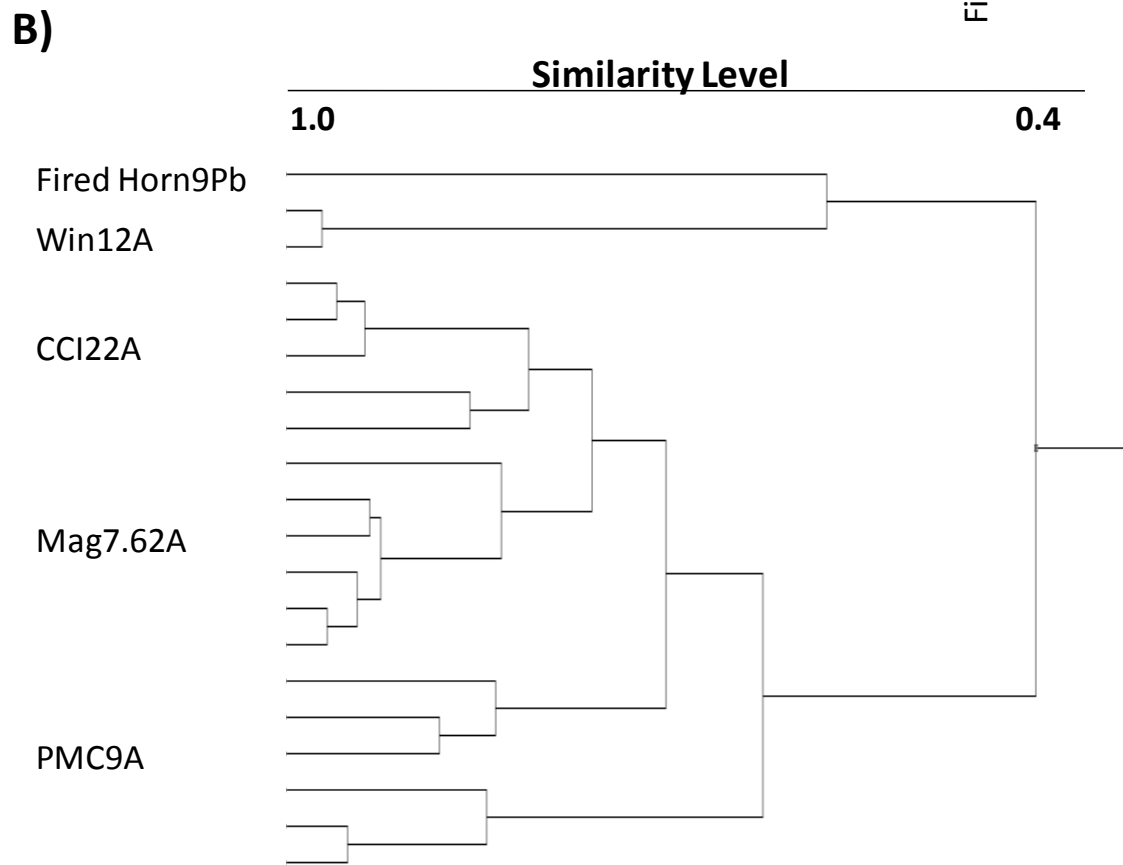
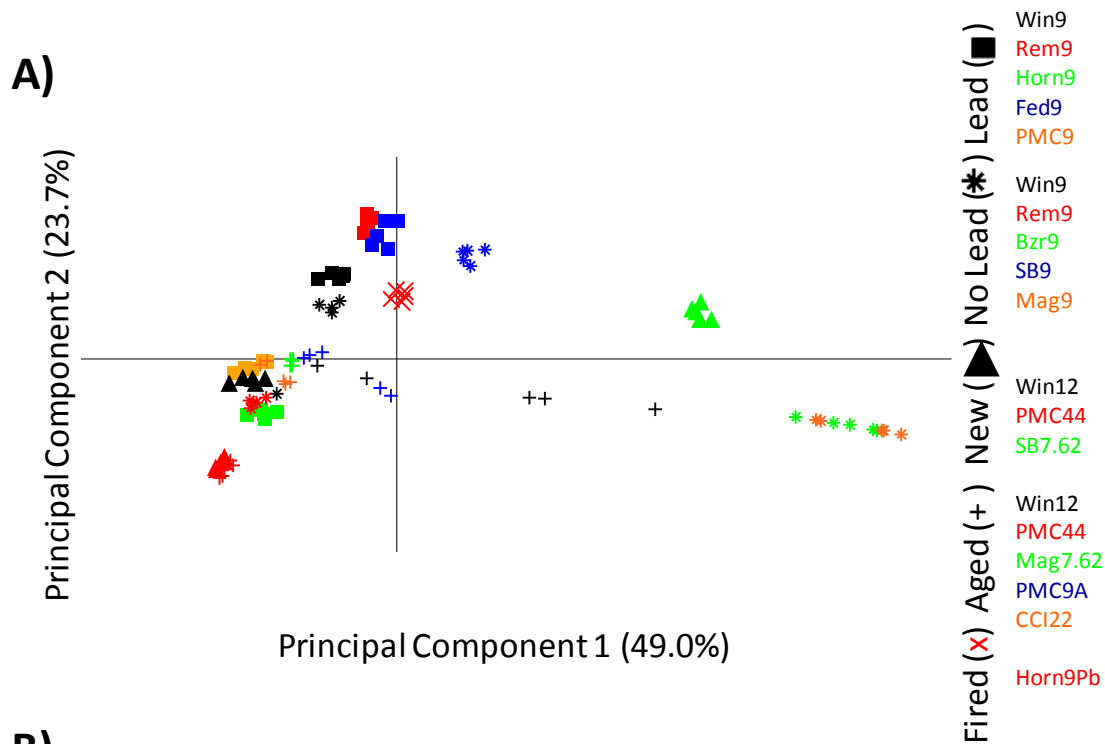


Figure A.5.2.3 Comparison of chemical profile for Fired Horn9Pb versus profiles from unburned smokeless powder (A) PCA scores plot and (B) HCA dendrogram.

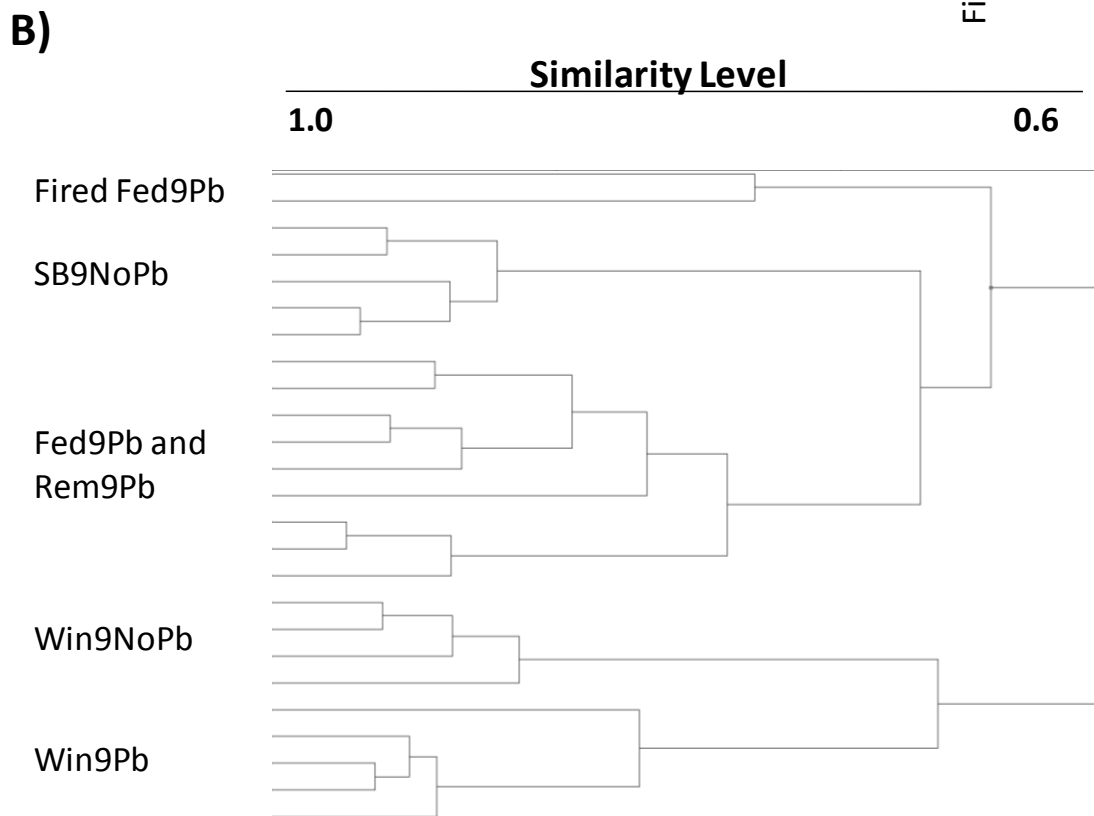
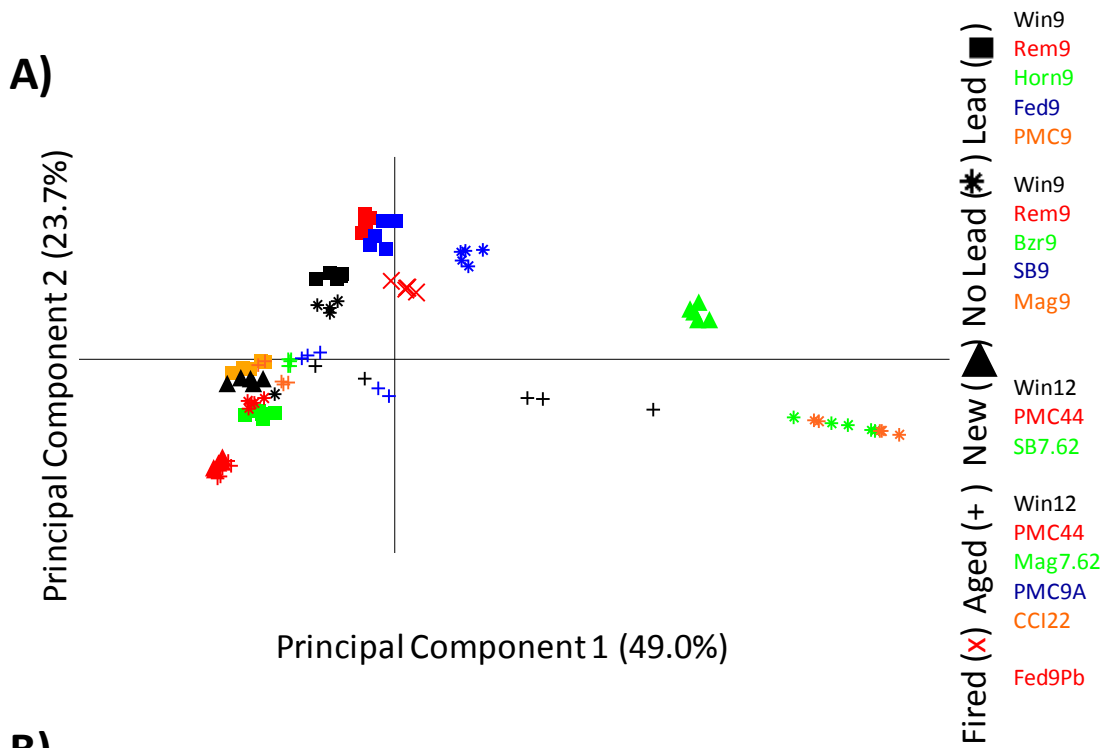


Figure A.5.2.4 Comparison of chemical profile for Fired Fed9Pb versus profiles from unburned smokeless powder (A) PCA scores plot and (B) HCA dendrogram

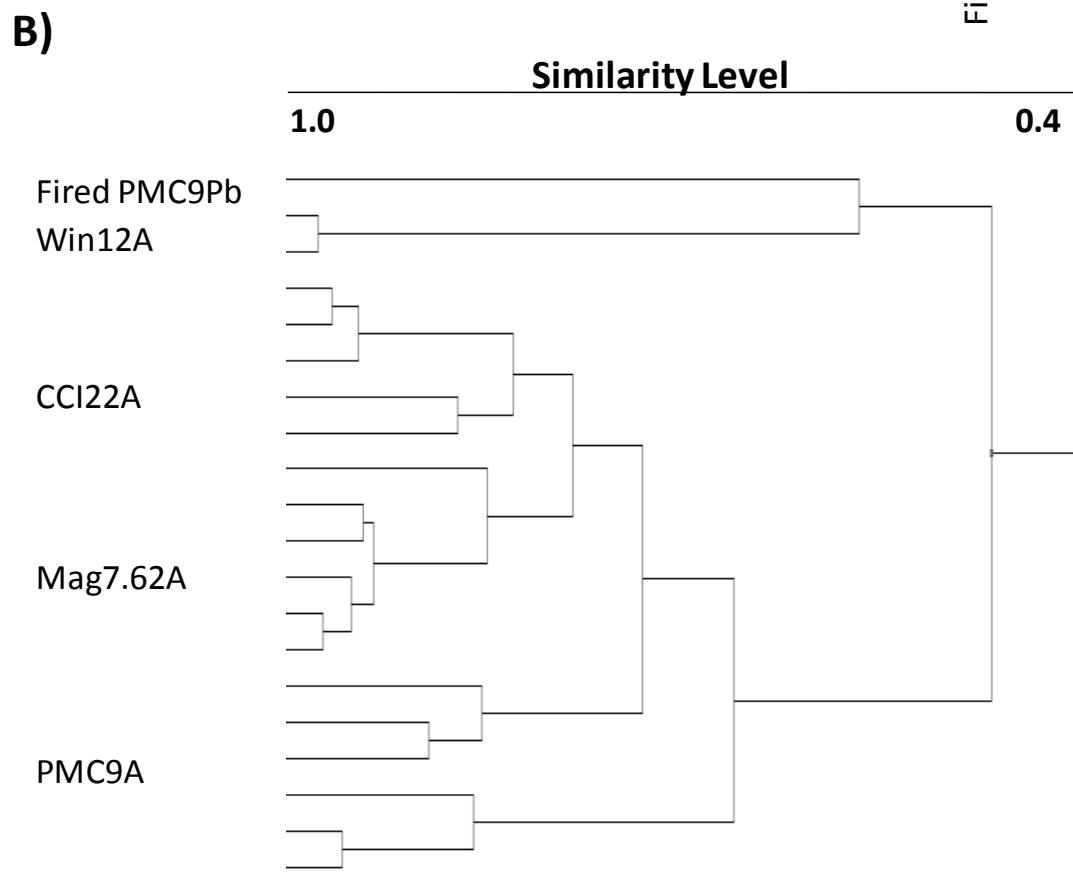
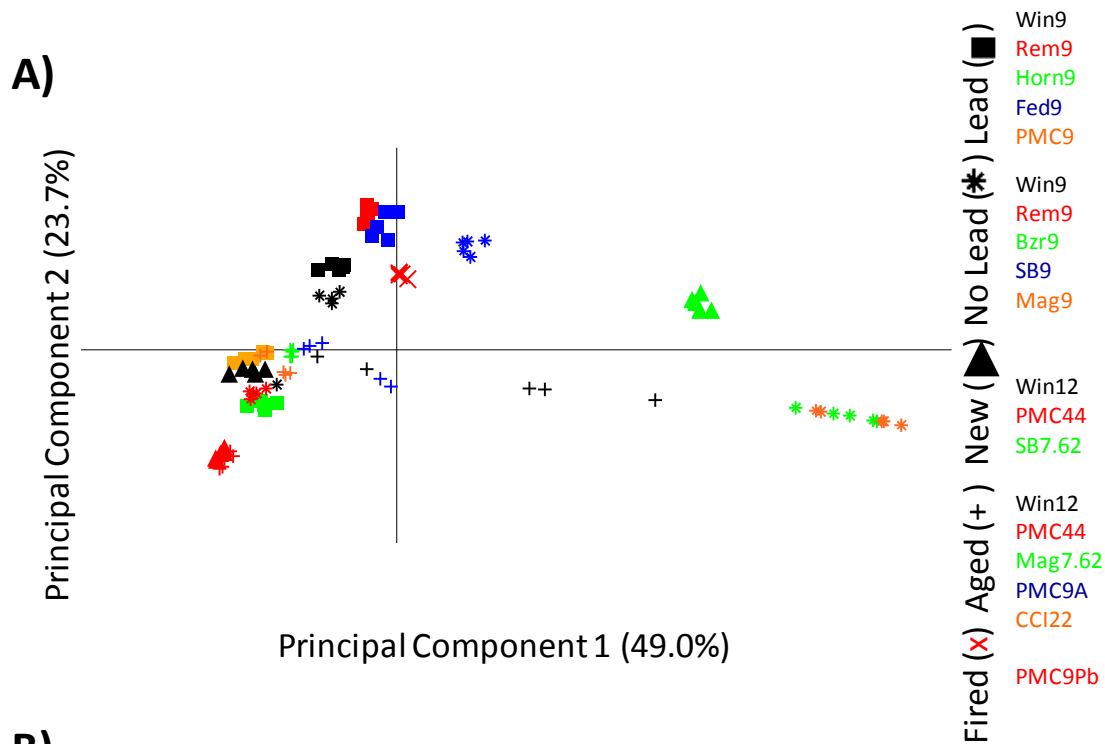


Figure A.5.2.5 Comparison of chemical profile for Fired PMC9Pb versus profiles from unburned smokeless powder (A) PCA scores plot and (B) HCA dendrogram

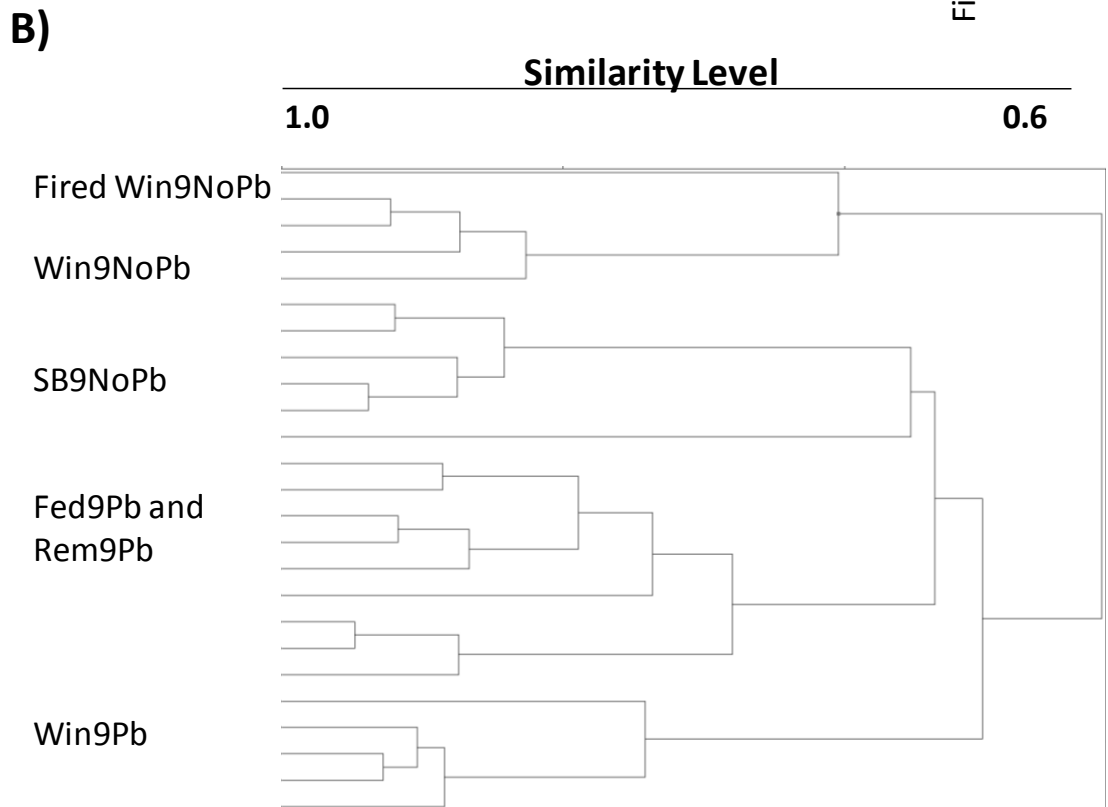
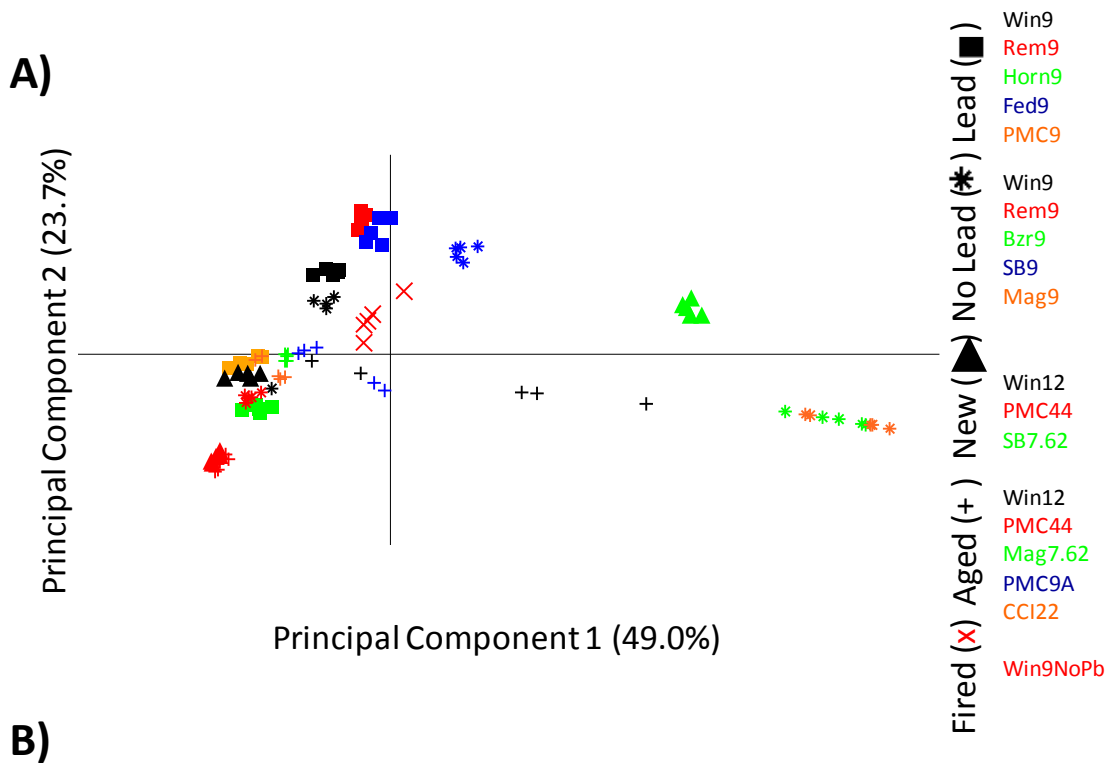


Figure A.5.2.6 Comparison of chemical profile for Fired Win9NoPb versus profiles from unburned smokeless powder (A) PCA scores plot and (B) HCA dendrogram

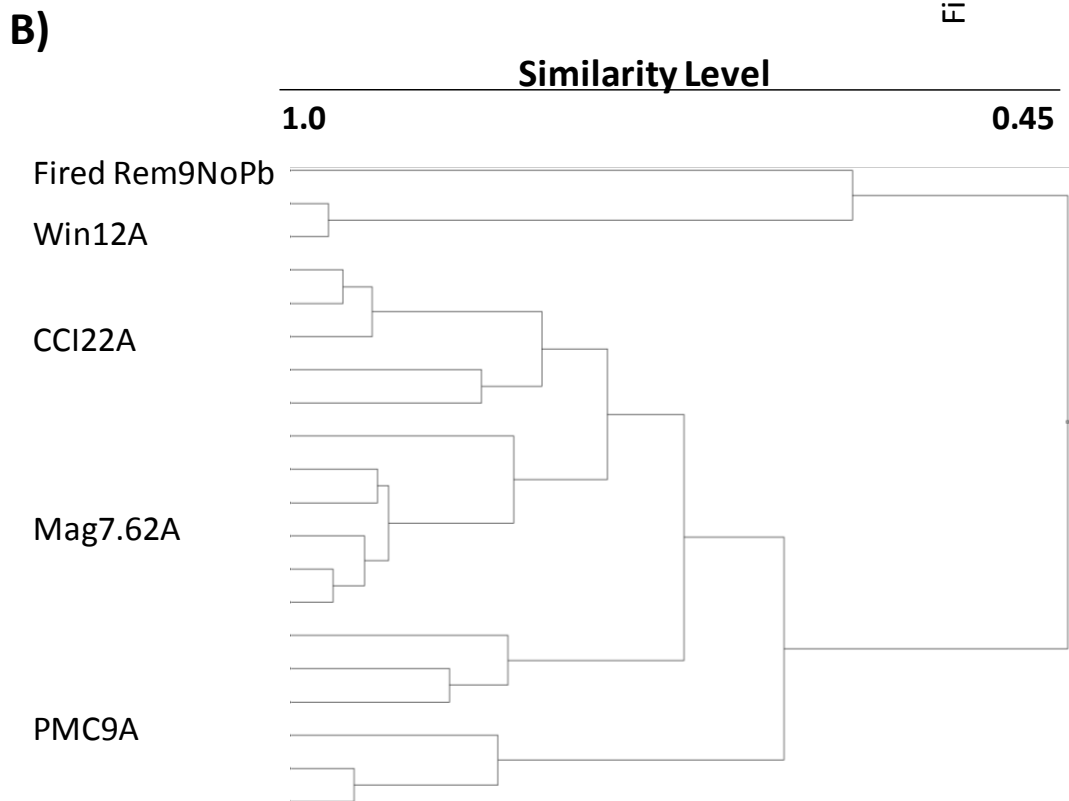
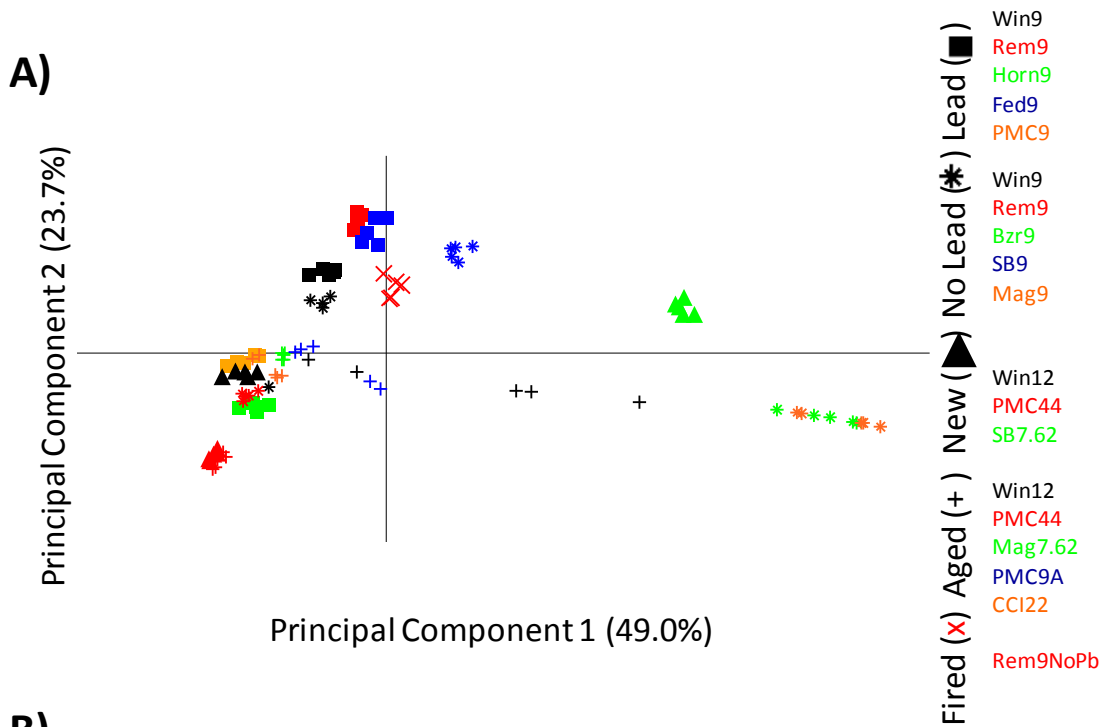


Figure A.5.2.7 Comparison of chemical profile for Fired Rem9NoPb versus profiles from unburned smokeless powder (A) PCA scores plot and (B) HCA dendrogram

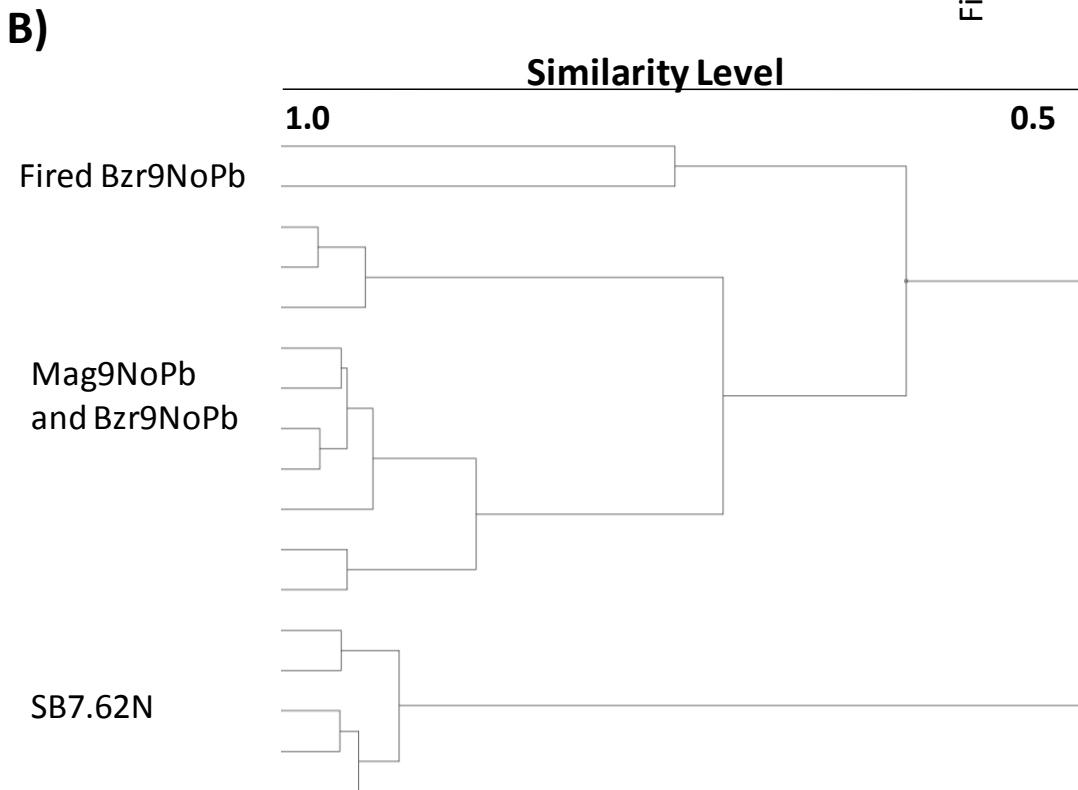
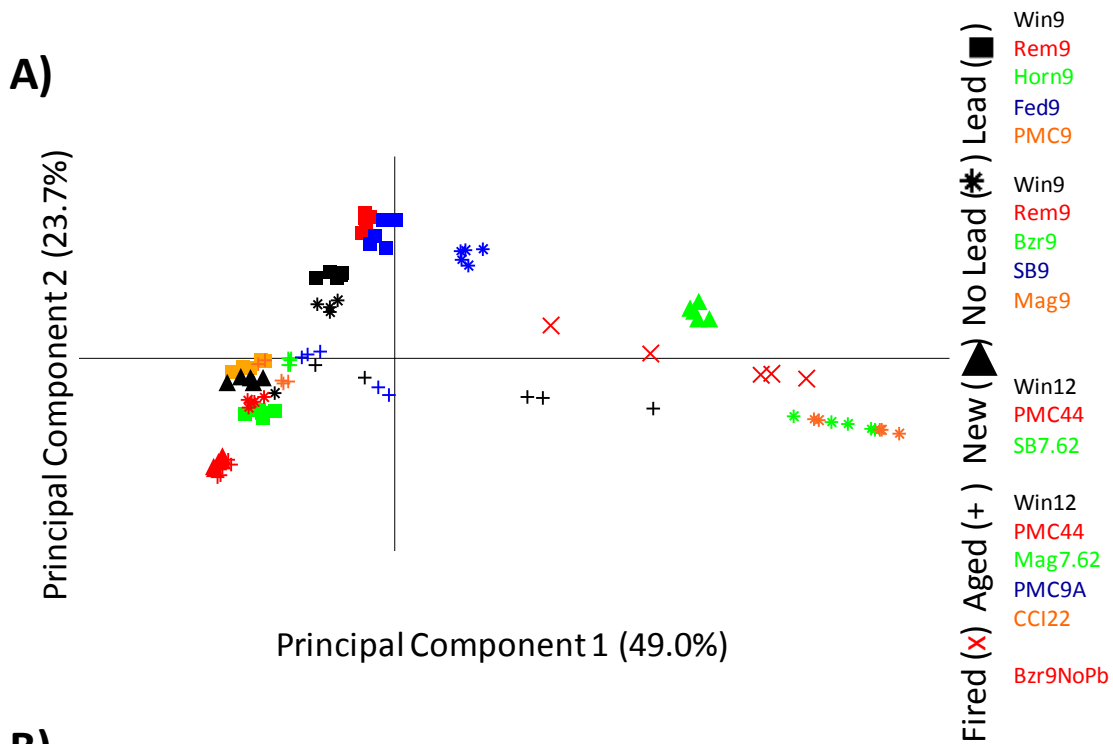


Figure A.5.2.8 Comparison of chemical profile for Fired Bzr9NoPb versus profiles from unburned smokeless powder (A) PCA scores plot and (B) HCA dendrogram

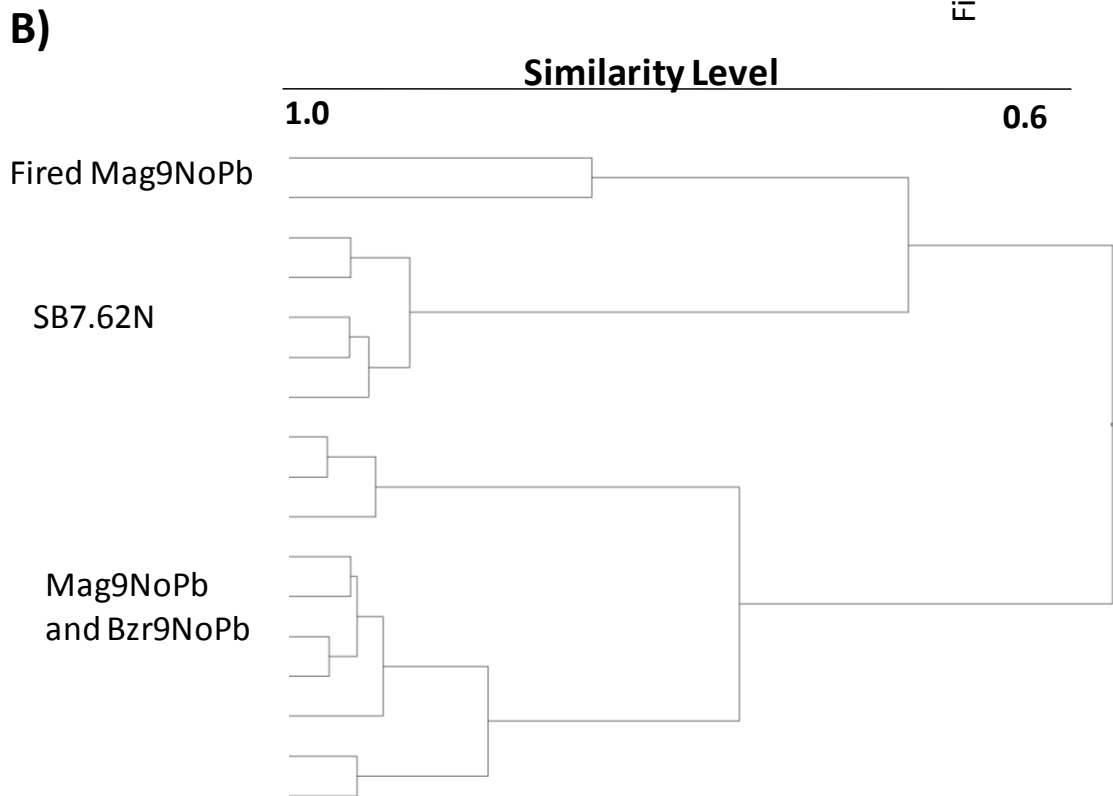
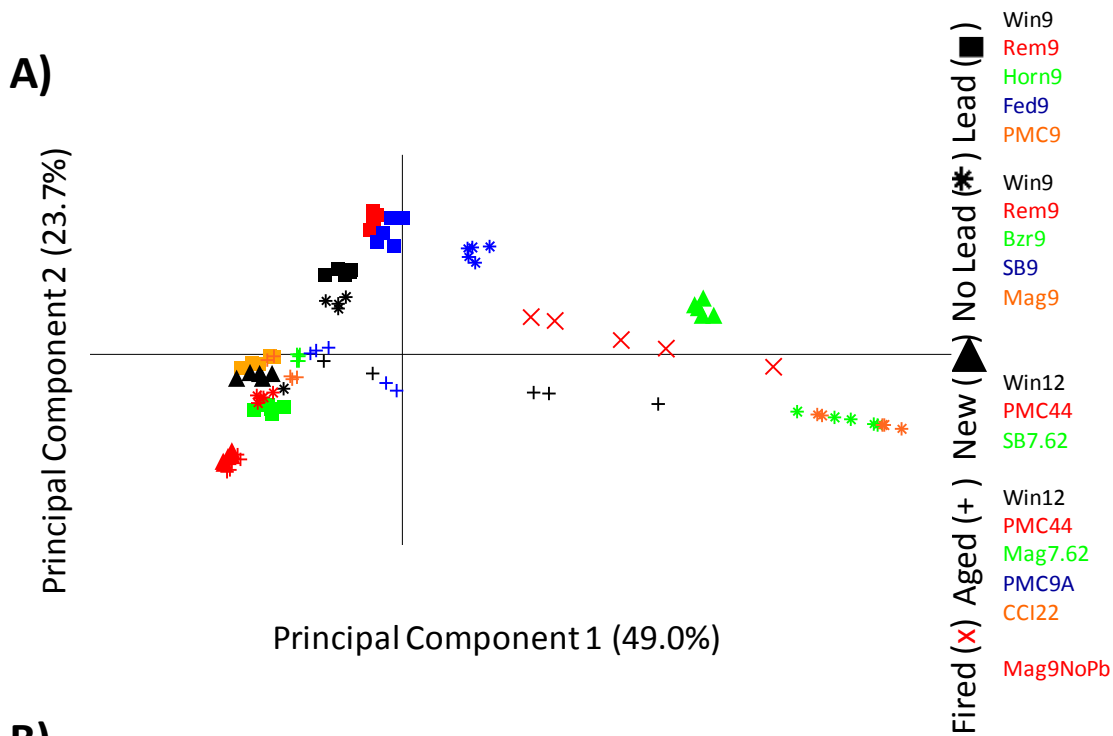


Figure A.5.2.9 Comparison of chemical profile for Fired Mag9NoPb versus profiles from unburned smokeless powder (A) PCA scores plot and (B) HCA dendrogram

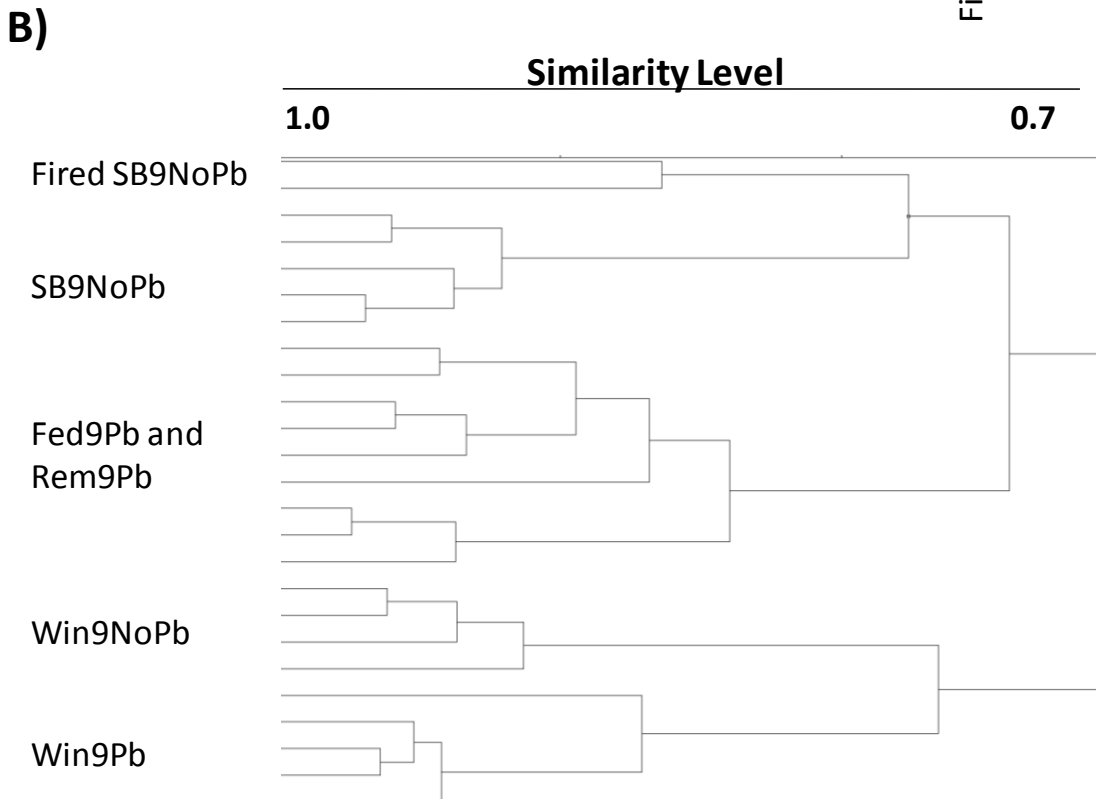
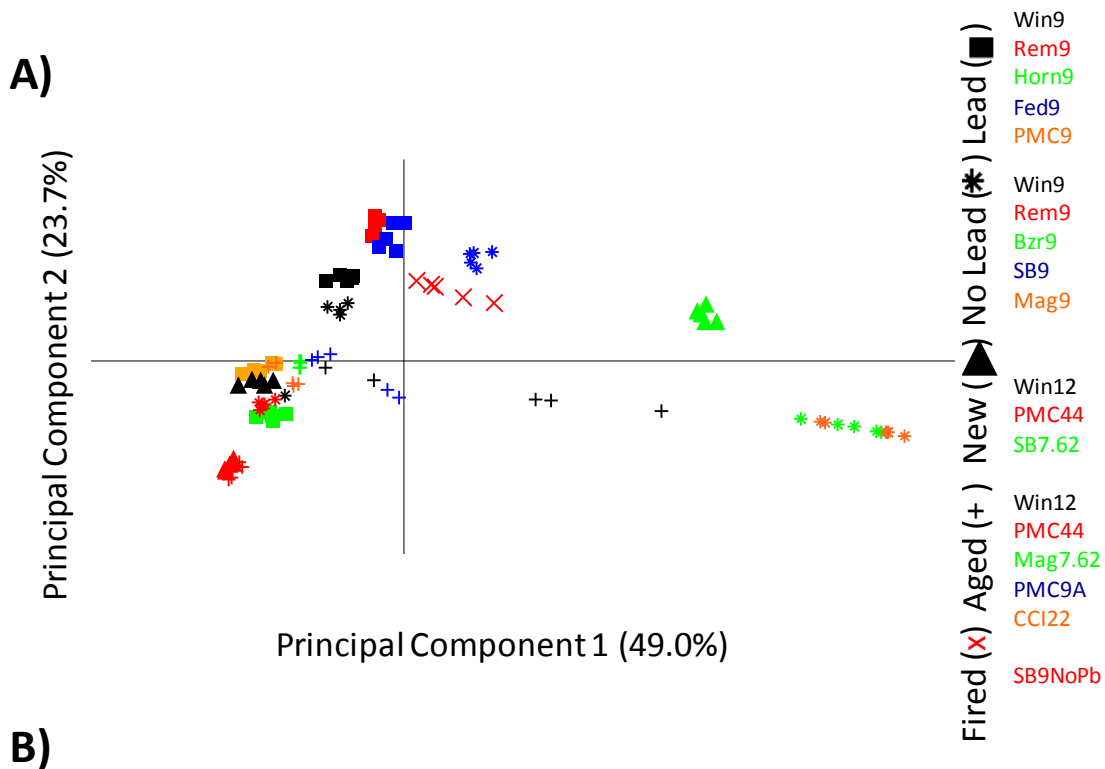


Figure A.5.2.10 Comparison of chemical profile for Fired SB9NoPb versus profiles from unburned smokeless powder (A) PCA scores plot and (B) HCA dendrogram

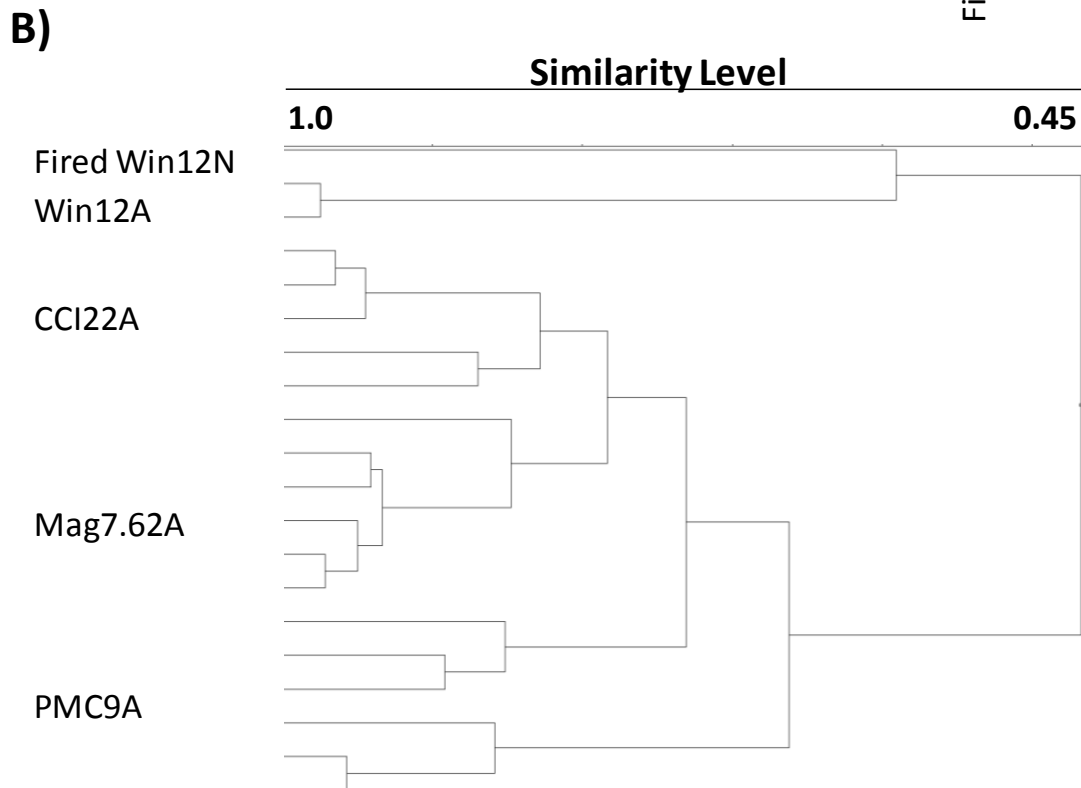
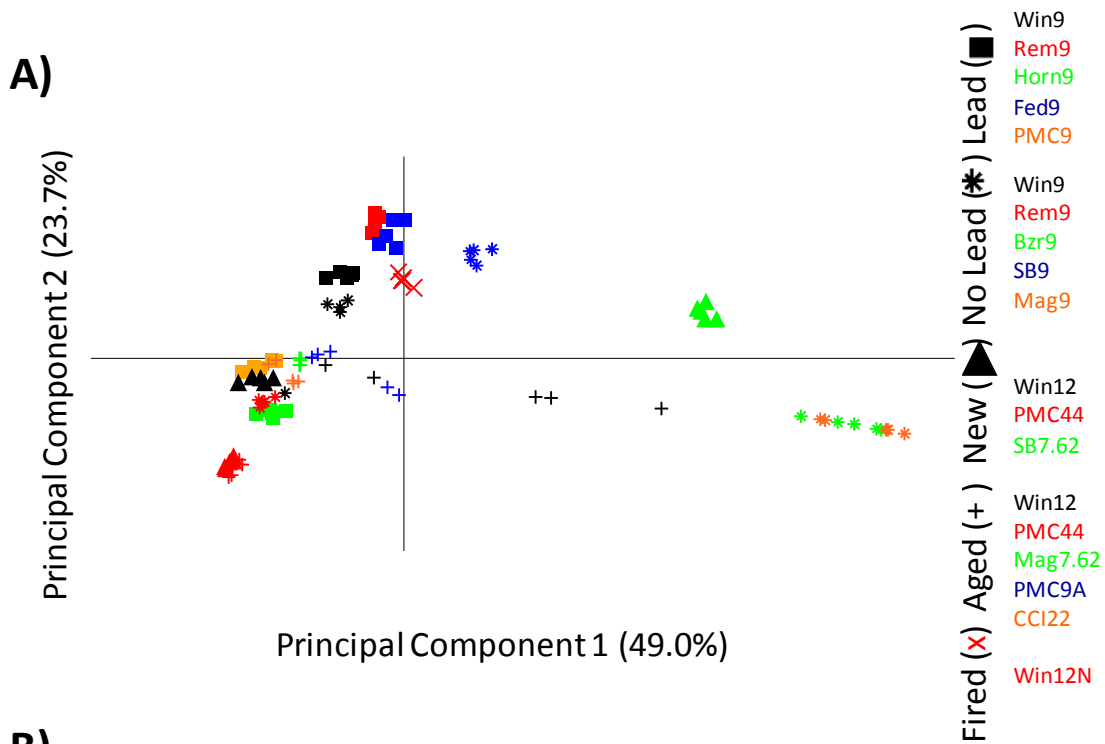


Figure A.5.2.11 Comparison of chemical profile for Fired Win12N versus profiles from unburned smokeless powder (A) PCA scores plot and (B) HCA dendrogram

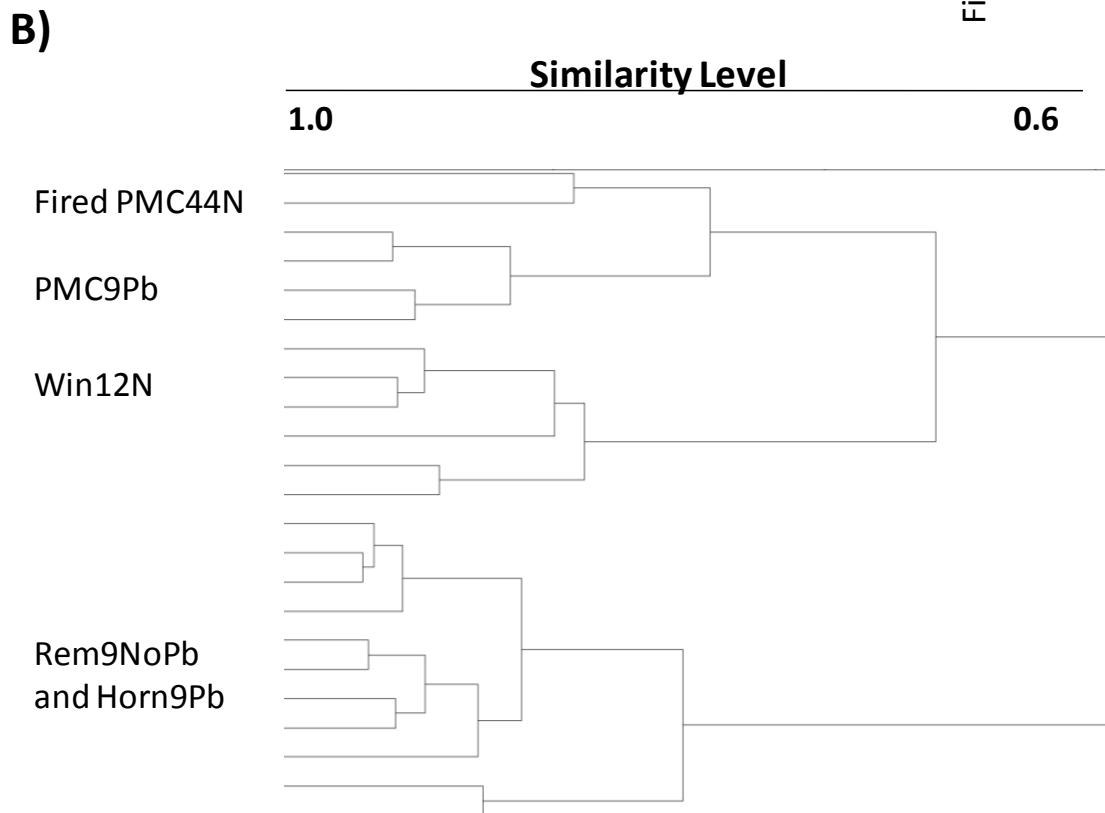
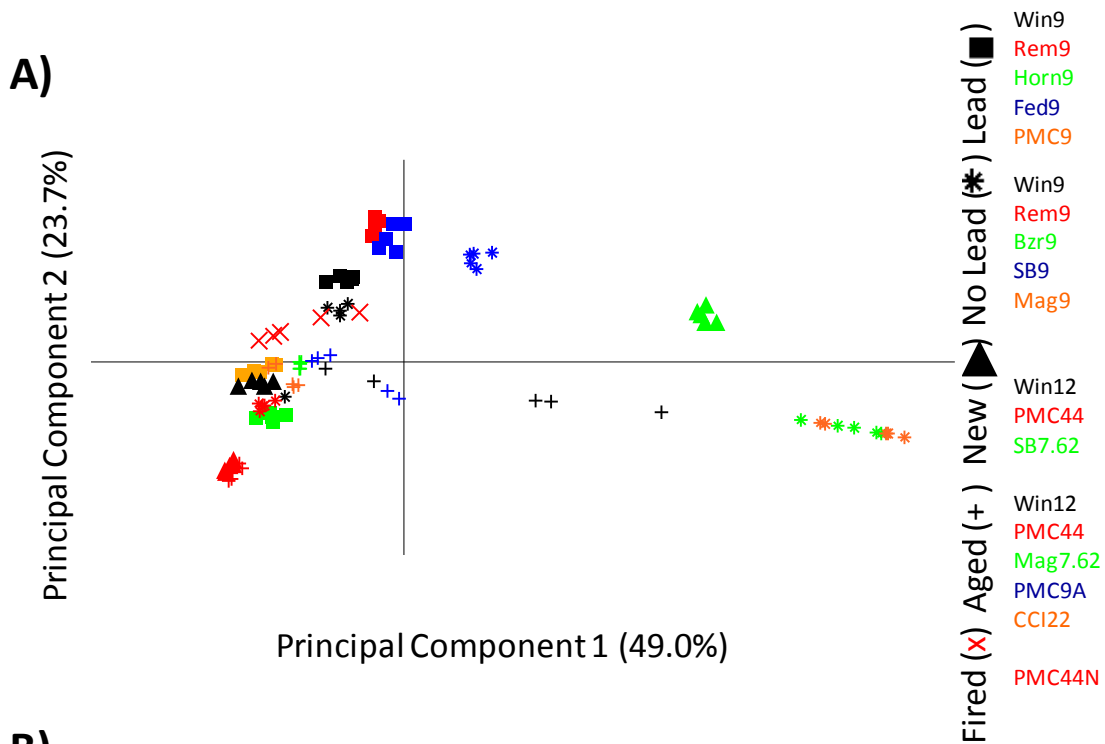


Figure A.5.2.12 Comparison of chemical profile for Fired PMC44N versus profiles from unburned smokeless powder (A) PCA scores plot and (B) HCA dendrogram

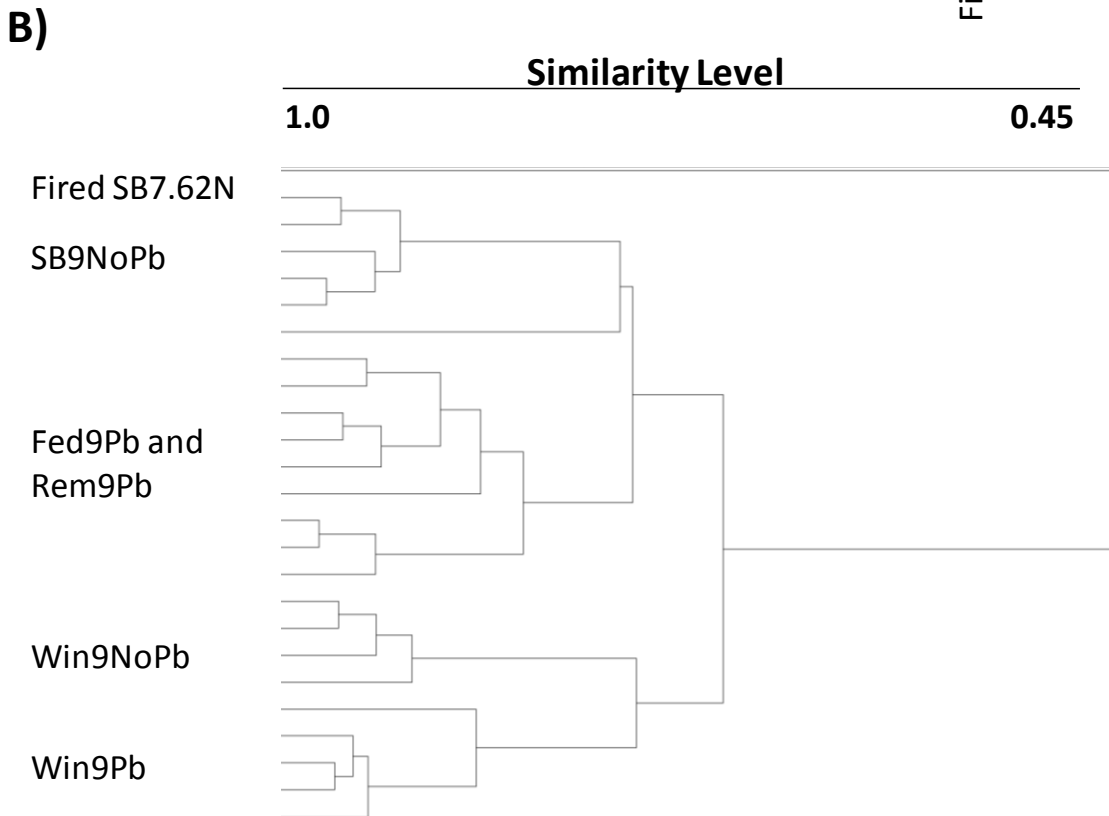
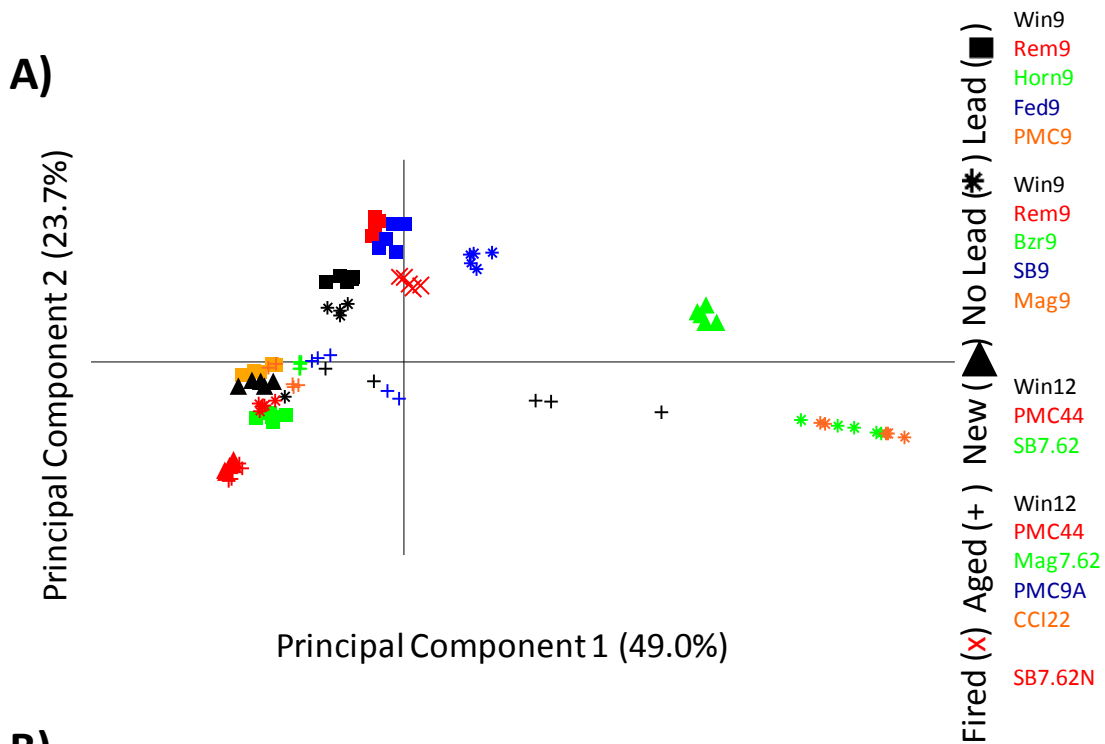


Figure A.5.2.13 Comparison of chemical profile for Fired SB7.62N versus profiles from unburned smokeless powder (A) PCA scores plot and (B) HCA dendrogram

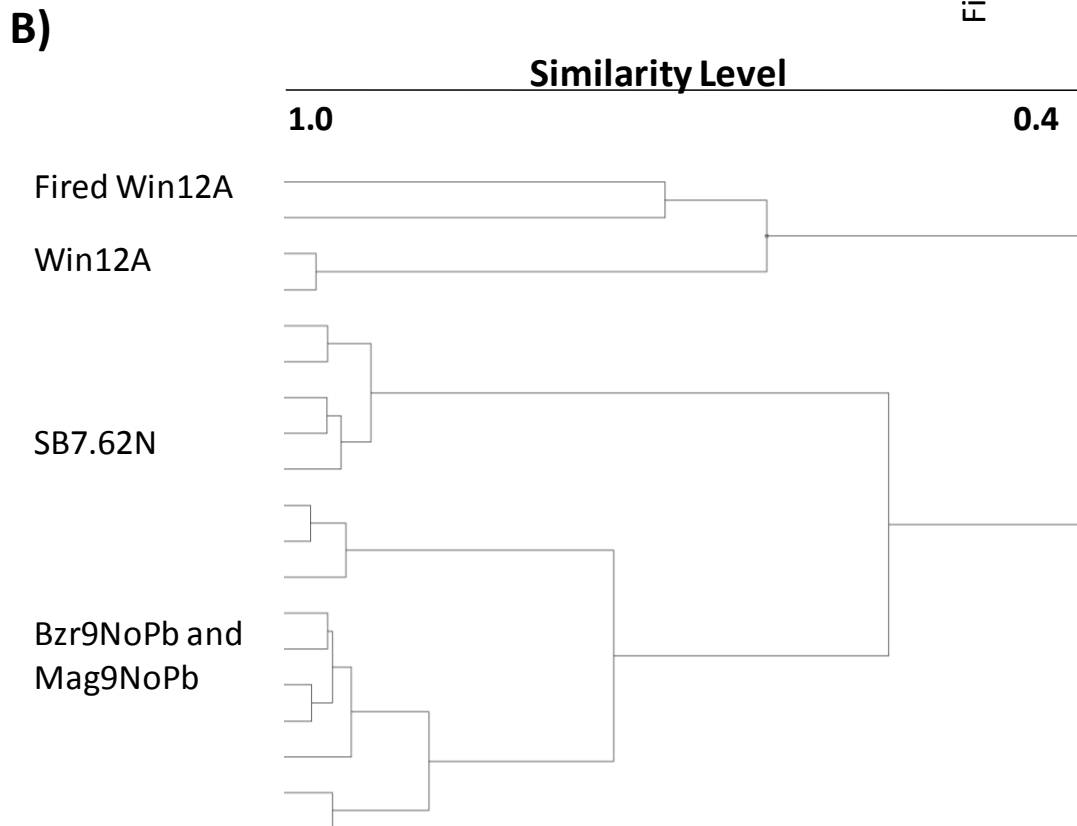
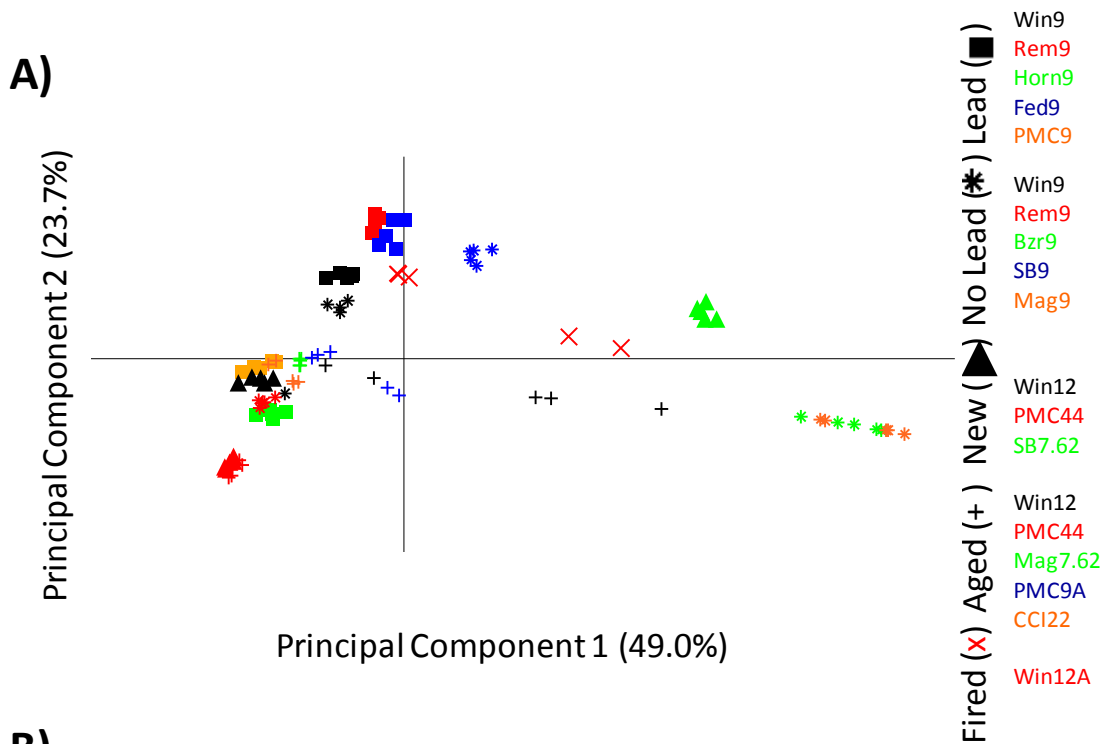


Figure A.5.2.14 Comparison of chemical profile for Fired Win12A versus profiles from unburned smokeless powder (A) PCA scores plot and (B) HCA dendrogram

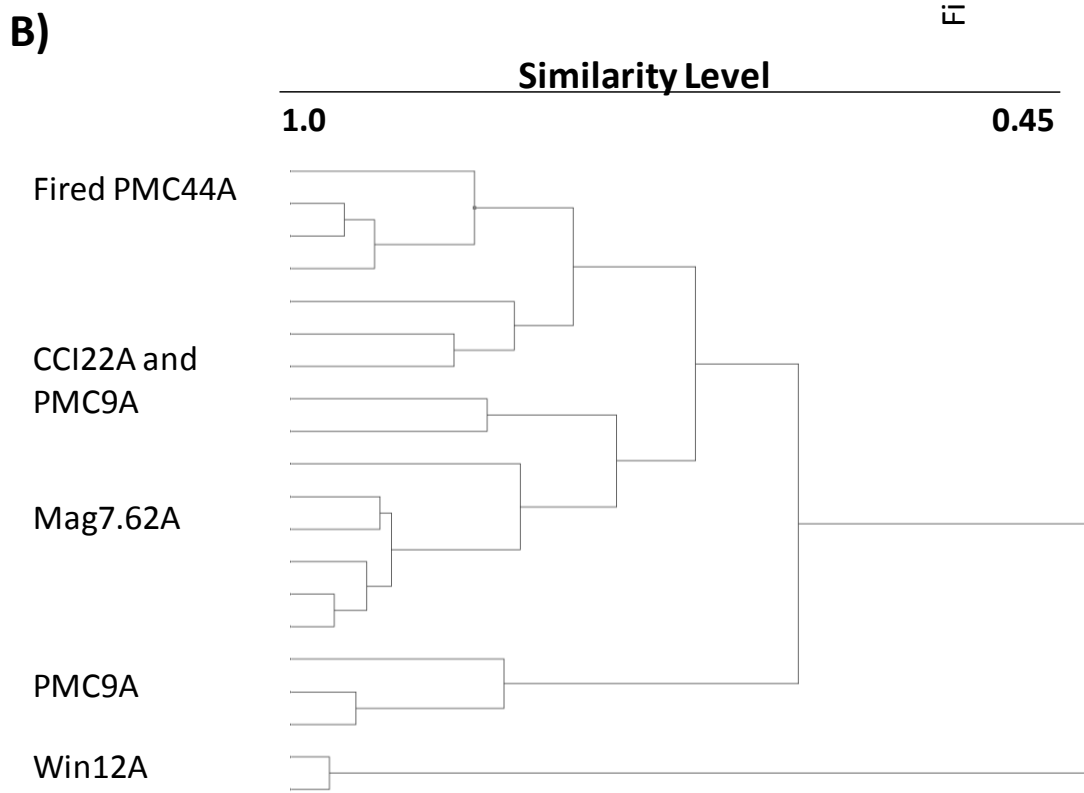
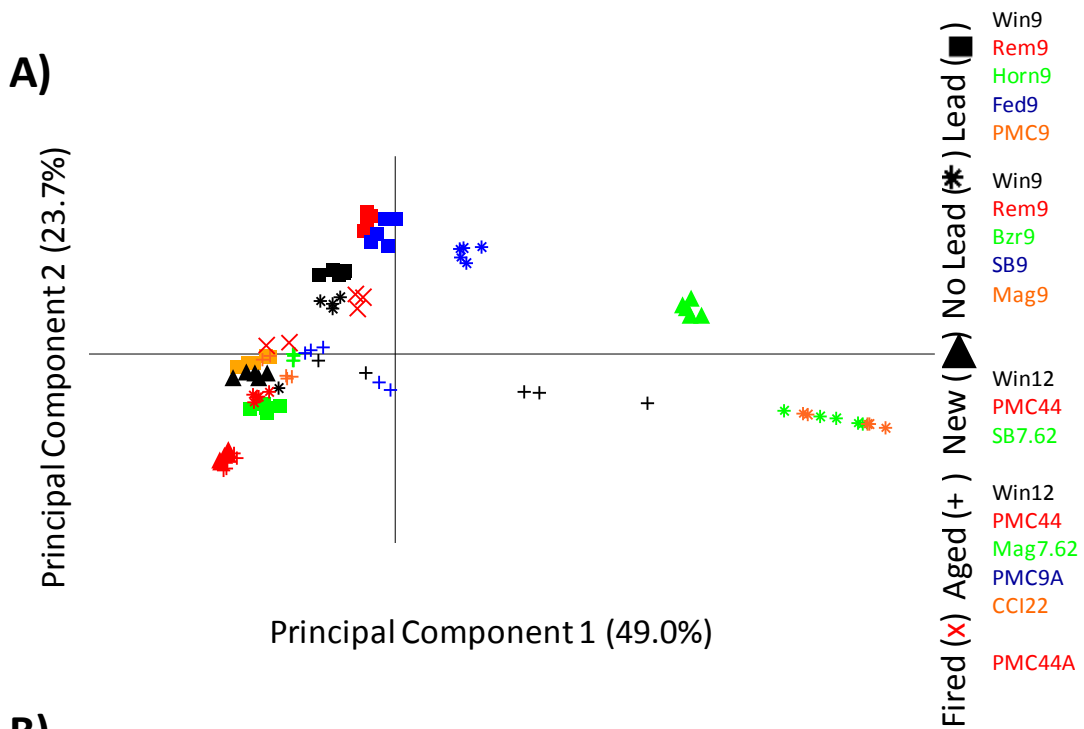


Figure A.5.2.15 Comparison of chemical profile for Fired PMC44A versus profiles from unburned smokeless powder (A) PCA scores plot and (B) HCA dendrogram

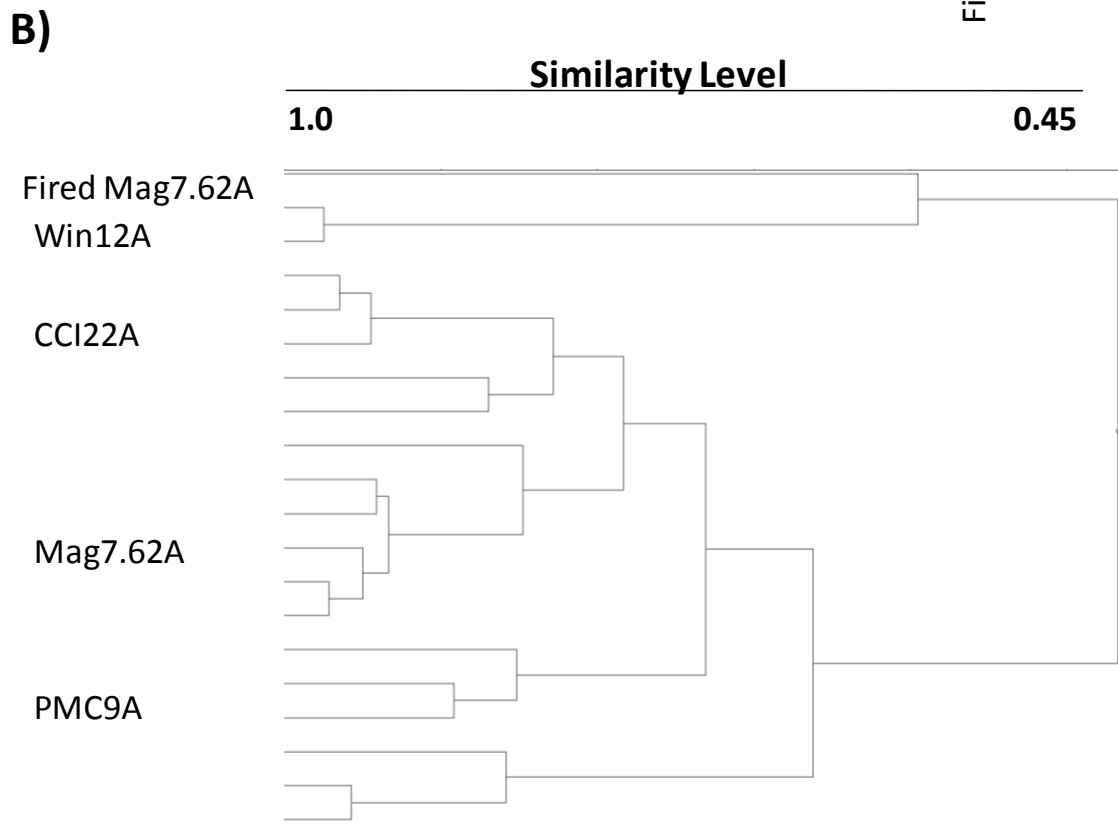
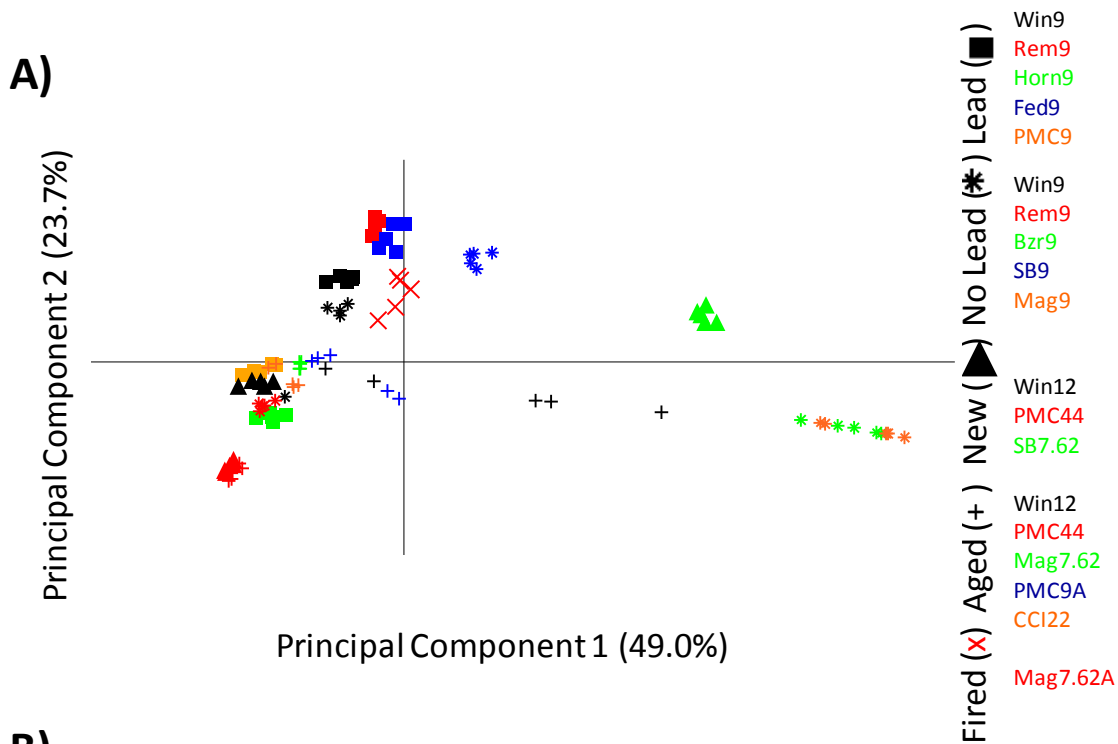


Figure A.5.2.16 Comparison of chemical profile for Fired Mag7.62A versus profiles from unburned smokeless powder (A) PCA scores plot and (B) HCA dendrogram

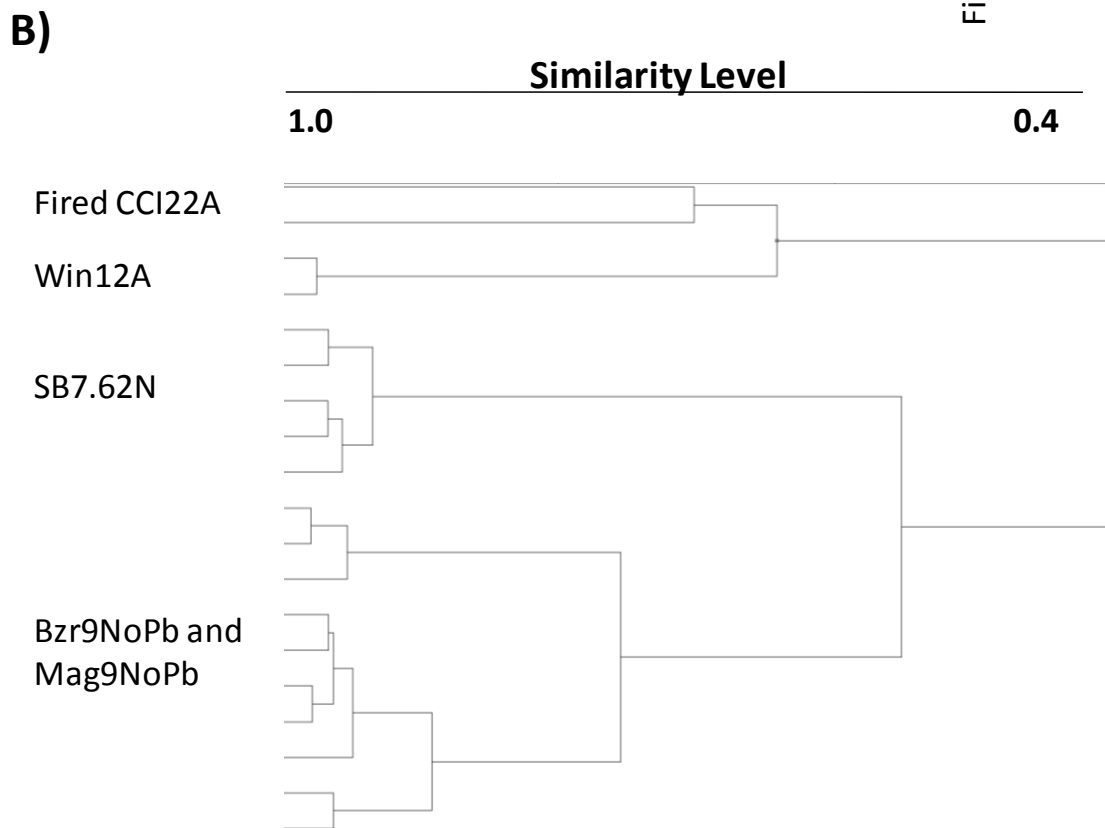
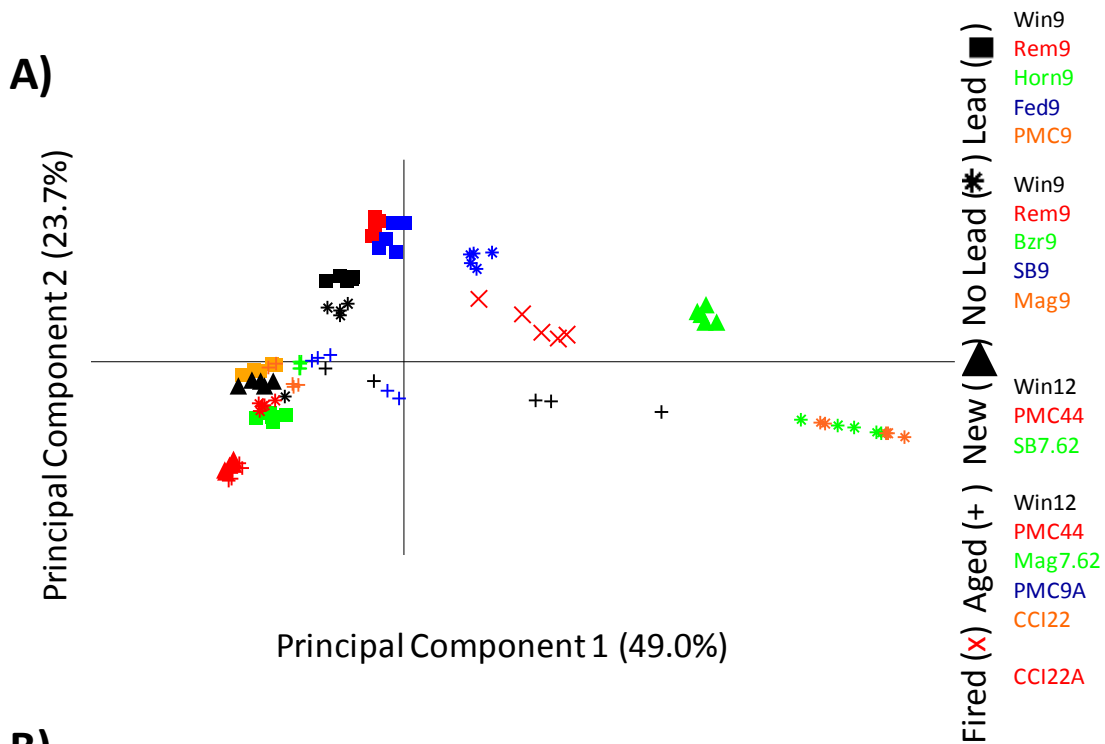


Figure A.5.2.17 Comparison of chemical profile for Fired CCI22A versus profiles from unburned smokeless powder (A) PCA scores plot and (B) HCA dendrogram

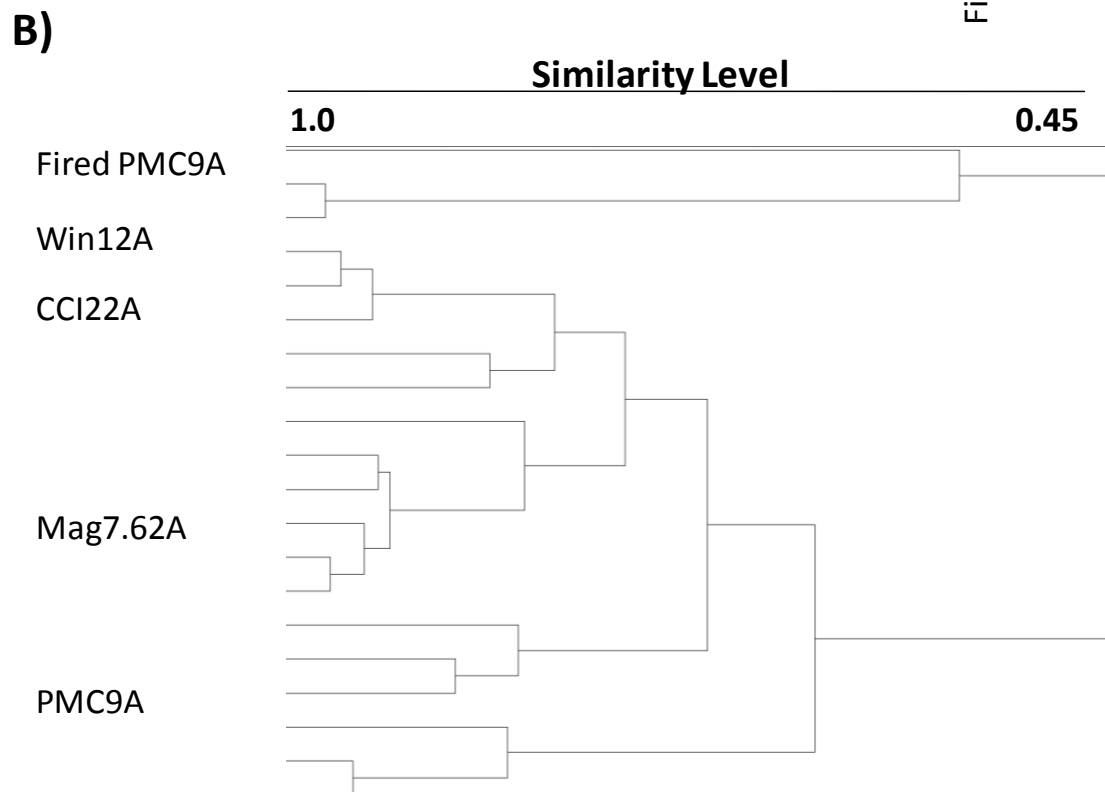
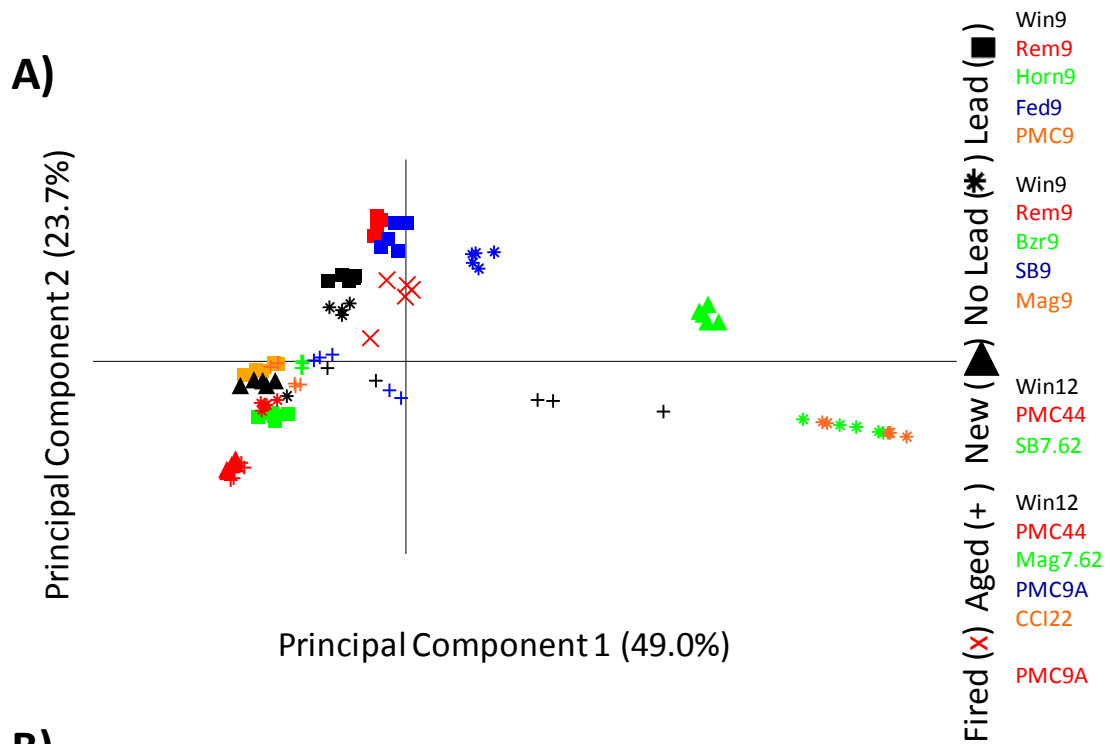


Figure A.5.2.18 Comparison of chemical profile for Fired PMC9A versus profiles from unburned smokeless powder (A) PCA scores plot and (B) HCA dendrogram

REFERENCES

REFERENCES

1. Eringen AC, Liebowitz H, Koh SL. Mechanics and Chemistry of Solid Propellants: Proceedings of the Fourth Symposium on Naval Structural Mechanics, Purdue University, Lafayette, Indiana, April 19-21, 1965: Elsevier Science, 2014.
2. Heramb R, McCord BR. The Manufacture of Smokeless Powders and their Forensic Analysis: A Brief Review. *Journal of forensic sciences*. 2002;4(2).
3. Mahoney CM, Gillen G, Fahey AJ. Characterization of gunpowder samples using time-of-flight secondary ion mass spectrometry (TOF-SIMS). *Forensic Science International*. 2006 4/20;158(1):39-51.

CHAPTER SIX: Conclusions and Future Directions

6.1 Conclusions

The identification and characterization of smokeless powders and burned residues are important aspects of forensic science work given the prevalence of firearms in committing misdemeanors or felonies. Forensic scientists can utilize evidence collected at a crime scene to identify the type of smokeless powder or to associate ammunition from a crime scene to ammunition belonging to a potential suspect. Morphological and/or chemical means have been used to examine smokeless powder evidence. In particular, the chemical approach to characterizing smokeless powders has greater discriminating power. Targeted liquid chromatography-mass spectrometry (LC-MS) methods have been previously successful in identifying compounds and distinguishing powders of different chemical compositions. However, these studies required available reference standards, which may not be feasible for many forensic laboratories.

This work investigated the use of multiplexed collision-induced dissociation (multiplexed CID) for a non-targeted approach to compound identification in the absence of available reference standards. Smokeless powders, both unburned and burned, were collected from samples of various ammunition brands, calibers, and relative ages. Preliminary morphological analysis was found to provide some discrimination, but was limited. Therefore, chemical analysis provided more definitive association and discrimination. High performance liquid chromatography (HPLC) was used to separate the compounds, while detection was performed with atmospheric pressure chemical ionization (APCI) coupled to a time-of-flight mass spectrometer (TOF-MS) utilizing multiplexed CID. Molecular and fragment ions were both utilized for the identification of unknown compounds in the absence of available reference

standards, generating a more comprehensive chemical profile.

Unique compounds or differences in normalized compound abundances between smokeless powder profiles were utilized as distinguishing features within the multivariate statistical analyses of principal component analysis (PCA) and hierarchical cluster analysis (HCA). For unburned powders, PCA provided a means of identifying which compounds provided the greatest levels of distinction between samples. HCA provided a numerical value to measure similarity between replicate measurements from cartridges with the same designation. Groupings of several samples provided broad differentiation, showing alterations in the chemical profiles were associated with the age of the powder but showing no preference for ammunition manufacturer, caliber, or primer composition. Morphological data was combined with the output from PCA and HCA to discriminate most samples. Those that were not distinguished were strongly suspected, but not proven, to have originated from the same smokeless powder manufacturer.

The chemical profiles of burned residue extracted from fired ammunition casings were likewise compared though HPLC-APCI-multiplexed CID-TOF-MS. While the total abundance of organic compounds was depleted, the use of extracted ion chromatograms allowed comparison of the relative abundances among all samples. Of noted importance was the depletion of diphenylamine (DPA) from most samples due to its interaction with products of the burning process and the irreproducibility of the normalized abundance of compounds within replicates of the same ammunition due to the firing process. Utilizing PCA and HCA, the chemical profiles of burned residues were associated or discriminated from the chemical profiles of unburned smokeless powders. Many burned residues were associated well or moderately. Finally, comparison of the known chemical profiles to the chemical profiles of unknown samples

could have use in classification purposes.

The impact of this work on forensics focuses on the use of multiplexed CID to characterize unknown organic compounds within a sample and the use of multivariate statistical analysis on relating unburned and burned smokeless powders. Multiplexed CID allows generation of a comprehensive chemical profile regardless of available reference standards, which is extremely important in regards to the association and discrimination of samples. Multiplexed CID could also be applied to other types of forensic samples for organic compound determination. Meanwhile, the chemical composition of burned residues is variable but useful for analyzing real world samples. The use of multivariate statistical analysis is critical to the analysis. HCA provides a numerical measure of similarity while PCA provides visual comparison through the scores plot and the contributions of individual compounds for differentiation through the loadings plot. Altogether, smokeless powder evidence collected at a crime scene can be compared to powder evidence collected from a suspect, potentially providing a substantial link for law enforcement.

6.2 Future Directions

Potential future experiments could involve the investigation of a large sample set in a single caliber, which would provide a greater comparison of samples across different manufacturers. Commercial ammunitions other than 9mm calibers could be examined. Lead-containing and lead-free primers could be investigated for all samples. Alternatively, acquiring powders directly from the manufacturer would remove any biases of an ammunition manufacturer for purchasing products from a particular powder manufacturer. As the possibility

of reloaded or blended powders is possible, a systematic comparison of mixed manufacturer powders could also be performed.

A larger study of aged ammunition could be performed, if samples permit. The analysis of aged ammunition is important as growing costs encourage the storage and conservation of unused ammunition. Preferably, the cartridges disassembled and/or fired should be known to be from the same ammunition batch. Additionally, the chemical profile of the powder within aged ammunition is affected by ambient storage conditions. However, to utilize controlled conditions would require a controlled study over an extended amount of time.

For purposes of chemical analysis, more replicates would be analyzed for each smokeless powder for both the unburned and burned smokeless powders. The use of a larger amount of samples would allow an analysis on how frequently certain compounds appear, in particular akardite II. Additionally, the irreproducibility of the firing process could be studied between different guns and/or cartridge types. Overall, there are many research opportunities possible for future work in the detection of unburned smokeless powders and the corresponding burned powders.